HEAVY-DUTY ENGINE LOW-LOAD EMISSION CONTROL CALIBRATION, LOW-LOAD TEST CYCLE DEVELOPMENT, AND EVALUATION OF ENGINE BROADCAST TORQUE AND FUELING ACCURACY DURING LOW-LOAD OPERATION

LOW NO_X DEMONSTRATION PROGRAM – STAGE 2

ARB CONTRACT 15MSC010

FINAL REPORT

SwRI® Project Number 03.22496

Prepared for:

California Air Resources Board

Prepared by:

Christopher A. Sharp, Institute Engineer - Program Manager

Southwest Research Institute
6220 Culebra Road
San Antonio, TX 78238

May 6, 2020

HEAVY-DUTY ENGINE LOW-LOAD EMISSION CONTROL CALIBRATION, LOW-LOAD TEST CYCLE DEVELOPMENT, AND EVALUATION OF ENGINE BROADCAST TORQUE AND FUELING ACCURACY DURING LOW-LOAD OPERATION

LOW NO_X DEMONSTRATION PROGRAM – STAGE 2

ARB CONTRACT 15MSC010

FINAL REPORT

SwRI® Project Number 03.22496

Prepared for:

California Air Resources Board

May 6, 2020

Prepared by:

Chris A. Sharp, Institute Engineer
Diesel Engine and Emissions R&D Dept.
Powertrain Engineering Division

Approved by:

Charles E. Roberts, Jr., Ph.D., Director
Diesel Engine and Emissions R&D Dept
Powertrain Engineering Division

POWERTRAIN ENGINEERING DIVISION

TABLE OF CONTENTS

LIST OF FIGURES

Figure **Page**

LIST OF TABLES

Table **Page**

LIST OF ACRONYMS

AMT	Automated Manual Transmission
ANR	Ammonia to NO_X Ratio
ASC	Ammonia Slip Catalyst
AT	Automatic Transmission
BMEP	Brake Mean Effective Pressure
CAN	Controller Area Network
CITT	Curb Idle Transmission Torque
CWF	Carbon Weight Fraction
DAAAC	Diesel Aftertreatment Accelerated Aging Cycles
DEF	Diesel Exhaust Fluid (32% urea by weight)
DOC	Diesel Oxidation Catalyst
DPF	Diesel Particule Filter
ECM	Electronic Control Module
EGR	Exhaust Gas Recirculation
EO	Engine Out
EU	European Union
EWMA	Exponentially Weighted Moving Average
FTP	U.S. Heavy Duty Transient Federal Test Procedure
FUL	Full Useful Life
GEM	EPA Greenhouse Gas Emission Model
GHG	Greenhouse Gas
GPS	Global Positioning System
HDIUT	Heavy Duty In Use Testing
IMAP	Intake Manifold Absolute Pressure
IMT	Intake Manifold Temperature
LLC	Low Load Cycle
LO-SCR	Light Off SCR Catalyst
MAW	Moving Average Window
MB	Mini-burner
MT	Manual Transmission
MY	Model Year
NIST	National Institute of Standards and Technology
NTE	Not-to-Exceed
OBD	Onboard Diagnostics
PAG	Program Advisory Group
PNA	Passive NO_X Adsorber
RMC-SET	Ramped Modal Cycle Supplemental Emission Test
RMS	Root Mean Square
SCR	Selective Catalytic Reduction (ammonia-based)
SCRF	SCR on Filter (SCR coated on DPF)
SPN	CAN Suspect Parameter Number
TM	Thermal Management
TP	Tailpipe
WBW	Work-Based Window
WHTC	World Harmonized Transient Cycle
zCSF	Zone Coated Catalyzed Soot Filter

EXECUTIVE SUMMARY

This report describes a program that was performed on behalf of the California Air Resources Board (CARB) to examine the potential for Low NO_X emissions from heavy-duty engines operating over low-load duty cycles, such as those typical of urban environments and vocational applications. The program described in this report is described as the Stage 2 Low NO_x Program, and it follows directly from efforts under the Stage 1 program that were described in the report "Evaluating Technologies and Methods to Lower Oxides of Nitrogen Emissions from Heavy-Duty Vehicles," submitted to CARB in April 2017.

The Stage 1 program focused primarily on the current regulatory cycles, the Heavy-Duty Transient Federal Test Procedure (FTP) and the Ramped Modal Cycle-Supplemental Emissions Test (RMC-SET). Some initial examination of lower load operating cycles was done using a preliminary set of Vocational Cycles, which were low load cycles from vocational applications that were developed based several existing cycles which CARB selected to enable a preliminary examination of the low-load operating region. However, a more robust examination of the potential for Low NO_X levels was needed in support of the regulatory efforts planned by CARB. The current regulatory approach provides for good emission controls in the range of duty cycles represented by the FTP and RMC-SET, but many current production systems do not provide as robust a level of NO_X emission control during lower load operations as what is observed in laboratory tests on the current certification cycles. To address this "low-load emission gap," as it is sometimes called, CARB asked SwRI to expand the original Low NO_X demonstration effort to focus on several topics relevant to low-load NO_X control.

Specifically, SwRI was asked to conduct three major tasks to address the potential low-load NO_X:

- Develop a new Load Low Cycle (LLC) which would represent low-load operating regions currently not covered by existing regulatory cycles.

- Extend the FTP/RMC calibration of the Stage 1 diesel Low NO_X engine and aftertreatment system to examine the potential to reach Low NO_X levels under low-load operation, as represented by the new LLC. The revised calibration must still comply with original FTP and RMC targets at 0.02 g/hp-hr tailpipe NO_X.

- Examine the accuracy of ECM broadcast torque and fuel rate measurements at low loads. This examination included analysis of other metrics for quantifying emissions at low loads. In order to support this alternate metric analysis, other ECM broadcast variables were also assessed for accuracy, as noted later.

Low-Load Cycle Development

The new Low-Load Cycle (LLC) was developed based on real-world operating data, measured from trucks operating in the field. For the cycle development process, SwRI engaged with the National Renewable Energy Laboratory (NREL) as a subcontracted partner. NREL provided several key resources for this cycle development effort. These included access to data from hundreds of in-use vehicles that were available in their FleetDNA[1] database, supercomputer resources to support a data-driven and computationally intensive analysis process, and significant experience with this kind of "big data" analysis for cycle development. The source data set was further augmented with the addition of data from another 100 vehicles that were taken by CE-CERT[2] for CARB.

The data set is described below in Figure 1 and it covered a wide range of applications considering some 751 different vehicles.

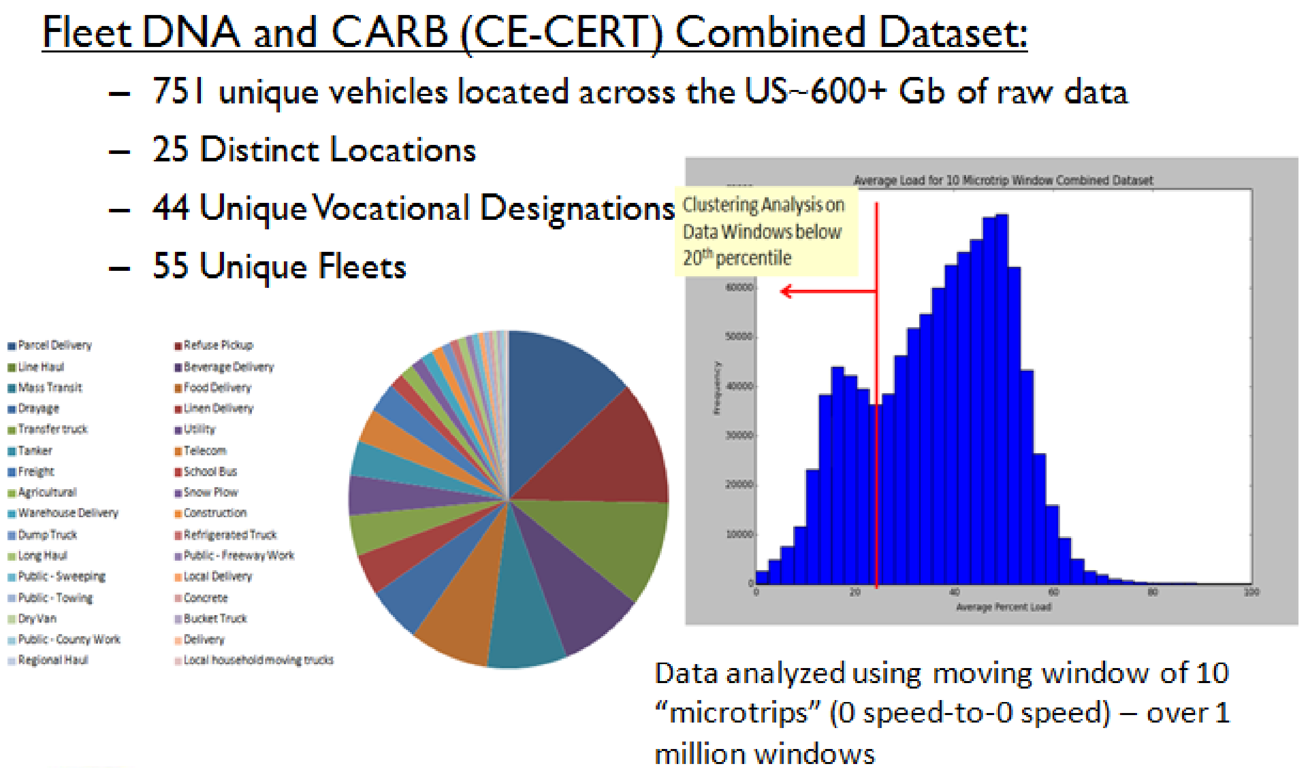

FIGURE 1. DESCRIPTION OF DATA INPUTS FOR LLC DEVELOPMENT

Because NO_X control behavior can be dependent on recent vehicle operating history, the data was examined in windows that incorporate a series of 10 "microtrips" (regions of operation between two points of zero vehicle speed). More than 1.2 million such unique windows were identified in the source data set. As part of the analysis, the region below the 20th percentile of average load was identified as the low-load region. The subset of windows in this space (about 250,000 data profiles) was analyzed by NREL using a k-means clustering process which was designed to identify common operation modes in the low-load operating space. Individual real-world examples of vehicle operation were then extracted from these areas to serve as building blocks for the final LLC. A total of 10 different profiles were ultimately selected based on this

[1] Fleet DNA as an online database which consists of high resolution commercial vehicle operation data that NREL collects from fleets around the country, www.nrel.gov/fleetdna

[2] Boriboonsomsin, Kanok, Johnson, Kent, and George Scora. 2017. "Collection of Activity Data from On-Road Heavy-Duty Diesel Vehicles." Technical Report for California Air Resources Board. Available from: http://ww3.arb.ca.gov/research/apr/past/13-301.pdf

analysis. The final clusters from which these profiles were picked similarly represented a wide range of different vocations and applications. Figure 2 shows an example of the distribution of applications for one of the final clusters (Cluster 1), from which several profiles were chosen.

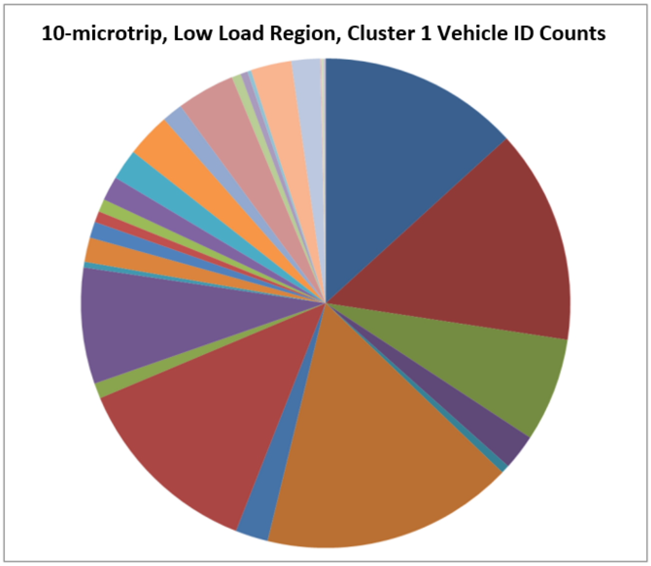

FIGURE 2. EXAMPLE VOCATIONAL DISTRIBUTION OF LOW LOAD CLUSTER 1

These vehicle profiles were translated to engine cycles using the EPA Greenhouse Gas Emission Model (GEM) to provide high time resolution engine activity validated against the engine CAN datalogs. The translated cycles were then examined via engine testing on current production engines, and the results were used to help select which of the profiles would be incorporated into the final LLC. Several candidate LLCs were assembled and tested, with a final set of candidates being presented to CARB, as well as a stakeholder group for feedback. The final LLC that was selected is given below in Figure 3. This particular cycle incorporates a number of characteristic challenges faced by a wide variety of vehicles and applications including low load transient operation, significant idling, engine motoring that forced cools today's products, and return to high power operation following periods of low load.

The LLC is designed to be run following the cold-hot FTP testing of the current certification process, following a 20-minute engine-off soak. It can also be run independently following a hot-FTP preconditioning cycle and 20-minute soak. The final cycle has a cycle average power generally in the range of 6% to 8% of maximum engine power. This contrasts with the current heavy-duty FTP at about 22% of maximum engine power. Testing of current production engines (certified to 0.2 g/hp-hr on the current regulatory cycles) over the newly developed LLC resulted in a wide variety of tailpipe NO_X levels ranging from 0.3 g/hp-hr to as high at 2 g/hp-hr. Most of the results observed were in the range around 1 g/hp-hr. This is consistent with the "low-load emission gap" often observed in field testing at lower loads. As a result, the LLC should be an effective tool in helping to ensure that future engines are equipped with systems and calibrations that control emissions effectively in this low-load operating region.

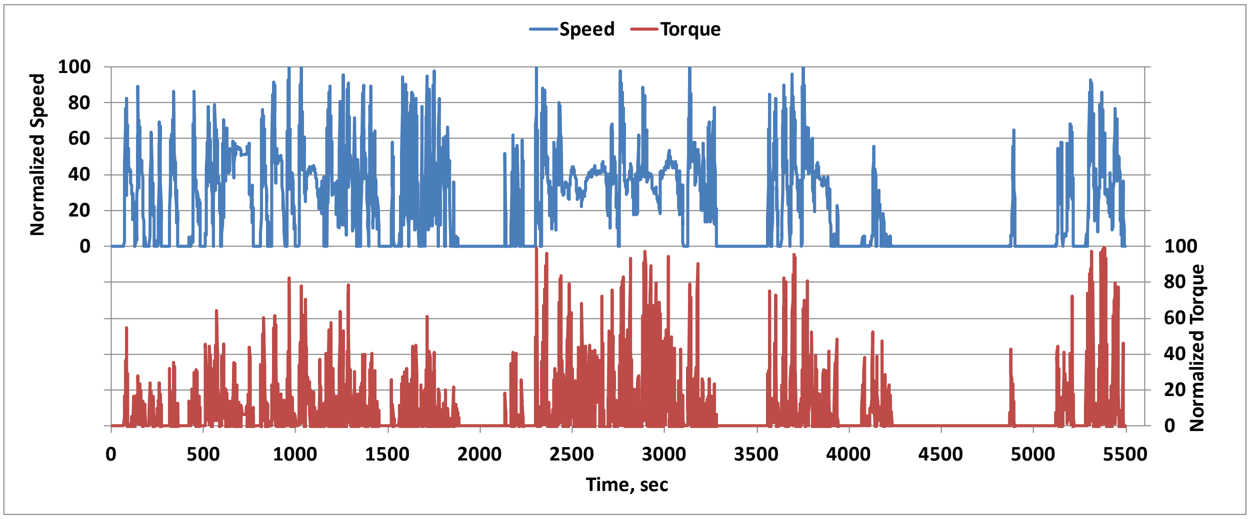

FIGURE 3. FINAL LOW-LOAD CYCLE – NORMALIZED SPEED AND TORQUE

Low-Load Calibration of the Stage 1 Low NO_X Engine

With the new LLC available, SwRI undertook the effort to extend the calibration previously developed for the Stage 1 Low NO_X engine system, to demonstrate Low NO_X levels over the LLC. This was done using a combination of engine calibration changes and thermal management strategy changes leveraging use of a mini-burner for flexible heat input. A range of calibration changes were investigated, as were the impact of those changes on CO_2 and criteria emission rates including on the other regulatory cycles.

A summary of the results of this effort is given in Figure 4 below. The final NO_X emissions levels ranged from 0.27 g/hp-hr to 0.02 g/hp-hr, with a corresponding range of CO_2 impacts from -2% to +2% as compared to the baseline engine. Ultimately, SwRI selected a calibration that was fuel consumption neutral compared to the baseline engine, and that calibration produced a tailpipe NO_X level of 0.07 g/hp-hr. At this same time, Low NO_X performance was re-checked after these calibration changes to make sure the system still performed as needed on the FTP and RMC-SET cycles. No changes in those cycle results were observed, indicating that the Low NO_X system still performed as intended on those other certification cycles, maintaining an emission level below 0.02 g/hp-hr using development aged parts (hydrothermal aging only[3]). LLC results were also checked on parts Final-Aged to full-useful life and achieved similar LLC performance. The performance of the Low NO_X system on the LLC in comparison to a current production engine is illustrated in Figure 5.

[3] The process of thermally cycling exhaust gases entering an aftertreatment system to simulate deterioration due to in field operation on an engine, typically in an accelerated fashion. Hydrothermal aging does not generally include chemical poisoning impacts.

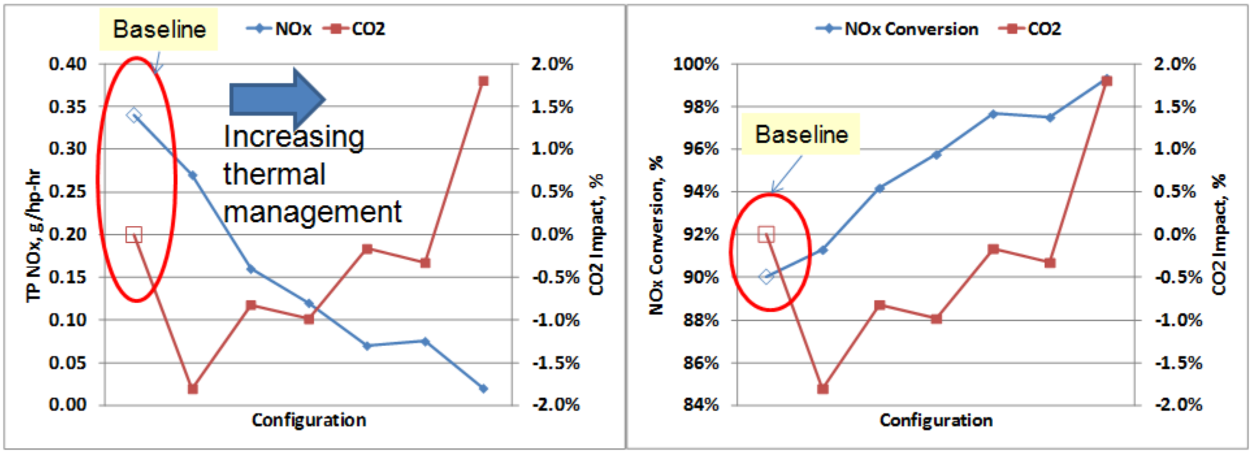

FIGURE 4. SUMMARY OF LOW-LOAD CALIBRATION EXTENSION EFFORTS ON THE STAGE 1 LOW NO_X ENGINE SYSTEM – NO_X AND CO_2 IMPACTS

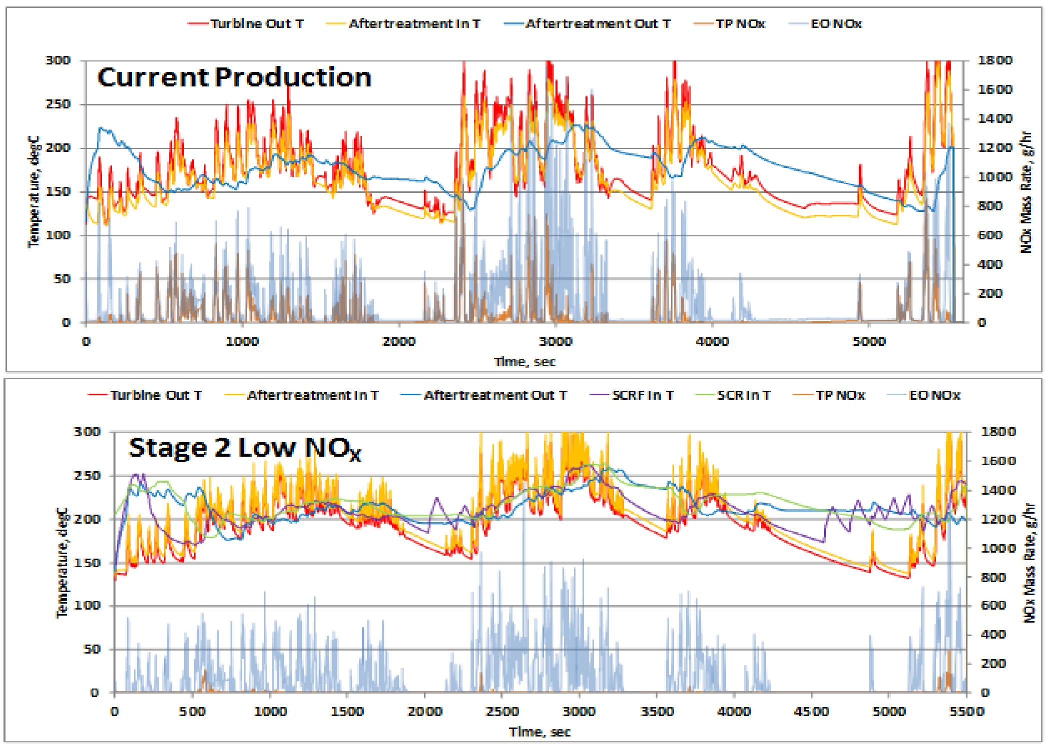

FIGURE 5. LLC DATA ON STAGE 2 RE-CALIBRATED LOW NO_X ENGINE COMPARED TO CURRENT PRODUCTION EXAMPLE AT SAME FUEL CONSUMPTION

As can be seen in the charts showing Tailpipe NO_X in red-brown compared to Engine-out NO_X in light blue, the Current Production engine permits a considerable amount of NO_X to reach the tailpipe, while the Stage 2 Low NO_X engine shows almost no tailpipe NO_X behavior apart from a few very small spikes and was accomplished over this cycle with a fuel neutral calibration compared to the baseline engine while preserving the FTP and RMC performance.

Low-Load NOx Sensor Accuracy and Metrics

SwRI examined the accuracy of key engine sensor-based measurements that would be needed to support an eventual sensor-based in-use compliance program. These measurements included fuel flow, exhaust flow, torque, and NO_X. Measurements were performed on multiple current production engines to assess the state-of-the-art in this area (all post MY 2017 engines from a number of manufacturers). The results of analysis looking at accuracy are illustrated in Figure 6 below. Exhaust Flow and Fuel Flow measurements were very good, while Torque measurement was problematic, especially at low loads. The NO_X sensor measurements were also problematic especially at the lower ranges typical of Low NO_X, and the measurements indicate the need for improvements on tailpipe NO_X sensor performance to support a robust in-use compliance program.

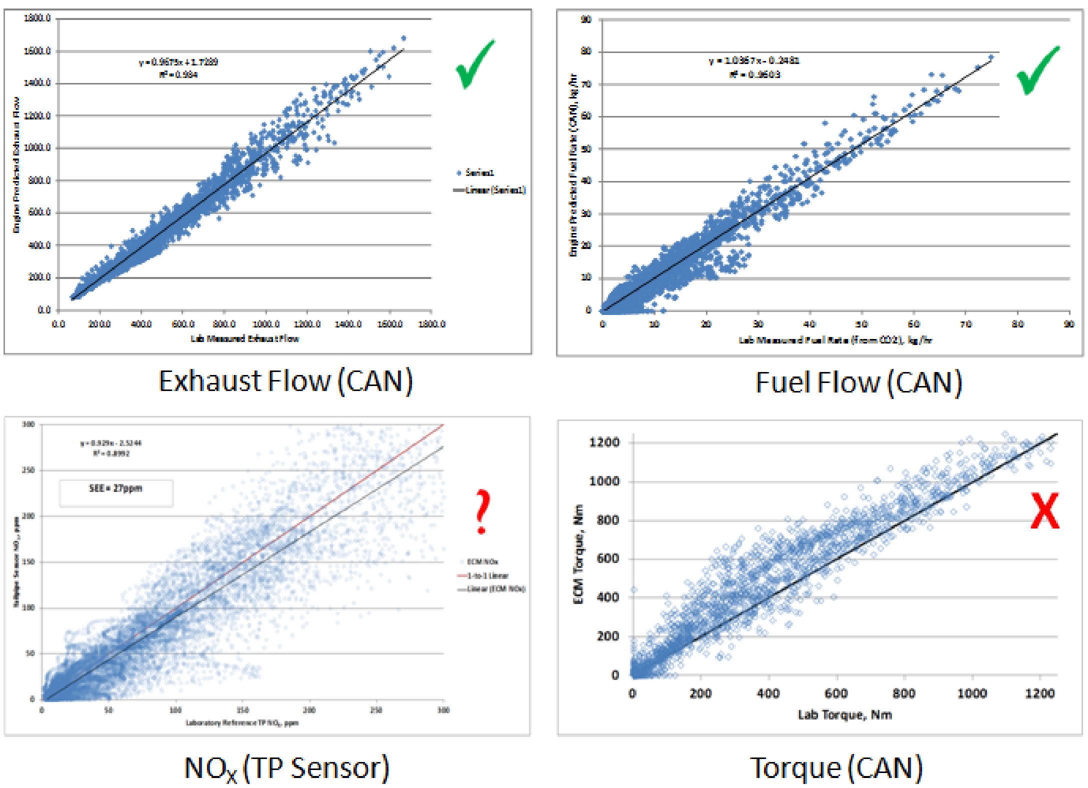

FIGURE 6. SENSOR ACCURACY ASSESSMENT – ECM SENSORS VERSUS LAB REFERENCE MEASUREMENTS

Multiple approaches to metrics for analysis of this type of continuous sensor data were examined over the course of the program. Two approaches that were examined most closely were an EU-style CO_2-based Moving Average Window (MAW), and an Exponentially Weighted Moving Average (EWMA). The MAW approach analyzes emissions over a window of fixed engine CO_2 mass output that is moved through a data set in one second increments. The EWMA applies an exponentially weighted filter to a continuous data set as a smoothing function to extract information from the raw data set. Examples of the results from these analysis approaches are compared in Figure 7 showing a histogram of results for both metrics, and Figure 8 showing the overall distribution of NO_X results from both metrics. The EWMA does appear to generate a somewhat more consistent shape to the data set, showing what looks like a logarithmic distribution of results, with the majority at very low NO_X levels, with some periodic spikes to higher levels. The MAW shows a somewhat less organized histogram with less clear behavioral patterns. There are pros and cons to both methods which are discussed in more detail elsewhere in the report

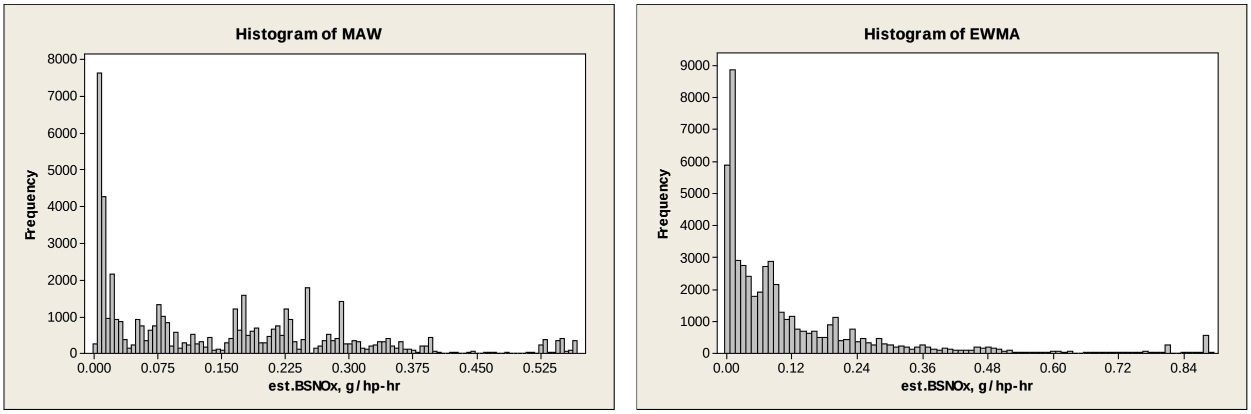

FIGURE 7. HISTOGRAMS OF IN-USE METRICS AT LOW NO_X LEVELS FOR VARIOUS DUTY CYCLES COMBINED

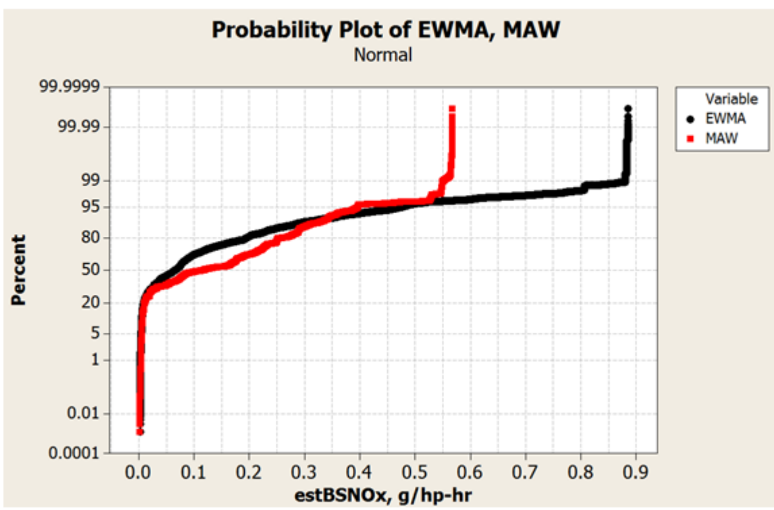

	estBSNOx, g/hp-hr	
Percentile	MAW	EWMA
5th	0.005	0.004
10th	0.006	0.005
50th	0.11	0.065
90th	0.33	0.32
95th	0.4	0.48
98th	0.55	0.8

FIGURE 8. DISTRIBUTION OF NO_X RESULTS FOR IN-USE METRICS AT LOW NO_X LEVELS

Whichever metric is ultimately selected, it will need to be paired to an appropriate compliance threshold value. This value might be a single threshold, or possibly a defined distribution that regulates, for example, both the 50^{th} and 95^{th} percentile of the overall distribution of results. It is recommended that more effort is needed to examine these and other metrics, and the implications of each approach. More effort is also needed to address NO_X sensor capability in this context.

Stage 1b Support Program

The Stage 2 program was supported by another program which was designed to answer durability questions left over from the Stage 1 program, as well as to provide a robust set of full-useful life Final Aged parts for the demonstration of the re-calibrated engine. This effort was called the Stage 1b program, and those results are summarized briefly here because several of those results were needed to support the Stage 2 data analysis. As part of this exercise, a new set of parts matching the original Stage 1 specifications was aged using an accelerated aging protocol based on the SwRI Diesel Accelerated Aftertreatment Aging Cycles (DAAAC) methodology. This method accounts for both thermal and chemical aging, and it was used in Stage 1b to age the aftertreatment to a simulated full useful life of 435,000 miles.

NO_X emission results for the Stage 1b program are shown below in Figure 9. The chart shows tailpipe NO_X emissions at various points along the Stage 1b aging exercise, including intermediate test points. The original Stage 1 data are also shown for comparison, although those results were compromised by a canning failure about 80% of the way through the aging process that disturbed the original experiment and left the questions which Stage 1b was designed to answer.

The Stage 1b results indicated that the final NO_X level that could be supported by the Stage 1 aftertreatment system design under "normal" aging was 0.023 g/hp-hr for the FTP cycle and 0.032 g/hp-hr for the RMC-SET cycle. A comparison to the Stage 1 results show that cold-start degradation between the two experiments was similar, but the system performance for the warmer hot-start and RMC-SET cycles was maintained much better, indicating that the failure did compromise performance on those cycles beyond normal degradation. These results essentially serve as the "final answer" with respect to the performance capability of the Stage 1-1b-2 system design approach.

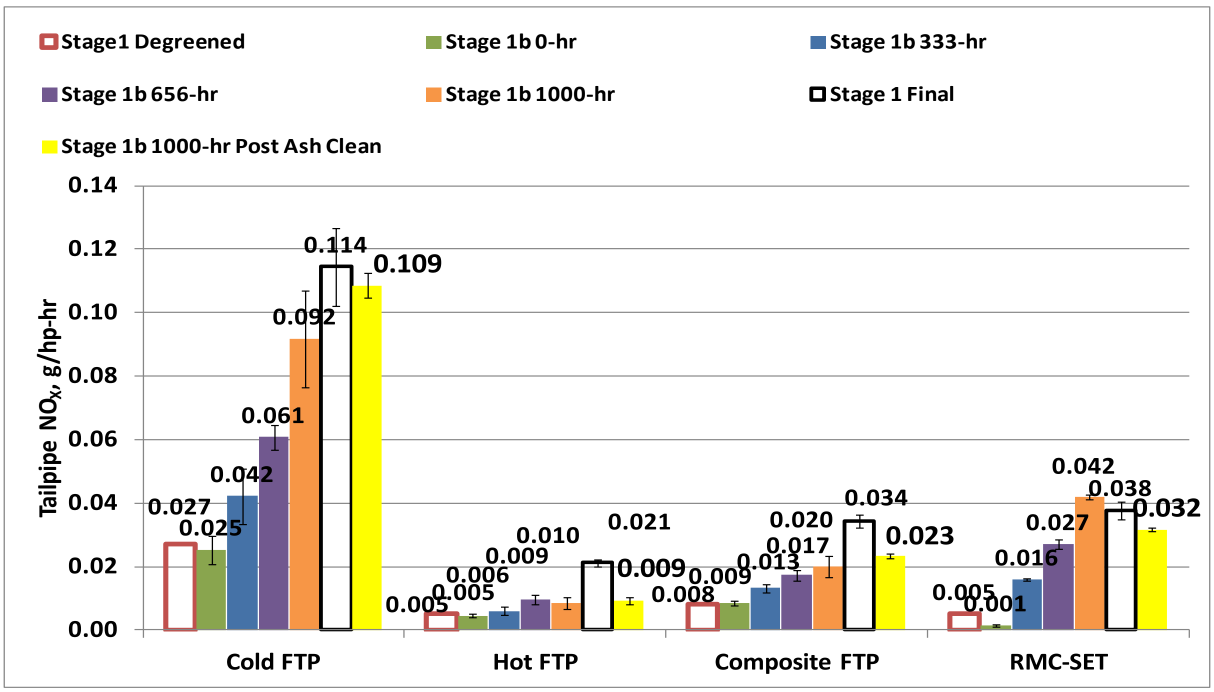

FIGURE 9. SUMMARY OF STAGE 1B NO_X RESULTS AT VARIOUS AGING POINTS

Taken as a whole, the Stage 2 program results, as supported by Stage 1b, provided a large body of information with respect to the potential for controlling tailpipe NO_X to Low NO_X levels on lower load duty cycles. The LLC developed in this program will help to ensure better emission control in these low-load operating regions in the future. The other Stage 2 program results provide additional information supporting that development of a robust NO_X standard covering all ranges of operation and including both laboratory testing and real-world in-use compliance.

1.0 INTRODUCTION AND BACKROUND

This report presents the description, results, and conclusions of a program conducted at Southwest Research Institute (SwRI) on behalf of, and sponsored by, the California Air Resources Board (CARB). The goal of this program was to examine the capability of advanced emission control systems to reduce emissions under Low-Load conditions that are typical of urban and vocational vehicle operation. This program follows directly from an earlier program entitled "Evaluating Technologies and Methods to Lower Nitrogen Oxide Emissions from Heavy-Duty Vehicles," also sponsored by CARB, which was completed in 2017. That earlier program is generally referred to as the Stage 1 CARB Low NO_X Program, and it involved demonstration of the feasibility of emission control technologies on both a Diesel-fueled engine and a Natural gas-fueled engine. The program detailed in this final report is referred to as Stage 2 of the CARB Low NO_X Program.

The Stage 2 program consisted of three primary tasks, with the overall goal of examining the capability of a Low NO_X emission control system at Low Loads. These three tasks were:

- The development of a new heavy-duty Low-Load Cycle (LLC) which could potentially be used as a new certification cycle in addition to the current FTP transient and RMC-SET steady-state cycles.

- Extension of the calibration of the Stage 1 Low NO_X Diesel engine test article to examine the capability of that system to control emissions under Low-Load conditions, including the new LLC developed in the first task.

- Examination of the accuracy of ECM broadcast torque and fuel rate measurements at low loads. This examination included analysis of other metrics for quantifying emissions at low loads. In order to support this alternate metric analysis, other ECM broadcast variables were also assessed for accuracy, as noted later.

The test article used for this program work was the Diesel heavy-duty Low NO_X engine system developed under the Stage 1 program. This engine was a modified 2014 Volvo MD13TC EU6 engine. Under the Stage 1 program, this engine was re-calibrated, and a new Low NO_X aftertreatment system was developed and calibrated for the updated engine. The Stage 1 engine is shown in Figure 10. The final Stage 1 Low NO_X aftertreatment system is shown in Figure 11.

It should be noted that the Stage 2 program was supported by an additional effort on this test article with additional funds provided by the South Coast Air Quality Management District (SCAQMD) and the Manufacturers of Emission Controls Association (MECA). This supplemental program is referred to as the Stage 1b program, and the objective of that program was to supply a robust set of Full Useful Life (FUL) aged aftertreatment parts for use with the Stage 2 effort. This was necessary due to a canning failure that occurred during the original Stage 1 aging effort (cite report and page number). This mechanical failure of a catalyst substrate mounting left the Stage 1 parts in a compromised state that was both unrepresentative in terms of performance, and fragile with respect to continued use. In addition, as part of the Stage 1b program, the engine baseline performance was re-checked, which also provided an opportunity to generate a baseline for the LLC. Because these results are relevant to the Stage 2 efforts that are being described in this report, a brief summary of the Stage 1b results is also included in this report.

FIGURE 10. STAGE 1 ENGINE – 2014 VOLVO MD13TC EU6 DIESEL ENGINE

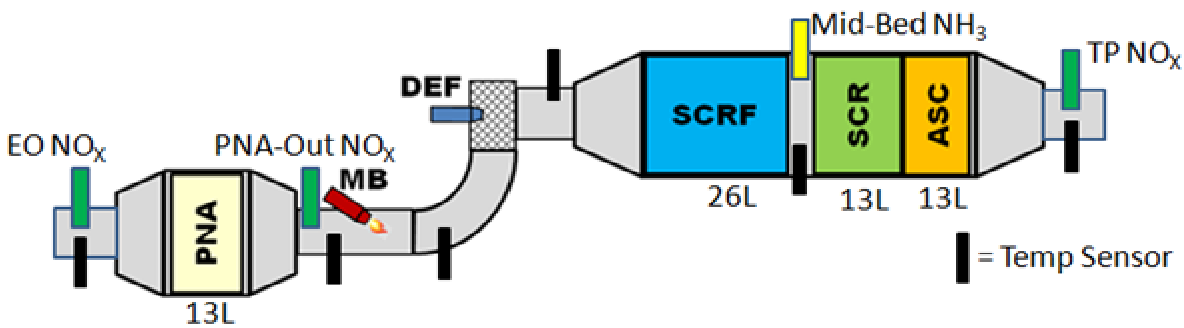

FIGURE 11. FINAL STAGE 1 LOW NO_X AFTERTREATMENT SYSTEM (ALSO USED FOR STAGE 2 PROGRAM)

2.0 LOW-LOAD CYCLE (LLC) DEVELOPMENT

The LLC was designed for potential use as an additional certification test cycle covering low-load engine operating regions that are not well represented by existing certification test cycles. The development of the LLC was done by leveraging data, tools, and expertise available at the National Renewable Energy Laboratory (NREL), which was engaged as a subcontractor on this effort, to quantify off-cycle low-load operating conditions characteristic of on-road heavy-duty vehicles.

The partnership with NREL provided access to several key resources that were utilized in the program. These included the FleetDNA database, which provided a major source of in-use data for the cycle development effort, and the High-Performance Computing resources that were applied to analyze the millions of miles of vehicle driving data that were examined in the making of the LLC. Additional data resources were also provided by CARB in the form of an additional set of in-use vehicle data which was generated by CE-CERT under a separate program.

The final output from NREL was a set of vehicle profiles which were representative of low-load operation. Each profile was a unique sample of actual in-use operation that had occurred on one of the vehicles in the source data set. These profiles served as the building blocks for the final LLC.

Having been recorded in the field, these profiles came in the form of vehicle-based data, whereas the final LLC needed to be in the form of an engine-based cycle. Therefore, it was necessary to translate the vehicle profiles into engine-based profiles that could be run on an engine dynamometer. SwRI utilized the EPA's Greenhouse Gas Emission Model (GEM) for this translation task, leveraging the ability of the GEM model to produce engine cycles from vehicle cycle data. These engine cycles were then normalized using the appropriate engine torque curve for each profile, resulting in a set of 10 normalized engine cycles that could be applied to any engine using the denormalization rules outlined in 40 CFR Part 1065.

The individual engine profiles were run on-engine to help determine the characteristics of each profile, and to assist in identifying the subset of profile data that would contribute to the final LLC. Key regions and challenges within the 10 final profiles were identified, and these operation segments were combined in different run orders to make a variety of different candidate Low-Load Cycles. The objective of this exercise was to identify the most efficient arrangement of the LLC that would present the desired series of representative operational challenges to the test engine in the minimum amount of time. The 10 individual profiles represented roughly 3.5 hours of driving, while the final combined LLC was a little over 90 minutes long.

Subsequent parts of this section of the report will provide more detail on the various steps in the cycle development process.

2.1 Source Data Description (NREL)

Two source data sets were used for this project, including Fleet DNA and CE-CERT data. Both data sets were collected from a variety of commercial vehicles operating in the field equipped with data recording devices to capture 1 Hz telematics and Controller Area Network (CAN) data.

Fleet DNA

In collaboration with fleet and industry partners across the country, the Commercial Vehicle Technologies team in NREL's Transportation and Hydrogen Systems Center focused on evaluating the real-world performance of alternative fuel and advanced vehicle technologies deployed in medium- and heavy-duty commercial fleets throughout the nation. The team has instrumented vehicles operating in the field with data recording devices to capture 1 Hz telematics and Controller Area Network (CAN) data. These data are then used to calculate in-use fuel economy and performance drive-cycle characterization and system-level duty-cycle analysis, which can be complemented by chassis dynamometer emissions and fuel economy data. These results are used to provide feedback to stakeholders such as fleets, technology providers, researchers, and government agencies, helping to inform and provide insight on the performance of advanced technologies and fuels operating under real-world conditions. The data for these evaluation projects is stored in the Fleet DNA database along with additional externally sourced data that have been supplied by Fleet DNA project partners. This online database and tool are available at http://www.nrel.gov/fleetdna. The Fleet DNA data used in this analysis included 666 unique vehicles located across the US, as illustrated in Figure 17. There was over 500 Gigabytes of raw data from 23 distinct locations, including 25 unique vocational designations, and 31 unique fleets. A summary of the number and types of vehicle included is shown in Table 1.

TABLE 1. FLEET DNA VEHICLE COUNTS BY VOCATION

Vocation	Number of Vehicles	Vocation	Number of Vehicles
Parcel Delivery	100	School Bus	11
Refuse Pickup	88	Snow Plow	9
Line Haul	73	Warehouse Delivery	9
Mass Transit	53	Dump Truck	7
Beverage Delivery	52	Refrigerated Truck	6
Food Delivery	52	Long Haul	6
Drayage	31	Local Delivery	4
Linen Delivery	30	Concrete	3
Transfer truck	29	Dry Van	3
Tanker	25	Bucket Truck	3
Utility	24	Delivery	1
Telecom	24	Regional Haul	1
Freight	22	**TOTAL**	**666**

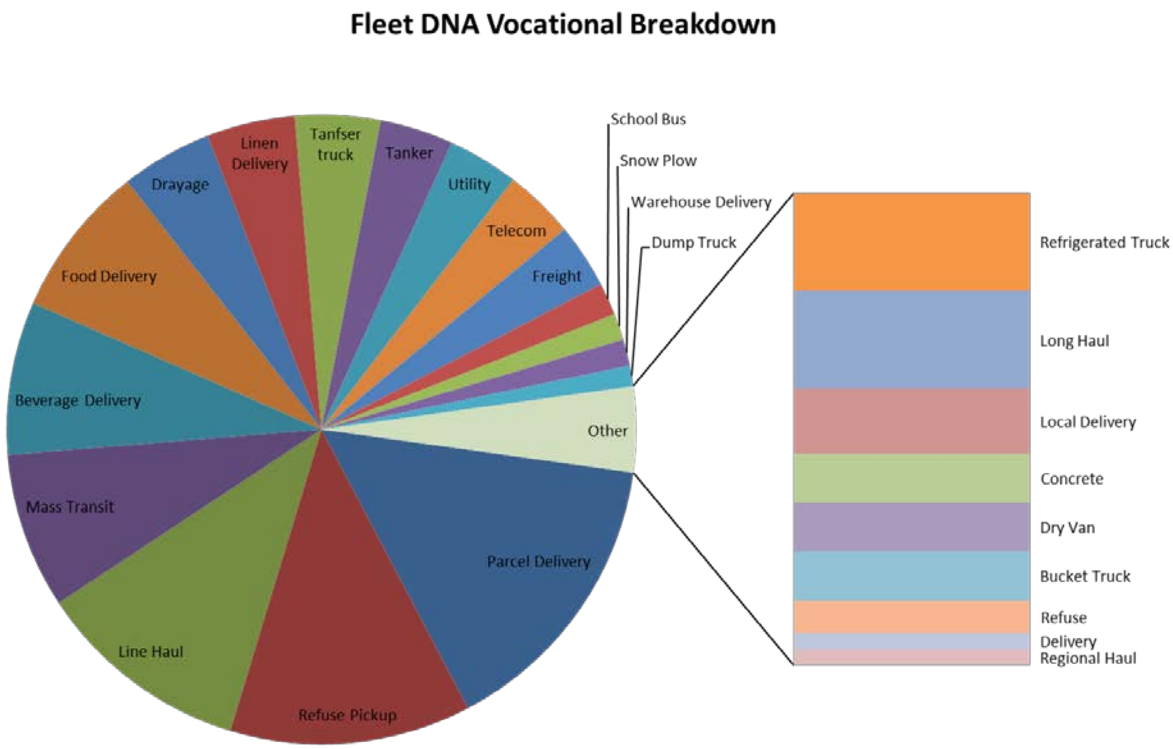

FIGURE 12. FLEET DNA VEHICLE VOCATIONS BY NUMBER OF VEHICLES

CE-CERT Data

In order to characterize the activity profiles of heavy-duty diesel vehicles in different types of vocations and identify the fraction of vehicle operations that SCR system may not function effectively, the CARB sponsored University of California at Riverside, College of Engineering – Center for Environmental Research and Technology (CE-CERT) to collect both vehicle and engine activity data from 90 heavy-duty vehicles operating in California, shown in Table 2. These vehicles consist of 18 different groups defined by a combination of vocational uses, gross vehicle weight rating (GVWR) and geographic region, as illustrated in Figure 13. Almost all the vehicles are of model year 2010 or newer and are equipped with SCR system. The collected data included vehicle position, speed and engine parameters. For more information about this database, please refer to the CE-CERT Technical Report for California Air Resources Board. Available at: http://ww3.arb.ca.gov/research/apr/past/13-301.pdf

TABLE 2. CE-CERT VEHICLE COUNTS BY VOCATION

Vocation	Number of Vehicles	Vocation	Number of Vehicles
Beverage distribution	13	Utility - Repair	5
Food distribution	8	Public - Towing	4
Agriculture - South CV	8	Public - County Work	3
Drayage - Southern California	7	Line haul - out of state	3
Construction - Heavy	6	Drayage - Northern California	3
Refuse	6	Urban diesel hybrid bus	3
Public - Freeway Work	5	Agriculture - North CV	2
Public - Sweeping	5	Construction - Small	2
Shuttle	5	Local household moving trucks	1
TOTAL			89

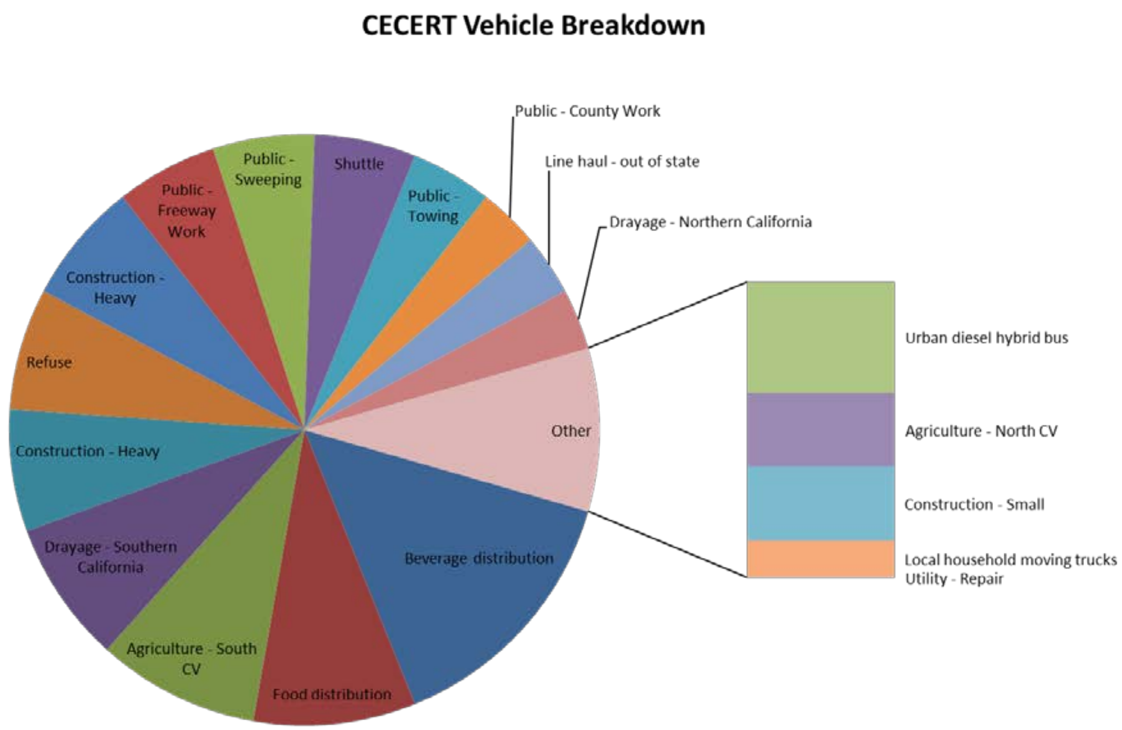

FIGURE 13. CE-CERT VEHICLE VOCATIONS BY NUMBER OF VEHICLES

2.2 Data Pre-Processing and Cleanup (NREL)

To account for the common errors associated with the analysis of GPS speed-time data, a common GPS data processing method has been developed that employs a series of linearly progressing logic-based data filters [4]. Both Fleet DNA and CE-CERT datasets were processed using standard Fleet DNA data filtration and interpolation scripts. The GPS data filtration approach consisted of six distinct filters to ensure consistent high-quality input data. The six-step filter to correct vehicle speed data includes:

1. Speed Limit filter - replaces data falling outside limits (default of 0 – 90 mph). Outlying data was removed and replaced with values interpolated based on neighbors.
2. Parked filter - replaces noisy GPS data captured from a parked car and replaces with zero speed. Specialized logic routines determine when a vehicle is parked
3. Dropout filter - replaces false zero speed records in data caused by signal dropout/poor signal quality. False zero data was removed and replaced with values interpolated based on neighbors.
4. Data Gap filter - improves data continuity and quality by filling in small gaps in data with interpolated values. If data gaps are large (>15 seconds) the filter routine ramps data to and from zero speed accordingly.
5. Acceleration filter - removes speed data that generates impossible accelerations (using constants determined based on generalized estimates for vehicle weight class and performance characteristics), replacing the data with interpolated results.
6. Smoothing filter - designed to remove signal noise from the repaired test data. Additionally, the smoothing filter provides a smooth driving trace that can used in repeat chassis dynamometer testing.

Figure 14 illustrates an example of the acceleration filter. Descriptions of the other filters may be found in the reference note earlier.[3]

[4] A. Duran, M. Earleywine. "GPS Data Filtration Method for Drive Cycle Analysis Applications.": 9 pp. 2013. https://www.nrel.gov/docs/fy13osti/53865.pdf.

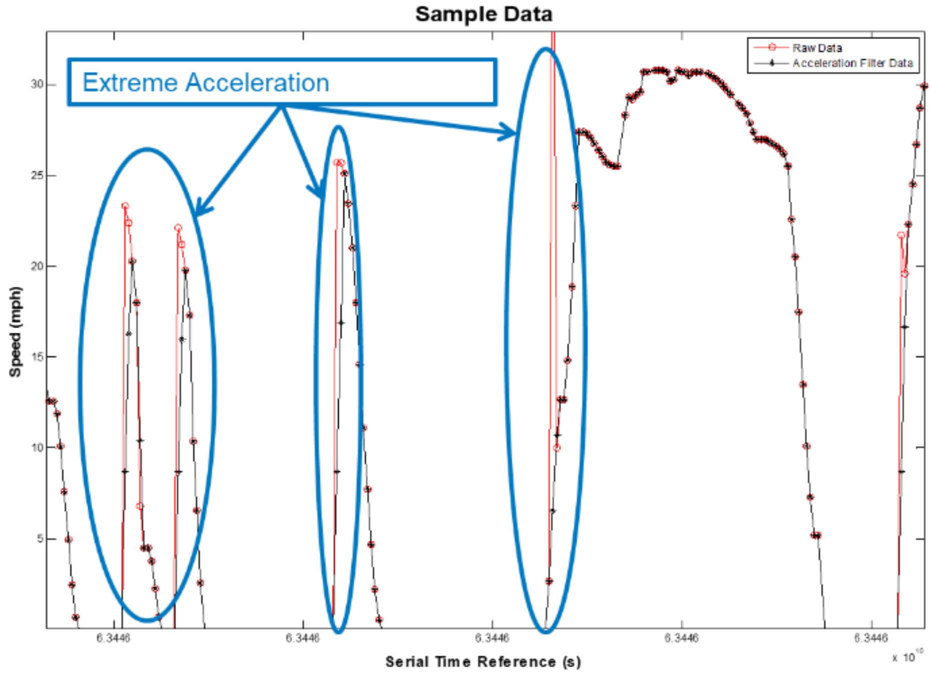

FIGURE 14. ILLUSTRATION OF ACCELERATION FILTER

2.3 Initial Analysis and Window Selection (NREL)

It was determined that a moving microtrip moving window analysis was the best approach for calculating the average load over a duty cycle. A microtrip is defined as the time elapsed from when the vehicle starts moving to the next stop. Figure 15 shows an illustration of a microtrip window with 5 micro-trip events. Each subsequent window is shifted by one microtrip and the average load over the microtrip window is recalculated. Next, we generated a frequency distribution of the average loads for and evaluated the impact of the microtrip window as shown in Figure 16.

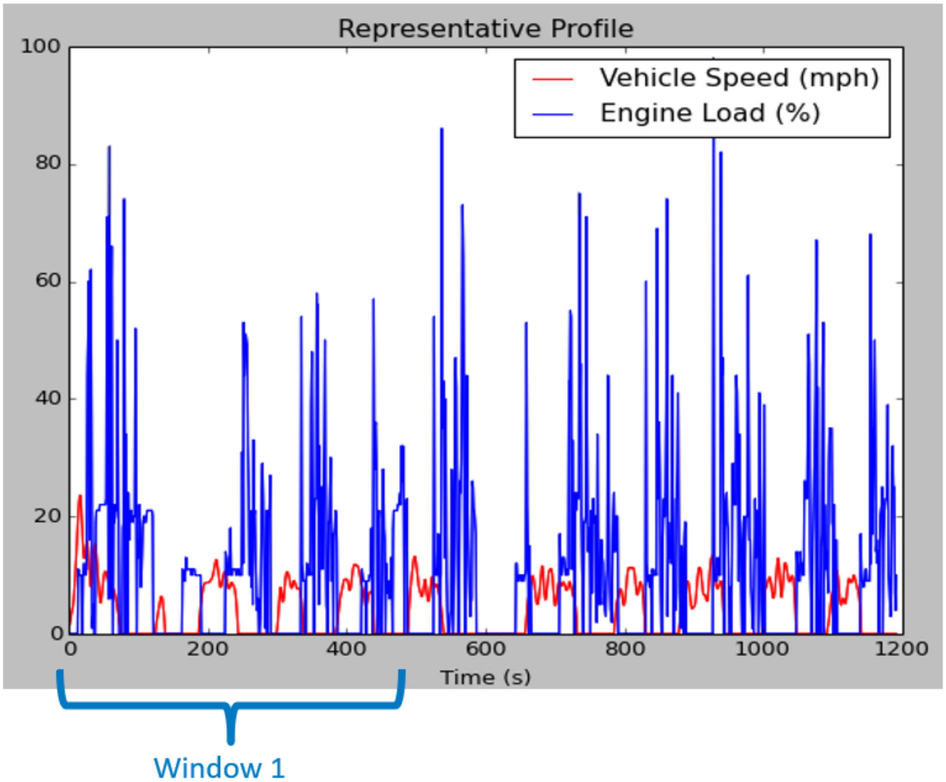

FIGURE 15. REPRESENTATIVE PROFILE WITH 5-MICROTRIP WINDOW

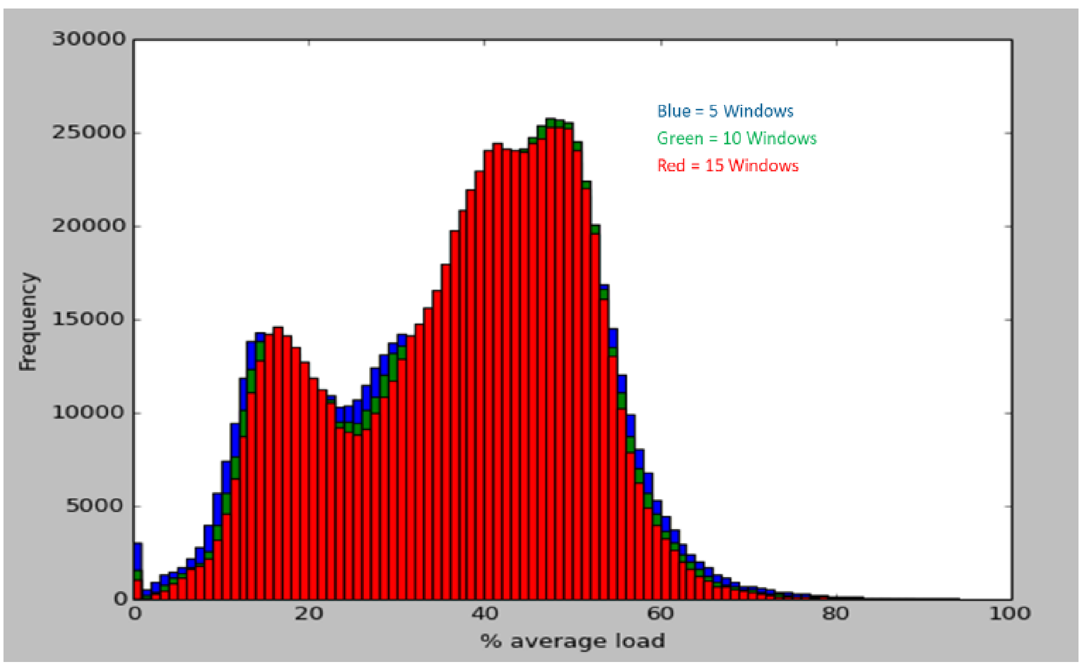

FIGURE 16. DISTRIBUTION OF % AVERAGE LOAD FOR 5, 10 AND 15 MICROTRIP WINDOWS

Increasing window size shifts distribution towards a normal distribution curve. Moving the distribution at the edges closer to the median of 40% load, the 10th percentile shifts from ~14.5% load up to 16.6%. Also note that the distribution is tri-modal in shape with two large primary peaks and a third lower power peak. The number of available microtrip windows decreases as the size of window expands.

2.4 Overall Distribution and Definition of the Low-Load Region (NREL and SwRI)

As noted earlier, the distribution of 10-microtrip windows in the combined data set was observed to have a tri-modal shape when examined over the full load range. With some initial input from EPA staff, analysis was conducted on the overall tri-modal shape to break that distribution down to a combination of three constituent single mode distributions. The result of this analysis is illustrated in Figure 17. In this case, the variable associated with Load is the CAN-recorded variable "Engine Percent Load at Current Speed" (J1939 SPN 92).

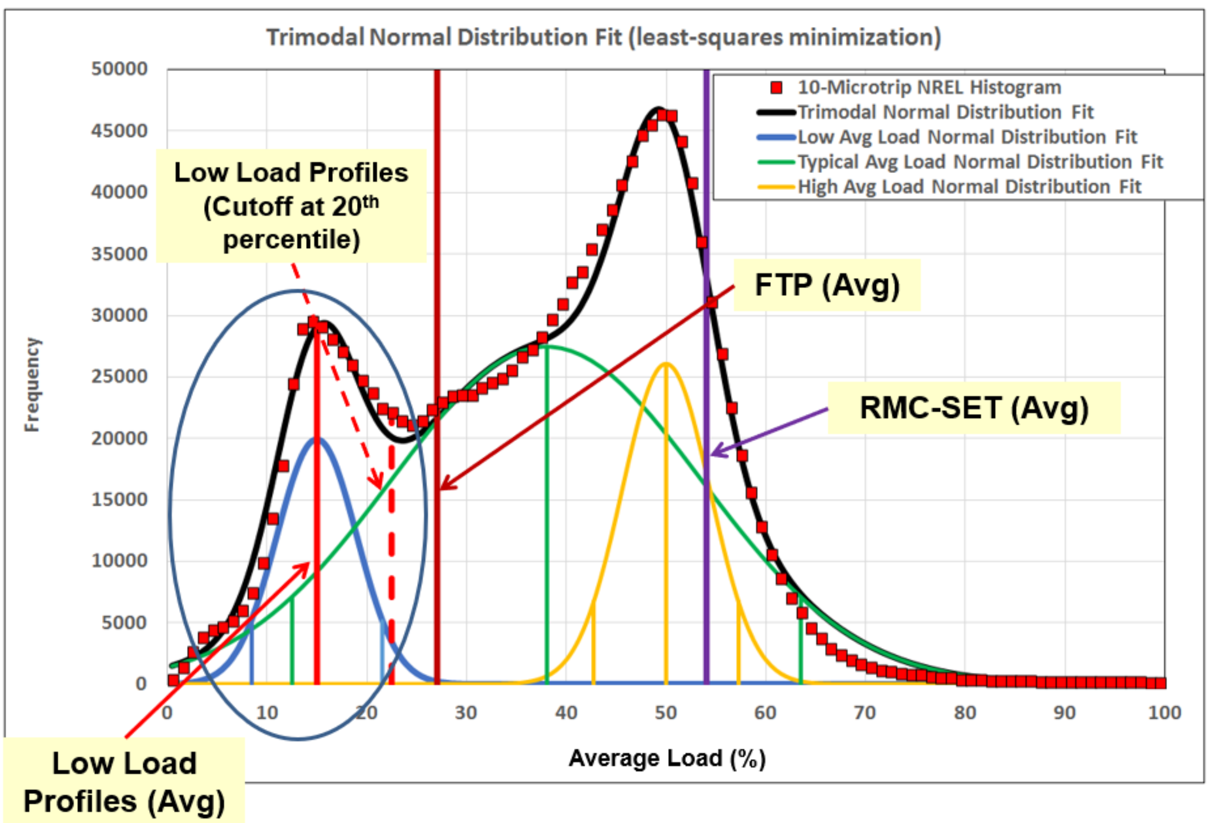

FIGURE 17. OVERALL DISTRIBUTION OF 10-MICROTRIP WINDOWS VS. WINDOW AVERAGE LOAD

In Figure 17, the three constituent distributions are labeled as Low-Load (blue), Typical Average Load (green), and High Load (yellow). For each constituent distribution, the 5th, 50th, and 95th percentiles are denoted as vertical lines. The average value for both the FTP and RMC-SET cycles are also illustrated in Figure 17. As shown in the figure, a significant portion of operation in the overall database occurs within this definition of the Low-Load region. The range of the Typical and High Load distributions is well represented by the FTP and RMC-SET, but the region around the Low-Load is well below even the FTP. It was determined that the windows in the region defined by the Low-Load distribution would serve as the source data set for the Low-Load cycle. The 95th percentile of this region is located at about 22% average load, and it also occurs at the 20th percentile of the overall distribution thus encompassing one fifth (1/5th) of the windows in the dataset. Therefore, that point was defined as the top end of the low-load operating region. As a result, of the 1.25 million windows in the full data set, the bottom 20 percent or about 250,000 windows were defined as the low-load operating region which would be analyzed via the subsequent clustering analysis. This low-load operating region was populated by windows contributed by each vocation represented in the data set with per-vehicle low-load window fractions ranging from 1% to 23% as shown in Figure 17.

2.5 Clustering Analysis (NREL)

NREL researchers utilized a set of metrics describing each drive cycle to define representative segments through clustering analysis. Clustering analysis is an analytical method where groups of data within a larger dataset are identified through statistical analysis using a handful of target metrics to judge for similarity. The metrics in this study were chosen given their role in previous NREL research to characterize engine load characteristics. Six primary metrics were chosen for the clustering analysis.

1. Average engine load
2. Maximum engine load
3. Median load
4. Standard deviation of engine load
5. Number of engine loading events per mile traveled
6. Loading ratio (ratio of increasing to decreasing loading rate time)

After exploring a range of clustering options, K-means clustering was applied to the combined Fleet DNA and CE-CERT Datasets. K-means was adopted over K-medoids[5] due to computational efficiency and removal of outliers during pre-processing. Quantitative approaches known as the “elbow” and variance analysis methods were compared for determining the optimal cluster number. The elbow method, illustrated in Figure 18, suggested three clusters. The elbow method looks for the point at which the slope of the relationship between variance and number of clusters flattens. The variance analysis approach, which looks for the point at which variance falls below a 10% variance threshold, suggested 12 optimal clusters. Final analysis of cluster composition results confirmed the elbow method findings of three primary clusters. When the large number of clusters suggested by the variance approach was used, many of the resulting clusters focused on just a few applications, and therefore they were not broad enough to be suitable for low load cycle development. The final three clusters suggested by the elbow method were found to contain a broad selection of vehicle applications. An example of this result is shown in Figure 19 for Cluster 1. Ideal representative cycles for each cluster were identified based on their relative “distance” or root mean square (RMS) error from cluster centroids.

[5] K-means and K-medoids refer to statistical partitioning techniques that clusters a data set of *n* objects into *k* clusters, with the number of clusters *k* presupposed. A medoid is the object of a cluster whose average dissimilarity to all the objects in the cluster is minimal (i.e. the most centrally located point in the cluster).

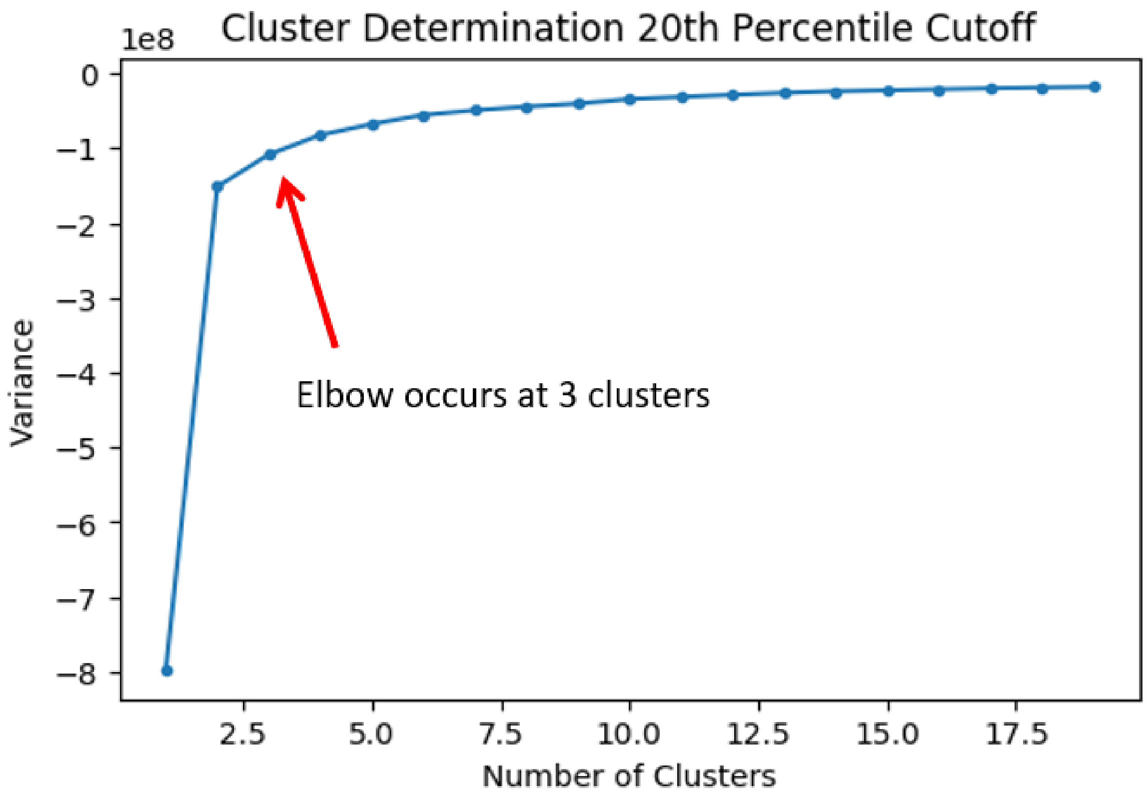

FIGURE 18. ELBOW METHOD FOR DETERMINING NUMBER OF CLUSTERS

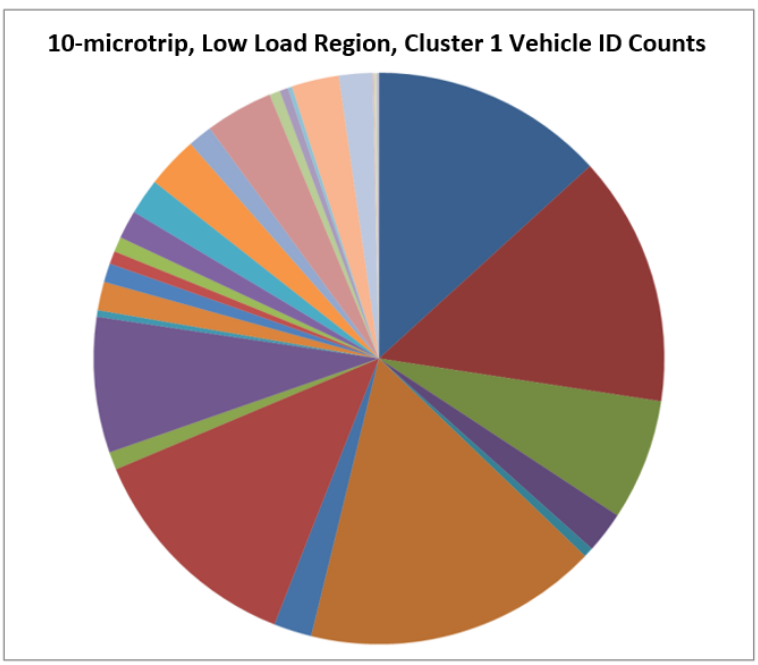

FIGURE 19. APPLICATION DISTRIBUTION FOR CLUSTER 1

The combined Fleet DNA and CE-CERT datasets were chosen for clustering analysis based on average load using the following criteria:

- 10 speed-time microtrip window sample size
- Average window engine load greater than 1% and less than 23% (corresponding to roughly lowest 20^{th} percentile of total population)

Over 220,000 sample windows were identified which met these criteria.

Figure 20 shows a three-dimensional representation of the clustered data on the axes of average engine load, number of load events per mile, and standard deviation of engine load percent. For visual clarity subsamples containing 250 points from each cluster are shown. Note that the actual clustering analysis was conducted in six dimensions.

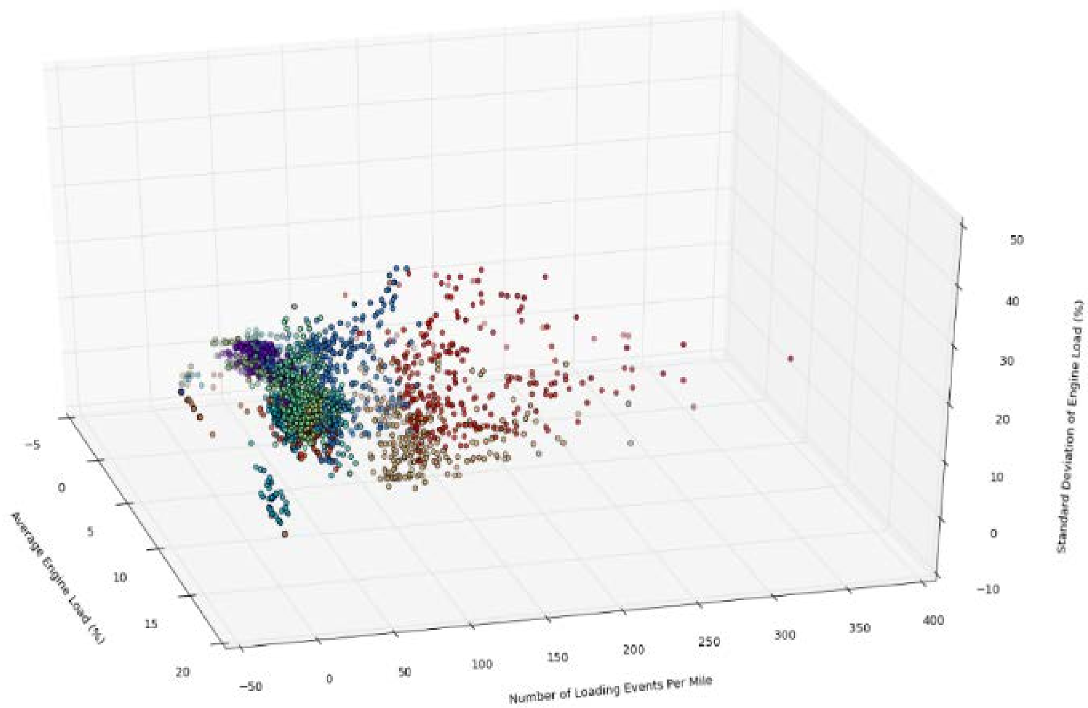

FIGURE 20. VISUALIZING CLUSTERS 3-DIMENSIONS – AVERAGE ENGINE LOAD (%), NUMBER OF LOADING EVENTS PER MILE, AND STANDARD DEVIATION OF ENGINE LOAD

2.6 Vehicle Profile Selection and Refinement (NREL)

To identify the most representative profiles, results from each cluster were ranked based on their distance to cluster center. Starting with profiles closest to cluster center, profiles were examined for behavior and final suitability for testing. Profiles with outlying behavior were removed from list, including:

o Extremely prolonged idle periods
o Long key-off periods during window
o Missing data

Ten candidate profiles were identified. The low-load profiles were categorized into three general operational modes, including:

1. Sustained light load
2. Low load to high load
3. High load to low load

Example profiles of each mode are shown in the graphs in Figure 21, Figure 22, and Figure 23, respectively.

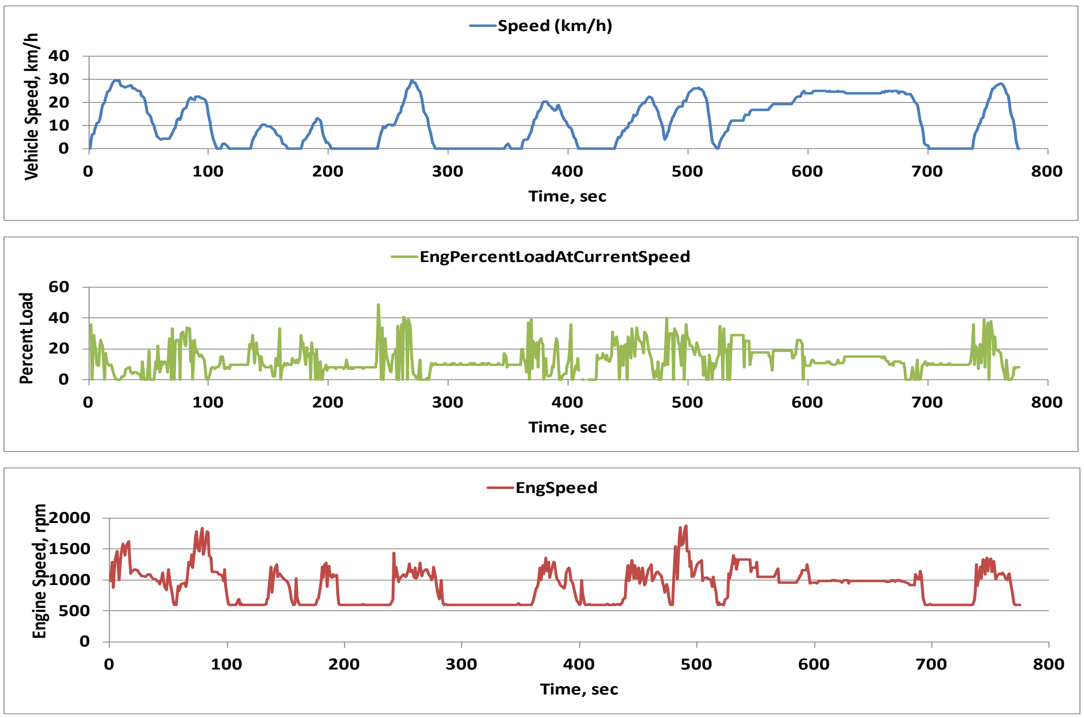

FIGURE 21. SUSTAINED LOW LOAD OPERATIONAL MODE

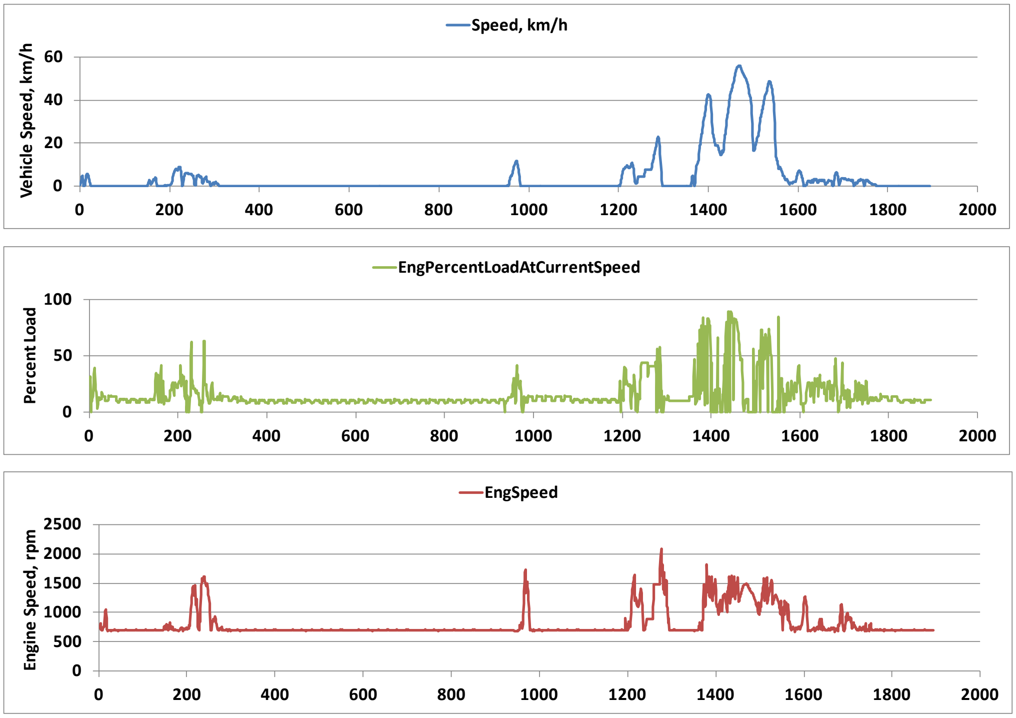

FIGURE 22. LOW LOAD TO HIGH LOAD OPERATIONAL MODE

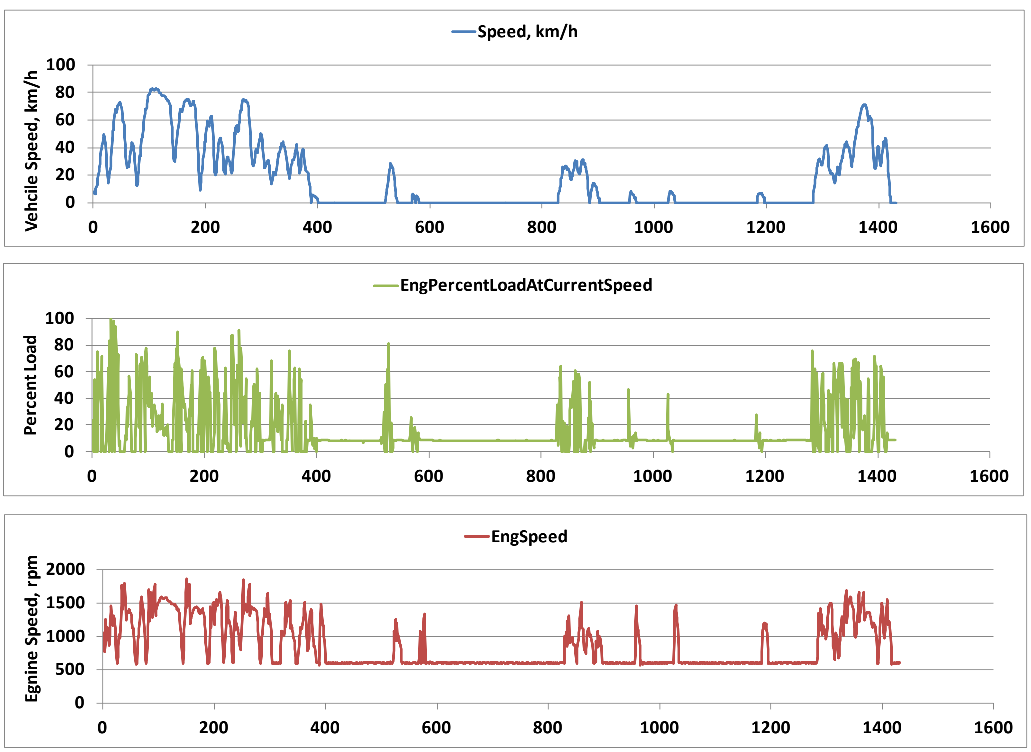

FIGURE 23. HIGH LOAD TO LOW LOAD OPERATIONAL MODE

Finally, a set of ten candidate profiles were provided to SwRI representing a range of vehicle vocations, weight classes, chassis manufacturers, and configurations. The ten profiles each fall in the range of 10 to 30 minutes in length and are summarized in Table 3.

TABLE 3. FINAL CANDIDATE LOW-LOAD PROFILES

Profile	Vehicle ID	Weight Class	Vocation	Chassis	Cluster ID	Profile Length (s)	Avg % Speed	Avg % Torque
1	v9892	8	Food Delivery	Volvo	0	800	26.9	6.9
2	v11660	8	Drayage	Mack	0	1295	21.4	6.6
3	v075	8	Drayage	Mack	0	1130	26.3	7.4
4	v11815	8	Transfer Truck	Volvo	1	1949	11.5	8.8
5	v11646	6	Parcel Delivery	Freightliner	1	904	15.9	10.7
6	v073	8	Drayage	Mack	1	1410	33.8	18.1
7	v9892	8	Food Delivery	Volvo	1	1616	27.0	10.6
8	v11660	8	Drayage	Mack	5	615	16.2	3.5
9	v11806	8	Transfer Truck	Peterbilt	5	1810	7.5	6.8
10	v11817	8	Transfer Truck	Peterbilt	5	739	15.3	7.7

2.7 GEM Translation (SwRI)

Once the final set of ten vehicle profiles had been selected, it was necessary to transform the vehicle-based profiles into engine-based cycles that could be run on an engine dynamometer. Although the vehicle profiles did have CAN broadcast torque data recorded with them, there was concern that this data was not always very accurate at low loads. Therefore, it was determined that vehicle modeling would be used to develop the engine speed and torque traces for the final cycles. This data could be checked against the recorded CAN data to ensure that the overall work performed over the profile was a reasonable match to what was observed in the field.

As for the modeling tool, SwRI elected to use the EPA GEM model. The GEM model is publicly available and well documented for regulatory purposes. It is also already designed to produce drive cycles suitable for engine dynamometer testing as an output. However, in order to support this task, several modifications needed to be made to GEM.

Normally, the GEM code contains only the three standard Phase 2 drive cycles. However, SwRI modified the code to allow the input of other, custom drive cycles. In addition, the allowable range of vehicle weight modifications was expanded to allow the simulation of a wider variety of vehicle masses, so as to allow for a better match with field conditions for some of the profiles. Vehicle model inputs were determined based on actual vehicle configurations recorded in the NREL database for each vehicle. However, these inputs were also cross checked using the VIN number information for the vehicles. Recorded transmission information was used to set up appropriate transmission input files based on published gear ratios for the different models and types.

The GEM configurations for each profile are summarized in Table 4. Note that some profiles required more than one test weight to rationalize the observed behavior as would be expected at certain points throughout a workday for a truck picking up or delivering cargo for example. The task of selecting the 20% of vehicle activity windows at the lower end of the load distribution can result in focusing on vehicle operation and real configurations or test weights that do not in some cases look like typical GEM default vehicle configurations, but note that the real world activity profiles they arise from were selected based on the representativeness of their engine loading within the three low-load activity clusters identified. The specific arrangement of test weight, vehicle configuration and grade that collectively give rise to the engine loading pattern in any specific vehicle activity profile is of less importance that the representativeness of that engine loading pattern within the cluster it is chosen from.

TABLE 4. GEM INPUT CONFIGURATIONS FOR LOW LOAD PROFILES

Vehicle	Profile	Config #	Regulatory Subcategory	Engine File	Transmission File	Drive Axle Config	Drive Axle Ratio	Aerodynamic Drag Coeff	Weight Reduction lbs	Default Weight lbs	Simulation Weight lbs	Net Alititude Change meters	Grade Pattern	Grade Adjustment
Used in Final LLC														
v9892	v9892_0	1	C8_DC_HR	v9892_D13.csv	v9892_AT2612D.csv	4x2	2.8	7.5	53995	69000	33003	-5	varying up and down	smoothed
v075	v075_1	2	C8_DC_HR	v075_MP8-415C.csv	v075_FRO-16210B.csv	6x4	3.55	7.5	45000	69000	39000	-3	varying up and down	none
v11660	v11660_5	3	C8_DC_HR	v11660_MP8-415C.csv	v11660-RTLO.csv	6x4	4.2	7.5	64000	69000	26333	-22	downhill	altered
v073	v073_1	5	C8_DC_HR	v073_MP8-415C.csv	v073-FRO016210B.csv	6x4	3.55	7.5	53995	69000	33003	-10	varying up and down	smoothed
v9892	v9892_1	1	C8_DC_HR	v9892_D13.csv	v9892_AT2612D.csv	4x2	2.8	7.5	53995	69000	33003	3	varying up and down	smoothed
v11806	v11806_5	1	C8_SC_HR	v11806_ISX.csv	V11806_LAS10C0D	6x4	3.7	10	2250	70500	69000	-1	varying up and down	none
Not Used in Final LLC														
v11815	v11815_1	1	C8_DC_HR	v11815_ISX.csv	v11815_RTLO.csv	6x4	3.11	10	53995	69000	33003	-52	downhill then flat	none
		2	same specs but heavier test weight after long idle segment - load attached during dwell						0	69000	69000	9	uphill	none
v11817	v11817_1	1	C8_DC_HR	v11817_ISM.csv	v11817_RTO.csv	6x4	3.67	7.5	0	69000	69000	-0.5	flat	none
v11646	v11646_1	1	LHD_U	v11646_ISB.csv	v11646_1000HS.csv	4x2	4.16	3.4	9990	16001	9341	0	flat	none
v11660	v11660_0	1	C8_DC_HR	v11660_MP8-415C.csv	v11660-RTLO.csv	6x4	4.2	7.5	64000	69000	26333	15	varying up and down	smoothed

Engine torque curves were determined from analyses conducted by NREL and supplemented by published torque curve data for the engines. Motoring torque curves were determined based on analysis of data from matching engines run at SwRI in non-proprietary data sets.

Where possible, the initially recorded grade data was utilized, although a grade smoothing algorithm was utilized to eliminate areas of excessive noise in the supplied grade data. Vehicle mass was not specified in the database, so a series of model runs at different masses was generally used to select a final vehicle mass for a given profile. Where necessary, grade profiles were sometimes modified to obtain a reasonable match between the model output work and the reference work predicted from the recorded CAN data, although a significant modification was required in only the case of v11660_cluster 5. Model output results were compared to the recorded data on the basis of cumulative work over the profile. The target was to match the accumulated work within 5%. In addition, it was desired that the general pattern of work accumulation over the course of the profile should match between the model output and the field data. An example of this comparison is shown in Figure 24 for one of the profiles.

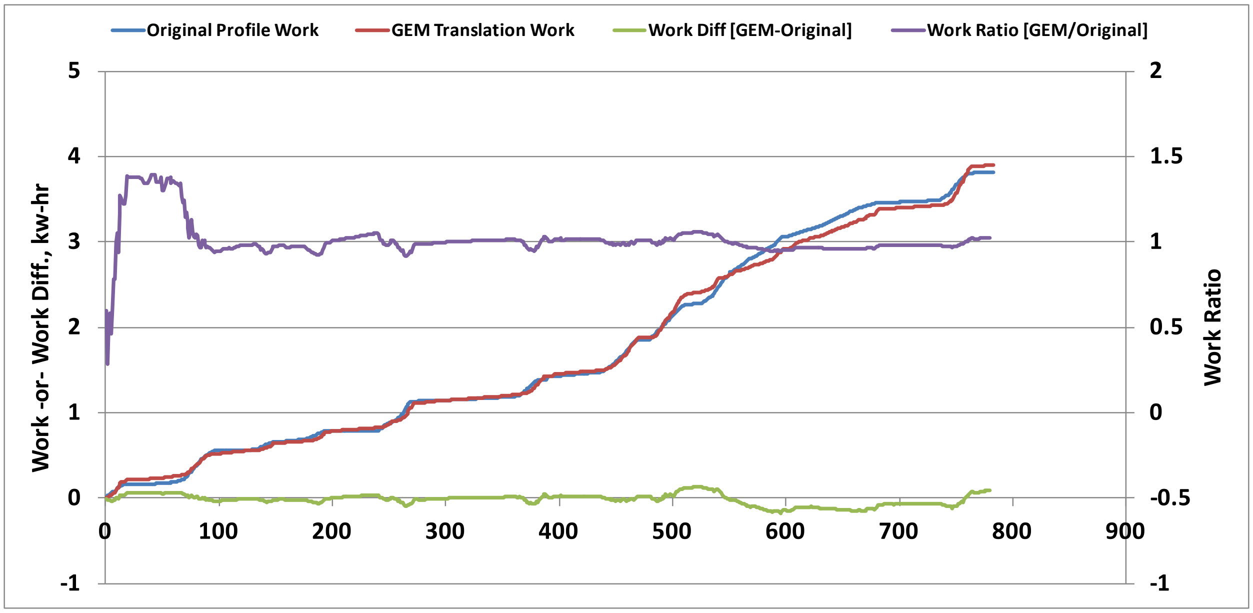

FIGURE 24. EXAMPLE OF GEM TRANSLATION QA FOR PROFILE V9892 CLUSTER 0

A second example is shown in Figure 25, along with an illustration of second-by-second power from both the recorded data and the GEM model output in Figure 26. It was not possible to match the field recorded data precisely on an instantaneous basis, but the data shows that the engine loading generally followed a similar profile between the two. This process was iterated as a function of vehicle mass and grade until an acceptable match was obtained.

When a given GEM profile translation was completed the profile was then normalized using the torque curve for that given engine. The normalization process was essentially the reverse of the equations in 40 CFR 1065 as follows:

$$\%\,Speed_i = \frac{(Speed_i - Idle\ Speed)}{(Max\ Test\ Speed - Idle\ Speed)} \times 100$$

$$\%\,Torque_i = \frac{Torque_i}{Max\ Torque\ at\ Speed_i} \times 100$$

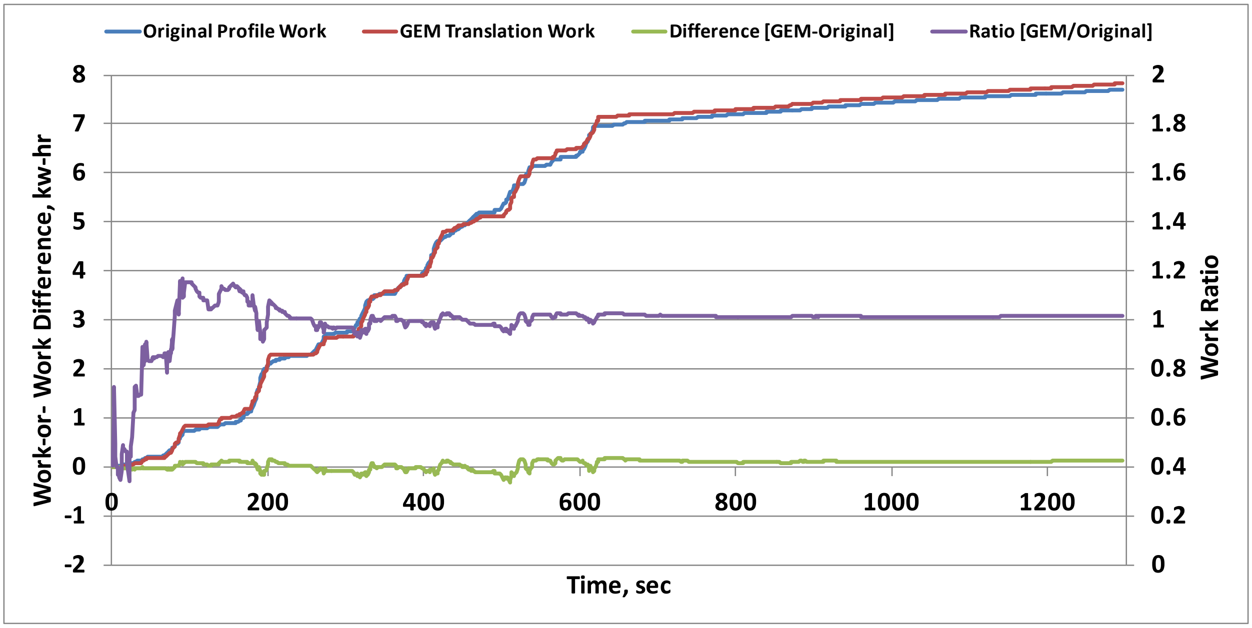

FIGURE 25. EXAMPLE OF GEM TRANSLATION QA FOR V11660 CLUSTER 0

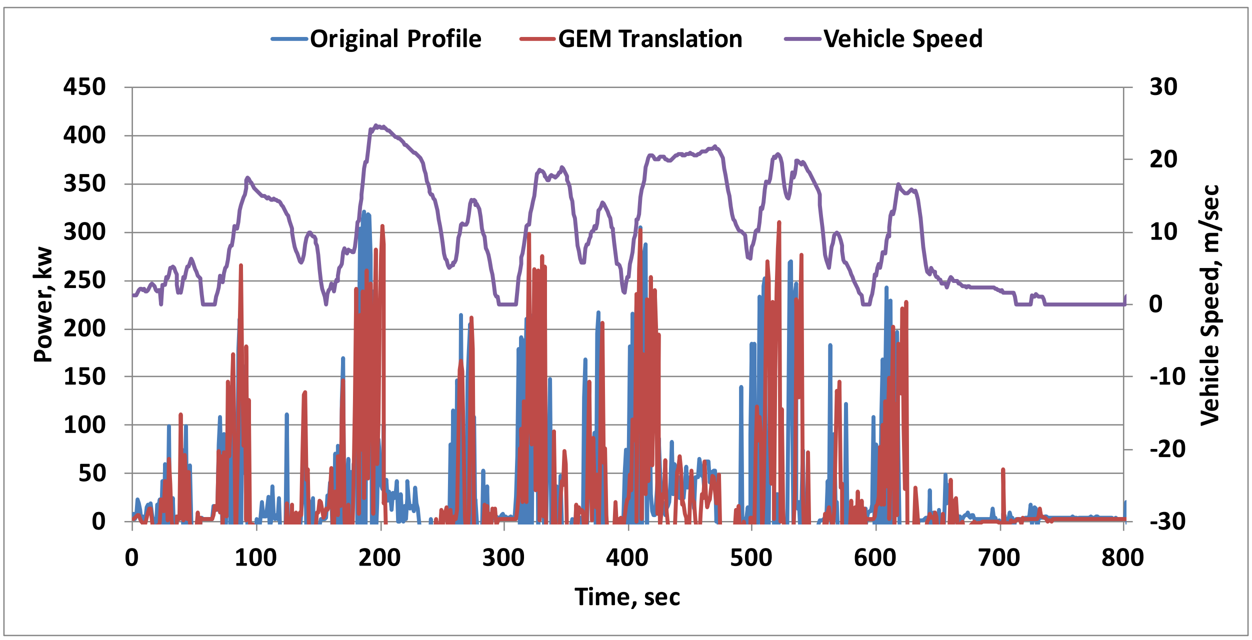

FIGURE 26. CONTINUOUS POWER DATA COMPARISON FOR V11660 CLUSTER 0

An example of an initial vehicle profile and the corresponding final normalized engine cycle for that profile is given in Figure 27 and Figure 28, respectively. This example is for vehicle 9892 cluster 0, which was a Class 8 4x2 chassis in a Food Delivery application, powered by a Volvo D13 405 hp engine, and having a 12-speed AMT transmission. This profile covered 2.5 kilometers at an average speed of 11 km/hr (or 16 km/hr counting only the portions of the profile where the vehicle was moving).

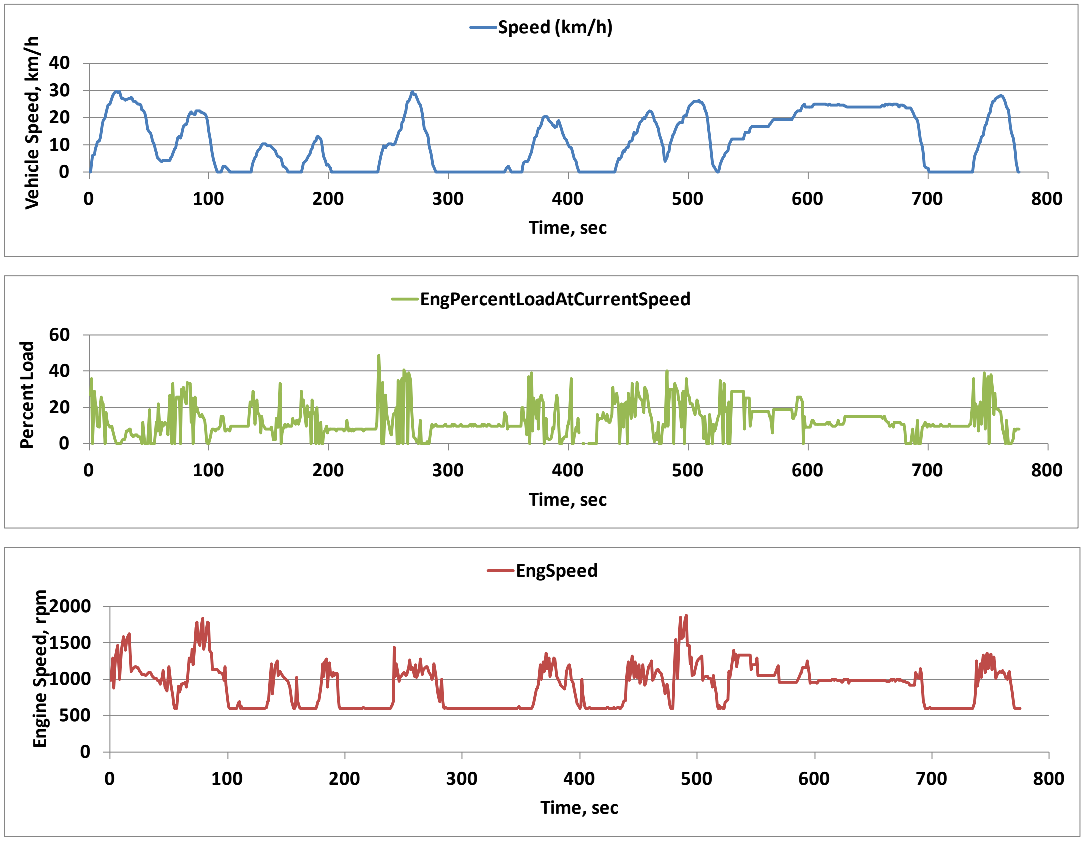

FIGURE 27. VEHICLE PROFILE FOR V9892 CLUSTER 0

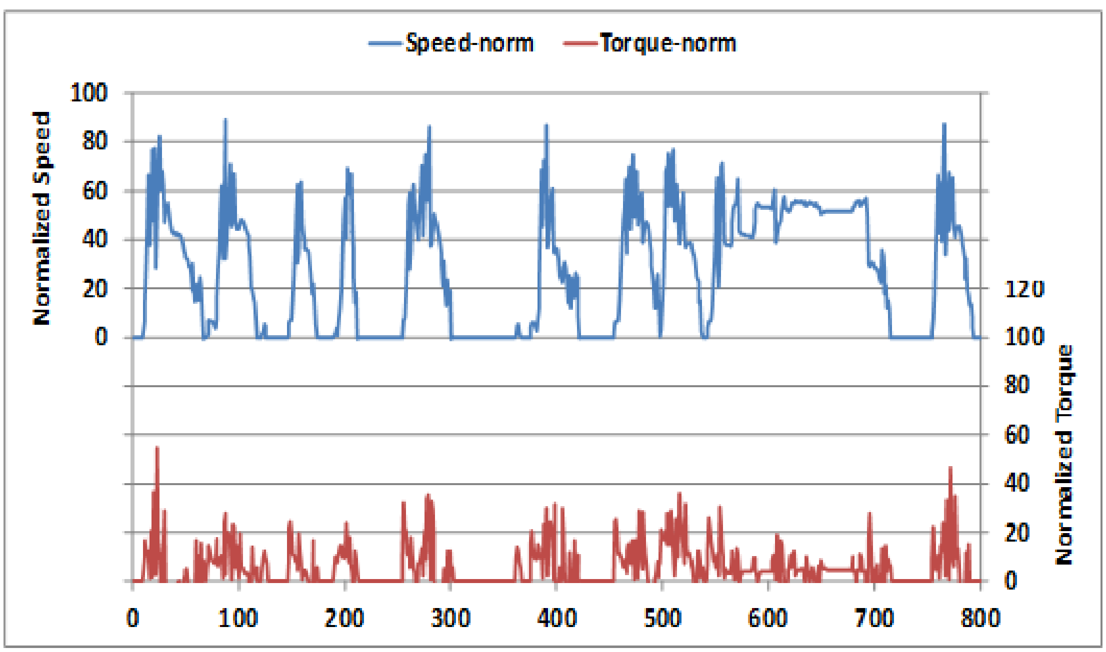

FIGURE 28. FINAL NORMALIZED ENGINE CYCLE FOR V9892 CLUSTER 0

These corresponding data sets are shown in Appendix A for all ten of the final vehicle profiles. Summary statistics for all ten of the profiles are given below in Table 5. These statistics are based on de-normalized values for one of the test engines used to run and evaluate the profiles. It should be noted that these values can be influenced somewhat by the shape of an individual engine torque curve, but these are generally representative for a Class 8 Line Haul Tractor engine.

TABLE 5. SUMMARY STATISTICS FOR FINAL TEN VEHICLE PROFILES

Profile	Average Power	Average non Motor Power	Average non Idle non Motor Power	Average non Idle Power	% Idle	Average Speed	Average Non Idle Speed	% Motor	Work, hp-hr	% FTP Work
v9892 cluster 0	5%	5%	8%	7%	31%	27%	38%	15%	4.2	12%
v11660 cluster 0	5%	6%	11%	9%	43%	21%	37%	25%	7.9	22%
v075 cluster 0	5%	6%	9%	7%	30%	26%	37%	19%	6.8	19%
v11815 cluster 1	6%	7%	17%	16%	62%	11%	30%	9%	12.9	37%
v11646 cluster 1	7%	8%	16%	15%	50%	16%	32%	16%	7.3	21%
v073 cluster 1	13%	14%	16%	15%	10%	33%	37%	28%	20.2	57%
v9892 cluster 1	8%	9%	14%	13%	34%	27%	40%	18%	14.9	43%
v11660 cluster 5	2%	3%	6%	5%	53%	16%	34%	15%	1.7	5%
v11806 cluster 5	4%	4%	12%	11%	66%	7%	22%	5%	7.1	20%
v11817 cluster 5	4%	4%	9%	8%	51%	15%	31%	8%	3.3	9%
FTP	21%	22%	32%	31%	32%	37%	54%	18%	35.1	n/a
Power is given as % of Engine Max Power										
Speed is given as 1065 % Speed (Idle-to-MTS)										
% Idle/Motor is idle/motor seconds versus total cycle seconds										

2.7.1 Note on Accessory Load at Idle

One issue that needs to be addressed arises from the normalization process that was used for the treatment of accessory loads, specifically at idle. It should be noted that all of the real-world vehicle profiles displayed a certain amount of accessory load at idle, as was appropriate for the manner in which the vehicle was configured. However, when an engine is configured in a dynamometer test cell for emissions certification testing, these loads are generally not represented, apart from those necessary to run the engine (such as the water pump, etc.). The GEM modeling process accounts for these real-world accessory loads in the output cycles it produces by included a fixed amount of power depending on the class of the vehicle being modeled. Those loads are 3.5 kw for a Heavy Heavy-Duty Engine, 2.5 kw for a Medium Heavy-Duty engine, and 1.5 kw for a Light Heavy-Duty Engine, respectively. The GEM output cycles for the various profiles included these loads.

However, in the process of normalizing these profiles to allow for later 1065 de-normalization, the idle points were defined as zero percent speed and zero percent load. If these cycles are later de-normalized using the standard 1065 rules, the idle load will be set to 0 for both a manual transmission (MT) or automated manual transmission (AMT), or to Curb Idle Transmission Torque (CITT) for an automatic transmission (AT) to simulate the torque converter. This interaction will have the effect of removing the accessory load at idle. This will result in engines being run with a load that is unrepresentative of field operations. While this issue may not be significant on other duty cycles, the low load nature of the LLC means that this is a more significant change of load on that cycle.

It is felt that maintaining a representative load on the engine at idle will be influential in the technology and calibration choices made to maintain aftertreatment system functionality under these low load conditions, and idle is a significant contributor to the LLC. For example, there are several thermal management levers that will react differently with as little as 0.25 or 0.5 bar BMEP of additional load at idle. It is important for the LLC to encourage the use of approaches that will be effective in real world operation, rather than only over the test cycle. Therefore, SwRI recommends that the accessory load should be added to the idle points of the LLC (i.e., any points with a normalized speed and torque of 0 percent). In the case of an automatic transmission application, this load would be added to any CITT that is already applied. In an engine test cell, these loads can be applied using the same dynamometer modes that are normally used to apply a CITT.

It is recommended that these loads should be consistent with the loads used by GEM for the different vehicle classes, as appropriate for the engine being tested. A target torque appropriate for the idle speed (zero percent speed) that is used by the engine should be calculated to produce the appropriate power level for the vehicle class (e.g., 3.5 kw for Heavy Heavy-Duty, and so on).

2.8 Engine Testing of Profiles and Results

The final set of ten normalized engine profiles was tested on several different engines available at SwRI to examine the characteristics of each profile, and to get a sense for the kinds of low-load challenges contained with each profile. It was also necessary to test each profile to ensure that the final engine profiles represented something that could be run properly on a dynamometer within the cycle validation criteria given in 40 CFR 1065.514. It should be noted that at the time these profiles were run, the question of idle accessory load had not yet been decided, therefore for manual transmission engines, a zero torque was applied at idle which could be taken as a worst case emissions control challenge of the possible range of idle loads.

The profiles were tested in sets of either three or four repeats, depending on the length of the profile. The repeats were arranged head to tail as a single run. Initially, each profile was run after each of two different kinds of preconditioning:

- One FTP transient cycle followed by a shut down and 10-minute engine off soak with the cycle beginning with engine start after the soak period. This approach generally resulted in the cycle starting with some residual stored heat.

- One FTP transient cycle followed by a 20-minute idle period, with the cycle started while the engine was still running directly following the idle period. This approach generally resulted in the cycle starting at a temperature below the normal level for that duty cycle.

The successive repeat cycles were run in order to allow the engine and aftertreatment to reach thermal equilibrium with the profile that was being run. The two different approaches to preconditioning were designed to examine how much the preconditioning impacted the system behavior, and how long it took for a given profile to reach thermal equilibrium with the given duty cycle. Following some of the initial data runs on some of the profiles, it was found that little additional information was gained from running both kinds of preconditioning on every profile, and therefore only the first preconditioning approach was continued for all tests. In general, thermal equilibrium was generally reached before the end of the first profile repeat in all cases.

In all cases, the preconditioning started with an FTP cycle warm-up, because the target for the LLC was generally warmed up engine operation at low load. The aftertreatment system might or might not be warm prior to the cycle, but it was desired that the engine should be fully warmed up (i.e., thermostat fully open). It was not as pressing to include cold-start in the scope of the LLC because cold-start operations are already regulated via the FTP.

An example of this testing process is illustrated in Figure 29 for testing after the FTP and hot-soak, and Figure 30 for testing after the FTP and 20-min idle period. As can be seen in comparing the two charts, there is some initial difference in temperature and performance due to the different preconditioning. However, that difference is essentially washed out before the end of the first repeat of the profile, and aftertreatment performance appears to be identical after about 300 seconds. From that point forward the two cycle runs are virtually identical.

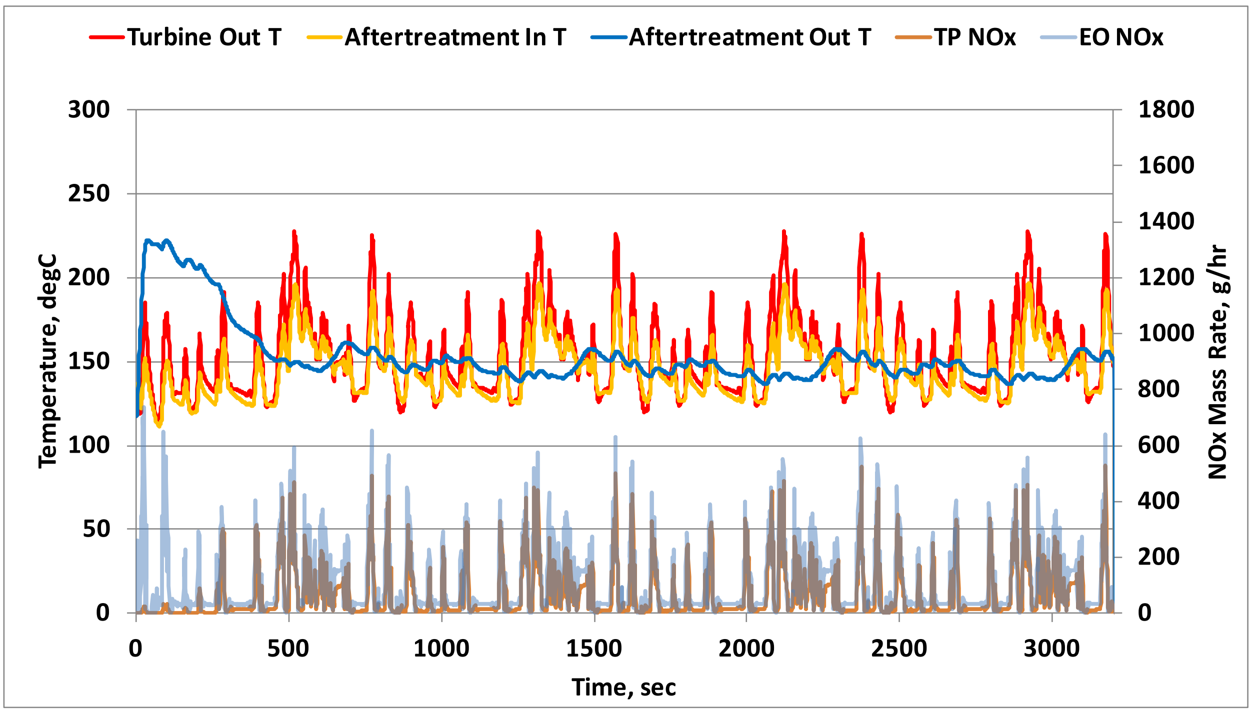

FIGURE 29. ENGINE TEST DATA FOR V9892 CLUSTER 0 – FOUR REPEATS FOLLOWING FTP AND 10-MINUTE SOAK

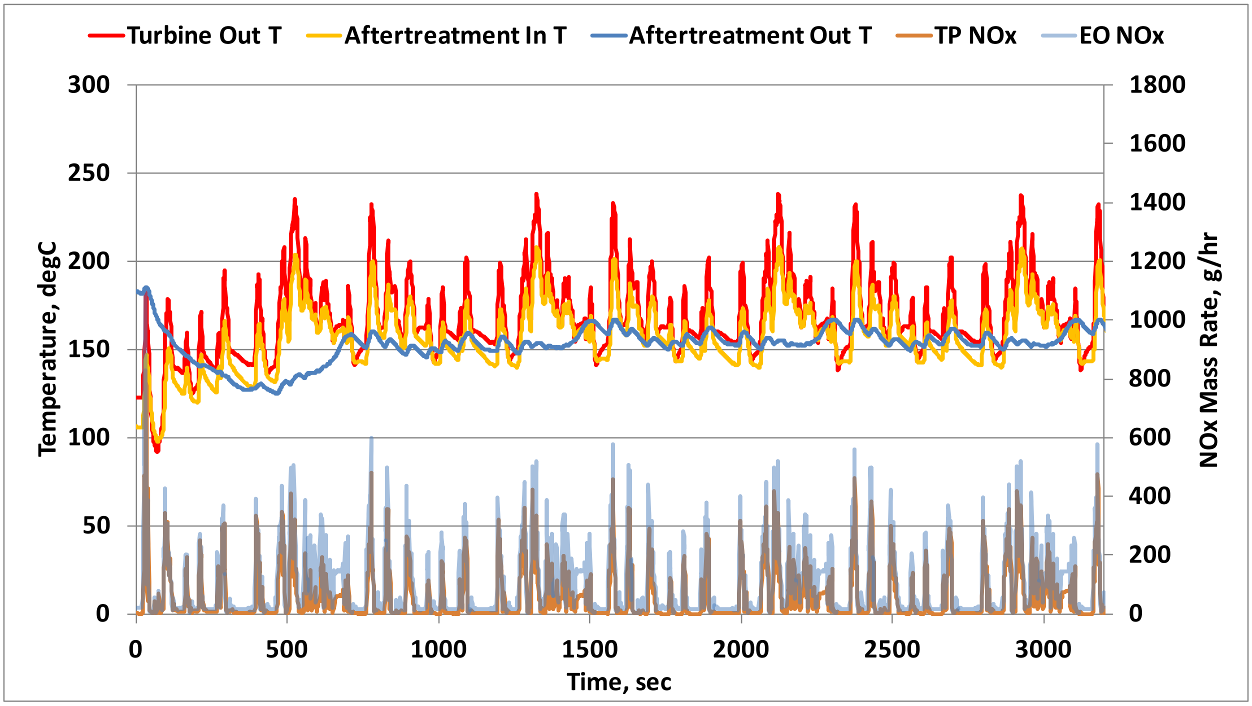

FIGURE 30. ENGINE TEST DATA FOR V9892 CLUSTER 0 – FOUR REPEATS FOLLOWING FTP AND 20-MINUTE IDLE PERIOD

This particular set of tests represented a good example of a sustained low-load challenge, wherein the engine is in a relatively stable period of low-load operation, neither increasing nor decreasing over the course of the profile. Aftertreatment temperatures generally hovered between 150 °C and 200 °C at equilibrium, with the outlet temperature generally staying around 150 °C. For this particular engine, NO_X reduction performance was relatively poor over this profile, generally averaging about 33% NO_X conversion efficiency.

All ten of the profiles were tested in this manner, and a summary of the results is given below. Detailed results for the profile tests are given in Appendix B. The profiles were then classified in terms of the types of low-load challenges that each of them included, and results of that classification process are given in Table 6. As seen in the table, there is some duplication in types of challenges among the profiles. As a result, only a subset of the profiles was actually selected for use in the final LLC. Those final building block profiles are summarized below in Table 6.

TABLE 6. PROFILES CLASSIFIED BY TYPES OF LOW-LOAD CHALLENGE

Type of Low Load Challenge	Profiles
Sustained Low Load – 5-6% Average Power	v9892 cluster 0 v075 cluster 0
Sustained Low Load – 2-4% Average Power	v11660 cluster 5 v11817 cluster 5
High-to-Low – Long Idle	11815 cluster 1 11806 cluster 5
High-to-Low – Motoring and Short Idle	v9892 cluster 1 v11660 cluster 0
Low-to-High – Return to Service Breakthrough	v9892 cluster 1 v073 cluster 1 v11806 cluster 5
Mid-Speed Cruise-Motoring	v073 cluster 1

TABLE 7. SUBSET OF PROFILES SELECTED FOR LLC USE

Profile	Vehicle	Cluster	Length	Avg % Speed	Avg % Torque	Repeats in SwRI Test Runs	Class	Chassis	Engine	Trans	Gears	Vocation
1	v9892	0	800	26.9	6.9	4	8	4x2	Volvo D13	AMT	12	Food Service
3	v075	0	1130	26.3	7.4	3	8	6x4	Mack MP8-415C	AMT	10	Drayage
6	v073	1	1410	33.8	18.1	3	8	6x4	Mack MP8-415C	AMT	10	Drayage
7	v9892	1	1616	27.0	10.6	3	8	4x2	Volvo D13	AMT	12	Food Service
8	v11660	5	615	16.2	3.5	4	8	6x4	Mack MP8-415C	MT	13	Drayage
9	v11806	5	1810	7.5	6.8	3	8	6x4	Cummins ISX 12	AMT	10	Transfer Truck

2.9 Low-Load Cycle Assembly and Candidate Testing

The assembly of individual profiles into a final low-load cycle was an iterative process, in which candidate cycles were put together, tested on engine, and then refined. The final cycle development was performed with several key objectives in mind:

- Provide at least one example of each of the key challenges observed in the field data and summarized in Table 6 earlier. Ideally multiple examples of both low-to-high load and high-to-low load transitions, as well as an adequate segment of sustained light load operation.

- As much as possible, present these challenges in a manner similar to how they would occur when each of the profiles was run on its own, considering the point at which the engine system had reached equilibrium with that profile's duty cycle.

- To the extent possible, minimize the time required to run the cycle, in terms of both, cycle run time and preconditioning effort.

- The cycle was intended to be run on a warm engine, although this did not necessarily mean that the aftertreatment would be fully stabilized at hot temperatures.

These objectives were sometimes in conflict with each other, and therefore the development of the cycle was a balance between presenting proper low-load challenges and minimizing laboratory effort. Considerable effort was required to strike a balance between regulatory objectives and laboratory efficiency. An early decision made with regard to this balance was that the complete profiles did not necessarily have to be used in assembling the final cycle. When possible, a portion of the profile capturing the key challenges was incorporated into the cycle, and any additional operation that was considered redundant was removed. This results in a cycle that actively examines the level of emissions control achieved in several representative emission control situations without needlessly extending the cycle to obtain an intrinsic weighting of those emission control challenges, a weighting which would vary somewhat across vocations, vehicle applications and as the vehicles pass into second and third life ownership .

Given that the intent was entry into the cycle with a warm engine at moderate aftertreatment temperatures, the FTP cycle was utilized as the primary preconditioning. Other cycles were examined and the use of idle segments following preconditioning cycles was considered. However, it was felt that these other cycles represented an arbitrary choice of preconditioning. In addition, the use of the FTP would make for easier and more efficient integration into the existing test process, as the LLC could then be run following the conclusion of the FTP hot test. Varying engine-off soak lengths were also examined as discussed later, but ultimately a 20-minute soak was chosen.

Where possible, candidate LLCs were run on multiple engines available at SwRI. In addition, candidates were distributed to Program Advisory Group (PAG) members in an effort to allow additional testing of some of the candidates in other laboratories. Some of the later candidates were tested by other laboratories which provided some feedback directly to CARB regarding the final cycle selection.

A total of ten candidate cycles were developed and tested as part of this process. Although the specific engines cannot be disclosed, candidate cycle testing and development was carried out on 3 different heavy-duty engines, all of which were MY 2017 or newer heavy-duty engines. The early cycles focused more on the basic ordering of the profiles, while later candidates focused on refinements for efficiency. In some cases, too much was removed in seeking a more efficient cycle. An example of one of the early candidates, showing one approach to ordering the low-load challenges is shown in Figure 31. Figure 32 and Figure 33 show two examples of test data from this Candidate 1 cycle for two different heavy heavy-duty engines from different manufacturers. The data indicates some differences in system performance, as might be expected given that the LLCs generally operate below the range covered by current US regulations. Both engines had tailpipe NO_X emissions generally in the vicinity of 1 g/hp-hr, with NO_X conversion rates generally 70% to 80%. This is generally well below the 95% and better conversion efficiency often achieved on the FTP. Engine-out (EO) and Tailpipe (TP) NO_X traces are shown in the charts for reference.

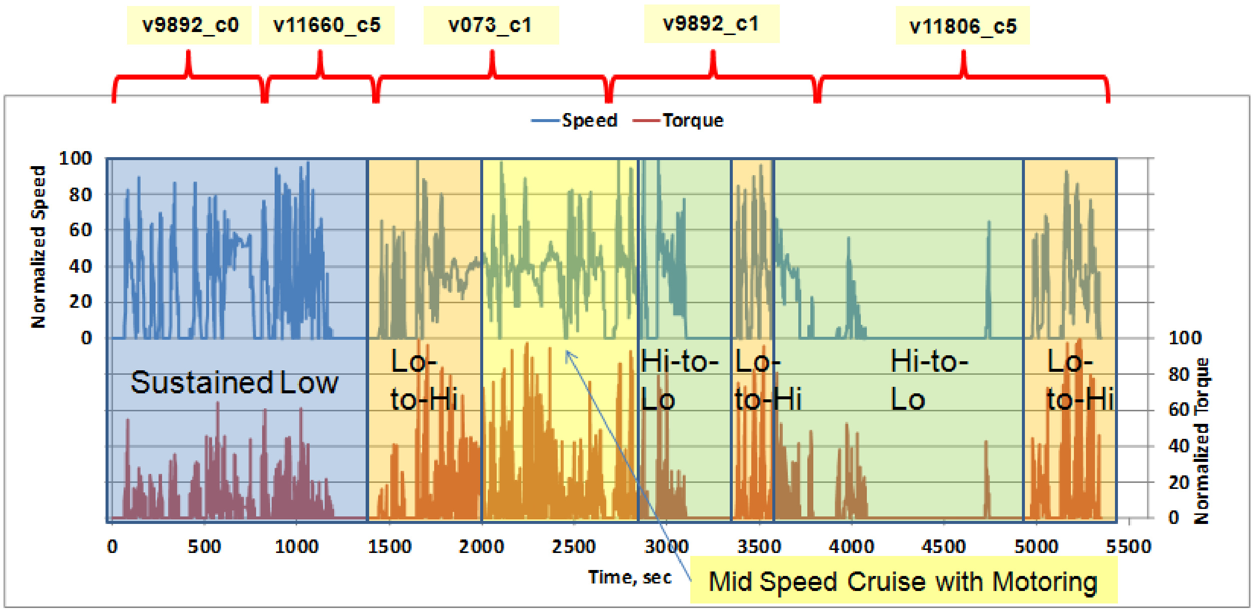

FIGURE 31. EARLY LLC CANDIDATE 1 SHOWING ORDERING OF LOW-LOAD CHALLENGES

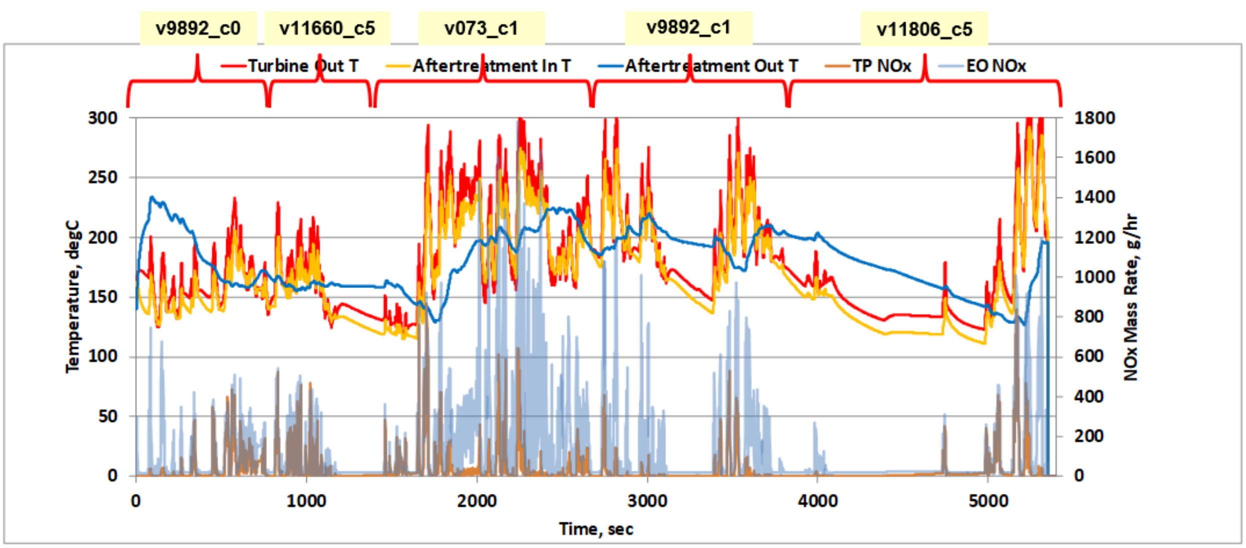

- Overall 72% conversion
- EO NO_X (g/hp-hr / g/kgCO_2) = 3.9 / 6.4
- TP NO_X (g/hp-hr / g/kgCO_2) = 1.1 / 1.8

FIGURE 32. EXAMPLE TEST DATA FOR LLC CANDIDATE 1, ENGINE 1

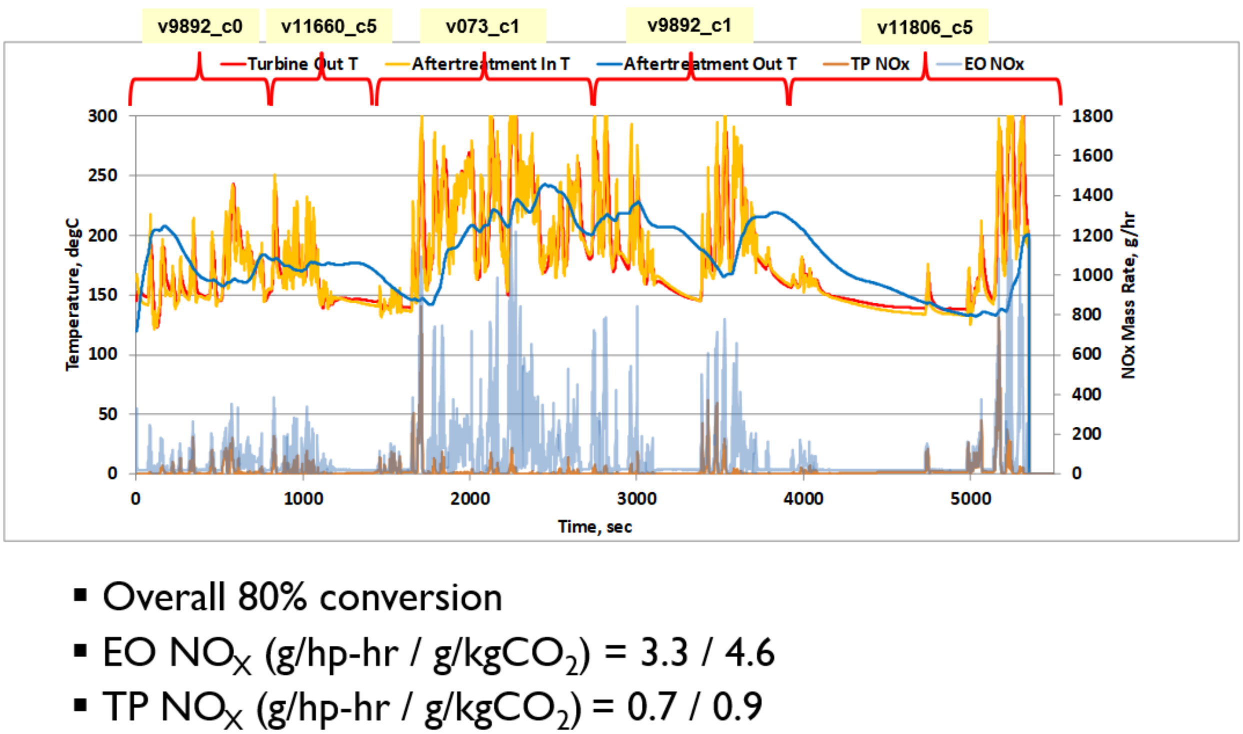

FIGURE 33. EXAMPLE TEST DATA FOR LLC CANDIDATE 1, ENGINE 2

At the end of this process, SwRI produced four final candidate cycles, each of which was a variation of the final basic profile order. These final candidates were presented to the PAG for feedback, along with a proposed preconditioning approach. Ultimately, CARB selected from among those candidates.

2.10 Cycle Details and Preconditioning

Some of the later cycles were used to examine additional issues or cycle details including:

- Length of soak time between preconditioning and test start
- Length of long idle segments
- Amount of sustained low-load operation
- Use of idle accessory load
- Identification of redundant areas of operation

The results of these more detailed experiments are given below.

2.10.1 Engine-Off Soak Length after Preconditioning

With regard to engine-off soak time, SwRI examined times as short as ten minutes and as long as one hour. It was ultimately determined that anything shorter than 20 minutes would be difficult when trying to append the LLC testing to the existing cold-hot FTP certification test sequence, due to the need to complete post-test maneuvers and prepare for the upcoming test. Soak times longer than one hour were considered impractical from the standpoint of laboratory operations, and generally anything over 30 minutes was felt to be a stretch. Table 8 shows the impact of varying soak length on the performance of one of the engines over the LLC. It was noted that while a longer soak time did have some effect on initial system temperatures, this effect was generally erased within roughly five minutes of the initial start. By even the second profile segment there was no difference between cycles of varying soak length. Therefore, it was determined that more practical shorter soak times could be utilized. Ultimately, a 20-minute soak was selected as a good compromise, allowing sufficient time to complete post-test and pre-test maneuvers following an FTP.

TABLE 8. PERFORMANCE PARAMETERS ON LLC CANDIDATE CYCLE 2 WITH VARYING SOAK TIME FOLLOWING PRECONDITIONING

	Whole Cycle		1st Profile	2nd Profile
Soak Time	Conversion	TP NO_X, g/kgCO_2	Conversion	Conversion
10 min	66%	2.04	72%	66%
30 min	66%	2.16	71%	66%
1 hour	65%	2.03	65%	66%

2.10.2 Long Idle Segment Length

One of the key challenge portions of the LLC was the relatively long idle segment that was taken from vehicle profile v11806_cluster5. This segment features a continuous idle roughly 21 minutes long before the start of a return to service event. This was taken from a transfer truck that appeared to be waiting in a queue, with one or two momentary creep events, before pulling away with a load. There was some question regarding whether this segment of idle should be made longer in order to capture a larger population of long idle events. However, this would have to be balanced by the significant amount of additional lab time that such a longer event would require.

This question was examined by inserting extra idle time into that profile segment, raising the idle time to 36 minutes, longer than the current CARB extended idle test mode length. The results of this examination are shown in Figure 34 and Figure 35 for the normal and extended length idle segments, respectively. As can be seen in the figures below, the added idle time did not significantly alter the challenge associated with either the idle itself or the subsequent return to service event at the end of the profile. It was noted that the primary control of idle heat retention and thermal management in this case is not necessarily the idle itself, but rather the presence of the return to service event after idle.

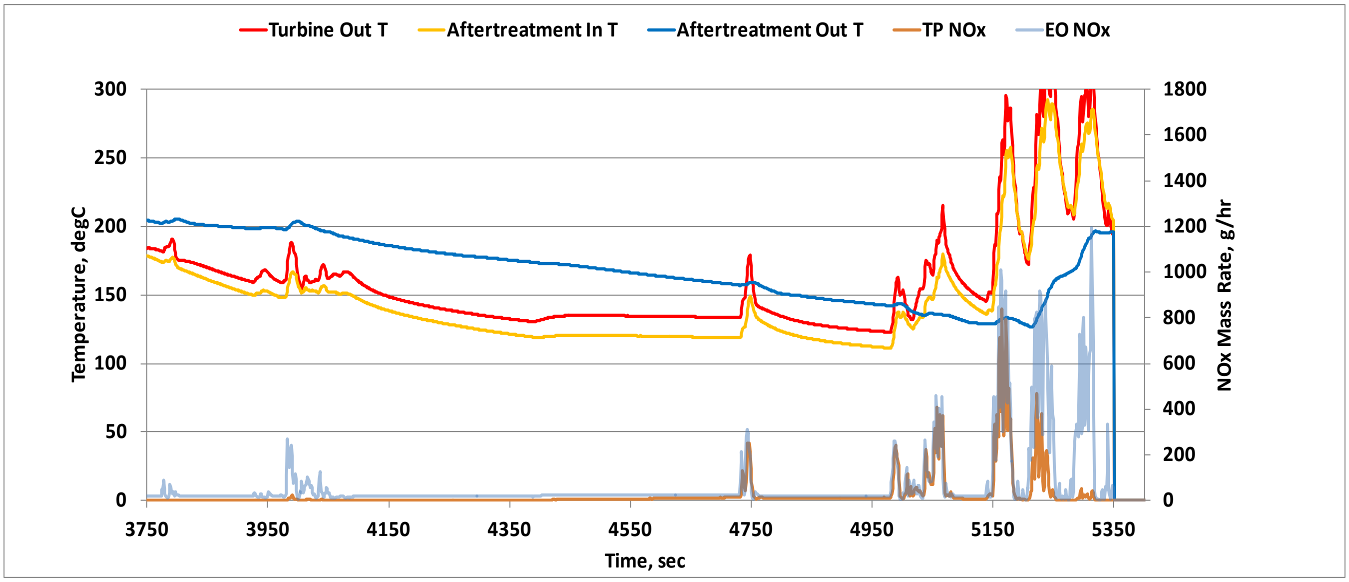

FIGURE 34. LONG IDLE PROFILE SEGMENT (V11806_CLUSTER 5, 21 MINUTES OF IDLE)

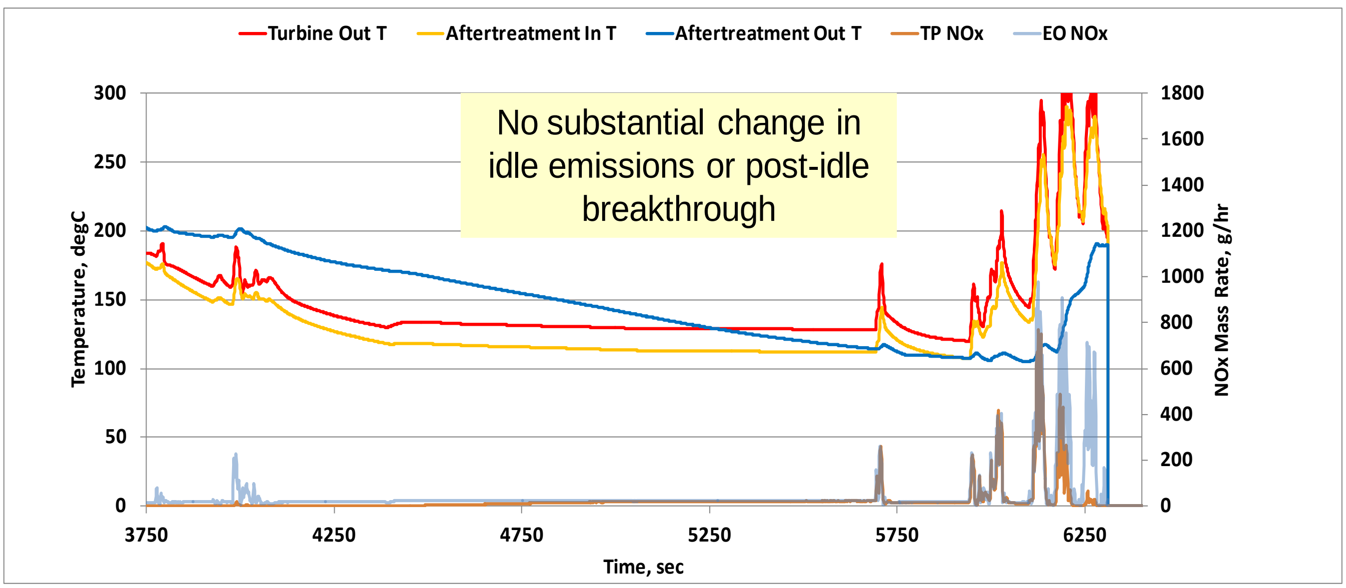

FIGURE 35. LONG IDLE PROFILE SEGMENT WITH EXTENDED DURATION (36 MINUTES OF IDLE)

It is clear from the two figures that the additional idle time would not likely change thermal management practices substantially for a properly calibrated system, as compared to the field version of the profile with the actual 21-minute idle event. The added time would serve to lengthen the test further, with little added gain in terms of emission control challenge. In the final cycle, the segment was left as it was taken in the field.

It was noted that this idle segment might serve as an adequate check of idle emissions (perhaps by examining idle emissions at the later end of the segment), and that it might be possible to use this in lieu of the current low idle segment of the CARB Clean Idle test. As noted earlier, the presence of the return to service acceleration at the end of this segment helps to ensure that strategies will be incorporated to maintain a state of sufficient readiness for potential real-world accelerations occurring after long idles. However, this determination will have to be made by CARB.

2.10.3 Length of Sustained Low-Load Segment

In many of the final candidate LLCs, the sustained low-load challenge portion is placed near the front of the LLC. It was noted that in general, there is some residual heat left in nearly all aftertreatment systems tested following the preconditioning and 20-minute soak. There was some concern on the part of CARB that the originally designed segment, consisting of two profiles (v9892_cluster 0 and v11660_cluster5), and having a duration of roughly 20 minutes, might not be sufficiently long to really enter into a "sustained" operating pattern, especially for systems featuring a high amount of thermal inertia in their design. Therefore, SwRI was asked to examine possibilities for a longer such segment. Another sustained low-load operating profile was chosen from the data set, v075_cluster0, and this profile was inserted between the existing two. It was felt that this approach would capture a more representative variety of operations rather than simply repeating of the existing segments.

The resulting data is shown in Figure 36 for the original segment and in Figure 37 for the revised segment including the third profile from v075_cluster0. In both cases, the temperature data for the engine under test appears to indicate that aftertreatment has exhausted any residual heat from the preconditioning after roughly 500 seconds. This means that nearly a third of that segment was spent in transition to the lower load thermal state. Given the concern about higher thermal inertia designs, the added profile in the expanded segment would reduce this to less than 20 percent of the sustained low-load segment. It should be noted that in both cases, this segment is followed by a low-to-high load acceleration at the start of the next segment, and similar to the case of the long idle segment, this return to service event provides an additional measurement of control by requiring some amount of system readiness in the form of thermal management.

It was not clear from experimental data whether this lengthened segment was more effective in controlling NOx during under sustained low-load operation. However, a more conservative approach with wider applicability of an extended sustained low-load segment was preferred. Ultimately, the final choice among candidates was influenced in part by the use of this longer sustained low-load segment.

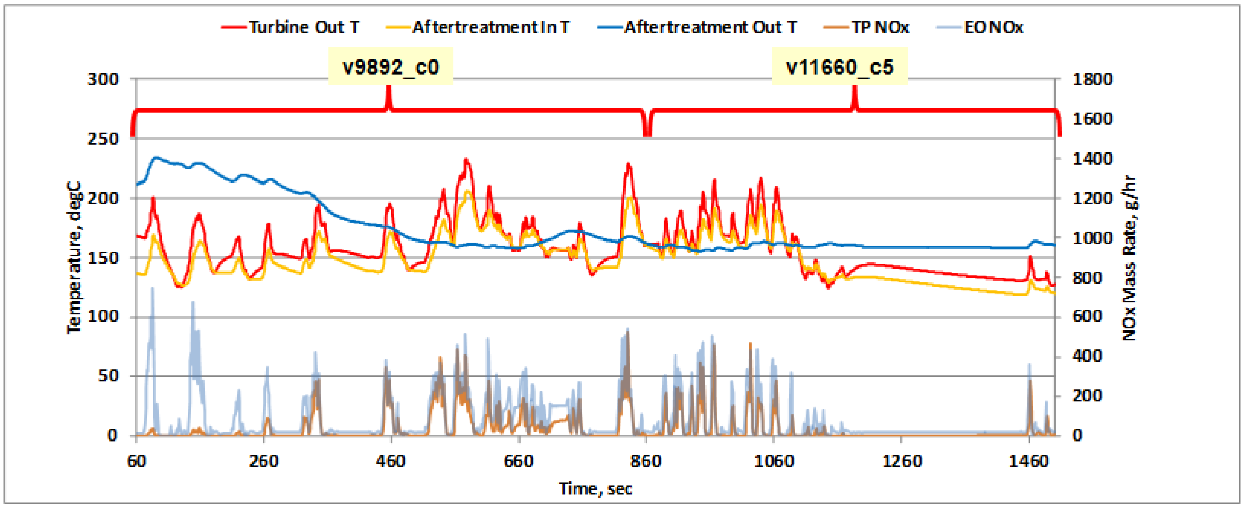

FIGURE 36. ORIGINAL SUSTAINED LOW-LOAD SEGMENT AT START OF LLC

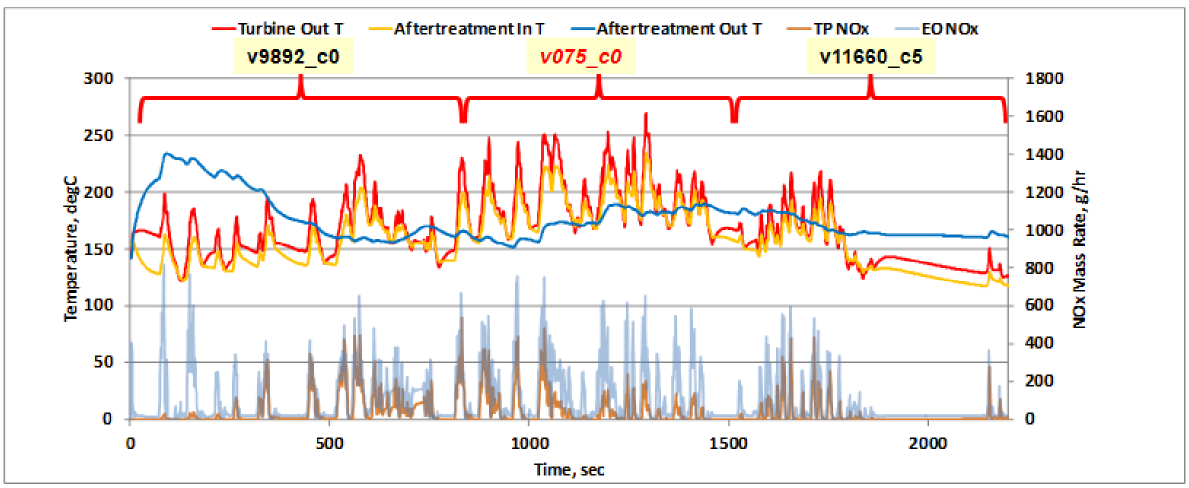

FIGURE 37. REVISED SUSTAINED LOW-LOAD SEGMENT WITH V075_CLUSTER 0 PROFILE INSERTED

2.10.4 Use of Idle Accessory Load

As noted earlier, SwRI recommended the use of a representative accessory load at idle to make the LLC more representative of real-world operation at low-load. This was considered important to ensure that the technology choices driven by the LLC would represent choices that would also be effective in real in-use conditions. However, there was some concern that this addition would potentially reduce some of the other challenges posed by the cycle, especially in regard to several of the low-to-high load transitions. SwRI examined this by looking at cycles both with and without accessory loads. Figure 38 and Figure 39 show the long idle segment of the LLC for one example engine both without accessory load at idle and with accessory load, respectively.

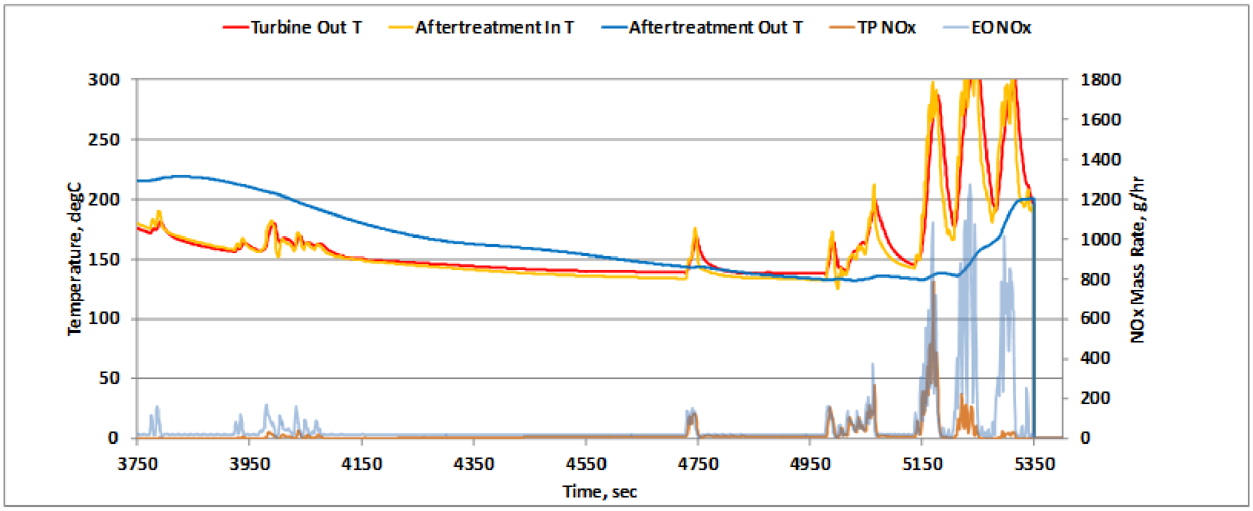

FIGURE 38. LONG IDLE SEGMENT WITH ZERO TORQUE AT IDLE

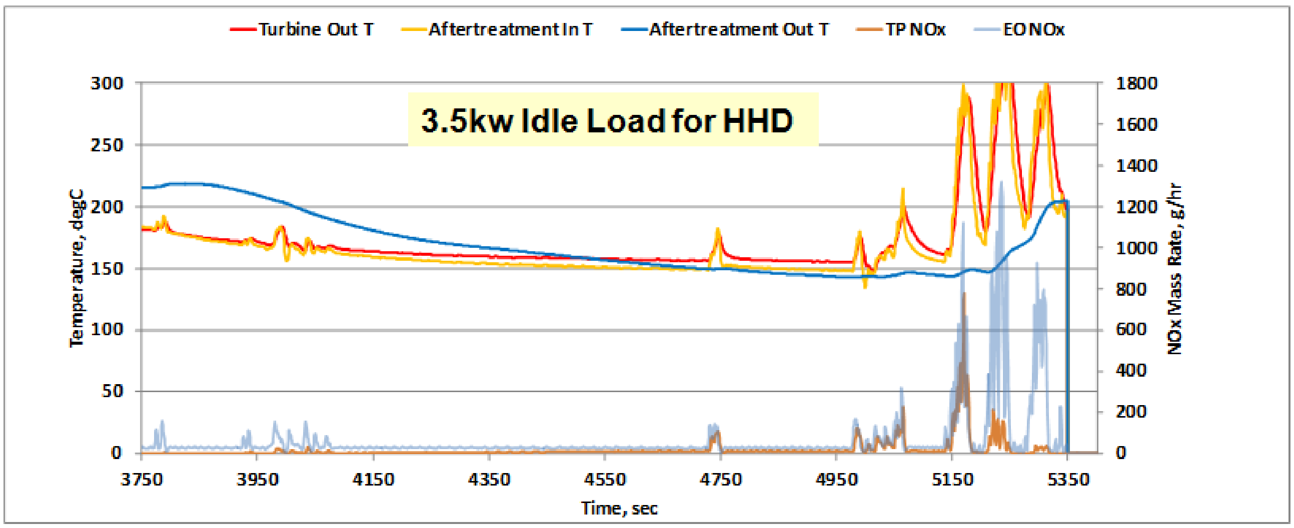

FIGURE 39. LONG IDLE SEGMENT WITH ACCESSORY LOAD AT IDLE

As seen in the figures, the addition of the accessory load did not substantially alter the behavior of the system significantly, nor did it substantially lessen the challenge associated with the return to service event at the end of this segment. However, given the more representative nature of the operation with accessory load, SwRI recommends that the use of accessory load at idle should be adopted as part of the LLC. This was run during testing by either adopting an effective CITT in the cases where the idle torque would normally be zero (i.e., manual transmissions), or by increasing the already existing CITT in the case of automatic transmissions.

2.10.5 Identification of Redundant Profile Sections

From the early candidate cycles, several areas were identified that were suitable for removal from the original profiles as incorporated into the LLC, without significantly impacting the overall challenge presented by the LLC. These included portions of the last three profiles incorporated into the LLC. One such example is shown in Figure 40 which depicts an area of the v9892_cluster1 profile that did not contribute substantially to the challenge associated with that segment. The primary feature of this profile is the motoring and short idle transition that begins about 400 seconds into the profile. That feature, and the subsequent return-to-service acceleration are very similar whether the previous portion of the profile is run or not. Therefore, the use of only the later portion of this profile in the LLC provides the desired challenge but manages to shorten the final cycle by nearly 7 minutes. A similar added portion occurs near the end of this profile after the primary challenge has been negotiated, removing an additional 5.5 minutes.

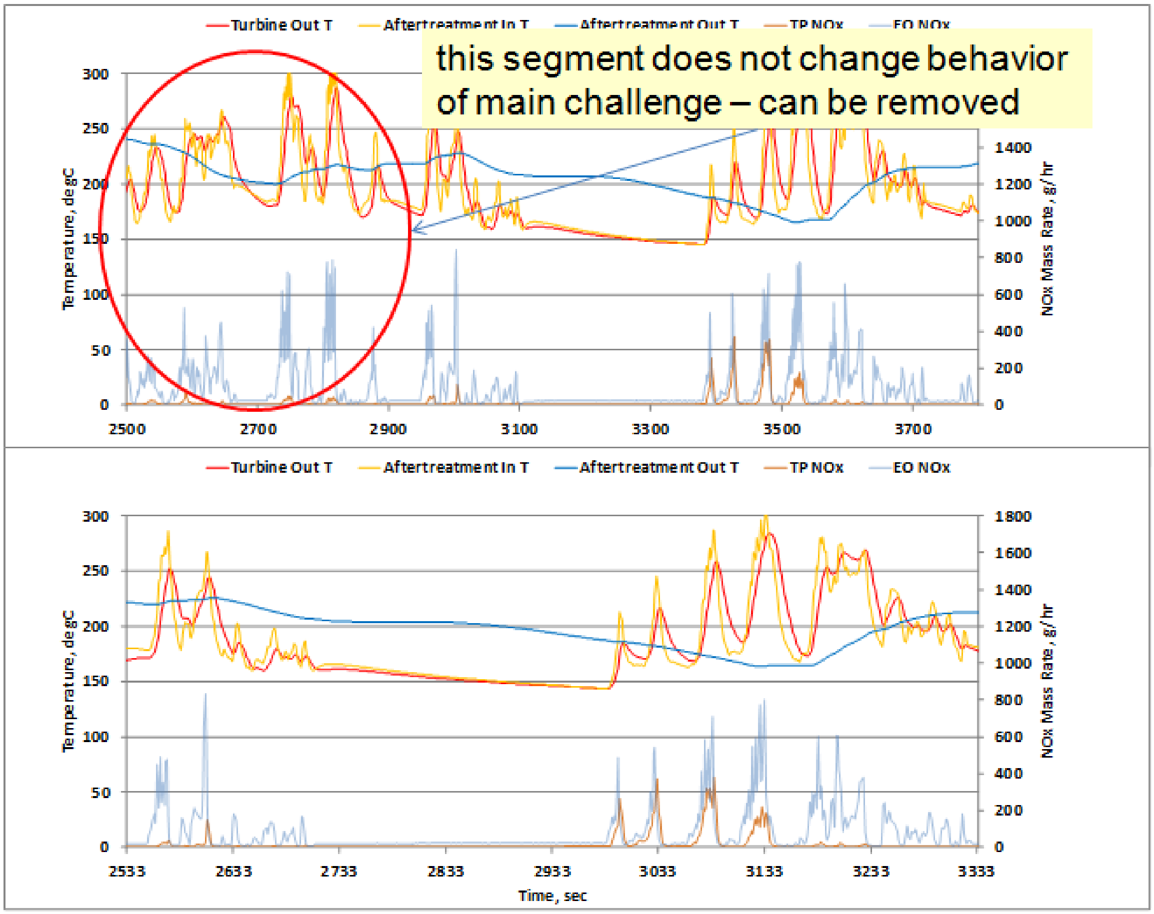

FIGURE 40. REMOVAL OF REDUNDANT SEGMENT OF V9892_CLUSTER 1 PROFILE FROM LATER LLC CANDIDATES

Other such areas included the later portions of the mid-speed cruise motoring segment under v073_cluster1, a portion of the added sustained low-load segment under v075_cluster0, and the ending portions of v11806_cluster5 following the return to service event near the end of the LLC. In total these efforts shortened the final LLC by roughly 32 minutes, as compared to what the duration would have been if complete profiles had been used. This is a substantial savings of laboratory effort while preserving the essential challenge nature of the final LLC.

2.11 Final LLC Selection

Eventually, SwRI arrived at a set of four final candidates provided to CARB for consideration. The base candidate among these options was Candidate 7. The other three options involved potential approaches to further trim the length of the cycle. These three options essentially revolved around two questions:

- Was the extended Sustained Low-Load segment near of the front of the cycle needed (via the inclusion of the v075_cluster0 profile portion)?
- Was the mid-speed cruise-motoring portion of the cycle valuable, or could it be further shortened?

These final four candidates are shown in Figure 41, Figure 42, Figure 43, and Figure 44, for Candidate cycles 7 thru 10, respectively.

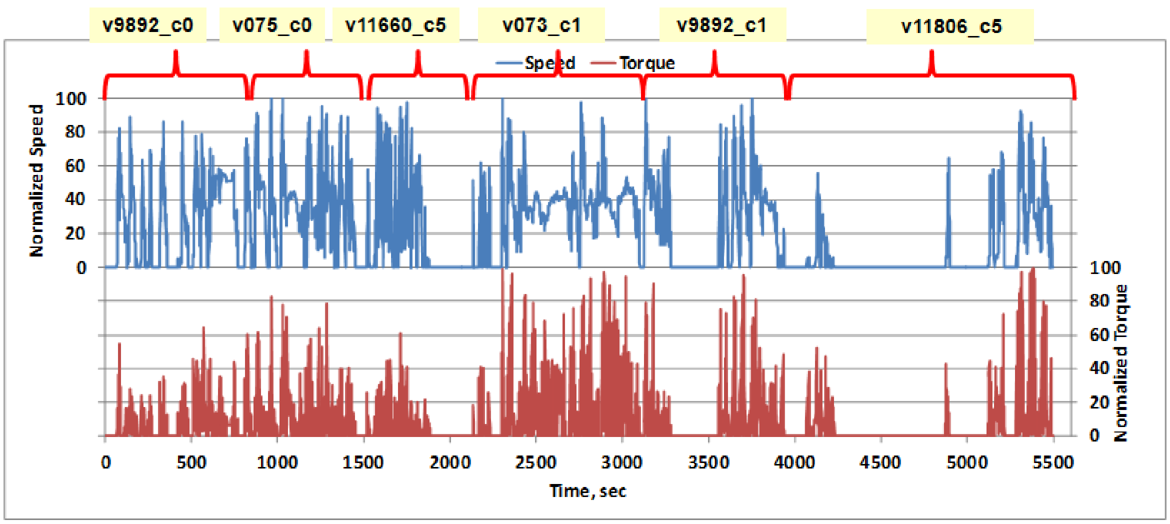

FIGURE 41. LLC 7 CANDIDATE 7 (BASE) – FINAL CYCLE SELECTED

The base cycle, Candidate 7, is roughly 90 minutes in length, candidates 8 and 9 are each roughly 80 minutes in length, and Candidate 10 is roughly 70 minutes long. Test data on these various candidate cycles generally indicated a similar level of challenge on all four cycles, though not identical. However, CARB remained concerned about the shorter sustained low-load segment at the start of the cycle. Therefore, Candidates 9 and 10 were removed from consideration. Following additional feedback from stakeholders, CARB elected to proceed with Candidate 7 as the final cycle.

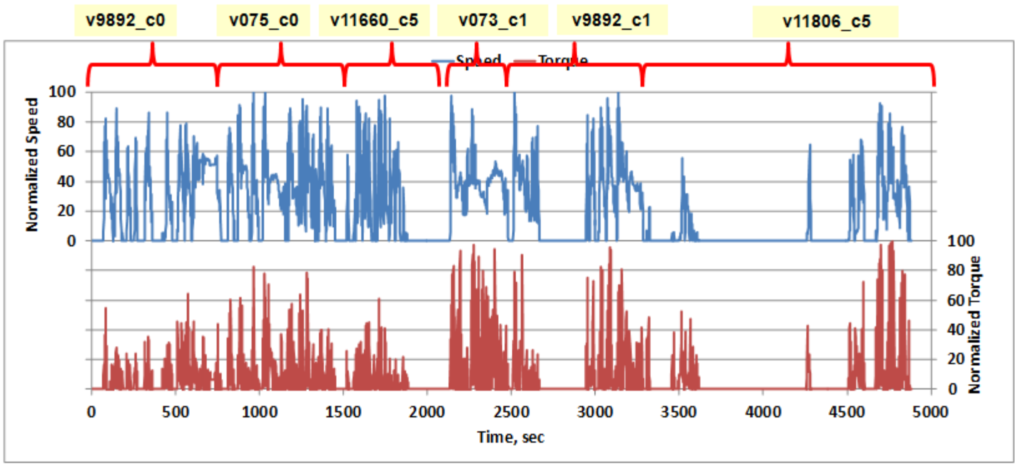

FIGURE 42. LLC CANDIDATE 8 (SHORTER CRUISE-MOTORING)

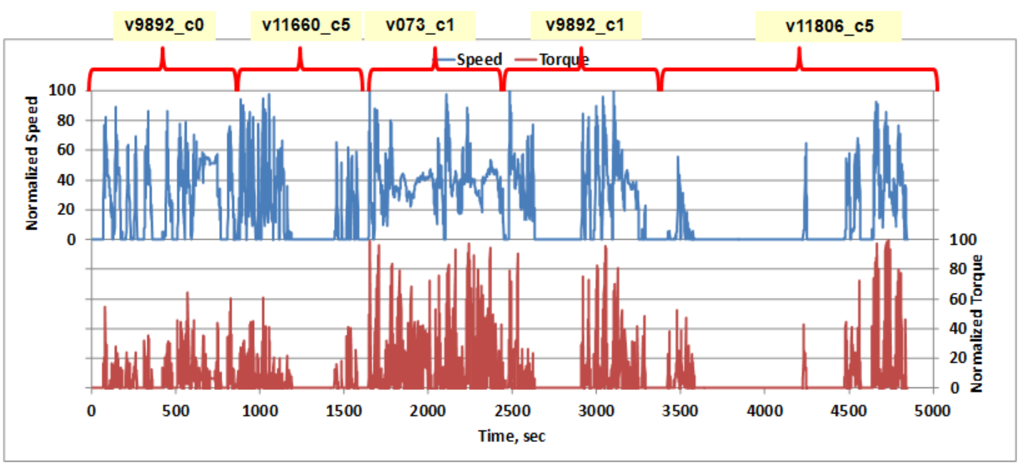

FIGURE 43. LLC CANDIDATE 9 (SHORTER SUSTAINED LOW-LOAD)

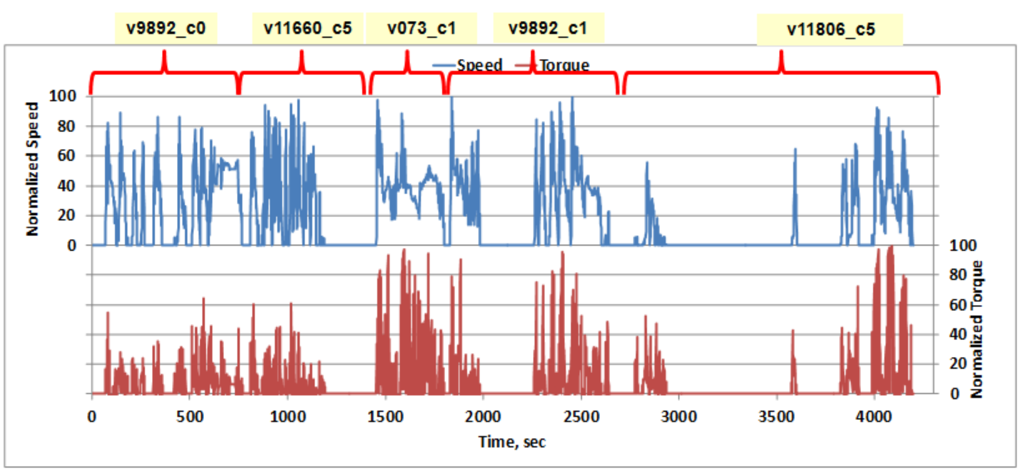

FIGURE 44. LLC CANDIDATE 10 (SHORTER SUSTAINED LOW-LOAD AND CRUISE-MOTORING)

3.0 LOW-LOAD CYCLE CALIBRATION

As part of this task, the Stage 1b engine and aftertreatment system were utilized for the low-load cycles re-calibration and optimization efforts. The intent was to generate one calibration that would encompass all of the low-load cycles tested during the course of the program while maintaining demonstrated Stage 1 performance over the FTP and RMC-SET cycles. The strategy development process entailed evaluating the cycle profiles and refining the selected approach to achieve ultra-low NO_X targets (e.g. 0.02 g/hp-hr). No specific tailpipe NO_X target was given in the program for the LLC. Therefore, several engine and aftertreatment calibration scenarios were developed to understand the required level of effort for several different tailpipe NO_X levels, to quantify the CO_2 impact at each of those. Unless otherwise noted, testing can be assumed to be on a development system that was exposed to hydrothermal aging only. However, it should be noted that the performance final “optimized” calibration was also verified using the Final Aged parts produced under the Stage 1b program.

3.1 Low-load Cycle and Shorter Development Cycles

As previously mentioned, the LLC was down-selected from a number of candidates that simulated vehicle specific real world challenge areas. Figure 45 shows the final candidate profile that CARB selected from the proposed cycles. Given the relatively long run time and required calibration efforts, it was necessary to conduct evaluations on specific areas of interest. In the case of the final cycle selection, the profile was split into four short development cycles. This provided a more focused evaluation on key areas where the aftertreatment system required additional intervention to generate high NO_X reduction performance. While four cycles were evaluated as part of this study, all were not used to screen potential low NO_X solutions. Because of this, some of the cycle work ceased after the baseline was completed and continued on cycles that were observed to have problems controlling NO_X emissions. The normalized cycles are shown in Figure 46 through Figure 49.

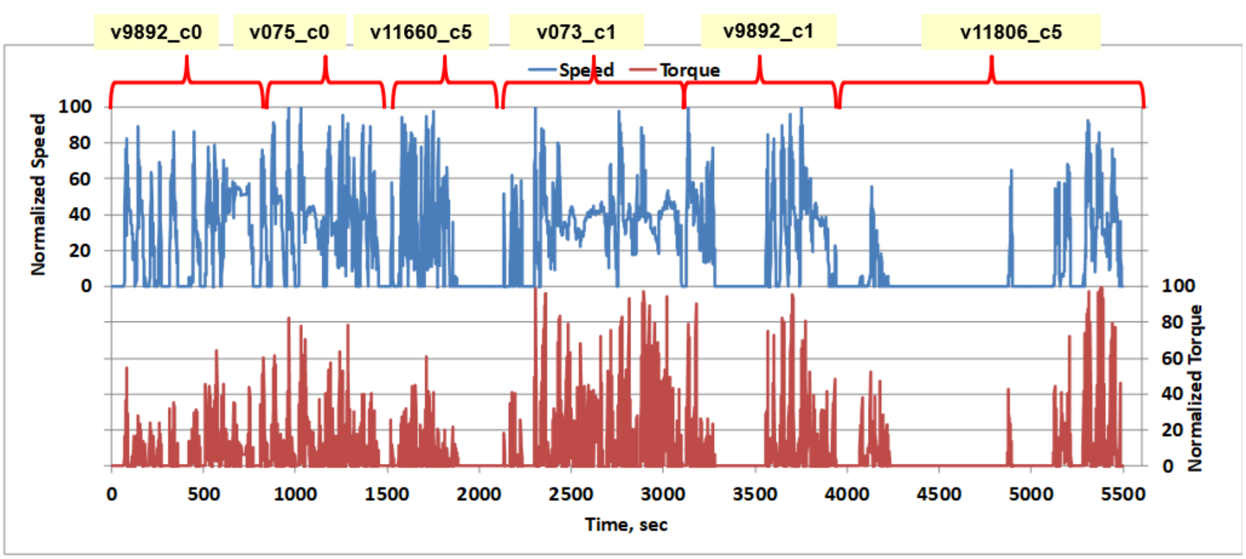

FIGURE 45. FINAL LOW-LOAD CYCLE

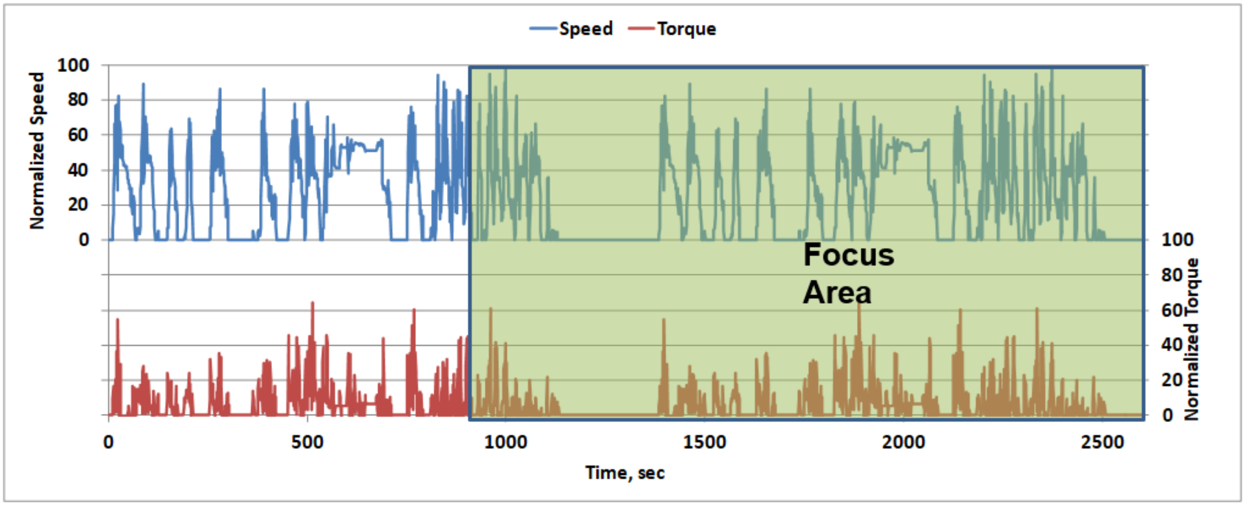

FIGURE 46. LLC DEVELOPMENT CYCLE 1 – SUSTAINED LOW-LOAD SEGMENT

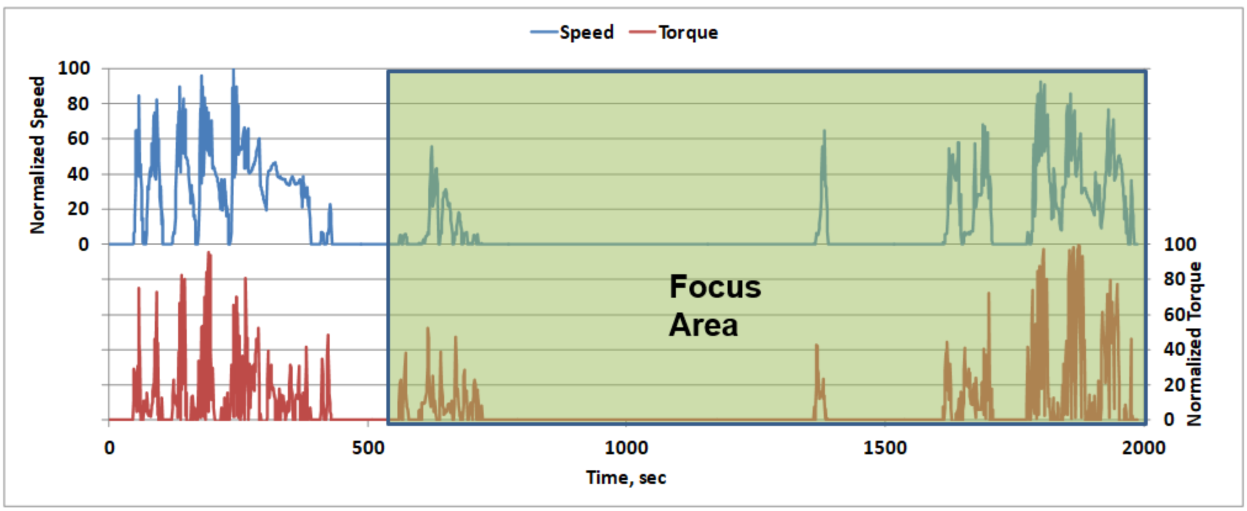

FIGURE 47. LLC DEVELOPMENT CYCLE 2– LONG IDLE SEGMENT

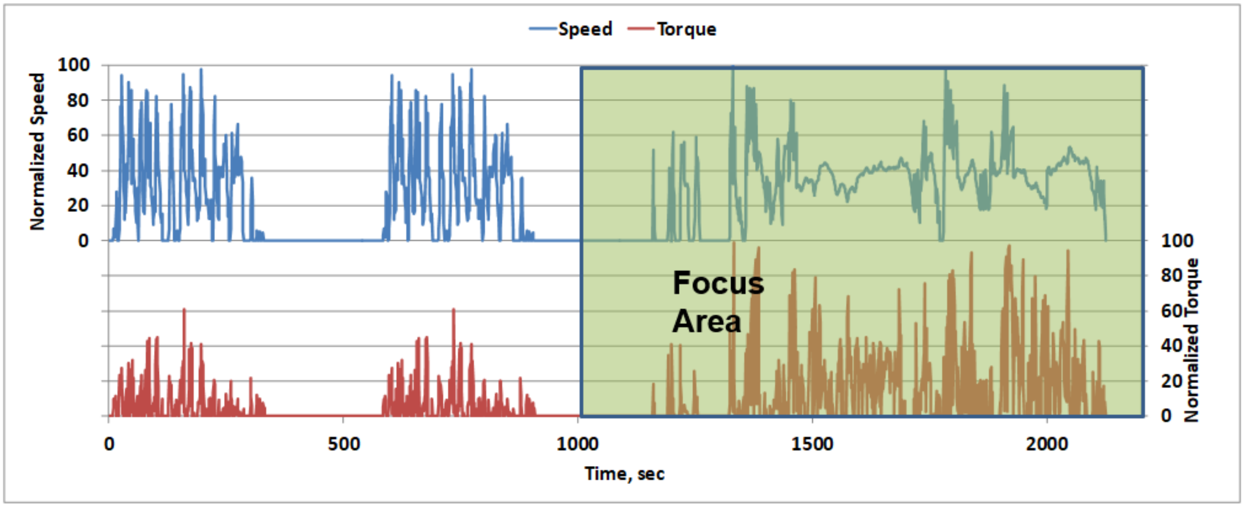

FIGURE 48. LLC DEVELOPMENT CYCLE 3– MOTOR / CRUISE BREAKTHROUGH

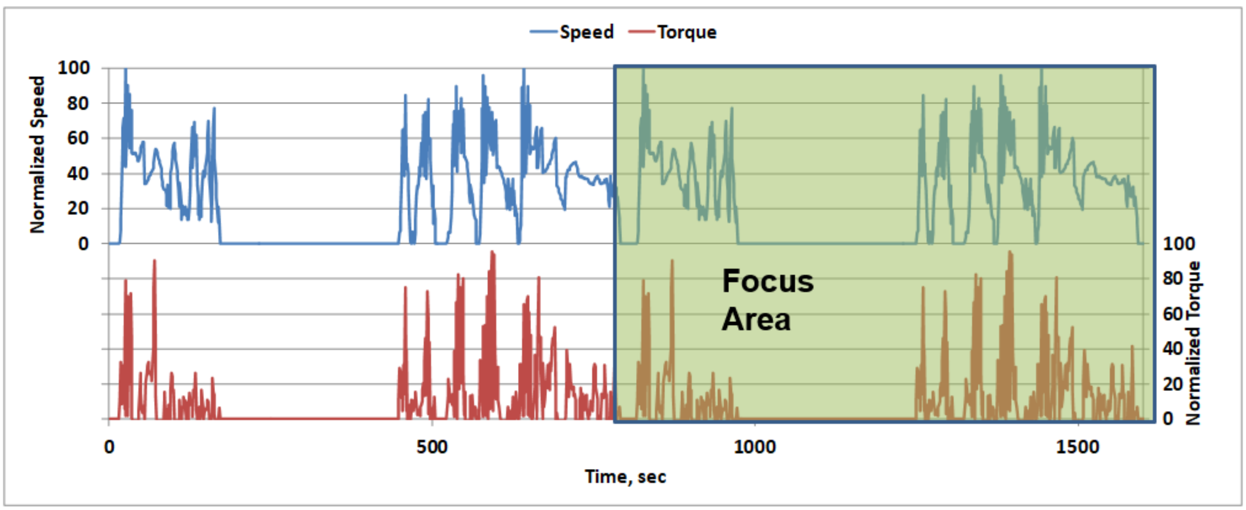

FIGURE 49. LLC DEVELOPMENT CYCLE 4 – MOTOR / SHORT IDLE BREAKTHROUGH

Included in the figures are non-highlighted and highlighted sections that identify the areas of interest. The non-highlighted areas also provide valuable information as they are considered the preparatory segment before the actual focus area. Additional measures were taken to evaluate the cycles with either a HD-FTP prep cycle followed by a 10-minute hot soak (i.e. engine off) or by testing with duplicates of the same profile, as shown in Figure 49. This was determined to provide sufficient aftertreatment stabilization (i.e. adequate ammonia (NH_3) storage accumulation on the SCR catalysts) based on the requirements for these cycles.

Emissions performance improvement efforts involved leveraging several approaches to develop a practical low NO_X strategy. Figure 50 introduces the two main approaches for improved aftertreatment performance. The first explores the possibility of achieving low NO_X emissions utilizing the engine calibration without mini-burner intervention. This required careful attention to the NO_X and CO_2 tradeoff as a significant fuel penalty can begin to diminish or eliminate the emissions reduction benefit completely. Potential options were considered to address the requirements for solutions without the supplemental exhaust energy enhancers.

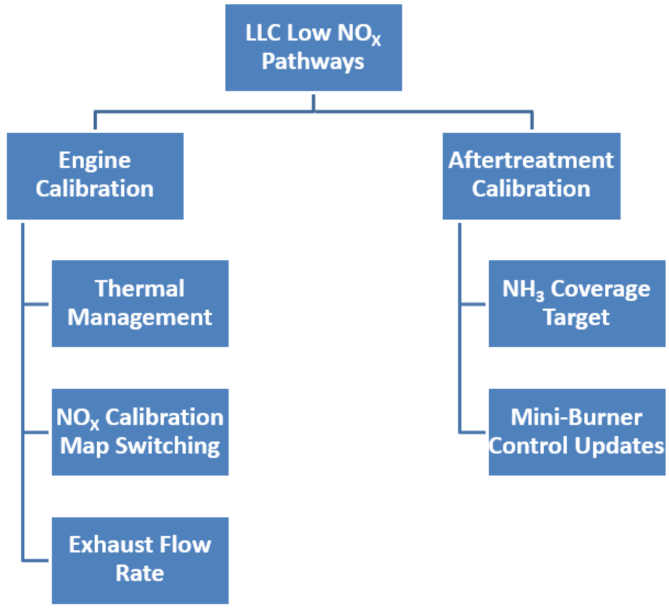

FIGURE 50. EXPLORED CALIBRATION PATHWAYS FOR LLC

The other pathway involved minor re-calibration of the aftertreatment NH_3 coverage targets and intermittent use of the mini-burner as needed for aftertreatment thermal management. While calibrating the NH_3 coverage targets provide minor benefits during the cycle, the mini-burner is the easiest solution to apply since it operates independently of the engine and provides a near instantaneous temperature increase. With that being said, there is an associated fuel penalty that needs to be considered as part of the mini-burner use. As will be discussed in section 3.6, this can be optimized by implementing strategies like burner cycling.

3.2 SCR Controls Description

Given that this program involved making modifications to the SCR controls developed in the Stage 1 program, this section provides a brief description of the SCR dosing controller to help the reader understand what modifications were being made.

A schematic of the dosing controller approach is given in Figure 51. This controller was developed by SwRI to operate in a manner similar to a production dosing controller, and in fact this approach and its associated algorithms are now being applied to production controls. The controller algorithms are designed to allow the controls to run within the constraints of an engine ECM.

The SCR controller is a model-based dosing controller that incorporates a physics-based lumped parameter kinetic model that allows the controller to monitor the NH_3 storage state on the SCR catalysts. Each section of SCR is split into a series of model cells, which allows the model to track the NH_3 storage state along the axial length of that section. That storage state is then used as a virtual sensor to drive the dosing controller.

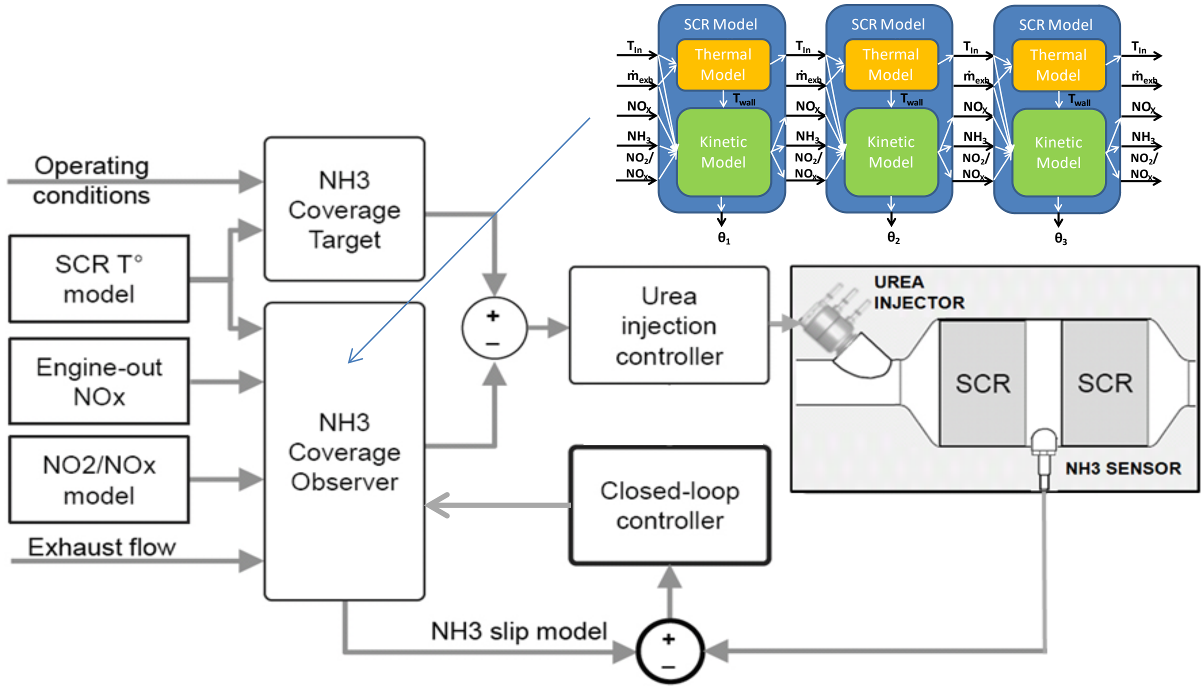

FIGURE 51. SCHEMATIC OF STAGE 1-1B-2 SCR MODEL-BASED CONTROLLER

The calibration of the dosing controller consists of several system gains, and a set of NH_3 coverage targets for each section of SCR catalyst. The coverage targets are mapped out based on measured catalyst parameters including temperatures and inlet NO_X mass flow rate. This means that there is one set of coverage targets and gains that are calibrated, but the controller is flexible enough to apply this single unified calibration to whatever duty cycle the engine is running. The controller incorporates a short-term feedback mechanism in the form of a mid-bed NH_3 sensor which is used to correct the NH_3 coverage observer. A production version of this controller also incorporates a long-term trim function that adjusts coverage targets over time based on a tailpipe NO_X sensor feedback, and an aging model (although calibration of that aging model was well beyond the scope of this program). At the time of this program, the long-term trim function was not yet automated.

For the Stage 1 program, the controller was calibrated using FTP and RMC-SET cycles, but the single calibration was also tested over different Vocational Cycles. For the Stage 2 program, the calibration was extended to also cover the LLC, although in practice it was found that only minor changes were made to coverage targets in some temperature ranges to account for the LLC. Those changes had no effect on FTP and RMC-SET performance. For Stage 2, these dosing calibration adjustments were combined with adjustments to thermal management strategy which are outlined below. Again, these features were already present, but thresholds were adjusted from initial calibration values in order to better encompass the lower temperature range of the LLC.

3.3 Initial Results with Stage 1 Calibration

An initial assessment of system performance was made to provide a base level of performance in the Stage 1 AT system configuration without the use of the mini-burner for thermal management. This would provide a start point for examining different calibration options. Testing was executed on the five cycles mentioned in section3.1. To understand the existing performance potential, the warm start HD-FTP engine and aftertreatment calibrations were used for the cycle evaluations. A separate objective of this testing was to define the required temperatures to exercise a mini-burner re-light strategy. This was completed by assessing the SCR catalyst gas temperatures and assigning minimum operating temperatures based on NO_X reduction performance. It is important to note that the cycle was evaluated following a hot start HD-FTP prep cycle and a 20-minute hot soak period.

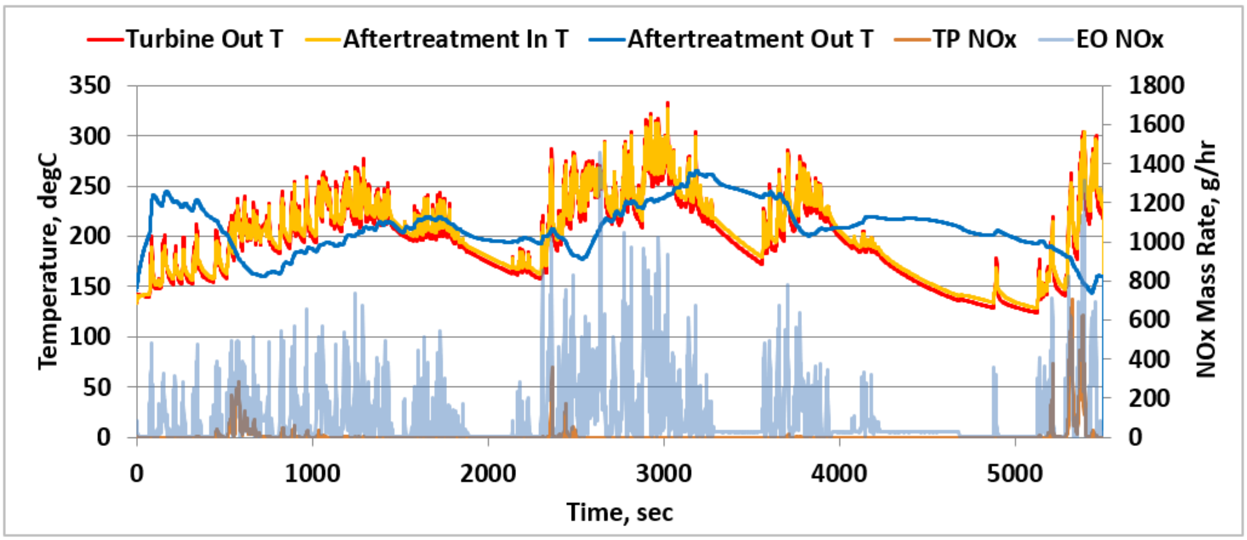

FIGURE 52. INITIAL AFTERTREATMENT PERFORMANCE WITH STAGE 1 CALIBRATION AND NO MINI-BURNER ACTIVITY

The initial cycle, shown in Figure 52, provides insights regarding the different challenge zones for this particular aftertreatment system. The test was conducted without the use of the mini-burner or engine calibration modifications from the HD-FTP Low NO_X engine maps. It can be shown that there are several areas where the inlet and outlet aftertreatment gas temperatures are below 200 °C. At these conditions, it is also observed that tailpipe NO_X breakthrough occurs due to the decreased catalyst activity. The most problematic area is the final 500 seconds as it accounts for approximately 60% of the total tailpipe NO_X emissions and contains the lowest temperatures. In this case, the inlet aftertreatment temperatures decrease below 150 °C. Still, the system appears to be mitigating the tailpipe NO_X breakthroughs by retaining heat. This resulted in an overall $BSNO_X$ of 0.27 g/hp-hr at the tailpipe and a $BSCO_2$ of 598 g/hp-hr. This actually represented an improvement of 2% over the baseline engine LLC $BSCO_2$ levels of 609 g/hp-hr, which are detailed later in Section 5 of the report.

3.4 Engine Calibration Approach

To understand the fuel economy impact from thermal management, engine calibration efforts focused on identifying a viable strategy to maintain ideal aftertreatment temperatures. This approach omitted utilizing the mini-burner as one of the primary pathways to achieve the low NO_X emissions targets. The emphasis was, therefore, to quantify the potential for a traditional thermal management solution without the need of a supplemental exhaust energy technology. As will be discussed, several calibration parameters and engine maps will be utilized to improve aftertreatment performance.

The engine calibration is the same as the one that was used for the final demonstration of Stage 1 components. To maintain similar fuel economy and NO_X reduction performance for the HD-FTP, it was important that the modifications to the calibration made to optimize the LLC should not interfere with the strategy for the other transient cycles. Periodic testing with the HD-FTP cycle was conducted to ensure that the engine performance remained similar.

Since the calibration was already developed for the ULN engine, this section will mainly report on developed maps that were triggered according to different engine conditions and aftertreatment temperatures. Table 9 details the engine maps that were used as part of these experiments to understand the impact from the engine thermal management. During the initial screening process, decisions were made to conduct some investigations on the engine map use, as well as to mitigate the fuel penalty in anticipation of the mini-burner use.

TABLE 9. ENGINE MAP DESCRIPTION

Engine Modes	Description
High Thermal Management (TM)	High temperature thermal management strategy used primarily during cold and warm starts
Fuel Economy	High EO NO_X and no aftertreatment thermal management for reduced fuel consumption
Low TM High NO_X	EGR strategy for minimal impact in NO_X reduction, but with improved fuel economy performance
Low TM Low NO_X	EGR strategy to improve NO_X reduction performance, but with increased fuel penalty

It is worth pointing out that the "Low TM High NO_X" and "Low TM Low NO_X" names require some additional explanation. These maps are intended to be the engine-out NO_X calibration component of the engine strategy, with some thermal management actions present, but not as much as the High TM mode. The other maps (i.e. High TM and Fuel Economy) reflect the strategies utilized to increase exhaust temperature during critical cycle segments or to improve fuel economy. For "Low TM High NO_X", the EGR flow rates are reduced to improve the engine fuel economy for either the High TM or the fuel economy maps but have slightly elevated engine out NO_X. The objective of the "Low TM Low NO_X" maps is to reduce the engine out NO_X during low temperature operation.

An additional component was added to this approach by applying a reduced idle exhaust flow rate. Since there are several extended idle segments, heat retention becomes a key issue as temperatures decrease below 150 °C. Therefore, there was a need to identify an approach to maintain temperatures above 200 °C, but without significantly altering the engine calibration. The best pathway to achieve this was to reduce the idle exhaust flow rate. The results for the reduced idle results are shown in Table 10.

TABLE 10. LOW NO_X CALIBRATION IDLE COMPARISON

Speed [rpm]	Torque [N-m]	Power [kW]	Exhaust Flow Rate [kg/hr]	EO NO_X Mass Rate [g/hr]	CO_2 Mass Rate [kg/hr]	Fuel Flow Rate [kg/hr]
550	0	0	105	26	327	1.02
550	0	0	48	2.8	283	0.91
550	61	3.5	50	1.6	451	1.42

The revised flow rates provide several benefits that promote improved performance during LLC testing. By reducing the flow rate, the catalyst temperatures can be maintained within the catalyst activity range for a longer period of time, which will also reduce the dependency on the mini-burner system. A slight fuel economy improvement is also observed along with a lower engine out NO_X mass rate for improved tailpipe NO_X performance. This revision is one of the only ways to achieve reduced engine out NO_X and fuel consumption without additional hardware. It is speculated that the reduced engine pumping losses are contributing to reduced fuel consumption. This would need to be confirmed via modeling, which is not within the work scope of this program.

After incorporating the reduced idle exhaust flow rate, calibration work started by focusing on the area that necessitated the most thermal management. For this cycle, it is the extended idle section at the end. To shortcut the effort required, a modified variant of the LLCDEV2 cycle was utilized to conduct the initial calibration screening efforts. The changes made to optimize for this cycle would prove to be sufficient for this calibration to address issues at other low temperature conditions within the experiment. The difference between the original cycle and the modified cycle was the prep conditions leading into the extended idle, which makes the cycle longer by approximately 700 seconds. With the modified variant, the temperatures were not elevated as they were on the original cycle.

Figure 53 shows the cycle for the High TM and Low TM Low NO_X engine map combination. This calibration utilized high TM operation for the entire cycle. Overall, there is a very subtle increase in the aftertreatment inlet gas temperature, but not significant enough to improve the catalyst activity. The aftertreatment-out temperature stays flat for different sections of the cycle due to the reduced exhaust flow rate at idle. The NO_X is also shown to be decreased towards the end of the cycle for the transient events and indicates that the high NO_X map is working to reduce the overall engine-out NO_X rate. For the last 1300 seconds, this calibration was able to reduce the tailpipe NO_X mass by 50% with a 0.5% fuel penalty over the Initial cycle previously shown in Figure 52.

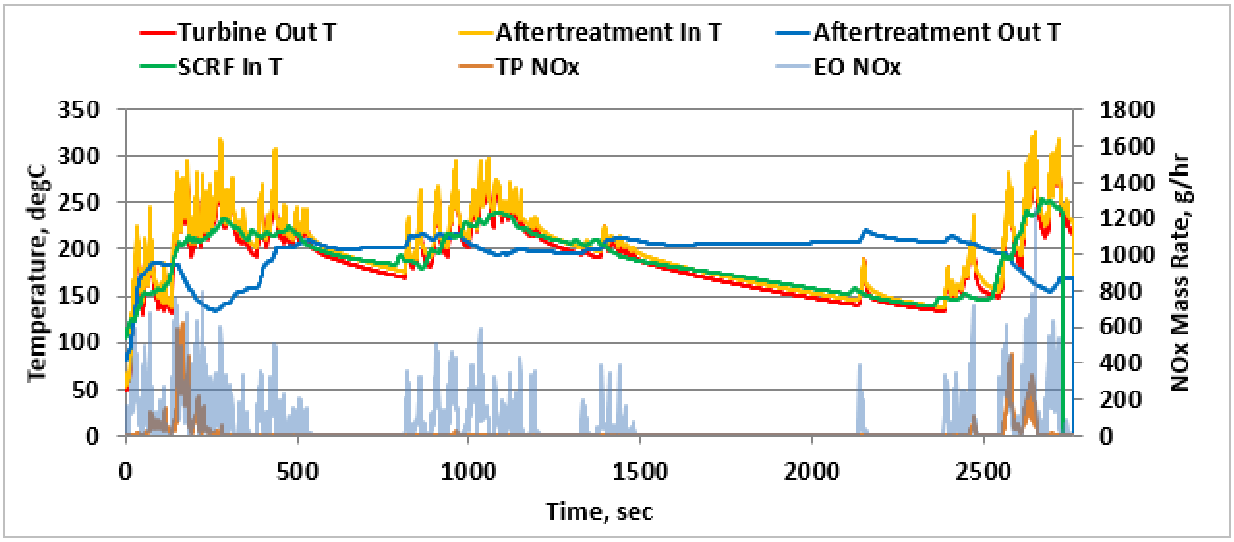

FIGURE 53. LLC DEV2 CYCLE VARIANT RESULTS: HIGH TM / HIGH NO_X

Comparatively, the High TM and Low TM High NO_X map was utilized for the next iteration of the engine out calibration. The data in Figure 54 does not show a significant improvement for the aftertreatment system inlet temperature, as temperatures below 150 °C are still observed. However, the lower exhaust flow rate at idle still helps to preserve heat in the aftertreatment system. The engine out NO_X for this calibration is also higher in the later sections of the cycle, following the extended idle. In this case, the engine out NO_X is 20% lower for the final 1300 seconds of the cycle compared to the Initial run and 3% better on fuel economy. It is important to decouple the fuel savings, which are mainly due to the idle exhaust flow rate revision. This calibration demonstrates the impact of utilizing the high NO_X or low NO_X calibration on fuel economy.

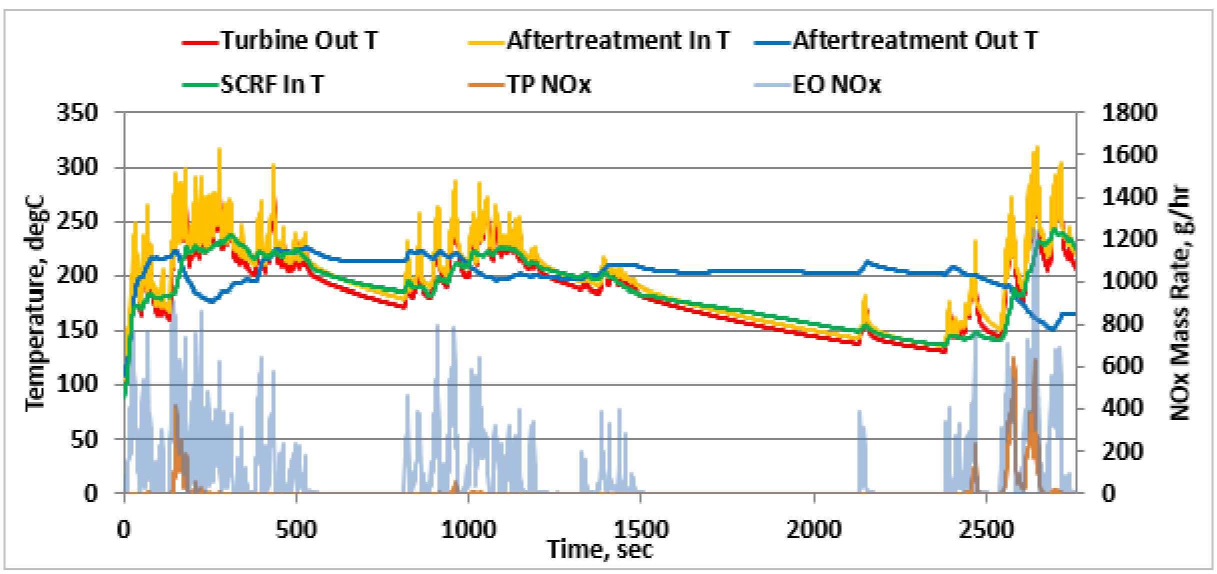

FIGURE 54. LLC DEV2 CYCLE VARIANT RESULTS: HIGH TM / LOW NO_X

The discussion, up to this point, has relied on a singular engine state for the entire cycle. However, during different engine conditions, there is the possibility of optimizing the engine-out strategy by switching between the fuel economy map and the High TM map to further improve the fuel consumption. Map switching, in this case, is triggered by the aftertreatment temperatures for on demand exhaust temperature management. The engine mode value shown below corresponds to an engine map calibration based on aftertreatment temperatures and engine sensor feedback (e.g. coolant temperature). Data presented in Figure 55 provides further insight on the engine map switching as a function of aftertreatment exhaust temperatures. In these charts, engine mode switching is shown in purple, with a value of 18 indicating a mode targeting higher fuel economy, and a value of 15 indicating a transient operating mode used at lower AT temperatures that is more focused on heat preservation. In the case of the High/Low NO_X switching (shown in black), a value of 100 indicates High NO_X, and a value of 0 indicates Low NO_X

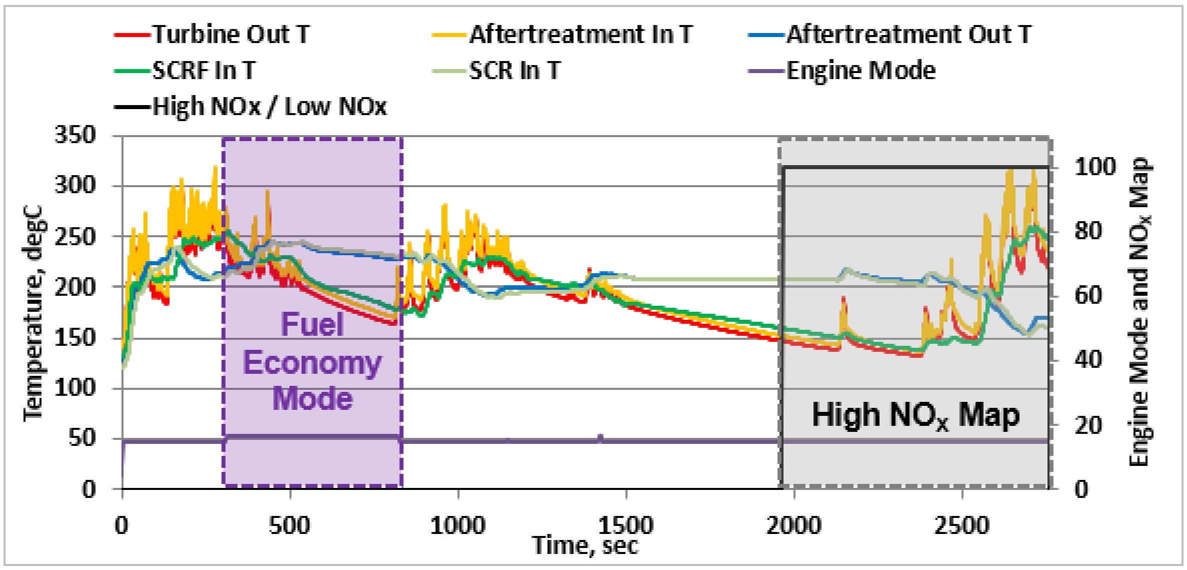

FIGURE 55. ENGINE MODE SWITCHING FOR TEMPERATURE AND ENGINE OUT NO_X CONTROL

In the control schemes explored, the SCR inlet gas temperature is used as the sensor feedback to determine the level of emissions and temperature control from the engine. As can be seen, low temperatures above 150 °C are shown to trigger the High TM engine map. One interesting observation to note is that fuel economy mode can be leveraged despite the fact that the aftertreatment inlet temperatures are low. This is because the SCR catalyst is hot enough to reduce NO_X during the period from 250 to 800 seconds. Once the aftertreatment temperatures at the inlet drop below 150 °C, additional NO_X reduction is required from the engine, which may result in a fuel penalty. The performance of this cycle was actually reasonable in that it did not incur a fuel penalty but did decrease NO_X by approximately 53% in the final 1300 seconds of the cycle. This result shows promise for a systems-level approach utilizing the mini-burner.

The next test involved migrating the strategies utilized in the short cycles to the complete cycle. Figure 56 and Figure 57 show the result of applying the aftertreatment engine calibration from the screening cycles to the LLC. Figure 56 depicts constant mode switching near the middle of the cycle to manage the decreasing idle temperatures. As discussed in the previous paragraph, focusing the high NO_X map on the cooling temperatures assists in mitigating the tailpipe NO_X breakthrough due to potentially inactive catalysts. Coupling this with alternating calibrations can decrease the NO_X by as much as 50% near the end of the cycle and without a substantial fuel penalty. Figure 57 provides additional insight on the continuous NO_X emissions. The calibration seems to do well at reducing the NO_X at the end of the cycle, but it cannot do much in other regions of the LLC. Nevertheless, the calibration was still able to achieve a 0.161 g/hp-hr at the tailpipe NO_X and 611 g/hp-hr of CO_2. This CO_2 level has no fuel penalty compared to the base engine, while achieving tailpipe emissions that are 50% below the original base engine calibration, without the use of the mini-burner for active thermal management.

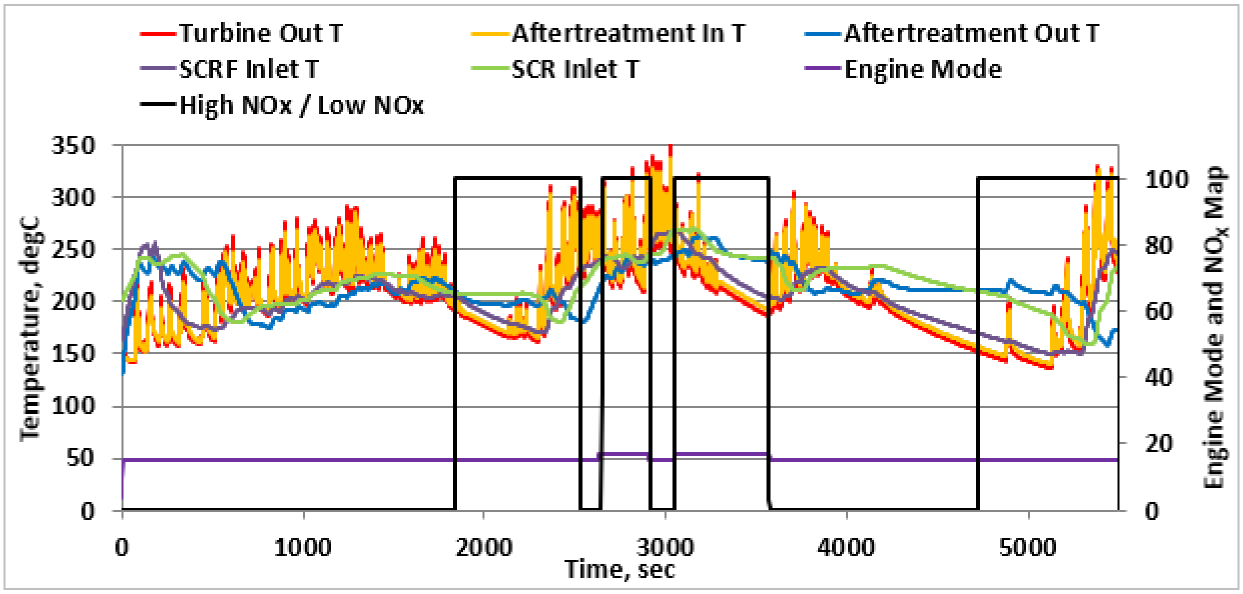

FIGURE 56. LLC ENGINE CALIBRATION WITHOUT MINI-BURNER

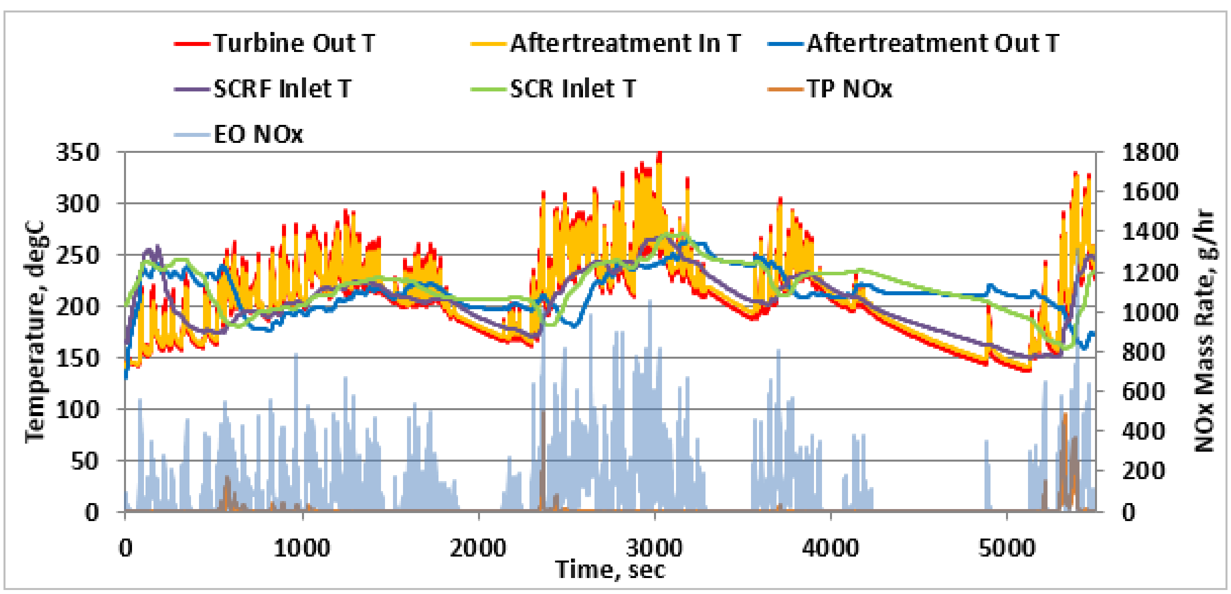

FIGURE 57. LLC EMISSION RESULTS USING ENGINE CALIBRATION ONLY

3.5 Aftertreatment Calibration Approach

The aftertreatment calibration approach was centered on utilizing the mini-burner to control catalyst temperatures within the cycle. Though the details of the mini-burner have been reported, it is worth mentioning the high-level overview of normal system operation. The primary burner hardware is comprised of the air supply pump, fuel supply system, ignition electronics, and the burner head. When the system is commanded "on", fresh air and diesel fuel are metered into the burner head. The head atomizes the fuel and swirls the air flow to create a plume, which then ignites over the spark plug. It takes approximately 8 - 10 seconds for the mini-burner system to ignite the fuel and air mixture. This includes the time required for the various systems (i.e. air supply and fuel system) to reach the stabilized conditions for proper ignition and sustained operation. While the components (excluding the burner head) were mounted remotely, the system was designed to be integrated onto a vehicle with minimal changes to the engine platform.

The burner control logic operates utilizing a state machine control framework and references the SCRF / SCR catalyst gas temperatures to determine the control state. The temperatures that determine the state conditions were made calibratable for the purposes of this approach. Based on the state, the burner would target a fixed heat input (calibrated on kilowatts of heat delivery) during early light and heat-up stages of a given burner cycle, and then switch to closed-loop control to achieve the target SCRF gas inlet temperatures. A maximum heat input limit was still utilized in closed loop control to prevent excessive fueling and stay within burner limits. These target and maximum heat input values were also made adjustable to optimize fuel consumption during different modes of mini-burner operation. A built-in provision to establish a minimum burner "on" time enabled further flexibility, as well as ensuring that the burner was not rapidly "short-cycled" (i.e. very short on times), which could lead to durability and ignition problems.

The first round of testing focused on the start of the cycle where the burner was operated following the hot soak period until defined aftertreatment conditions were achieved. The baseline NH_3 storage targets and burner settings remained the same as the HD-FTP calibration. The only engine calibration change that was carried over from section 3.3 was the reduced idle exhaust flow rate for optimal aftertreatment heat retention. Figure 58 shows the impact on SCRF inlet gas temperature following the cycle start with burner operation. The SCRF inlet gas temperature is observed to rapidly rise due to burner operation, which also helps maintain the aftertreatment out temperature near 250 °C. This results in reduced tailpipe NO_X breakthrough for the first 1900 seconds of the cycle. While the idle exhaust flow rate was lowered, the impact in the first segment of the cycle is considered minimal. Overall, the NO_X conversion performance for the initial 1900 seconds of the cycle improved from 91.7% (without mini-burner) to 99.7%.

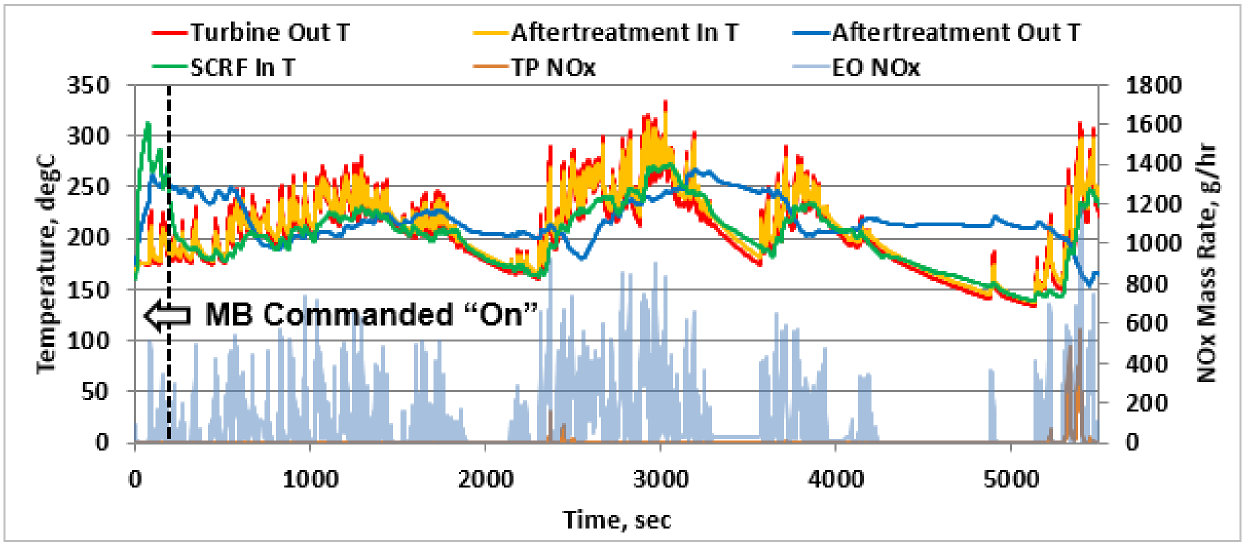

FIGURE 58. LLC MINI-BURNER ITERATION #1: BURNER OPERATION IMPACT AFTER ENGINE START

The remainder of the cycle shows improved NO_X tailpipe emissions, which is a result of the reduced idle exhaust flow rate. The two biggest improvements are shown in the extended idle segments between 1900 – 2100 seconds and 4300 – 5100 seconds where the aftertreatment-out temperatures are constant for a longer period of time. In addition to the temperature benefits, reduced NO_X is also observed in the latter idle segment when compared to baseline. This also helps improve the overall tailpipe emissions by reducing NO_X during conditions where the aftertreatment system is the most vulnerable. The combined impact from the burner and idle exhaust flow rate update reduced the brake-specific NO_X emissions from 0.27 g/hp-hr to 0.13 g/hp-hr.

As expected, utilization of the mini-burner yields an improvement on the overall NO_X emissions. The next step in the process was to evaluate the other areas where NO_X tailpipe breakthroughs occur. This, however, requires a different burner strategy to maintain ideal catalyst temperatures. The state, known as burner "re-light," references temperatures that were determined during the Stage 1 baseline evaluations to prompt burner use during a cycle. The use of the burner enables heat retention during cycle segments where the aftertreatment experiences "cool down" periods. As previously discussed, the baseline results shown in Figure 52 demonstrate that aftertreatment temperatures can decrease below 150 °C. While NO_X reduction is a challenge at this low temperature, the NO_X reduction performance is negatively impacted below a threshold of 200 °C. Therefore, it is important for the controller to predict the optimal moment to initiate the burner system. This will maintain high catalyst performance, while minimizing the amount of fuel required.

Table 11 summarizes the initial temperature target parameters for the SCRF and SCR catalyst re-light state. The re-light temperature in the second and third columns, represent the average temperatures across the catalyst required to initiate the re-light operation. It is important to note that both conditions must meet, or fall below trigger temperatures to command the state. The exit temperatures reflect the conditions required for the re-light state to be commanded "off". At this point, it is understood that the temperatures are high enough for the catalysts to perform well for some time. In the event that the catalysts are able to achieve the exit temperatures quickly, there is also a built-in minimum "on" time parameter that ensures the burner is utilized for at least 120 seconds. This parameter prevents fuel nozzle clogging issues in the event that the system is not able to reach stabilized conditions.

TABLE 11. MINI-BURNER RELIGHT INITIAL TEMPERATURE SETTINGS

Cycle	SCRF Re-Light Temperature	SCR Re-Light Temperature	SCRF Exit Temperature	SCR Exit Temperature	Minimum "On" Time
LLC7	185 °C	205 °C	205 °C	225 °C	120 s
LLC7DEV1	185 °C	190 °C	205 °C	210 °C	120 s
LLC7DEV2	175 °C	195 °C	195 °C	215 °C	120 s
LLC7DEV3	175 °C	180°C	195 °C	200 °C	120 s
LLC7DEV4	205 °C	215 °C	225 °C	235 °C	120s

Figure 59 highlights cycle segments utilizing the re-light feature according to the temperature conditions in Table 11 in row three (LLC7DEV2). The first segment represents the target warm start conditions following a "hot soak" where the engine is off. The three remaining segments represent an active re-light state to maintain or increase catalyst temperatures. The overall emissions are shown to be lower in these areas given the increase in temperature, which increases catalyst performance. Even the most challenging part of the cycle at the end shows significant improvement over the baseline and first iteration of applied modifications. This portion also signifies the part of the cycle where the burner "on" time is the highest. With the extended idle time, the thermal propagation is delayed, and the SCR catalyst does slightly go below 200 °C. Even though the SCR temperature decreases, the NO_X slip during this portion of the cycle is mitigated. This is likely due to the increased activity from the SCRF temperature that can aid the SCR in the event that it is cooling down.

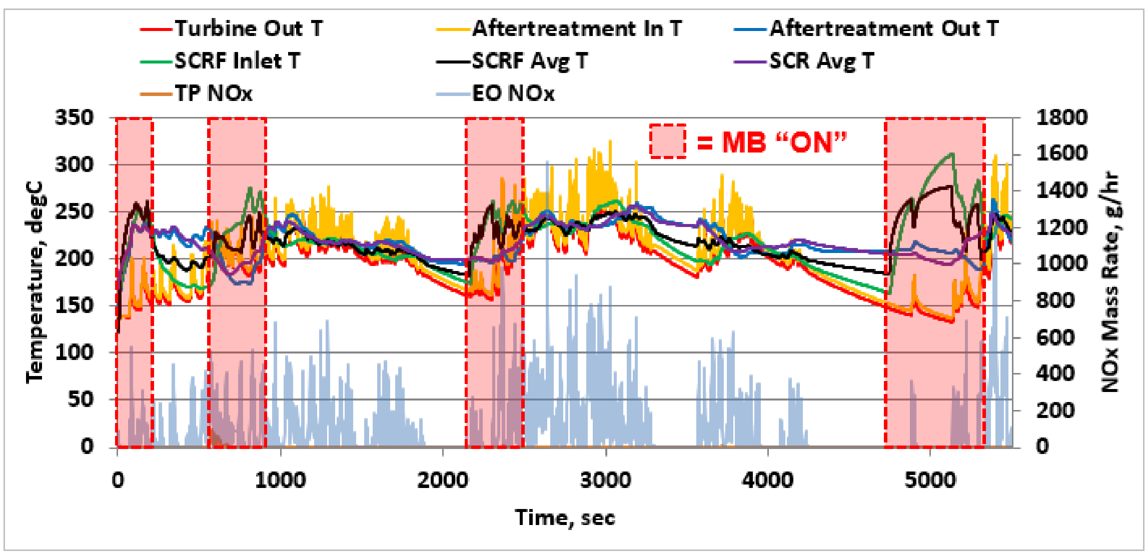

FIGURE 59. LLC MINI-BURNER ITERATION #2: RE-LIGHT FEATURE AUGMENTATION RESULTS ACHIEVING 0.02G/BHPHR WITH 2% FUEL PENALTY

The re-light strategy improved the overall tailpipe NO_X emissions performance from the previous cycle result of 0.13 g/hp-hr to 0.02 g/hp-hr. This result emphasizes the minimal effort required for substantial NO_X reduction. This was also accomplished without the need of engine calibration intervention aside from the idle exhaust flow rate decrease, which further simplifies the solution integration. As part of these efforts, additional experiments were conducted to explore the sensitivity of burner settings changes and will be discussed later in this section. For example, slightly altering the target temperature parameters could reduce cumulative burner utilization while providing effective aftertreatment thermal management.

In addition to the observed benefits presented, fuel economy impacts were also considered as part of the study given the existence of extended idle segments. The utilization of the burner and first iteration of parameters increased fuel consumption by approximately 4% over the Initial cycle to 622 g/hp-hr. This result stresses the need to refine the burner calibration to mitigate the fuel economy penalty, a 2% penalty compared to the baseline engine result. The calibration and mini-burner trigger changes made did not significantly affect FTP or RMC-SET fuel consumption, because these changes primarily impact the burner re-light function which does not come into play during those cycles due to the higher catalyst temperatures. Though this result meets the 0.02 g/hp-hr requirement, it must also be practical for future applications. What is labeled a 2% fuel penalty is referenced to the LLC fueling rate commensurate with its 6-8% average load and only applies to the portion of the vehicle duty cycle that is at low load (judging from the 20% of the NREL windows used to generate the LLC). The impact of this offset on real world customer fuel consumption will vary depending on application duty cycle, and it will likely be smaller if the duty cycle is higher than the 6-8% of average power represented by the LLC.

Given that no hard target had been established, there is some margin that has to be accounted for demonstration emissions results. Therefore, continued work focused on strategy optimization to minimize the fuel penalty and retain high NO_X performance reduction.

3.6 Strategy Optimization and Final System Approach

Experiments discussed in sections 3.3 and 3.4 utilized conservative settings to achieve high performance results. However, tradeoffs were observed with an increased fuel penalty due to aggressive engine thermal management and mini-burner operation. To address this problem, additional cycles were evaluated to consider the potential for a more optimized solution. The focus considered elements from the engine calibration and mini-burner approach. CARB has strong simultaneous emphasis on both its climate and criteria emissions reduction programs, so exploring a range of calibration choices was necessary to understand the interplay of NO_X and fuel consumption inherent to this Stage 1 technology set.

Section 3.3 outlined several maps and calibrations that were shown to be useful for reducing engine out NO_X. Though there wasn't a lot of temperature that was generated from the engine, emissions in certain sections of the test could still be reduced by 50%. This strategy proved to be ideal for a non-burner case, but the optimized solution requires a less conservative approach. It is more practical to allow the burner to increase the temperature in areas where high NO_X slip is reported. Figure 60 shows that the calibration for this is less aggressive than before. Areas that traditionally use the high NO_X map initiate settings sooner in the cycle because the burner turns on during low temperature conditions. It was also shown that, even with a conservative approach, the aftertreatment system required further intervention to reach the discussed target. The provided calibration is very similar to the original HD-FTP strategy.

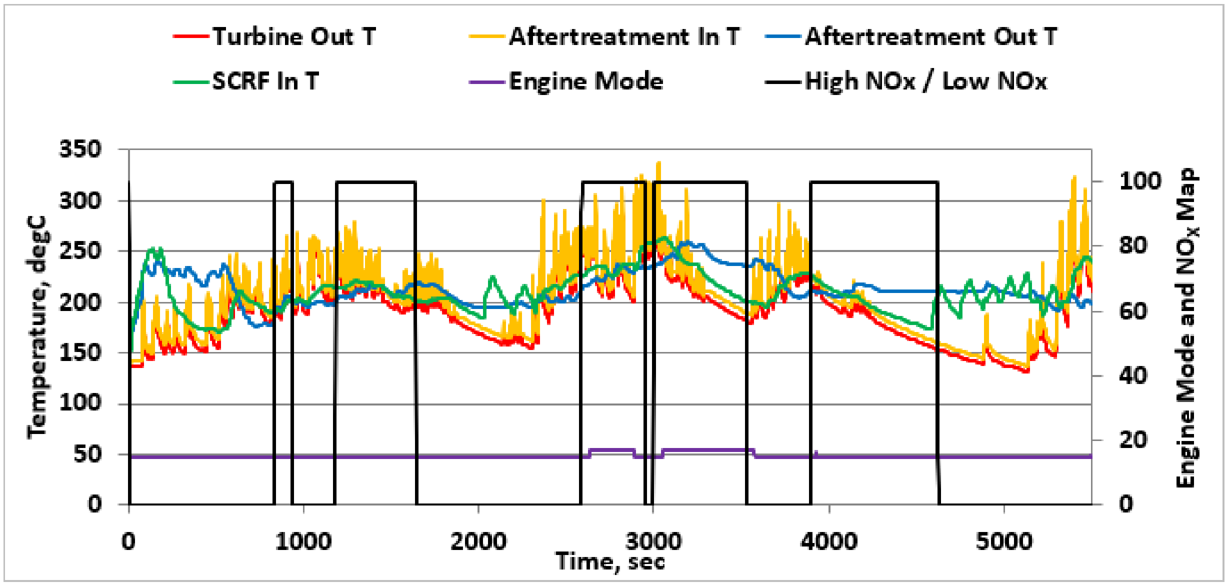

FIGURE 60. OPTIMIZED ENGINE CALIBRATION FOR FINAL DEMONSTRATION

In section 3.4, burner operation was observed to be online for extended durations, which increased fuel consumption. Because this strategy yielded very low tailpipe NO_X results, there was an opportunity to explore a less aggressive solution with the mini-burner. To start, the re-light temperature triggers were slightly adjusted to improve aftertreatment thermal management. For this strategy, the relight temperatures for SCRF and SCR were adjusted to 190 °C and 210 °C, respectively.

The mini-burner was controlled to produce a target heat output rate, and that heat rate was adjusted during these re-light modes to a lower level than what was used during cold-start warm-up, as a means to conserve fuel. However, there was a lower limit to the reduction of this heat rate due to issues of flame stability as the burner was operated leaner. This lean limit also prevented the use of closed loop temperature control on the burner, because this would have required very lean setpoints as the temperatures approached targets. Therefore, a cycling approach at the fixed heat rate was implemented where the burner would by operated for a 60-second period, which was generally more than enough to reach target temperatures, and then shut off. If the temperature dropped back below the threshold, the burner would be utilized again. In practice this approach allowed operation well above the lean limit of the burner, while at the same time preventing excessive “short cycling,” which would be detrimental to the durability of the burner system.

Figure 61 shows the optimized variant of the results discussed in section 3.4. The same areas are emphasized at the engine start-up, sustained low temperature operation, and extended idles. In this iteration, the burner activity cycling maintained the aftertreatment temperatures near 200 °C with small tailpipe NO_X breakthroughs. The SCRF inlet gas temperatures (shown in green) provide an insight on the burner cycling being that the temperature increases immediately following the burner light-off. A good example of this strategy is shown near the end of the cycle at 4500 seconds. The SCRF inlet temperature is cycling on and off, which causes a sharp increase and decrease in temperature.

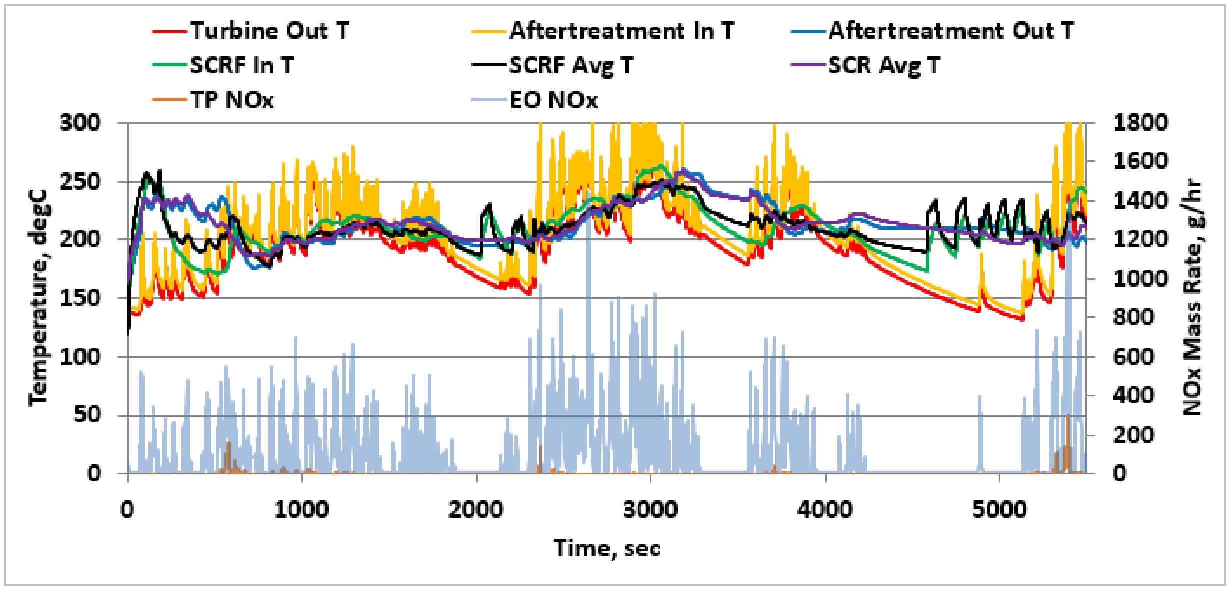

FIGURE 61. LLC MINI-BURNER ITERATION #3: OPTIMIZED BURNER CYCLING STRATEGY

This cycle resulted in a tailpipe NO_X result of 0.075 g/hp-hr or a 98% NO_X reduction. In regard to the $BSCO_2$, this iteration yielded 607 g/hp-hr or a which is essentially fuel economy neutral compared to the baseline engine. The dual approach provided reasonable results given the available technology and engine operation. Ultimately, given the desire to balance both NO_X reduction and GHG targets, SwRI selected a calibration point that provided maximum NO_X reduction at a fuel consumption neutralCO_2 level.

3.7 Final Demonstration System Results

Though the majority of the results that were presented were from the development system, it was still of interest to evaluate the Stage 1B system. The Stage 1B system was representative of full useful life aging that included hydrothermal and chemical aging. Aging was conducted utilizing an accelerated aging protocol known as DAAAC, or Diesel Aftertreatment Accelerated Aging Cycle. Because the system was exposed to sulfur and lubricant derived poisoning, understanding the impact on low temperature performance was crucial. Additionally, the Stage 1b system was subjected to ash loading so the temperature behavior would be altered due to the increased backpressure.

Figure 62 shows the temperature difference between the two systems and the impact that the added backpressure has on exhaust temperatures. The information is for the cycles without mini-burner intervention. It is evident that the final demonstration system has higher temperatures, which improved the overall NO_X reduction performance. Also, the higher aftertreatment temperatures yielded improved fuel economy since the trigger was not reached. Therefore, the fuel economy map was utilized for a longer period of time. The same could be said for the aftertreatment strategies that used the mini-burner for improved NO_X performance. For the non-burner cycle, NO_X reduction improved by 24% and a fuel economy benefit of 0.5% was reported.

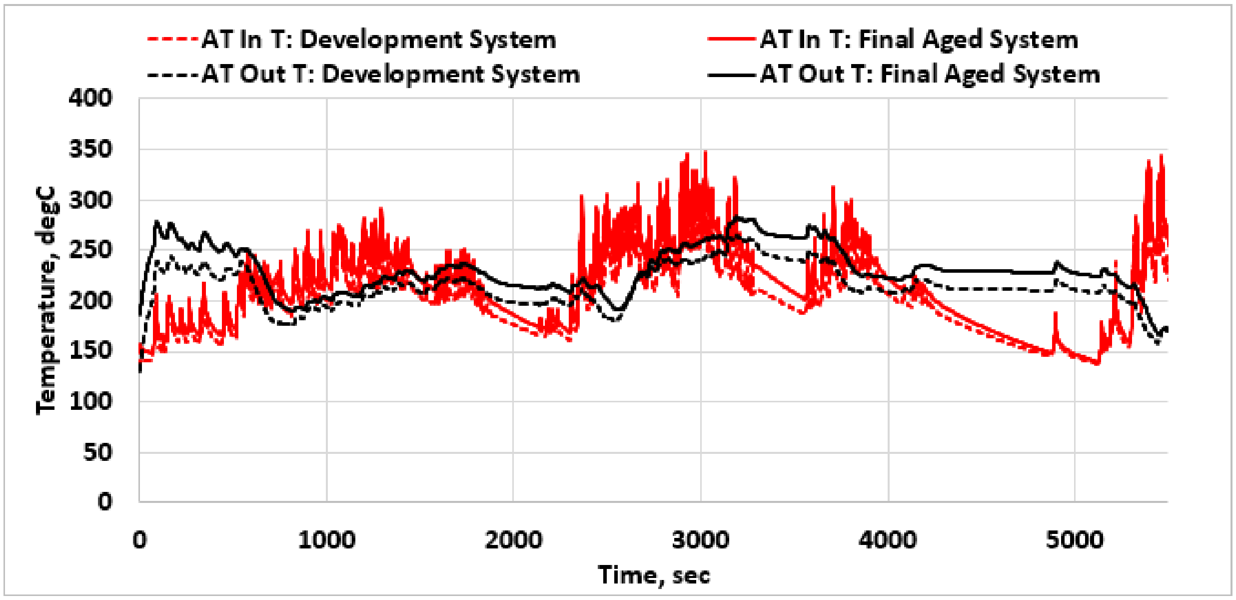

FIGURE 62. TEMPERATURE COMPARISON BETWEEN DEVELOPMENT SYSTEM AND FINAL AGED SYSTEM

The optimized mini-burner and engine calibration approach did not experience the same performance benefits that the engine calibration only approach reported. The tailpipe NO_X results remained similar and fuel consumption increased by approximately 0.5%. As previously mentioned, the backpressure increase over the development system is the likely root cause.

3.8 Results Summary

The results presented in Figure 63 represent the culmination of efforts that were characterized for this aftertreatment system. Throughout the process, it was evident that an optimized strategy encompassing both the engine calibration and the mini-burner was required to meet the performance demands. Trends shown in the figure highlight the increase in fuel penalty to increase the NO_X performance. To meet 0.02 g/hp-hr on the LLC required a 2% fuel penalty (from the extended burner utilization). The engine calibration was also examined for this case but did not achieve the Low NO_X target.

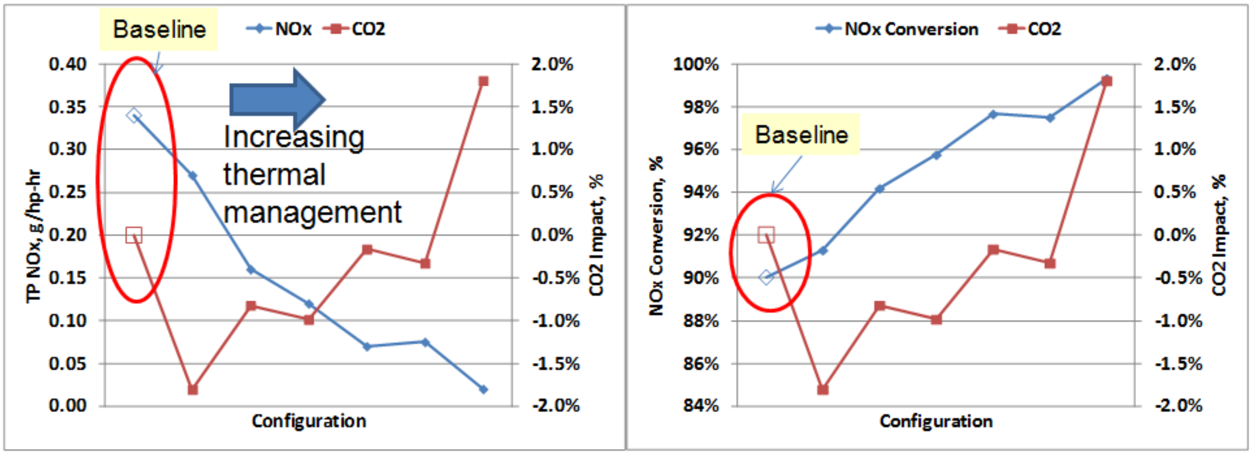

FIGURE 63. NO_X PERFORMANCE AND CO_2 TRADEOFF RESULTS

For reduced targets (e.g. 0.06 - 0.08 g/hp-hr), the fuel penalty over the LLC was near zero, assuming that the strategy was optimized. The calibration and thermal management techniques did not significantly affect FTP or RMC-SET fuel consumption. The results shown here are promising given that the low NO_X system provided a significant improvement over a commercially available system.

Table 12 presents the final results summary for the aftertreatment systems for the optimized cycles and the final integrated solution. Both the development aged and the final aged aftertreatment systems are shown.

TABLE 12. LLC RESULT SUMMARY

System	Calibration Approach	Engine Out NO_X [g/hp-hr]	Tailpipe NO_X [g/hp-hr]	CO_2 [g/hp-hr]	Idle Accessory Load
Development System	Engine Calibration Only	2.75	0.161	603	No
	Engine Calibration + MB	3.02	0.075	607	No
	Engine Calibration Only	2.60	0.098	594	Yes; 3.5 kW
Final Aged System	Engine Calibration Only	2.79	0.122	609	No
	Engine Calibration + MB	2.98	0.075	610	No
	Engine Calibration Only	2.58	0.095	615	Yes; 3.5 kW

4.0 IN-USE MEASUREMENT SIGNALS AND METRICS

A key portion of any upcoming NO_X regulation will be a likely update to the in-use testing and compliance portion of the standards. Although updates to the certification standards and the addition of the LLC will provide emission reductions and help extend emission reductions to the lower load operating space, these must be paired with a robust in-use compliance program to ensure that the expected reductions are being realized in-use.

In support of anticipated updates to the in-use compliance portion of the regulations, SwRI was asked to investigate two areas relevant to the upcoming revisions.

- Examine the accuracy of available engine-based parameters needed to support a sensor-based in-use compliance program, using current production engines.

- Investigate potential in-use metrics for emissions measurements, given the desire to extend in-use compliance requirements to the preponderance of the collected emissions data including currently off-cycle low-load engine operating regions.

Each of these two related topics will be discussed below in greater detail. It should be noted that this effort was not intended to design a new in-use metric per se, but rather the objective was to investigate a range of potential options and assess their strengths and weaknesses.

4.1 Accuracy of Engine Broadcast Variables

This effort involved the investigation of the accuracy of various engine broadcast parameters that could potentially be used to support various in-use metrics. The approach for this task was to obtain access to several current production (MY 2016 thru MY 2018) engines, and to record both broadcast parameters from the engine CAN bus and comparable laboratory reference measurements. This would allow assessment of the accuracy of the broadcast parameters as compared to the associated laboratory reference. A combination of steady-state and transient duty cycles was run to allow for comparison under a wide variety of conditions. It should be noted that the transient cycles generally focused more in the area of low load transient operation, given that there was more concern about these parameters at lower loads.

Three different production heavy heavy-duty diesel engines were used for the evaluation, as directed by the original program scope. Engines from three different manufacturers were used. The three engines were examined over the following duty cycles:

- The Phase 2 ARB Transient (40 CFR Part 1037 Appendix 1), a cycle included in GEM modeling of GHG compliance. The 9 GEM default Tractor application vehicles (40 CFR Part 1036.540 Table 3) were used to generate a set of 9 different ARB Transient engine cycles, and these were run in a manner similar to that of Phase 2 GHG mapping tests.
- The Stage 1 utilized engine translated ARB Heavy Heavy-Duty Diesel Truck Cruise-Creep cycle.
- The RMC-SET certification cycle to represent higher load and cruise operations.
- The newly developed LLC was also used where available.

The ECM parameters of interest for this effort were:

- ECM Broadcast Torque
- ECM Fuel Rate
- ECM Intake Air Flow Rate (or Exhaust Flow Rate)
- Tailpipe NO_X Concentration (based on the Tailpipe NO_X Sensor)
- Tailpipe O_2 Concentration (if available from the Tailpipe Sensor)

Engine Speed was also recorded but was generally very accurate and did not require much in the way of analytical effort to examine. These parameters were evaluated in comparison to laboratory measurements as detailed below.

4.1.1 ECM Broadcast Torque

It should be noted that ECM Broadcast Torque via the CAN bus is not necessarily a straightforward measurement, given that there is no single parameter utilized to determine net engine torque at the output shaft. Given that the same values were not always available on the J1939 CAN bus for all engines, SwRI recorded several different parameters to support this measurement.

The primary approach used for determining net engine torque involved the following parameters:

- Actual Engine Percent Torque (SPN 513) – Indicated % torque as a percent of Reference Torque
- Nominal Friction Percent Torque (SPN 514) – Friction torque and other parasitic losses as a percent of Reference Torque
- Engine Reference Torque (SPN 544)

ECM Broadcast Net Engine torque was then calculated as the difference between Actual Engine Percent Torque and Nominal Friction Torque, scaled using the Reference Torque. This value was used for comparison to the Laboratory measured torque. It should be noted that it was generally necessary to make this comparison using 10 Hz recorded data. Although it was possible to compare the data streams at 1 Hz, the low data rate would sometimes cause the two data sets to be out of phase with each other due to aliasing issues. This phasing would complicate the data analysis, resulting in large dynamic errors in both the positive and negative direction. However, even at 1 Hz, some of the trends observed at low-load torque remained apparent.

Figure 64 shows an example data set from one of the test engines, in this case showing a segment of data at lower loads, generally below 30% of maximum torque. A comparison data set is given in Figure 65 showing a region of higher load transients, with torque reaching 80 to 100% of maximum torque. Both traces show the Torque Error, the difference between ECM Torque and Lab Torque, in green. As can be seen, at lower loads a high bias can be seen in the torque error, while at higher loads the error is seen to be relatively symmetrical around zero. This general pattern was observed across multiple engines, although the magnitude of the errors did vary somewhat from engine to engine.

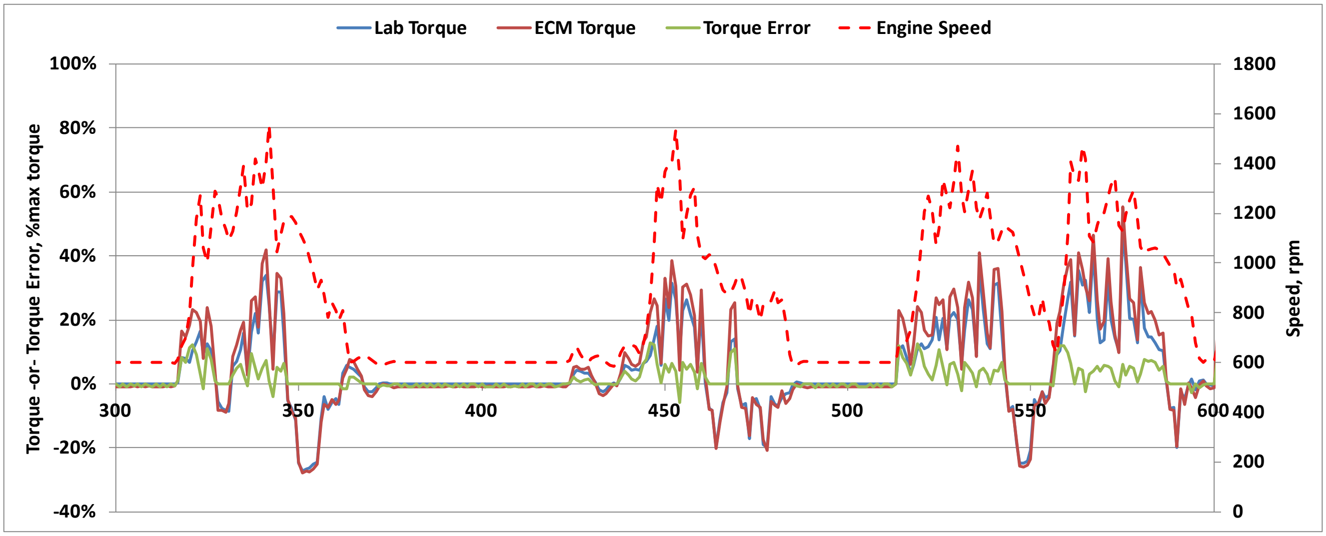

FIGURE 64. EXAMPLE OF TRANSIENT TORQUE COMPARISON UNDER LOW TRANSIENT LOADS

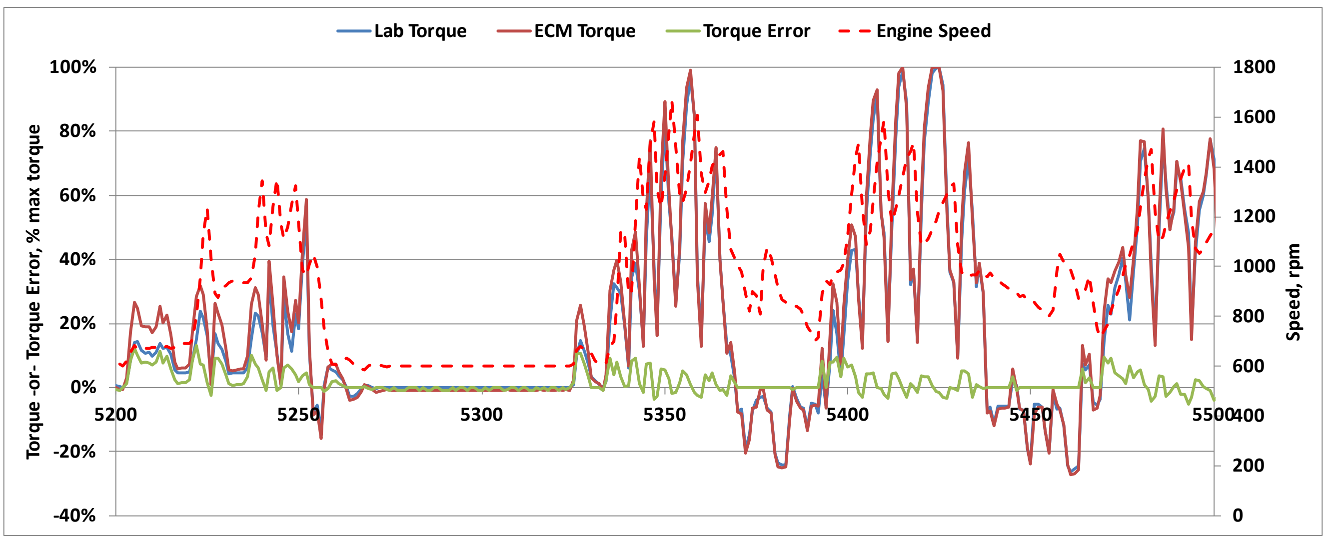

FIGURE 65. EXAMPLE OF TRANSIENT TORQUE COMPARISON UNDER HIGH TRANSIENT LOADS

Figure 66 shows a collected data set including LLC, ARB Transient, and RMC data for one of the test engines for the full range of measured torque, while Figure 67 shows the same data set only from the bottom of the torque range. Both charts also show a reference line representing one-to-one correlation between ECM Torque and Lab Torque. Over the full range, the torque is generally symmetrical to the reference line, but near the bottom of the torque range, a high bias is present.

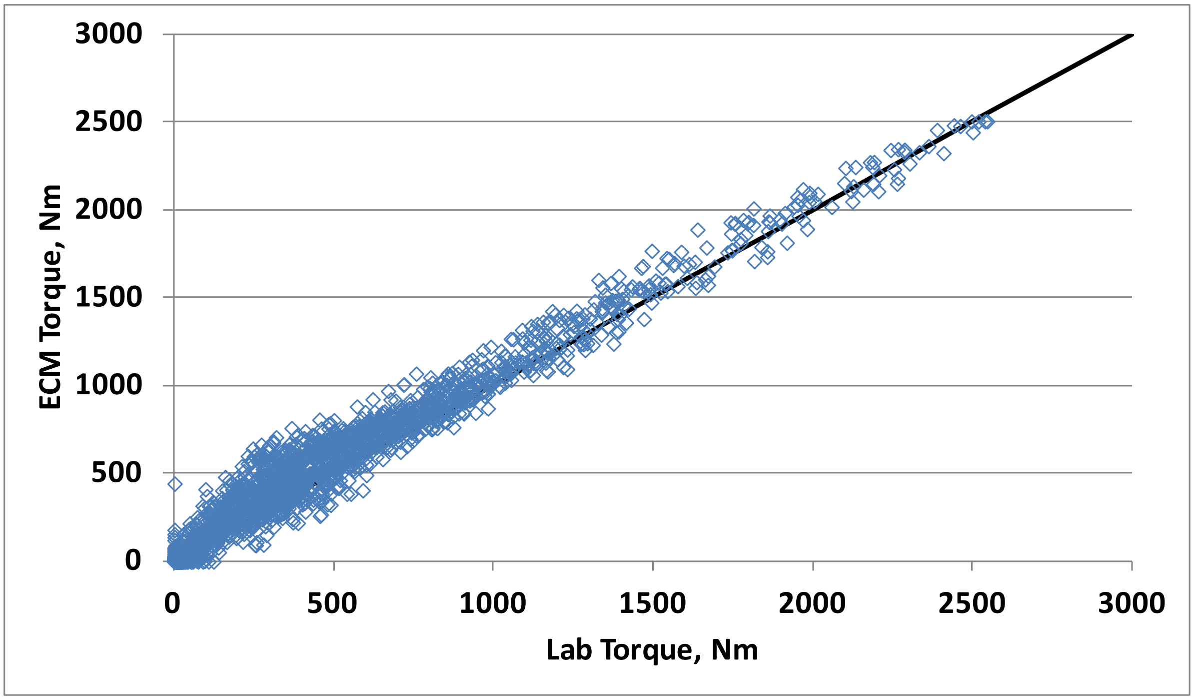

FIGURE 66. REGRESSION OF ECM TORQUE VS. LAB TORQUE - FULL TORQUE RANGE

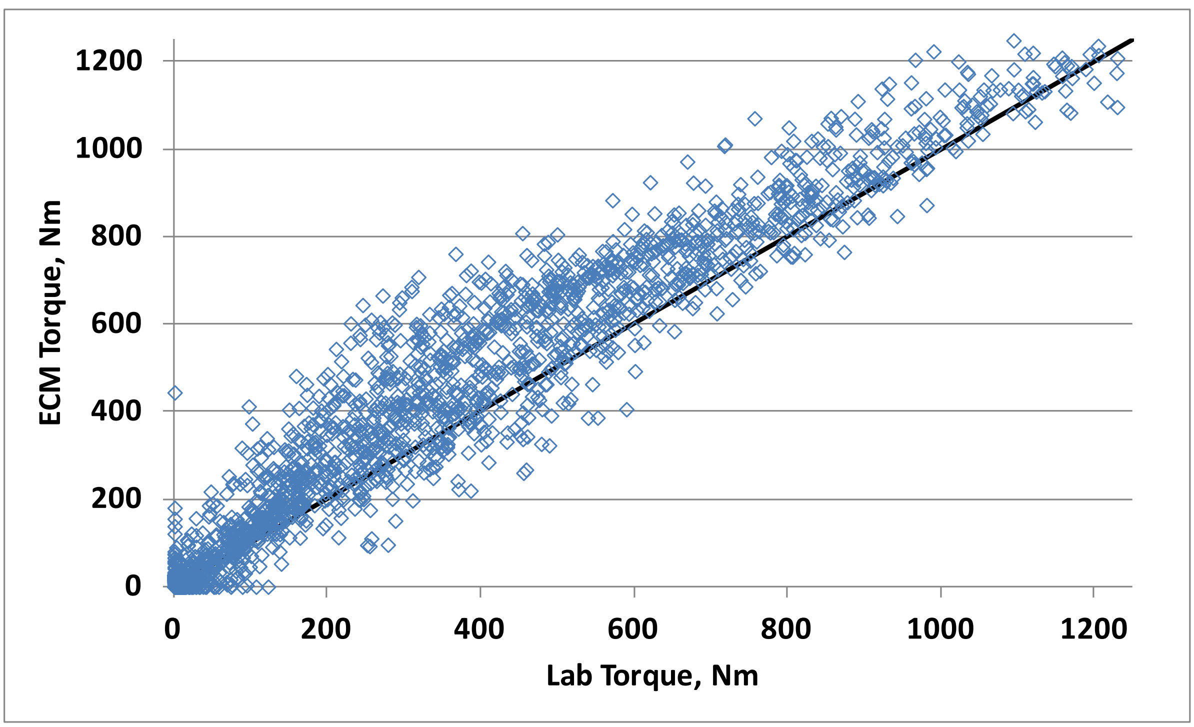

FIGURE 67. REGRESSION OF ECM TORQUE VS. LAB TORQUE – FOCUSED ON LOW-LOAD RANGE ONLY

The ECM Torque data set is summarized below in Table 13. The table shows the distribution of relative torque errors, for various ranges of torque from low load to high load. Some of the spread observed in this data set, especially at the 10th and 90th percentiles, is likely due to the recorded data sets being slightly out of phase. This may be due to in part to aliasing and the manner in which the data were recorded, even with a 10 Hz recording frequency. However, the distributions give a sense of the relative magnitude of the errors observed, as well as the presence of any bias observed between ECM Torque and the Lab Torque. At high loads the broadcast torque is relatively accurate, showing only a slight positive bias. However, at progressively lower loads, larger errors are observed, and an increasing trend towards a positive bias on the ECM Torque can be seen. This trend is consistent across multiple engines.

TABLE 13. DISTRIBUTION OF TORQUE ERRORS AT VARIOUS LOAD RANGES

	Torque Error Distribution, % pt			
	Percent of Max Torque			
Percentile	< 10%	10-20%	20%-40%	40%+
10th	-26%	-9%	-2%	-3%
25th	8%	8%	4%	0%
50th	**31%**	**32%**	**11%**	**4%**
75th	71%	50%	22%	9%
90th	118%	75%	30%	14%

This observed trend has two implications regarding the use of ECM Torque as a load metric for in-use compliance measurements. First, the direct use of ECM Torque is subject to significant errors in the Low-Load operating regions and could also result in a low bias on a brake-specific measurement. This is compounded by the fact the direct use of measured torque and/or power in the denominator of any metric will result in problematic behavior as the net output torque nears zero. Given that CARB has indicated a desire to extend the load range of in-use compliance to idle and near zero net power operating regions in the future, these problems are very significant for metrics with torque (or torque derived work) in the denominator. Therefore, it is recommended that some other form of load metric should be used in the denominator of any in-use compliance structure, at least at low-loads.

The observed behavior does have another implication even when applied indirectly. It is understood that there is some consideration being given to a "binning" approach, wherein in-use emissions may be grouped into one or more load regimes. If this binning is based on a power metric, such as an average percent of maximum power over a measurement window, then these torque errors could result in the misclassification of measurement windows near a low-load bin. Therefore, even if torque and power are not used as a direct load metric, it is still recommended that improvements in ECM Torque accuracy would be useful under such a classification scheme.

4.1.2 *ECM Fuel Flow (and Predicted CO_2)*

ECM Fuel Flow is relevant in two areas. First it is a component of calculating ECM Exhaust Flow, unless that direct channel is utilized. Second, ECM Fuel Flow can be used as an alternative load metric in the denominator of an in-use compliance. This can either be done directly as fuel-specific emissions (g / kg-fuel), or by using fuel rate to calculate a CO_2 rate for use in a CO_2-specific metric.

For fuel rate, SwRI recorded the CAN variable Engine Fuel Rate (SPN 183). This value is given in units of liters/hr. In order to get to a mass flow rate, an assumed density of 0.851 kg/L was used. Furthermore, in order to translate mass fuel rate into a CO_2 rate, the following transfer function was used:

$$CO_2 Rate\ \left(\frac{kg}{hr}\right) = Fuel\ Rate\left(\frac{kg}{hr}\right)\ \times \frac{CWF_{fuel}}{CWF_{CO2}}$$

Where CWF_{fuel} (carbon weight fraction in the fuel was set to 0.869), and CWF_{CO2} is 0.273. It should be noted that in this case, both the assumed fuel density and the assumed CWF_{fuel} are a potential source of variability in a metric relying on this approach, because the properties of the actual fuel being used cannot be measured in a practical way continuously during in-use compliance testing. However, it should also be noted that there is some relationship between these two parameters, such that they do not vary completely independently from one another. Any assessment of measurement accuracy would need to properly account for this potential source of variation.

Fuel rate tends to be a very dynamic parameter during transient duty cycles, and therefore it was found that comparisons needed to be made using at least 10 Hz data in order to avoid issues with phasing and aliasing. Due to the fact that there is inherently some lag in the Laboratory direct fuel flow measurement instrument, especially on transient duty cycles, the Lab Reference for this ECM measurement was chosen as the measured CO_2 Mass rate based on emission measurements. So as to compare to the ECM fuel rate, the transfer function given above was used to translate the Lab CO_2 Mass Rate into a Fuel Mass Rate for direct comparison to the ECM fuel rate.

As with the torque measurements, data from several transient duty cycles were aggregated for the analysis. Figure 68 shows an example of the resulting comparison data. Regression analysis of this data set produced the statistics as given in Table 14 below. The regression statistics are given in a format similar to what would be used to validate the linearity of measurements instruments for laboratory usage in 40 CFR Part 1065. It should be noted that these values are close to the levels that would normally be required to validate a laboratory instrument against a NIST-traceable reference signal. Considering this comparison involves an ECM broadcast signal compared to a Lab reference, this measurement of performance is quite good. It should be noted that it is possible that some of the observed slope error could be due to fuel properties. It is also likely that on the order of 1% of the positive slope observed is due to carbon balance error in the test cell.

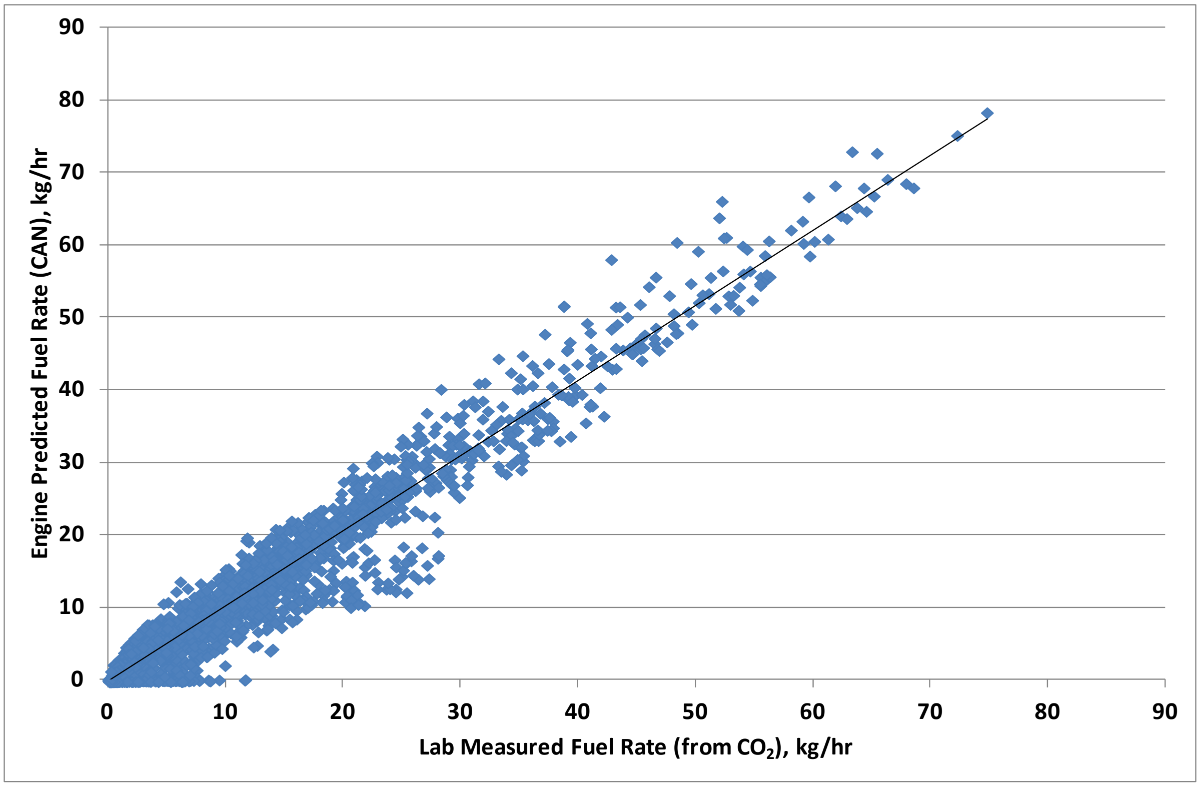

FIGURE 68. EXAMPLE OF CAN FUEL RATE VS. LAB FUEL RATE COMPARISON

TABLE 14. REGRESSION STATISTICS FOR EXAMPLE DATA SET – CAN VS. LAB REFERENCE

Slope	1.037	
Intercept	-0.3%	%max
SEE	2.7%	%max
R-squared	0.960	

As noted earlier, at least some the scatter observed in the 10 Hz data shown in Figure 68 is likely due to a small amount of phasing offset and aliasing, but this would likely be eliminated when the data is integrated over any reasonable measurement window. Therefore, these data indicated that ECM Fuel Rate is likely to be quite accurate for in-use compliance purposes.

Similar results were obtained for the other two engines examined in the program.

4.1.3 ECM Exhaust Flow and ECM Intake Air Flow

For all of the metrics examined, the numerator would be the mass rate of emissions for a given pollutant, with NO_X being the pollutant of highest interest for this effort. Because NO_X is reported as concentration by on-engine sensors, an exhaust flow rate signal must be used to translate that concentration into a mass rate. For the ECM signal, the exhaust flow was calculated as the sum of:

- ECM Fuel Mass Rate – as calculated from SPN 183 as noted earlier
- ECM Engine Inlet Air Mass Flow Rate (kg/hr) – SPN 132

Although there was concern regarding whether the Inlet Air mass rate would be available in all cases, this parameter was in fact available on all engines that were tested under this program. No difference in fidelity was observed analyzing the data at 10 Hz as compared to at 1 Hz.

In all cases, the Lab Reference is generated via methods given in 40 CFR Part 1065, using measured intake air flow rate and the chemical balance equations in 1065.655 to determine exhaust flow rate. The molar flow rate was translated into a mass flow rate to allow for direct comparison to the ECM predicted exhaust flow rate.

Table 15 shows a summary of regression statistics on the comparison of ECM Exhaust Flow and the Lab Reference Exhaust Flow. Continuous data from all three engines is shown in Figure 69, Figure 70, and Figure 71, for Engines 1, 2, and 3, respectively. For all three engines a combination of ARB Transient cycle and LLC data is shown.

TABLE 15. REGRESSION STATISTICS FOR ECM EXHAUST FLOW VS. LAB EXHAUST FLOW – THREE ENGINES

		Engine 1	Engine 2	Engine 3
Slope		0.997	0.976	0.956
Intercept	%max	0.3%	0.1%	0.7%
SEE	%max	2.4%	2.1%	2.4%
R-squared		0.971	0.984	0.984

As can be seen in the table and the subsequent figures, ECM predicted exhaust flow is generally well correlated with the Lab Reference. The slope for all three engines was very close to one and intercepts were near zero, indicated no biases. In addition, the standard error of estimate (SEE) was nearly good enough to meet the linearity requirements given in 40 CFR 1065.307 for a laboratory grade instrument when compared to a NIST-traceable standard. In general, this indicates good accuracy for exhaust flow as an input for in-use compliance testing.

It should be noted all three of these engines determined their intake air flow rate using a speed-density calculation involving Engine Speed, IMT, IMAP, and some form of calibrated volumetric efficiency assumption to determine a charge flow. In addition, all three engines featured a venturi-based EGR flow rate measurement, with that EGR flow rate being subtracted from the charge flow to determine a final Intake Air flow rate.

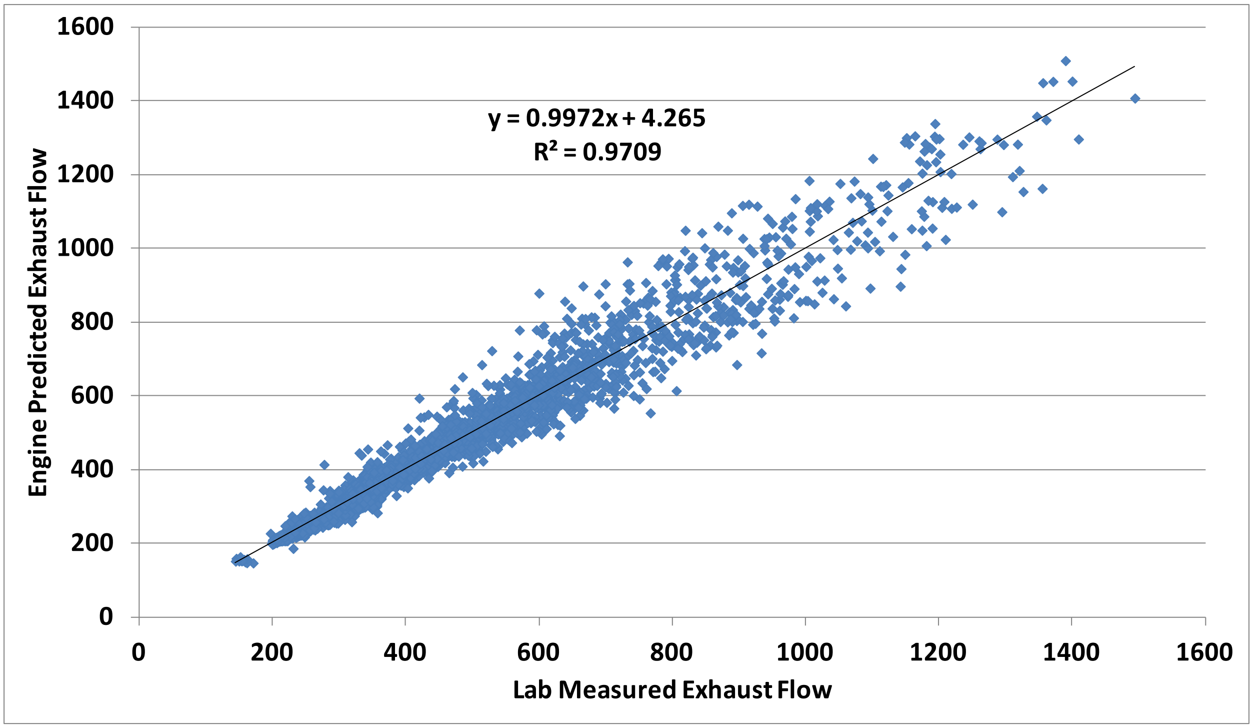

FIGURE 69. ECM VS. LAB EXHAUST FLOW – ENGINE 1

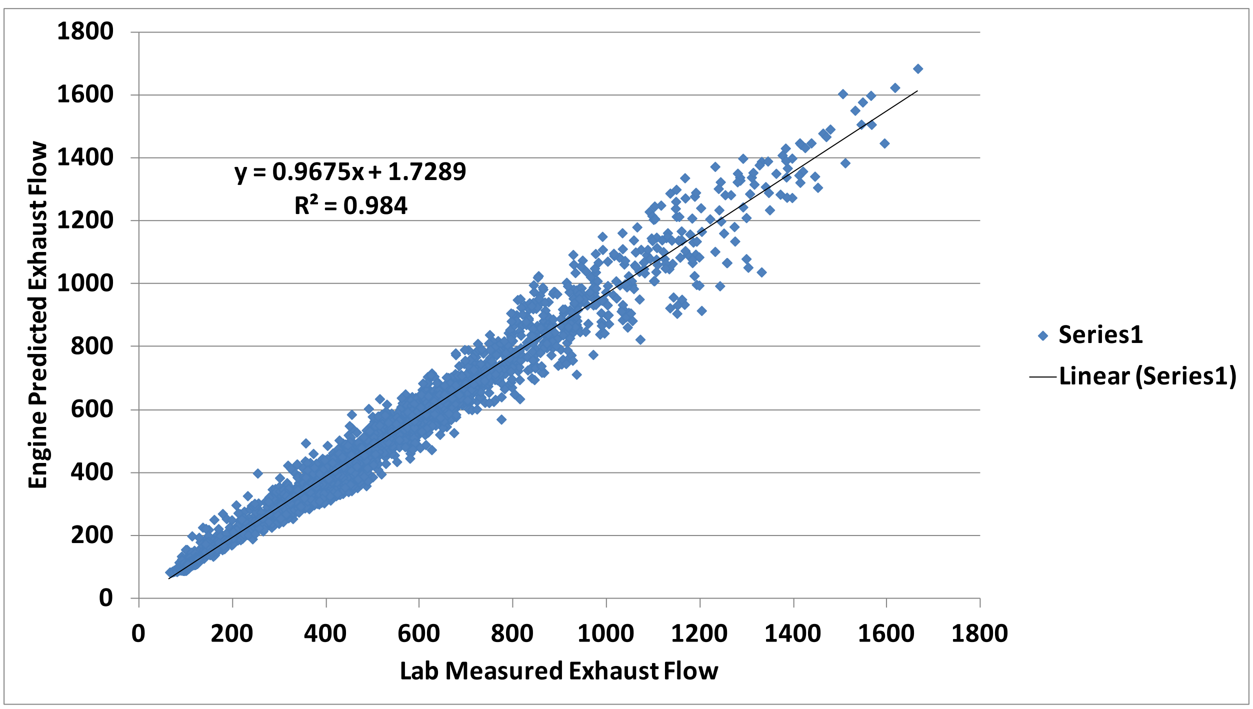

FIGURE 70. ECM VS. LAB EXHAUST FLOW – ENGINE 2

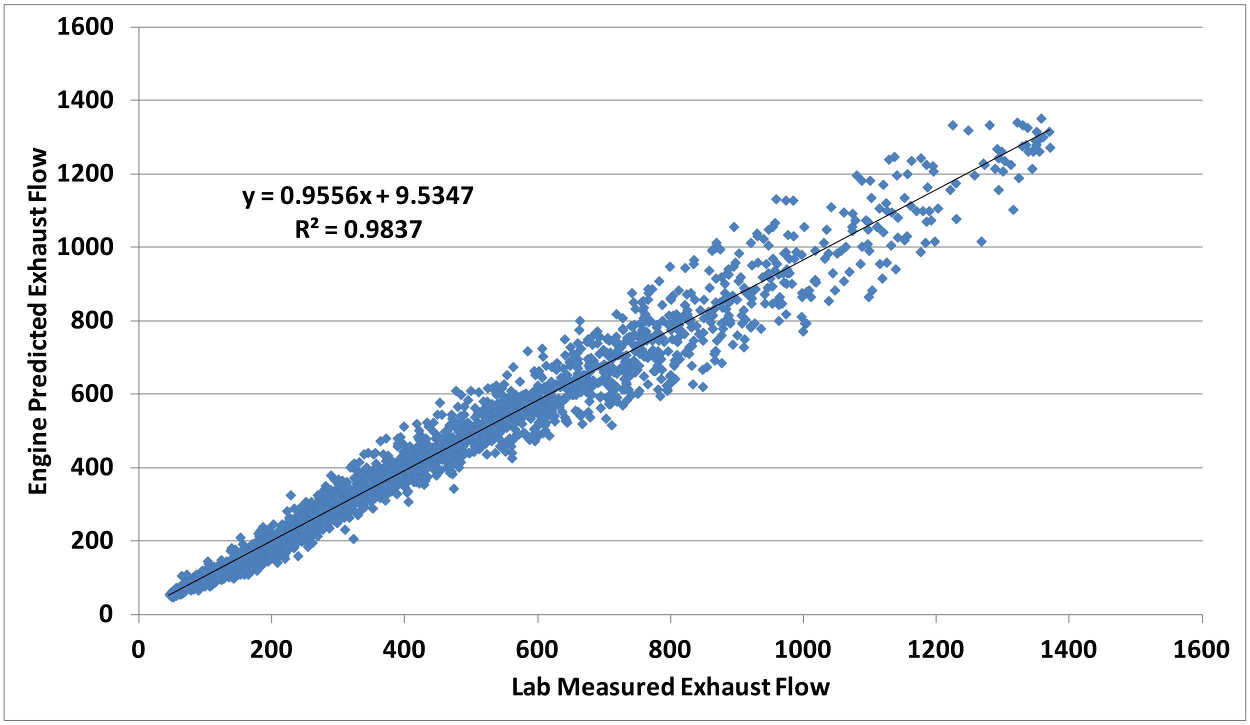

FIGURE 71. ECM VS. LAB EXHAUST FLOW – ENGINE 3

4.1.4 Tailpipe NO_X Sensor

A robust examination of the accuracy of tailpipe NO_X sensors is a complex task, and that was generally beyond the scope of the efforts included in this program. Other program efforts are currently in progress which will examine the accuracy of these sensors in great detail, along with a wide variety of factors that could potentially influence measurement variability on the field.

Although a detailed examination regarding NO_X sensor accuracy was beyond the scope of this effort, some observations may still be drawn regarding NO_X sensor capability based on the data recorded during this program. Figure 72 shows a comparison of tailpipe NO_X Sensor data and Lab Reference tailpipe NO_X, based on 10 Hz data after time alignment of the two data streams. The data shown here represents more than 98% of the total data set, which covers a range up to 300ppm of NO_X. The SEE for this data set was 27ppm, or about 9% of the maximum value of the data, and this fit shows an r-squared less than 0.9. It should be noted that there was no ammonia slip present for any of these data sets.

Data from both the Lab and the Sensor data set was used to calculate NO_X mass rates using the same set of ECM exhaust flow data. In order to eliminate some of the impact of data phasing and aliasing, the NO_X mass rate data was summed over 20-minute windows for both data sets. It should be noted that in areas where the NO_X sensors were not turned on, the affected data were scrubbed from the overall data set before this analysis was performed. Figure 73 shows the result of this analysis. Even when significant NO_X mass is present, substantial errors can be seen on the order of 10% to 20%, and the errors grow larger at low overall NO_X mass levels. It is clear that the NO_X sensor data at present is not yet at the same level of accuracy as some of the other ECM broadcast measurements, such as exhaust flow.

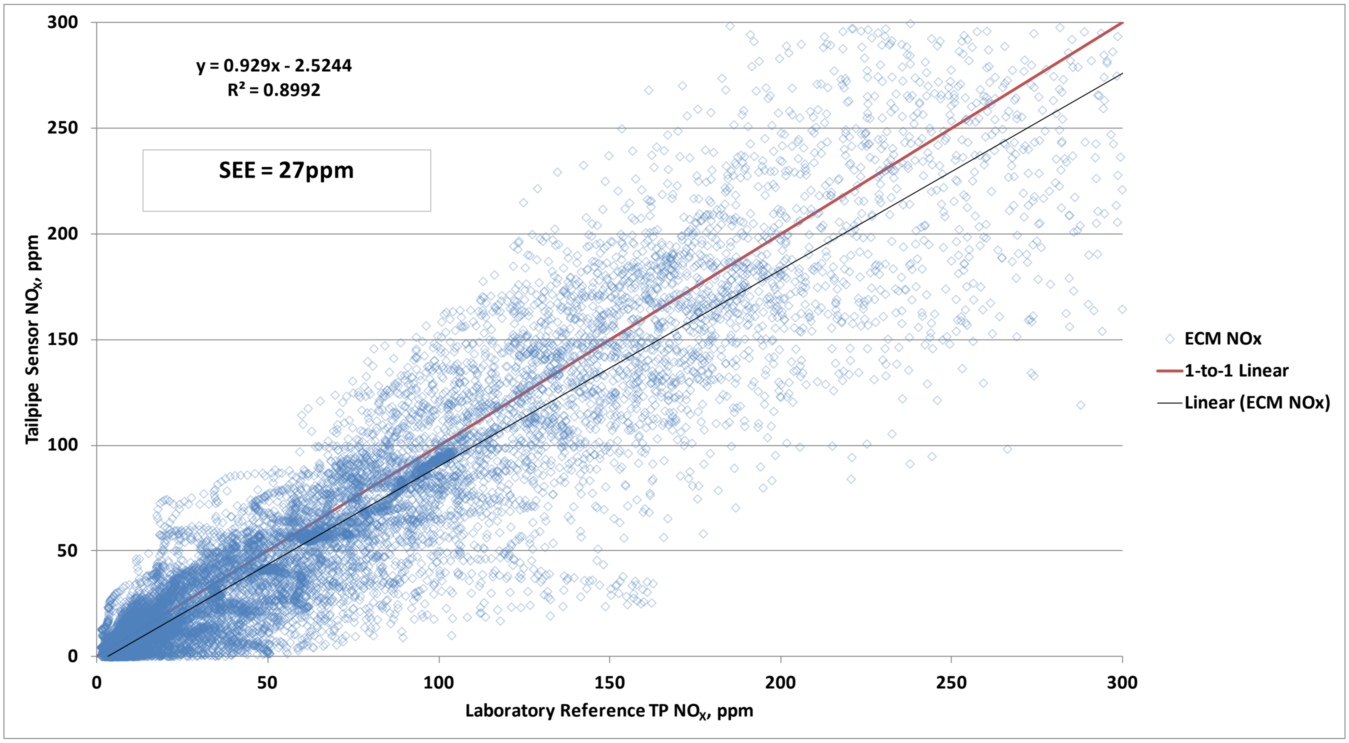

FIGURE 72. EXAMPLE TP NO_X SENSOR VS. LAB REFERENCE TP NO_X CONCENTRATION – LLC AND ARB TRANSIENT CYCLES

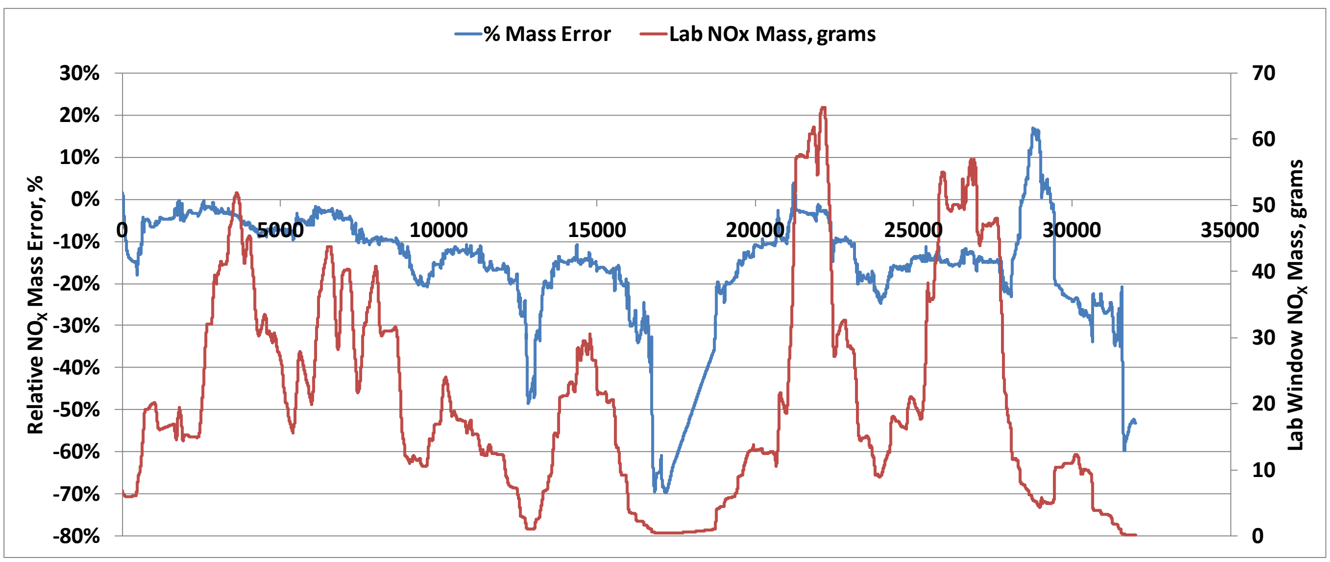

FIGURE 73. NO_X MASS RATE ERROR OVER 20-MINUTE INTEGRATION WINDOWS BASED ON SENSOR VS. LAB CONCENTRATIONS (WITH SAME EXHAUST FLOW)

4.2 Potential Metrics for In-Use Compliance

A second portion of the work related to in-use measurement was to investigate potential metrics for in-use compliance. Based on previous evaluations of fraction of daily activity assessed, the operational modes included, typical vehicle activity patterns, and observed in-use emission rates from studies conducted by CARB, EPA, ICCT, UCR CE-CERT, WVU and others, it has become clear that the current Not-to-Exceed (NTE) approach to in-use testing does not provide adequate in-use emissions controls, especially at low loads. In addition, there is a desire to move towards a compliance program which is based around on-board sensors, rather than a small selection of periodic PEMS measurements. These changes would require a different in-use compliance metric.

SwRI examined several possible approaches to working with continuous in-use data sets, with the aim of developing options that would be more suitable for low-load emission controls, and that would leverage larger portions of the data set than the current NTE approach.

4.2.1 Metric Basics

Fundamentally, an emission metric is a form of filter designed to extract information about compliance from a stream of continuous measurement data. As with any filter, a metric must be designed to strike a balance between smoothing the data sufficiently to allow for information to be extracted from the data, while at the same time maintaining enough responsiveness to not miss critical information.

The basic form of any engine emission metric is as follows:

$$\frac{Pollutant\ Mass}{Engine\ Output\ Metric}$$

For heavy-duty engines, the denominator has traditionally been in the form of Work performed (Power output over time). This allows the metric to scale with engine size, and is also consistent with the current emission certification standards, which feature a fixed known duty cycle. However, when the metrics must be applied to unknown duty cycles of varying lengths, brake-specific emission can become problematic, especially at low loads where output work can in fact drops to zero.

It would be possible to simply use pollutant mass over time (or distance), but this could potentially place an undue burden on larger engines and vehicles, so some form of scaling is still needed. Possible alternative output metrics could include fuel, CO_2 emissions, or more simply, results could even be scaled to engine maximum power. In the following analyses, SwRI focused on CO_2-based load metrics.

In the numerator, SwRI chose to retain the use of emission masses (or mass rates), rather than moving to a concentration-based metric or a flow-weighted concentration metric. The approach of using masses is also more compatible with subsequent potential use of in-use data for modeling and inventory purposes.

In the case of the results shown they were given in two forms:

- CO_2-specific mass in units of g NO_X / kg CO_2.
- An "estimated" brake-specific emission level, wherein the CO_2-specific emission level would be multiplied by a $BSCO_2$ level for the engine (usually the FTP certification value) to determine an est. $BSNO_X$ in g/hp-hr.

4.2.2 Metrics Examined

SwRI examined three basic approaches to windowing or filtering the data. In each of these approaches, emission mass would be determined, and a matching engine-output metric would be calculated on a similar basis. The approaches considered included:

- A Moving-Average Window (MAW) based on fixed time length windows. In this approach, both emission mass and CO_2 mass would be integrated over a window of pre-determined length (we examined 5 to 20-minute windows).
- A CO_2-Based Moving Average Window (CO_2-MAW), where the size of the window would be based not on time but on an amount of CO_2 emitted. In this case that amount of CO_2 mass would equate to some portion of the CO_2 emitted of an FTP certification test interval. This approach would be very similar to the current European window approach, but using only CO_2-based windows for compliance rather than the work-based windows.
- An Exponentially Weighted Moving Average (EWMA) wherein an algorithm is used to weigh the current data along with previous data points, in manner that produces an exponential decay in the influence of a given data point over time. This is an alternate filtering approach to using an averaging window as a filter.

The fixed-time windows were only examined for a short period of time with this study's analytical emphasis shifting toward the second two approaches which seemed closer to existing methods manufacturers are already using in other regions or applications. Recent CARB and EPA discussions are reconsidering the benefits of fixed time windows to mitigate weighting implications at low load of launching new windows at 1hz but ending them based on accumulated work that could be bunched at the conclusion of a long idle or low load period. Work based windows potentially overweight return to service events after a long low load period due to the linear in time launching of new windows whose lengths are all truncated at essentially the same absolute time one work window after the engine begins working again thus creating hundreds or thousands of windows defined by that return to service emissions performance.

4.2.2.1 EU-style MAW (CO_2-based)

Under this approach a window of CO2 mass is defined equivalent to some portion of the mass of CO2 emitted over an FTP. SwRI examined various potential windows sizes from 0.25 x FTP windows to 1.5 x FTP. Much of the data show later will focus on the 1 x FTP windows. Windows less than 0.5 x FTP were found to be too small and did not provide sufficient filtering, while going beyond 1 x FTP in windows size did not provide any benefits, and appeared to compromise responsiveness too much.

An example of the CO2-based window process is illustrated below in Figure 74. Once the first window is defined, the start point is then incremented one second at a time through the data with this windowing approach being repeated until there is not enough data left to form a complete window. Typically, emissions are quantified over each window, and the aggregated set of window results would be evaluated against some kind cap or distribution requirement.

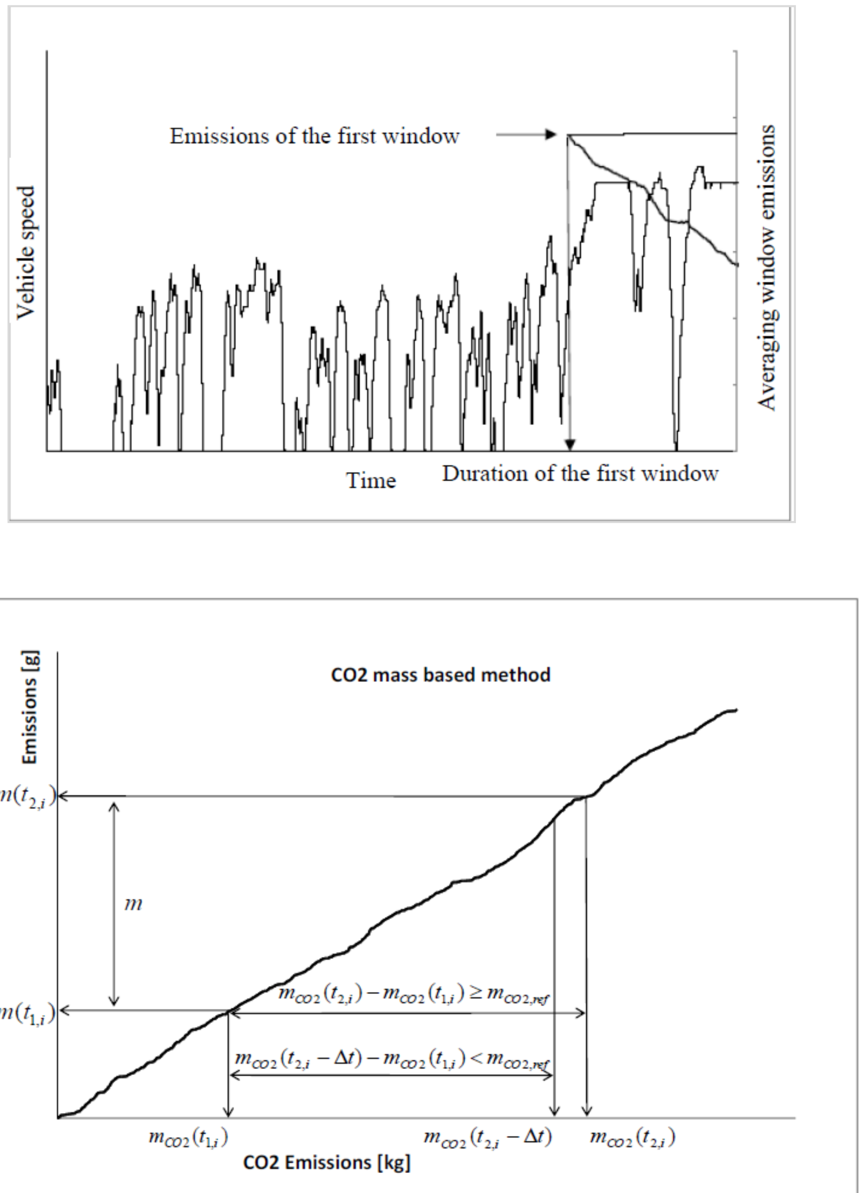

FIGURE 74. ILLUSTRATION OF CO_2-BASED WINDOWING PROCESS

In the current EU process, a valid window must have an average power of at least 10% of maximum engine power. However, for the current analysis, no such limits were imposed. An example of such an analysis on low-load data is given in Figure 75 showing input data, and Figure76 which shows the resulting analysis. Figure 76 shows resulting CO_2-based metric (in g NO_X / kg CO_2), and it also shows the average power (as a percent of maximum engine power) for the windows. Results are shown for window sizes of 0.25 x FTP, 0.5 x FTP, and 1 x FTP.

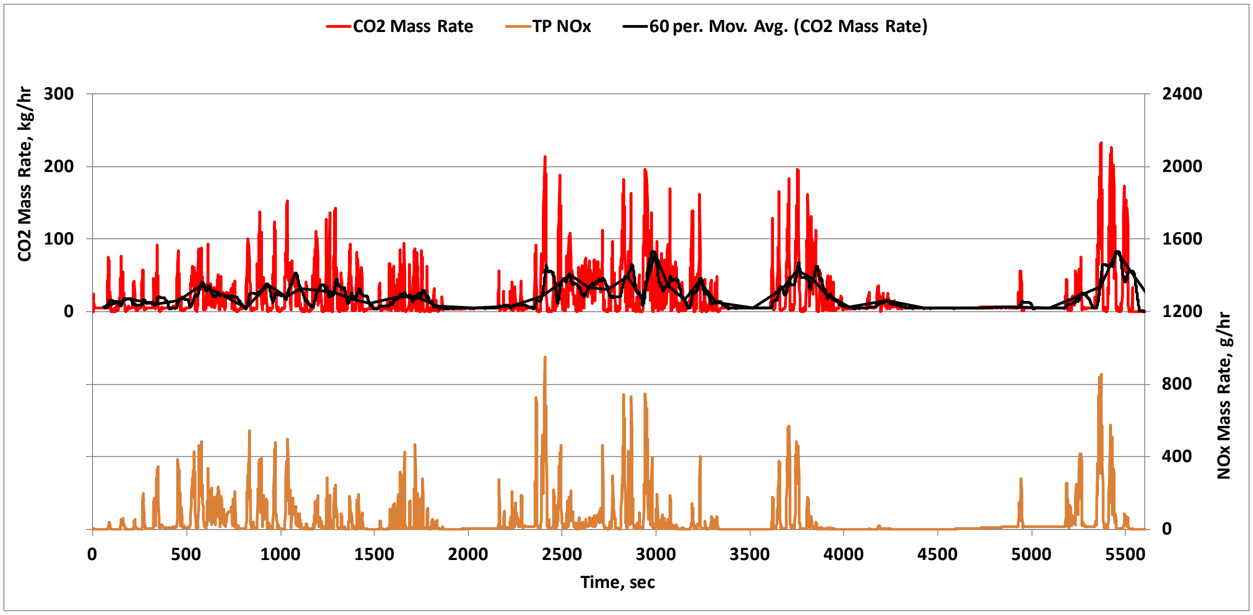

FIGURE 75. LOW-LOAD CYCLE DATA SET EXAMPLE FOR MAW ANALYSIS

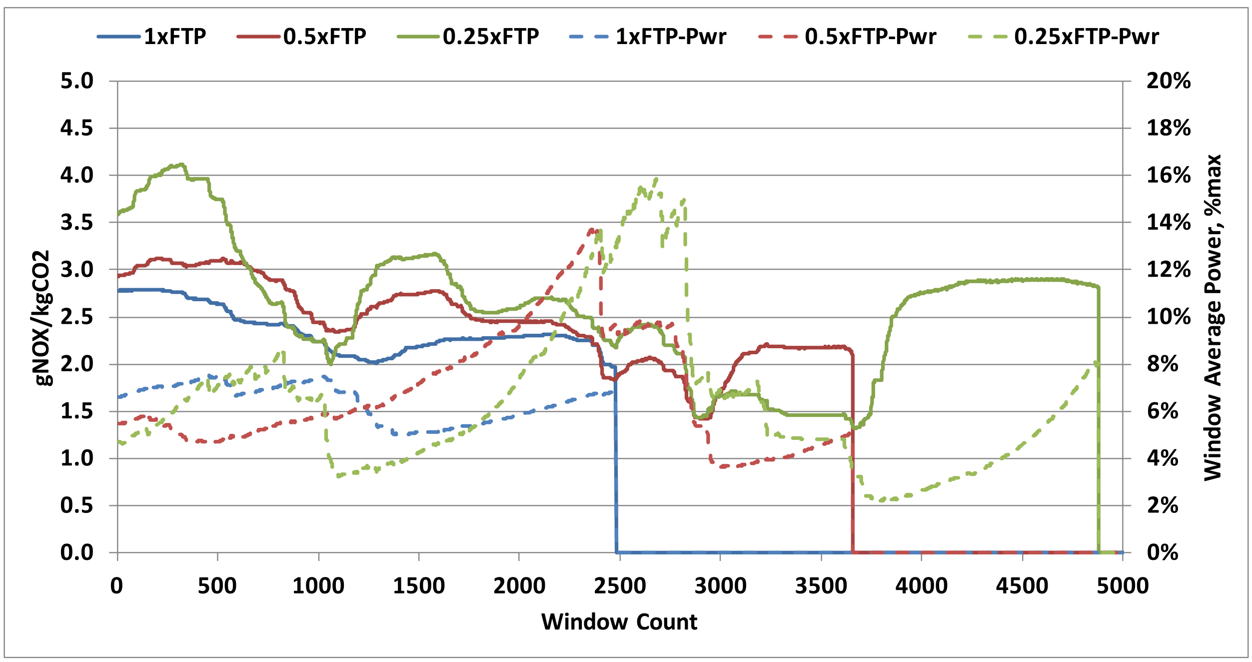

FIGURE 76. CO_2-BASED MAW ANALYSIS OF EXAMPLE LLC DATA SET (AT VARIOUS WINDOW SIZES)

It is possible to translate the result from the CO_2-based metric into an estimated $BSNO_X$ value using a cycle-averaged $BSCO_2$ result. Initially it was suggested that this translation could be done using the FTP cycle $BSCO_2$, which is a result readily available from certification data. However, at lower loads this could result in a low bias in the results. Therefore, it is recommended that if this translation is to be used, a binned approach should be adopted wherein lower load windows, generally below 10% average power, should use the LLC $BSCO_2$ instead of the FTP. This translation is illustrated below in Figure 77 using both the FTP and LLC values, although the latter is recommended in this case for the low power windows.

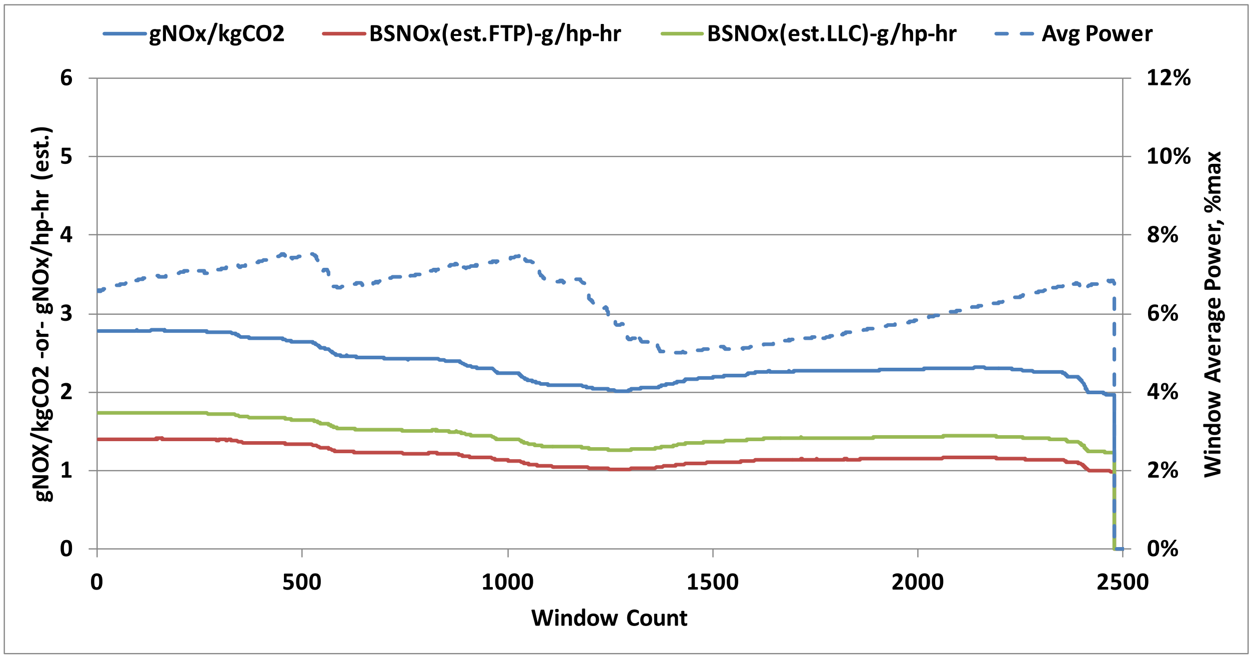

FIGURE 77. MAW NO_X RESULTS FOR 1 X FTP CO_2 WINDOWS – CO_2-SPECIFIC AND BRAKE SPECIFIC ESTIMATES

It should be noted that while the MAW approach is familiar to manufacturers who also sell products in the EU, that familiarity would not hold in cases where the MAW is applied to a wider range of duty cycles. Currently the EU places bounds on the range of duty cycles which may be considered valid for compliance but controlling the proportions of driving in 3 different vehicle speed bins to defined limits. One significant concern with the MAW approach at low loads is the elasticity of time at very light loads. On very light load duty cycles, well below FTP average loads, the windows can become very long covering larger segments of operating time, so that a single measurement event could be resident in large number of windows. However, the compliance metric typically rank-orders all of these windows, regardless of length. There is a concern that this approach could result in an overemphasis of these relatively brief spikes in a Low NO_X environment. The current EU regulation ignores this problem by effectively removing windows with average power below 10%. This potential issue must be examined carefully when that window power threshold is removed.

4.2.2.2 Exponentially Weighted Moving Average (EWMA)

As an alternative to a window-based approach, SwRI also investigated a more continuous metric that might be more conducive to simplified ECM calculations. In order to provide the required smoothing, SwRI looked at the use of an Exponentially Weighted Moving Average (EWMA) approach. This approach was selected in part because it is already frequently employed on engine ECMs in the context of OBD, where it is utilized to provide smoothing in order to reduce noise in a data set to allow for more robust pass-fail decisions with respect to an OBD threshold. A relatively simple closed-form equation can be implemented to calculate an EWMA, as shown in the equations below:

$$EWMA_i = EWMA_{i-1} \times (1 - \alpha) + Data_i \times \alpha$$

$$\alpha = 1 - \tau$$

$$\alpha = weight\ factor$$

$$\tau = system\ time\ constant\ in\ seconds$$

This calculation effectively weights the most recent data point against previous data points, and results in an exponential decay pattern over time in the weight of any give data point. An example of this weighting pattern is shown in Figure 78 for a weight factor of 0.2 (τ = 5 seconds). By adjusting the time constant τ, the relative weight of the latest data point and previous data can be changed, such that increasing the time constant will provide more of a filtering and smoothing effect. SwRI investigated a variety of different time constants as part of this work.

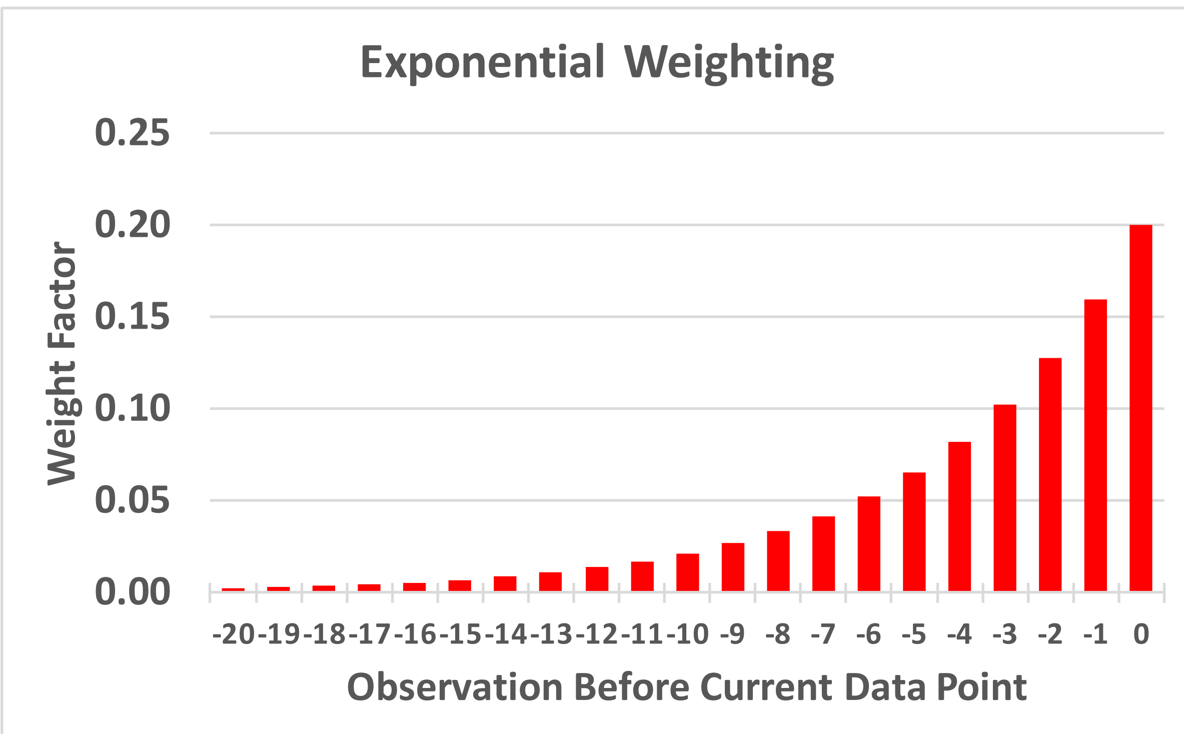

FIGURE 78. ILLUSTRATION OF EMWA WEIGHTING (ALPHA = 0.2, CURRENT DATA POINT ON THE RIGHT SIDE)

Another feature of the EWMA is that the algorithm can rapidly be started and restarted following an interruption or other disturbance by temporarily setting the time constant to a smaller number. In OBD algorithms, this is generally referred to as a "rapid response" feature. That feature could potentially be used in this context to start the EWMA calculation quickly after an engine start, or to restart the algorithm following some kind of interruption, such as a loss of CAN communication or a temporary sensor fault which could be considered as an alternative to longer full window length restart gaps or potentially concatenating available data sections across the data interruption gap.

In the cases studied by SwRI, the same time constant was used in both the numerator and the denominator of the metric. The numerator was thus the EWMA NO_X mass rate, and the denominator was the EWMA CO_2 mass rate. As with the MAW results shown earlier, the metrics are given as CO2-specific (g NO_X / kg CO_2), but this can be translated to $BSNO_X$ using a cycle $BSCO_2$ in a similar fashion.

Figure 79 shows an example of EWMA analysis for various time constants, based on the same data set illustrated in Figure 75 earlier for the MAW example. The longer time constants provide more smoothing of the data, while the shorter time constants are more reactive. Based on analysis of the various options, SwRI recommends a time constant on the order of 300 seconds as a good balance between smoothing and responsiveness. However, it is noted that in some cases at very low CO_2 values, the CO_2-specific metric can tend to "hang" a bit, even when NO_X emissions are also very low. Therefore, SwRI also investigated the possibility of a Scalable time constant (Scalable Alpha) wherein the value of the time constant would be reduced for CO2 values below 10% of the maximum value, as shown in Figure 80, which would reduce the time constant by a factor of up to 3 from a base constant of 300 seconds (alpha = 0.0033). As seen below in Figure 79 this scalable alpha approach provides a simple mechanism to keep the metric from run into hanging issues at low loads, while still being responsive to NO_X spikes.

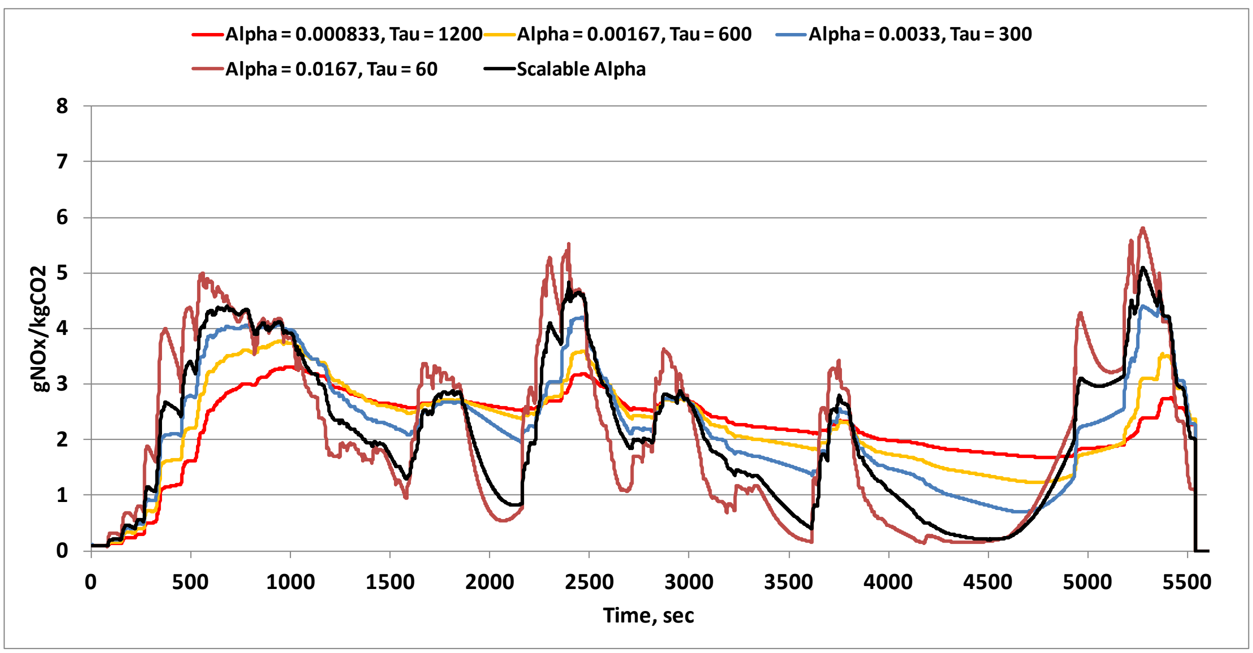

FIGURE 79. EXAMPLE OF EWMA ANALYSIS AT VARIOUS TIME CONSTANTS – BASED ON EARLIER LLC EXAMPLE DATA

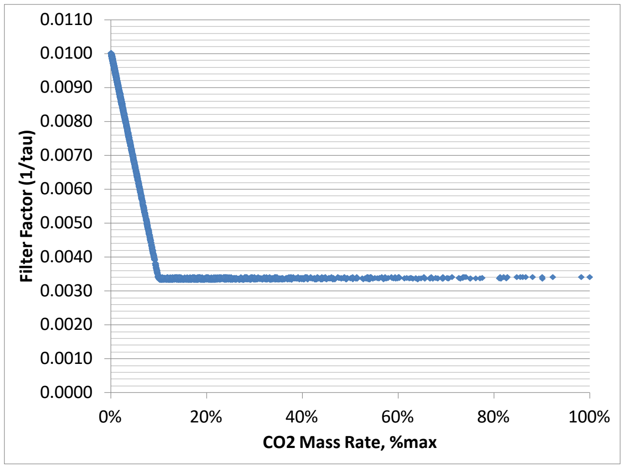

FIGURE 80. SCALABLE ALPHA (1 / TIME CONSTANT) FOR LOW CO_2 VALUES

The resulting data set from the EWMA with a properly scaled time constant provides better resolution in the data and appears to do a better job than the MAW algorithm at separating high NO_X regions from the rest of the operations. This better resolution would produce a result more useful for identifying the types of operation that are causing high NO_X regions to occur. This data would be somewhat more obscured by the MAW window approach as can been seen comparing Figure 79 to Figure 76. However, this higher degeneration of resolution also results in more dynamic behavior from the metric, which means that any compliance threshold must be calculated with this behavior in mind.

It is suggested that for a more responsive metric, it would likely be more appropriate to regulation compliance based on a distribution, rather a single compliance threshold (such as a conformity factor). Under this scenario, one could potentially regulate the 50th percentile of the distribution of EWMA results to a value that is near the standard, and then allow the 95th percentile to float to a significantly higher value (i.e., 5 times higher or even more). This would ensure that the majority of the data would be near the desired value, while permitting occasional excursions to higher values. If those high values become too frequent, they would begin to push up the 50th percentile as well, even if the 95th percentile value was still below a higher threshold value. This kind of distribution-based compliance would also provide more flexibility to individual manufacturers to plan a compliance strategy by either controlling high values more, or by pushing down the majority of the population to lower values. Either approach would achieve the desired goal of lowering in-use emissions.

The downside to the EMWA is that it represents an unfamiliar approach to compliance, and therefore might meet with resistance while manufacturers work to understand the implications of a different compliance metric.

4.2.2.3 Comparison of Metrics

Table 16 shows a comparison of distributions for results from the various NO_X metrics using the LLC data discussed earlier. The MAW results appear to cluster together more closely given the greater smoothing imposed by the window approach. It should be noted that with a long enough time constant and no scaling, the EWMA approach eventual begins to look quite similar to the MAW approach, with results for a 1200-second time constant EWMA being fairly close to the 1 x FTP MAW. The EWMA does do a better job of separating infrequent high events from more frequent operations, but the question will be whether this added level of information is valuable enough to change to a less familiar regulatory scheme.

TABLE 16. DISTRIBUTIONS OF RESULTS FROM VARIOUS NO_X METRICS

Percentile	EWMA-tau=300	EWMA-tau=600	EWMA-tau=1200	EWMA-scalable	MAW-1xFTP	MAW-0.5xFTP	MAW-0.25xFTP
	gNOx/kgCO2						
10th	0.82	1.27	1.69	0.37	2.04	1.74	1.46
50th	**2.26**	**2.40**	**2.39**	**2.00**	**2.29**	**2.45**	**2.66**
75th	2.80	2.77	2.70	3.01	2.78	3.07	3.64
95th	**4.05**	**3.60**	**3.17**	**4.37**	**2.78**	**3.09**	**3.96**
98th	4.22	3.72	3.27	4.62	2.79	3.11	4.06
	gNOx/hp-hr (using LLC CO2)						
10th	0.51	0.79	1.05	0.23	1.27	1.08	0.91
50th	**1.41**	**1.50**	**1.49**	**1.25**	**1.43**	**1.53**	**1.66**
75th	1.75	1.73	1.68	1.88	1.74	1.91	2.27
95th	**2.53**	**2.24**	**1.98**	**2.73**	**1.74**	**1.93**	**2.47**
98th	2.64	2.32	2.04	2.88	1.74	1.94	2.53

To assess the behavior of the two approaches more fully, it is also important to examine the metrics under Low NO_X conditions. Therefore, a similar analysis was run using results from the Stage 2 engine, which had an LLC NO_X level at about 0.06 g/hp-hr, near a potential LLC standard. If this is to be considered a valid engine-aftertreatment system, then any associated in-use metric must be able to identify these behaviors as valid. Figure 81 shows an example data set for one of these tests on the LLC, while Figure 82 and Figure 83 show analyses by both MAW and EWMA respectively. This data set shows a tailpipe NO_X level near zero most of the time, with three relatively small breakthrough spikes that do not result in the overall cycle exceeding 0.06 g/hp-hr.

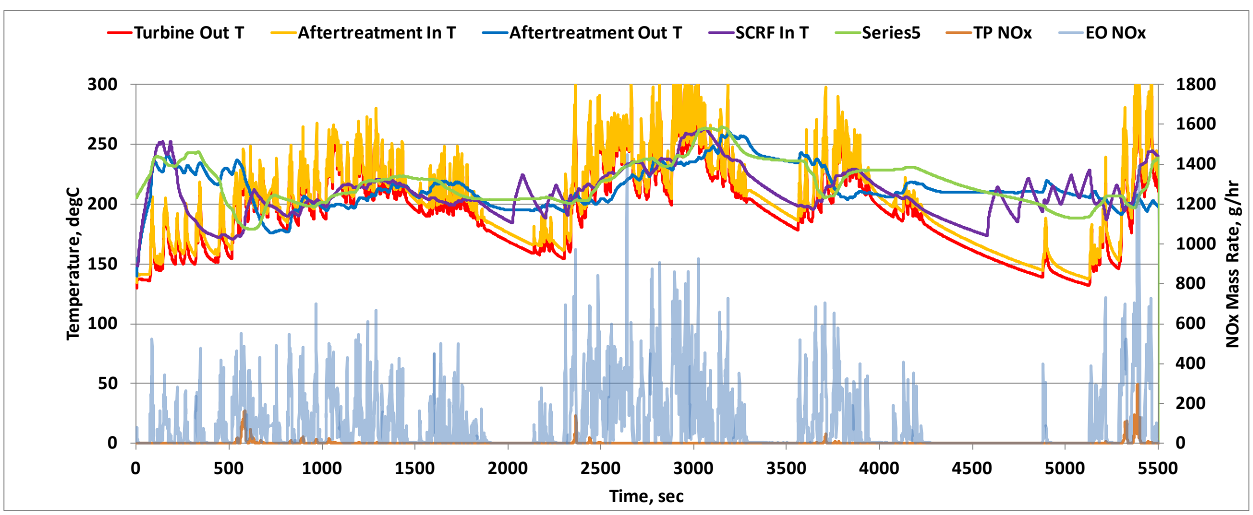

FIGURE 81. STAGE 2 LOW NO_X ENGINE LLC RESULT

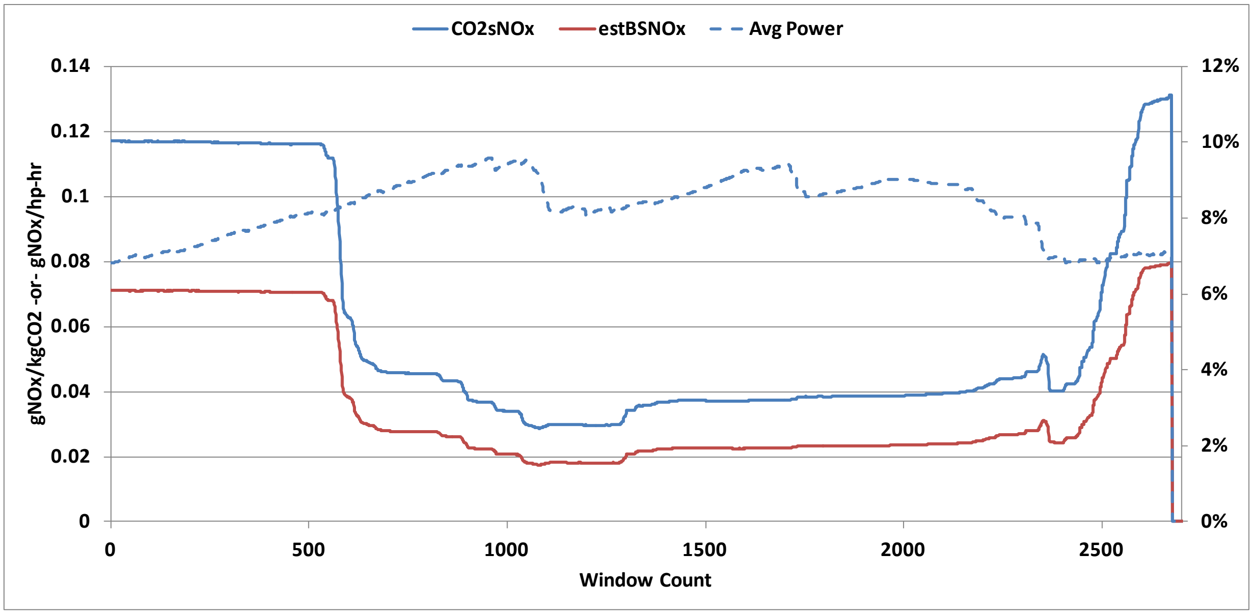

FIGURE 82. 1 X FTP MAW ANALYSIS OF LOW NO_X ENGINE LLC DATA

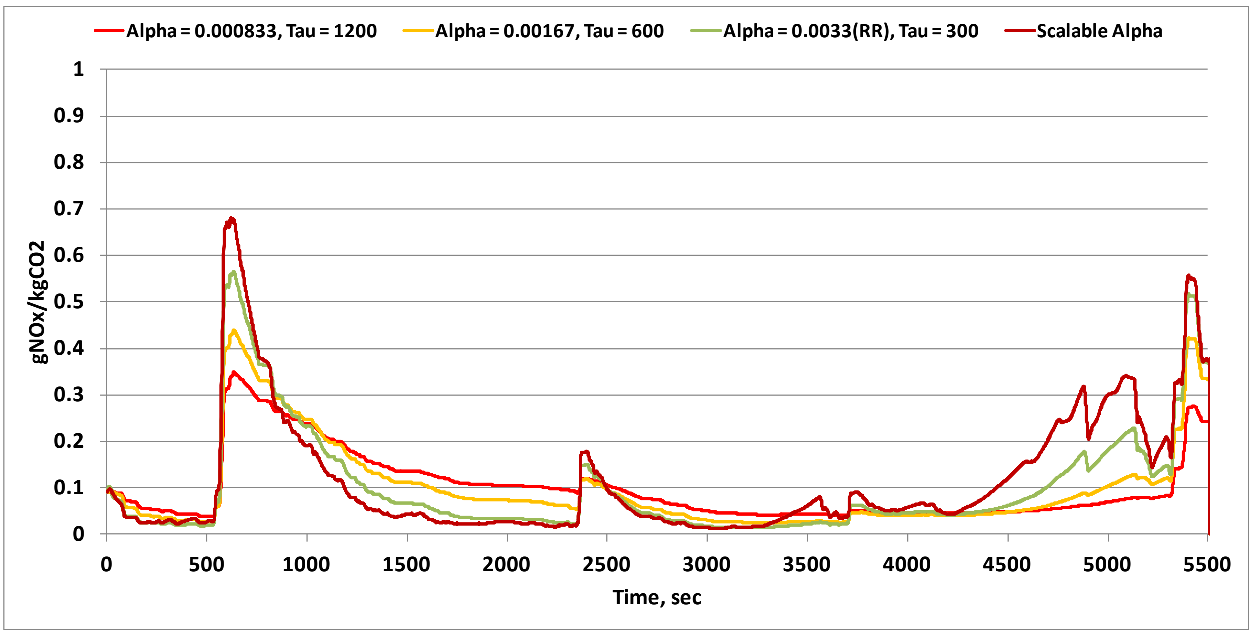

FIGURE 83. EMWA ANALYSIS OF LOW NO_X ENGINE LLC DATA

Figure 82 shows the reaction of the MAW metric, which appears to plateau at several spots where one of the short NO_X spikes is within the window. This results in a large number of windows being driven by a small number of breakthroughs. This would seem to indicate that 25% of the cycle is above the standard, when there are actually only three relatively short events, and it is difficult to discern the circumstances of the breakthrough events. The length of time the EWMA remains above the standard is affected by the magnitude of each given isolated spike.

Figure 83 shows the EWMA behavior, wherein the time constant set of 300 seconds appears to capture behavior of the three breakthrough events more accurately. It should be noted that the Scalable time constant under this Low NO_X data set appears to result in a wind-up of the metric near 5000 seconds due to only a small increase in NO_X emissions. Therefore, the fixed time constant may be a better choice at Low NO_X levels to avoid over-emphasizing emissions at near zero loads.

Table 17 summarizes the results for various metrics again as distributions of both CO_2-specific and estimated brake-specific values. The 300-second EWMA correctly identifies a small number of spikes in a larger body of emissions that are below a potential standard of 0.06 g/hp-hr on the LLC. Those 95th percentile spikes can be up to 8X the standard without disturbing the final cycle average results. On the other hand, the MAW values, even at the 75th percentile would exceed 1.5X the standard, even for a valid cycle, indicating that with a single compliance threshold, a 1.5X factor may be difficult to manage. Again, as noted earlier, given that these data are coming from an LLC which could be considered in compliance with a standard set of 0.06 g/hp-hr, any metric must be able to identify the behavior in this cycle as valid. Therefore, it is recommended that careful consideration be given to balance the metric design with the stringency for light load duty cycles.

TABLE 17. DISTRIBUTIONS FOR VARIOUS METRICS AND LOW NO_X LEVELS ON LLC EXAMPLE DATA SET

Percentile	EWMA-tau=300	EWMA-tau=600	EWMA-tau=1200	EWMA-scalable	MAW-1xFTP	MAW-0.5xFTP
	gNOx/kgCO2					
10th	0.02	0.03	0.04	0.02	0.03	0.01
50th	**0.05**	**0.07**	**0.07**	**0.05**	**0.04**	**0.05**
75th	0.13	0.11	0.12	0.16	0.12	0.19
95th	**0.37**	**0.33**	**0.27**	**0.38**	**0.12**	**0.21**
98th	0.51	0.41	0.31	0.55	0.13	0.25
	est. gNOx/hp-hr (using LLC CO2)					
10th	0.01	0.02	0.03	0.01	0.02	0.01
50th	**0.03**	**0.04**	**0.04**	**0.03**	0.02	0.03
75th	0.08	0.07	0.07	0.10	**0.07**	**0.12**
95th	**0.23**	**0.20**	**0.17**	**0.23**	**0.07**	**0.13**
98th	0.31	0.25	0.19	0.33	0.08	0.15

4.2.3 Metric Behavior over Larger Data Sets

To examine the behavior of the different metrics over larger data sets covering a wider array of duty cycles, cycle data for both a current production engine and the Stage 2 Low NO_X engine from a variety of different test cycles was assembled into a single large "simulated measurement shift," covering roughly 12-16 hours of operation. This discussion will focus primarily on the Low NO_X engine data, given that those data sets are more relevant to any discussion of future in-use standard. The data set was still focused more at the low load range but covered a broader range of average power over the course of the simulated shift, as shown in Table 18.

TABLE 18. DISTRIBUTION OF AVERAGE POWER FOR ASSEMBLED SIMULATED MEASUREMENT SHIFT DATA SETS (BASED ON 1 X FTP MAW ANALYSIS)

	Power Distribution, % max	
	Low NOx Engine	Current Engine
10th	2%	2%
25th	4%	4%
50th	6%	9%
75th	15%	17%
90th	20%	24%
Average	10%	14%

Figure 84 shows the full set of window results from MAW analysis of this data set, using a 1 x FTP CO_2 window. Figure 85 shows an EWMA analysis of the same data set using τ = 300 seconds for the time constant.

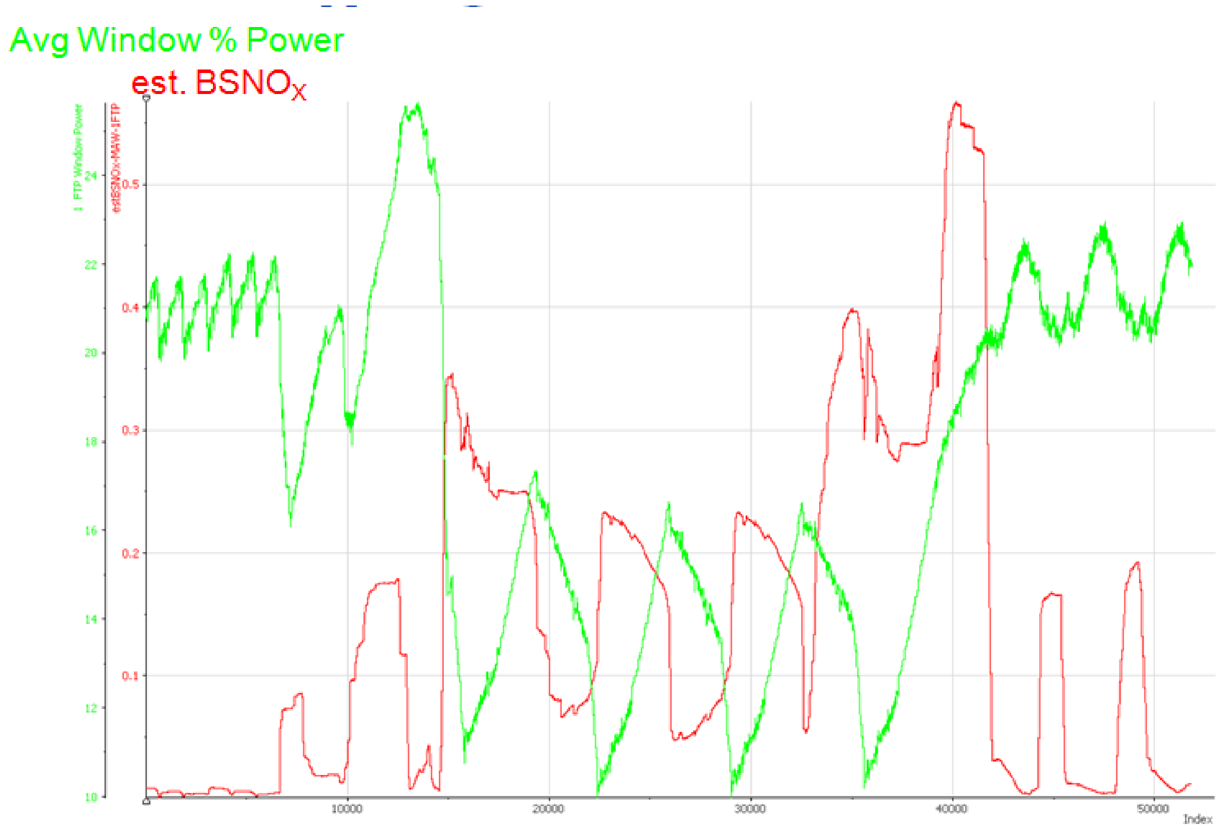

FIGURE 84. MAW ANALYSIS RESULT FOR SIMULATED MEASUREMENT SHIFT ON LOW NO_X ENGINE

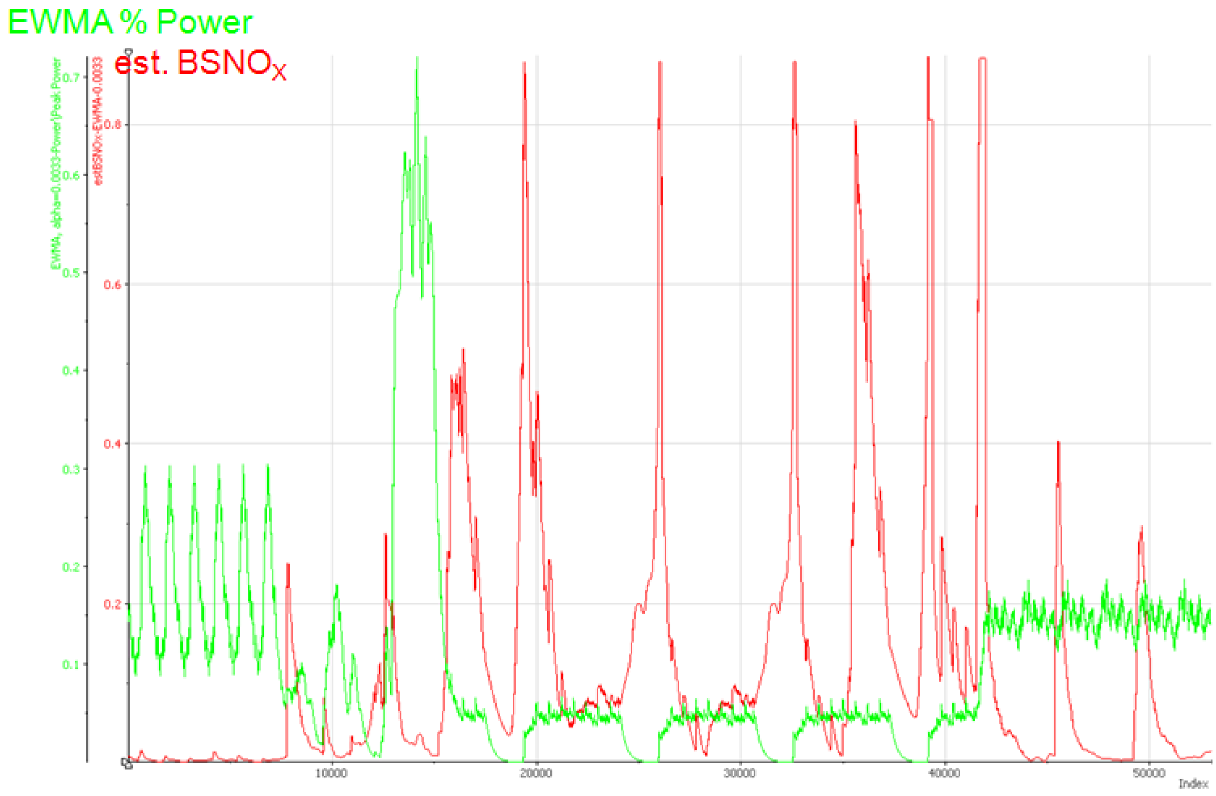

FIGURE 85. EWMA ANALYSIS (TAU = 300 SECONDS) FOR SIMULATED MEASUREMENT SHIFT ON LOW NO_X ENGINE

Figure 86 shows a comparison of histograms of estimated $BSNO_X$ from both metrics. The MAW indicates no clear trend, other than a high frequency of very low number, but the rest of the distribution is scattered somewhat randomly between 0.05 and 0.35 g/hp-hr. On the other hand, the EWMA indicates a logarithmic behavior to the distribution, with the majority of the data points being below 0.1 g/hp-hr, but showing a fairly long tail of very infrequent spikes to about 0.3 to 0.5 g/hp-hr. Figure 87 shows this comparison side by side in a probability plot format, with some key points on the distribution shown in the figure for both metrics.

The two metrics diverge at about the 40th percentile, with the EWMA correctly identifying that NO_X levels remain in the range of a low-load compliance threshold of below 0.1 g/hp-hr, roughly 1.5 X a possible LLC standard level at 0.06 g/hp-hr, while the MAW analysis seems to indicate that the median data in this set is about 2x that value. A distribution tail set at the 90th percentile would be at roughly 0.35 g/hp-hr for both metrics, but again it is felt that picking a 50th and 90th (or 95th) percentile and regulating both areas of the distribution is a more valuable approach, recognizing that periodic brief excursions to these higher values might be acceptable, assuming that they stay relegated to above the 90th or even 95th percentile of behavior.

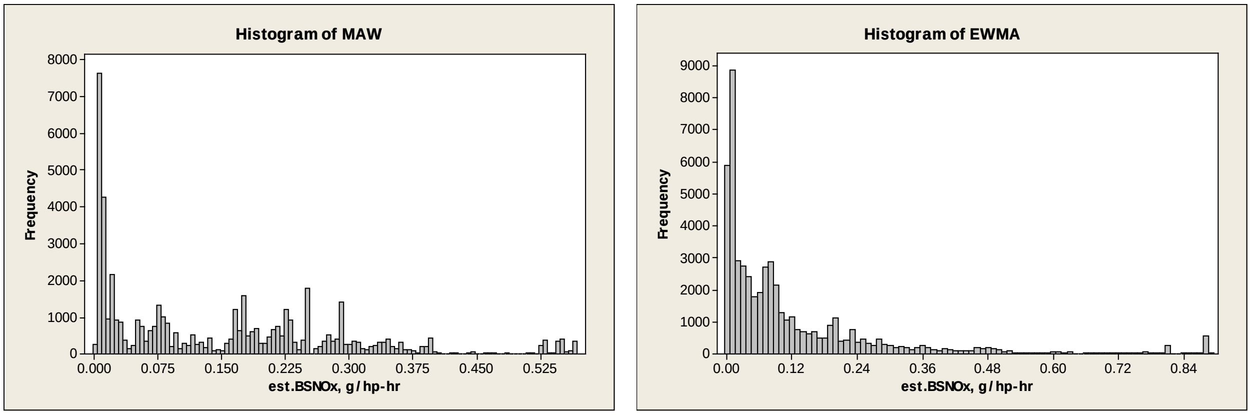

FIGURE 86. COMPARISON OF HISTOGRAMS OF EST. BSNO$_X$ FROM MAW AND EWMA ANALYSIS

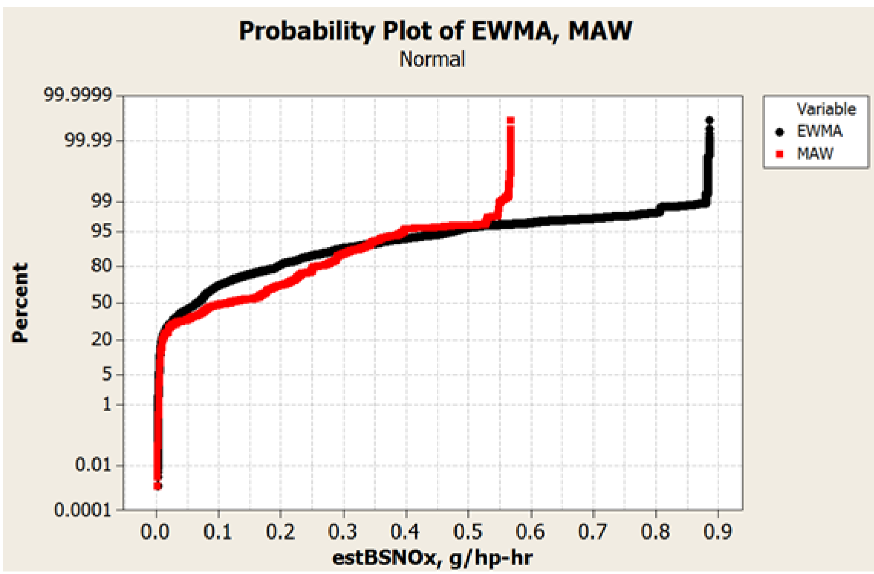

	estBSNOx, g/hp-hr	
Percentile	MAW	EWMA
5th	0.005	0.004
10th	0.006	0.005
50th	0.11	0.065
90th	0.33	0.32
95th	0.4	0.48
98th	0.55	0.8

FIGURE 87. PROBABILITY PLOT COMPARISON OF MAW AND EWMA METRICS AT LOW NO$_X$ LEVEL USING SIMULATED MEASUREMENT SHIFT DATA SET

Figure 88 and Figure 89 show an overview of the pros and cons for both in-use metrics, respectively. Overall the MAW has advantages in terms of familiarity based on current EU practices, and relatively long averaging window reducing concerns related to time alignment of data. On the other hand, the EWMA has advantages in terms of a simpler algorithm, and better resolution and identification of measurement events and the kinds of operation that they came from.

CO_2 MAW

- CO_2 MAW is familiar
  - OEMs and others will understand it
- Relatively long averaging windows reduce vulnerability to time alignment issues
- Measurement issues are quantified to some extent by EU JRC
  - at current EU VI levels
- Compatible with a relatively simple threshold
  - still need to account for low load windows…

EWMA

- More compatible with on ECM calculation via sensors
  - used this way now for OBD
- EWMA is more fault tolerant in terms of recovery from "bad" data points
  - "rapid response" feature can restart algorithm within a very short time after most disturbances
- EWMA provides more information about where emissions are coming from in terms of operating modes
  - tends to focus on spikes better

FIGURE 88. PROS OF BOTH METRICS EXAMINED

CO_2 MAW

- More difficult to assess compliance in real time
  - generally requires post processing
- Less tolerant of bad data points
  - larger segments of un-useable data, especially at low loads
- Provides little information where emissions are coming from in terms of operating modes
- Potential to overweight transient emission spikes at low loads

EWMA

- More of an unknown quantity
  - will require more explanation and justification
- There will be some work in the tuning of the weighting factors
- Compliance threshold likely not as straightforward
  - distribution is likely needed
  - likely to be some kind of ceiling calculation versus CO_2
- Sustained periods of Very Low CO_2 can cause some algorithm "wind-up"

FIGURE 89. CONS OF BOTH METRICS EXAMINED

5.0 SUMMARY OF STAGE 1B PROGRAM AND RESULT

The Stage 1b program has been reported and discussed elsewhere. However, given that the Stage 1b program provided a baseline for comparison of the updated calibrations, as well as providing a more refined estimate of the performance of the Stage 2 aftertreatment system over regulatory cycles, those results are important for interpretation of the data shown in this report. Therefore, a brief summary of the Stage 1b program is given in this section of the report.

5.1 Background and Motivation

The original Stage 1 ARB Low NO_X Demonstration program involved an examination of the feasibility of technologies to achieve a target tailpipe NO_X level of 0.02 g/hp-hr on both a diesel and natural gas engine platform. The diesel demonstration platform was a 2014 Volvo MD13TC EU6 engine. The final configuration of the Low NO_X aftertreatment system is shown below in Figure 90 below.

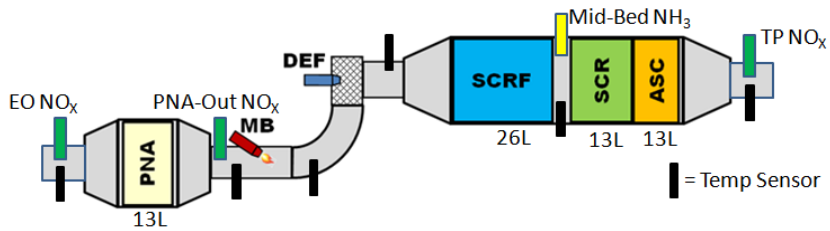

FIGURE 90. Final Stage 1 Low NO_X Aftertreatment System Configuration

A key part of the technical demonstration involved aging of the final system on engine in an accelerated fashion to simulate full useful life degradation, so that the system performance could be demonstrated at the end of useful life. However, during that aging process, an unexpected failure occurred which disturbed the experiment, resulting in the exposure of the aftertreatment system to unrepresentative conditions. The failure involved the canning of the Passive NO_X Adsorber (PNA), which in turn results in mat materials being ingested into the downstream SCR-on-Filter (SCRF). The failure is illustrated in Figure 91. Due to time and budget constraints, the experiment could not be restarted. Although the parts were repaired, and the experiment was completed, this left two lingering issues:

- How much of the degradation observed in the original Stage 1 experiment was "normal," versus how much was "abnormal" (resulting from the unrepresentative failure conditions).

- The SCRF was left in a fragile state following the failure, with several areas of channel micro-cracking that could later expand to a full failure with continued use. This was an issue because the parts were needed to support low-load calibration and demonstration efforts in the CARB Stage 2 program.

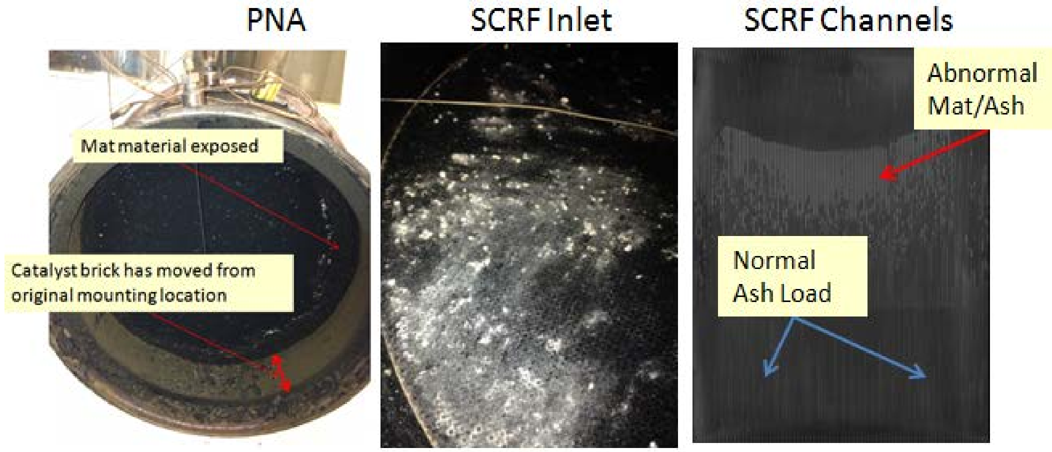

FIGURE 91. Illustration of Stage 1 Failure ON PNA AND Downstream SCRF

The Stage 1b program was initiated with funding from SCAQMD to address these issues and answer the lingering questions about the true full useful life performance of the Stage 1 aftertreatment design.

5.2 Test Plan and Results

The Stage 1b Test plan involved repeating the 1000-hour accelerated aging experiment that was performed under Stage 1, using a fresh set of parts identical to the original parts. To gain better insight into system degradation over time, the parts were tested at two intermediate points during aging, in addition to before and after the completion of the full aging duration. Tests were conducted at the 0-hour point (following de-greening), and at 33%, 67%, and 100% of the FUL aging duration of 1000 hours. The aging was conducted using the SwRI-developed DAAAC (Diesel Accelerated Aftertreatment Aging Cycles) methodology, which accounts for both thermal and chemical aging components. The aging cycle is shown in Figure 92 below. For this experiment, the aging achieved a full 10X acceleration of thermal aging, and a 4.5X acceleration of chemical aging. However, at the end of aging, the SCR-on-Filter contained a near maximum life duration of ash loading, prior to ash cleaning. To assess the impact of ash cleaning on the SCRF, an additional ash cleaning experiment and test were added to the test plan, supported by MECA (the Manufacturers of Emission Controls Association).

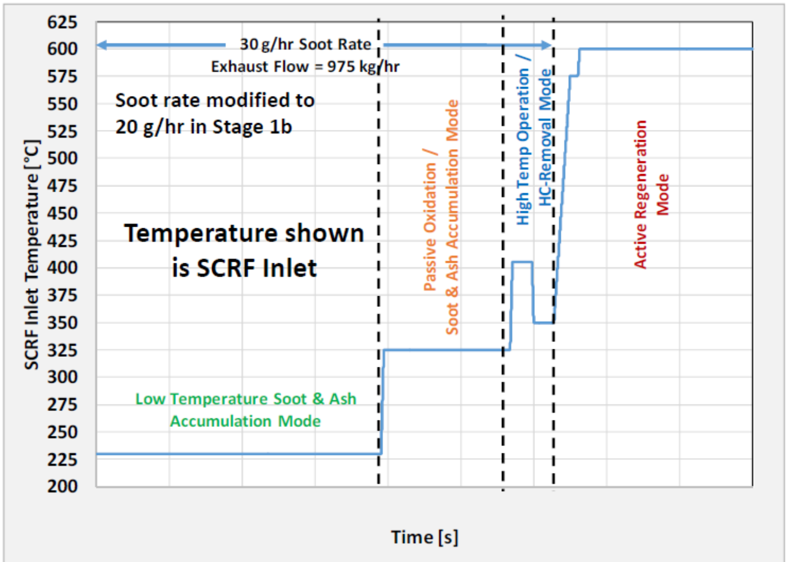

FIGURE 92. FINAL STAGE 1B AGING CYCLE – BASED ON SWRI DAAAC METHODOLOGY

The final results of the Stage 1b program are summarized in Figure 93. The figure shows emission results at before and after the FUL aging, as well as at two intermediate test points that were taken along the way. The results indicate the following trends:

- Cold-Start FTP performance on Stage 1b was similar to that observed during Stage 1. Cold-start performance loss is driven primarily by loss of PNA performance. This indicates that the canning failure did not disturb the aging of the PNA itself.

- Hot-Start STP performance on Stage 1b was considerably better than what was observed on Stage 1. The system maintained 99.6% NO_X conversion in Stage 1b, as compared to only 99.3% in Stage 1. This was primarily driven by the behavior of the SCRF, and it indicates that the SCRF was significantly disturbed by the upstream canning failure in Stage 1.

- **Composite FTP** NO_X levels were **0.023 g/hp-hr** after ash cleaning in Stage 1b, as opposed to 0.034 g/hp-hr in Stage 1, a considerable performance improvement.

- **RMC-SET** NO_X levels were **0.032 g/hp-hr** in Stage 1b as opposed to 0.038 g/hp-hr in Stage 1, again due primarily to the better performance of the SCRF that was not subjected to the upstream canning failure.

It should be noted that all these results including both FTP and RMC need to have a value of 0.004 added to them as an upward adjustment factor (UAF) to account for the impact of infrequent regeneration on NO_X emissions. The documentation of the development of that UAF is explained in detail in the Stage 1 final report.

One aspect of the results that needs to be mentioned is that part of achieving the results shown in Figure 93, especially on the hot-start and RMC cycles was the ability of the SCR dosing controller to make periodic, long-term trim adjustments to compensate for changes in system performance over time. In this program, some of these long-term trim adjustments had to be made manually, given the developmental maturity of the controller at the time. However, the results do highlight that a robust long-term trim system based on in-exhaust sensor measurements will likely be an important component of maintaining Low NO_X system performance over time. In the Stage 1 and 1b system, the controller incorporated both short-term feedback mechanisms based on a production mid-bed NH_3 sensor, and provisions for long-term feedback via the tailpipe NO_X sensor. These types of feedback systems will be important components of the controls for a Low NO_X system, especially during warmed-up operating modes where the system will be called on to maintain NO_X levels below 0.01 g/hp-hr.

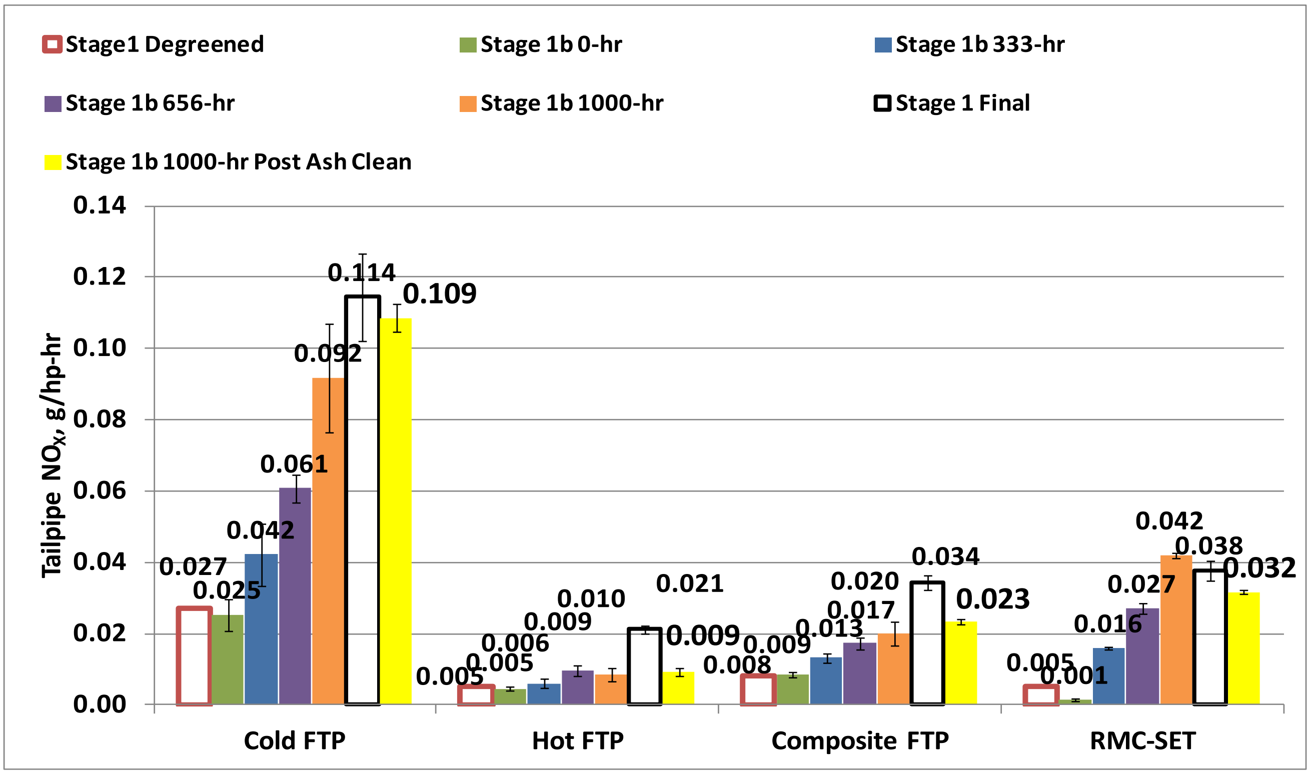

FIGURE 93. FINAL NO_X RESULTS FOR STAGE 1B PROGRAM (SHOWING COMPARISON TO STAGE 1 RESULTS)

At the conclusion of the Stage 1b program, the Volvo engine was returned to the baseline condition, and the stock aftertreatment system was re-installed. At that point, the baseline emission levels were re-checked for several purposes. The first was to verify the baselines for comparisons of CO_2, given that the original baseline had been conducted several years earlier in a different test cell, and the engine had been through several maintenance and repair events over the course of the program. In addition, it was necessary to run LLC baselines for proper comparison to the Stage 2 calibration results, given that the LLC did not exist at the time the original baseline testing was run.

Figure 94 shows a comparison BSNO_X levels for the Stage 1b baseline check and the original Stage 1 baseline tests. In general, the performance of the baseline engine and aftertreatment system was comparable to the previous baseline test result. Figure 95 shows a similar comparison for BSCO_2. The CO_2 levels were very close to original baseline levels, indicating that the original CO_2 comparisons and those made for the LLC baseline result remained valid.

As mentioned earlier, the baseline re-test was also an opportunity to generate a set of baseline results on the 2014 Volvo MD13TC EU6 engine over the LLC. Figure 96 illustrates the continuous data from one of these baseline runs. It should be noted that as a EU6 compliant engine, the Volvo MD13TC was actually calibrated to comply with the European work-based window (WBW) requirements. Although every WHTC-sized window on the LLC is well below the power threshold for valid window, the system still achieves a significant amount of control under these conditions, with the thermal management modes being engaged over a significant portion of the cycle. In addition, the baseline aftertreatment system is fairly large and contained in a thermally optimized, one-box type arrangement. As a result, the system temperatures were in a good range for much of the cycle, and the Volvo MD13TC baseline engine achieved some of the better tailpipe NO_X results observed among production engines tested on the LLC at SwRI. Compared to many other engines with LLC emissions in the vicinity of 1-2 g/hp-hr, these results indicate the potential for NO_X reduction on the LLC even for a conventional modern aftertreatment system.

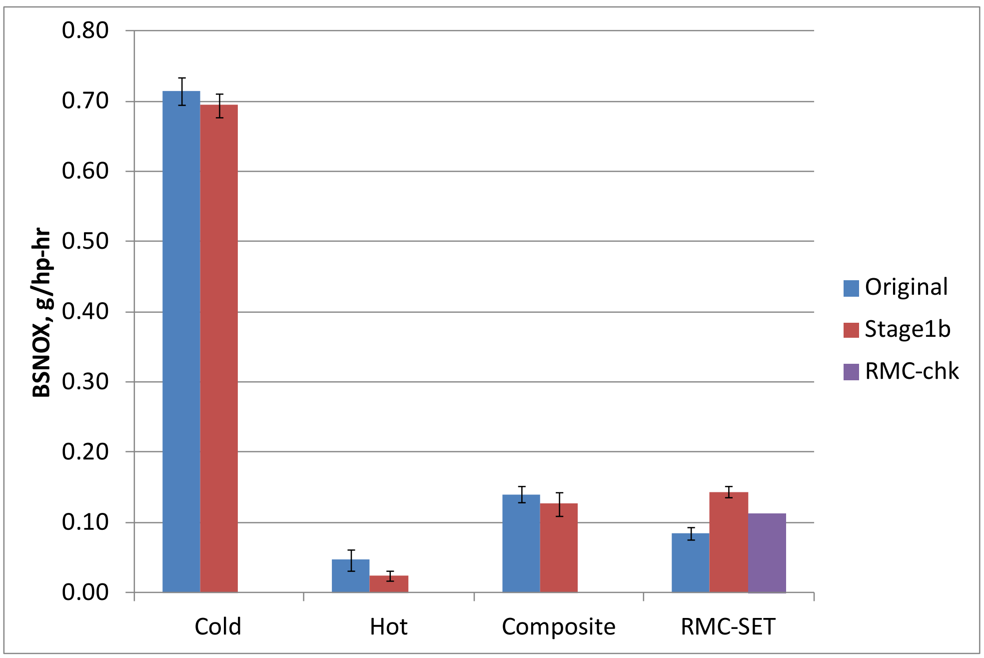

FIGURE 94. $BSNO_X$ COMPARISON OF STAGE 1B BASELINE CHECK TO ORIGINAL STAGE 1 BASELINE TESTS

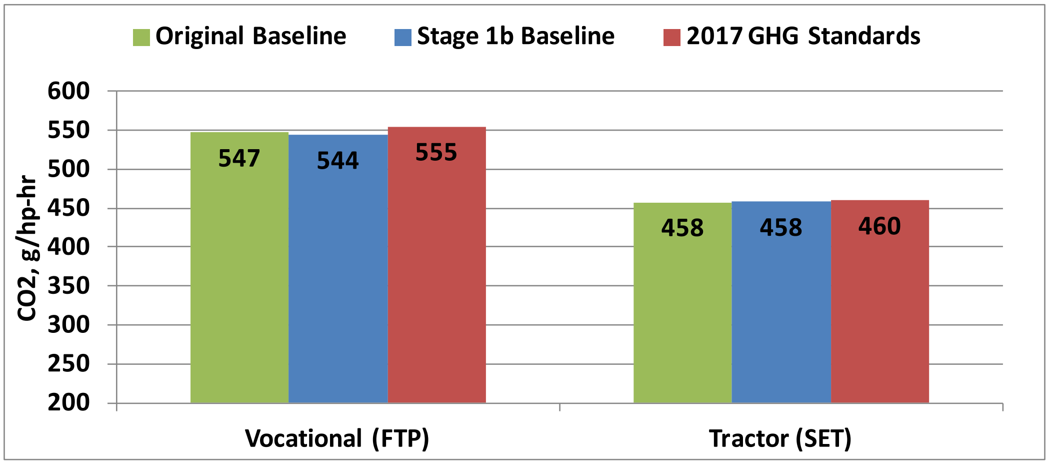

FIGURE 95. BSCO$_2$ COMPARISON OF STAGE 1B BASELINE CHECK TO ORIGINAL STAGE 1 BASELINE TESTS

Table 19 shows a summary of the baseline LLC results for the baseline Volvo MD13TC engine. The aftertreatment system achieved roughly 90% NO_X conversion, resulting on a tailpipe NO_X level of 0.34 g/hp-hr from a 3.4 g/hp-hr engine-out NO_X level. CO_2 emissions averaged 609 g/hp-hr on the LLC, and this is the baseline level that was used for CO_2 comparisons for the Stage 2 re-calibration effort.

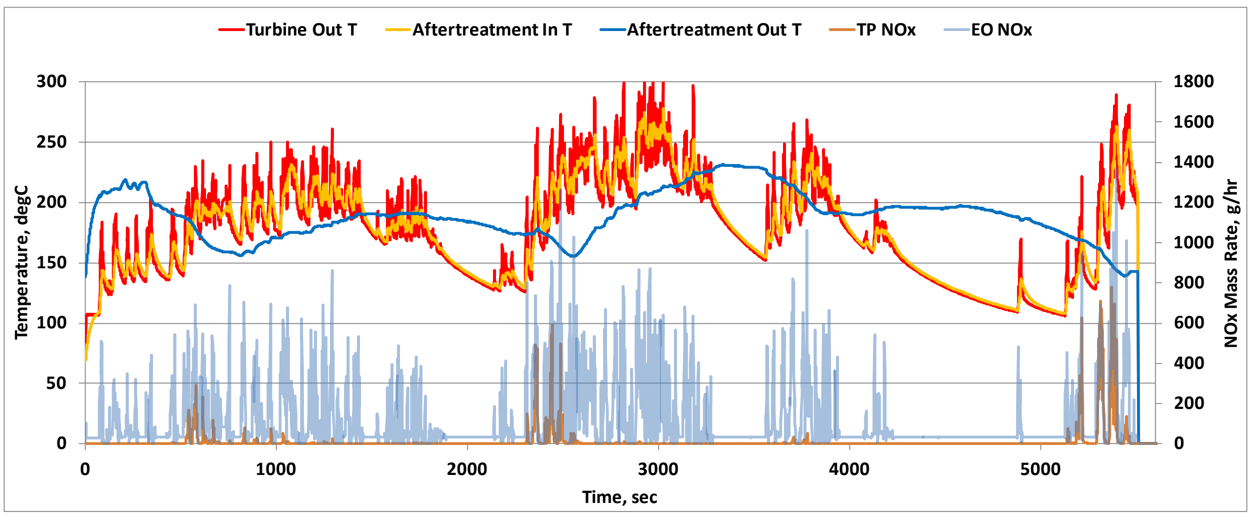

FIGURE 96. BASELINE LLC RESULT FOR THE 2014 VOLVO MD13TC EU6 ENGINE WITH STOCK AFTERTREATMENT

TABLE 19. SUMMARY OF BASELINE LLC RESULTS FOR 2014 VOLVO MD13TC ENGINE

Run		1	2	3	**Average**	Stdev	COV
		Tailpipe					
THC	g/hp-hr	0.034	0.000	0.036	**0.023**	0.020	87%
NMHC	g/hp-hr	0.033	0.000	0.036	**0.023**	0.020	87%
CO	g/hp-hr	0.167	0.157	0.198	**0.174**	0.022	13%
NOx	g/hp-hr	**0.352**	**0.338**	**0.339**	**0.343**	**0.008**	**2.3%**
PM	g/hp-hr	0.004	0.001	0.001	**0.002**	0.002	91%
CO2	g/hp-hr	606.5	612.3	608.6	**609.1**	2.9	0.5%
Work	hp-hr	50.90	50.88	51.05	**50.95**	0.09	0.2%
		Engine-Out					
THC	g/hp-hr	0.26	0.26	0.27	**0.26**	0.003	1.2%
NMHC	g/hp-hr	0.26	0.26	0.26	**0.26**	0.003	1.2%
CO	g/hp-hr	1.80	1.90	1.94	**1.88**	0.072	3.8%
NOx	g/hp-hr	**3.37**	**3.44**	**3.49**	**3.43**	**0.060**	**1.8%**
NOx Conversion	%	90%	90%	90%	**90%**	0.4%	n/a

6.0 SUMMARY AND CONCLUSIONS

A number of work efforts were undertaken in the Stage 2 program to support the development of a comprehensive Low NO_X regulation. These efforts were focused on expanding the reach of the technology demonstrated in the Stage 1 program into the Low-Load operating region. These efforts will contribute to emission control under real-world conditions in urban and vocational duty cycles.

A Low-load Cycle (LLC) for use as a potential future certification duty cycle was developed based on real-world field data. Data from several hundreds of vehicles was evaluated in a data-driven analytical process that leveraged the tools and computing resources of NREL to develop a set of representative driving profiles that characterized common low-load operating modes. These driving profiles were translated to engine dynamometer cycles using the EPA GEM model, and the translated engine cycles became the building blocks for the final LLC. SwRI assembled and evaluated a number of possible candidate LLCs, as well as examining a number of technical issues and questions regarding cycle details. These included areas such as the use of idle accessory load, determination of proper preconditioning, length of in-cycle idle periods, and others.

In the final analysis a set of 4 candidate cycles was offered for consideration by CARB. The cycles were also distributed to stakeholders to evaluate and test, so as to provide feedback to CARB for the final selection. Ultimately, CARB chose LLC Candidate 7 to become the final cycle. Eventually the decision was made to include accessory load at idle when running the LLC. It is understood that the LLC will be incorporated into the CARB Omnibus Low NO_X rule.

It should be noted that the LLC also has a vehicle speed trace associated with the normalized engine cycle. This was included to enable the eventual use of powertrain or vehicle-based testing as a means to demonstrate emission benefits, and possibly in the future compliance with criteria pollutant standards.

With the LLC now developed, SwRI was able to launch the second major program task, which was the extension of the Stage 1 engine FTP/RMC-SET calibration for better low-load control. This calibration effort was performed with the goal of determining how much NO_X emission control could be achieved on the LLC with the Stage 1 Low NO_X system, and how much varying levels of NO_X control might impact CO_2 levels, as compared to the baseline engine system and calibration.

As part of this calibration effort, SwRI developed four "development cycles" which focused on particular areas of the LLC but could be run in a shorter period of time to speed up the development effort. Those development cycles were used to examine a number of different calibration options. Further modifications to the Stage 1 Low NO_X engine calibration were made to examine on-engine options. In addition, a variety of different thermal management strategies were explored using the mini-burner, which gave a picture of the thermal input required to achieve different lower emission levels. A tradeoff between NO_X emission control and CO_2 impact was determined, which spanned a range of CO_2 levels from -2% to +2% from the baseline engine, and tailpipe NO_X levels from 0.27 g/hp-hr to 0.02 g/hp-hr.

Ultimately, SwRI decided on a final calibration that achieved 0.07 g/hp-hr at a level of CO_2 equivalent to the baseline engine (essentially a fuel consumption neutral calibration). This LLC NOx level is roughly 2 to 2.5 times the emission levels that the Stage 1 system demonstrated on the FTP and RMC-SET cycles. The modified calibration was also checked on the FTP and RMC-SET cycles and was found to have emission levels equivalent to the data generated before those changes were made.

Finally, several efforts examined on-engine sensor-based measurements for eventual in-use compliance testing. SwRI also examined alternate emissions metrics that could be used to analyze that emission data which would be compatible with a wider compliance range that includes low-load emissions in the field.

Regarding the engine sensor-based measurements, it was found that several key inputs to the calculation of in-use emissions had good accuracy on multiple current production engines. The key inputs included fuel flow and exhaust flow. Conversely, ECM predicted torque was found to be increasingly inaccurate at lighter loads, and therefore it was recommended that ECM torque should not be used in a future in-use emission metric unless substantial improvements in accuracy are made. It was also found that tailpipe NO_X sensors, while generally providing a useful indication of tailpipe NO_X levels, would likewise require considerable improvement in application and accuracy to support in-use compliance measurements at Low NO_X levels. Such improvements are outside the scope of this program, but it is understood that efforts are underway to examine NO_X sensor capabilities in detail and recommend areas for improvement.

Finally, several alternatives were examined for emission metrics compatible with eventual low-load in-use measurements. These metrics included a Moving Average Window (MAW) approach based on windows containing a CO_2 mass equivalent to that emitted on an FTP, similar in concept to the approach currently utilized in the EU for Euro VI heavy-duty vehicles. Another approach that was examined utilized an Exponentially Weighted Moving Average (EWMA) algorithm to extract compliance information from the continuous data. Various tuning parameters for these metrics were examined, such as MAW window size, or the proper time constants for an EWMA algorithm. Ultimately the two approaches were compared and contrasted over data sets from both current production engines and the Stage 2 Low NO_X engine. A final recommendation regarding in-use metrics was not given, but the features and issues with both methods were laid out to enable a regulatory decision. It is suggested that further investigation of these metrics is needed, as well as to set a proper compliance threshold for whichever new metric is chosen.

Another effort was carried out in support of this Stage 2 program, which was funded by the South Coast Air Quality Management District (SCAQMD) and the Manufacturers of Emission Controls Association (MECA). This supporting effort was termed Stage 1b, and it was designed to provide a robust set of aged parts for the Stage 2 program, given that the Stage 1 parts were left in a fragile state at the end of Stage 1 due to a canning failure that occurred during the later stages of the original aging. Under Stage 1b a "clean" aging effort was re-run using the same accelerated aging protocol based on the SwRI DAAAC methodology employed in Stage 1. Although that effort has been reported elsewhere, a summary of the Stage 1b program is given in this report, given that several key outputs from the Stage 1b effort were needed for Stage 2.

In addition to providing a robust set of full useful life aftertreatment parts, aged to 435,000 equivalent miles, the Stage 1b program also answered lingering questions regarding the true durability of the advanced aftertreatment system. The Stage 1b final aged parts demonstrated emission levels of 0.023 g/hp-hr NO_X on the FTP cycle and 0.032 g/hp-hr on the RMC-SET cycle at the end of useful life.

It is understood that the efforts from this program will be used to support several aspects of the CARB Omnibus Low NO_X regulatory proposal, which will be released during the 2nd quarter of 2020. The LLC developed as part of this Stage 2 program will become an integral part of emission certification testing as the new regulations take effect. The calibrations performed in this Stage 2 program provide indications of the potential NO_X performance during the low-load operating regions represented by the LLC, and show promise for closing the “low-load emission gap” that is frequently observed in the field.

While significant efforts were undertaken to investigate in-use sensor-based measurement and compatible low-load metrics, it is suggested to further efforts need to be undertaken, and more analysis needs to be performed before setting a final in-use measurement protocol, and the appropriate compliance thresholds for that protocol.

APPENDIX A

LOW LOW-PROFILES AND TRANSLATED NORMALIZED ENGINE CYCLES

PROFILE V9892_CLUSTER 0 (USED IN LLC)

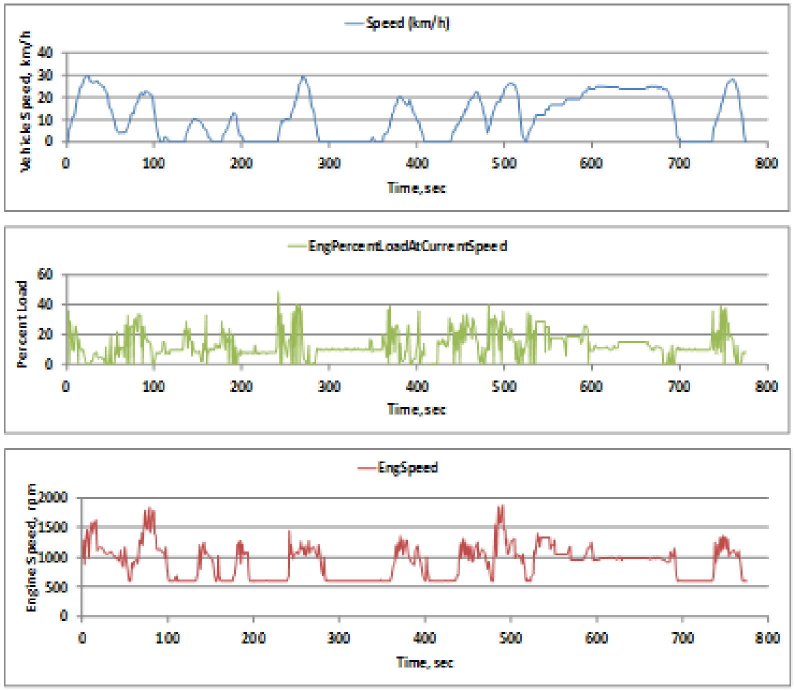

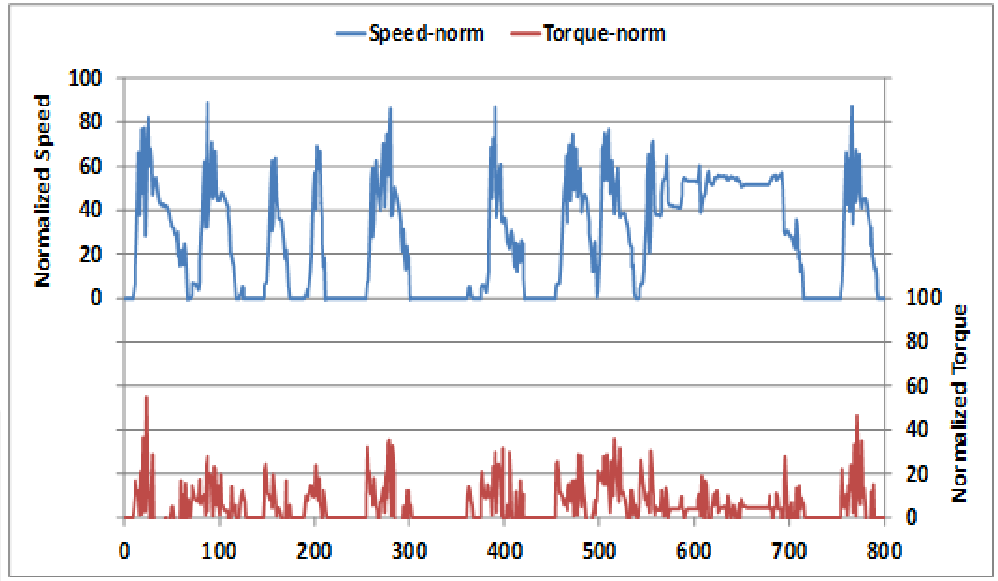

Real-World Vehicle Profile

- Class 8 Tractor, Food Delivery (Shamrock), 4x2
- Volvo D13 405hp, 12-speed AMT
- 1.5 miles travelled in 780 secs
- Average 11 kph, (16kph moving)

Translated Engine Test Profile

- 14% average load at speed
- 5% of max power
- 7% of max power moving
- 31% idle, 15% motoring

PROFILE V075_CLUSTER 0 (USED IN LLC)

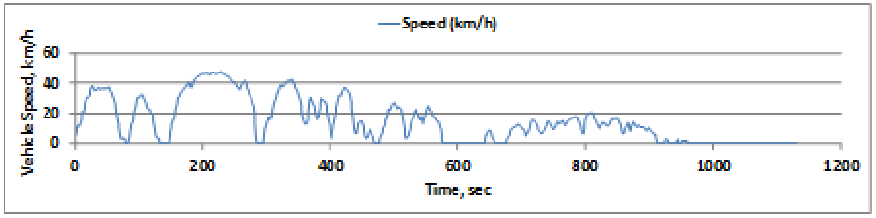

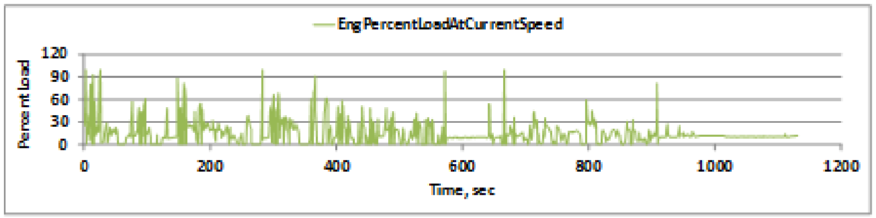

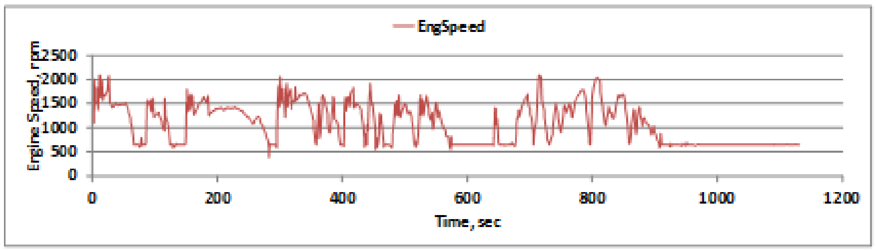

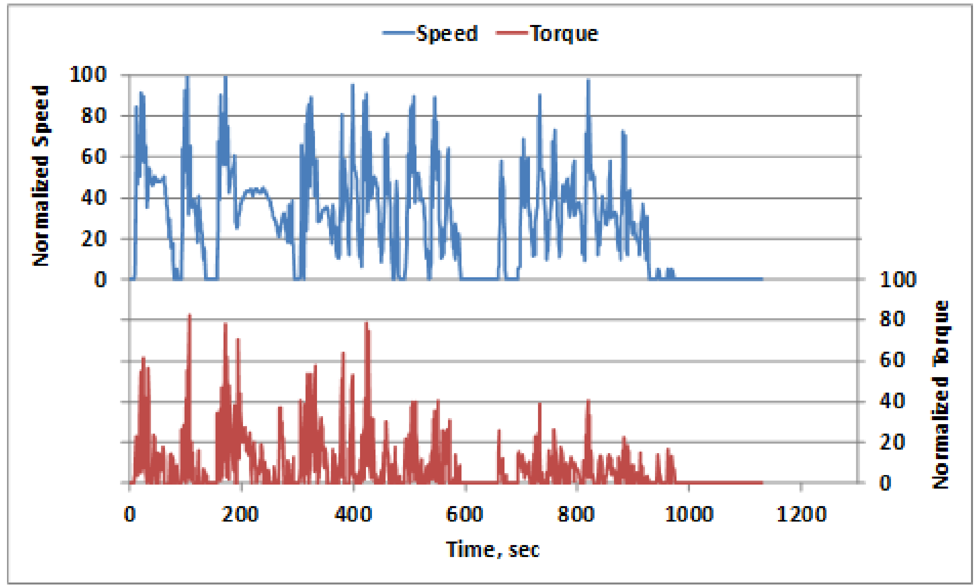

Real-World Vehicle Profile

- Class 8 Tractor, Drayage Truck, 6x4
- Mack MP8-415C, 10-speed AMT
- 2.8 miles in 1130 secs
- Average 14 kph (21 kph moving)

Translated Engine Test Profile

- 13% average load at speed
- 6% of max power
- 8% of max power moving
- 30% idle, 19% motoring

PROFILE V11660_CLUSTER 0

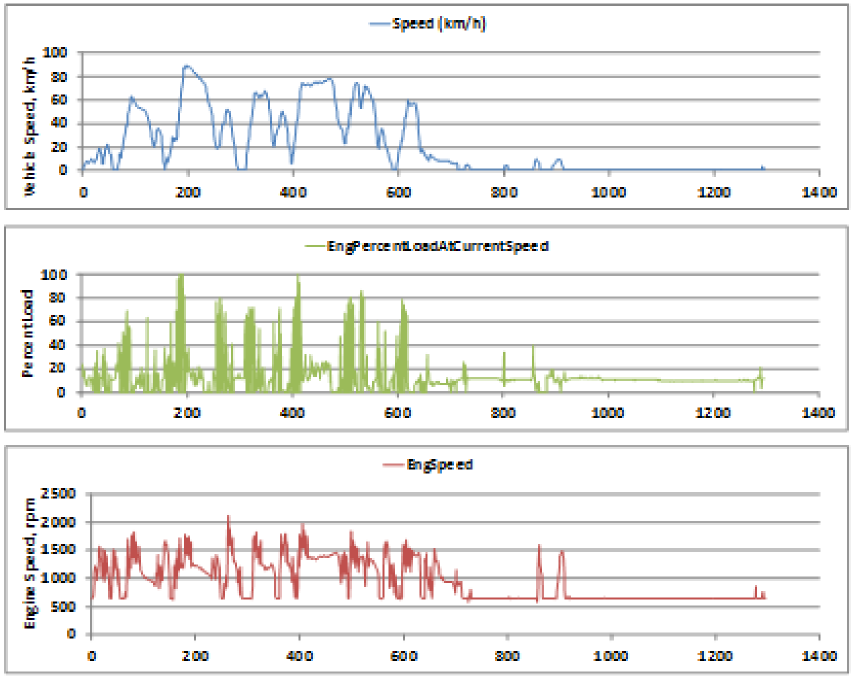

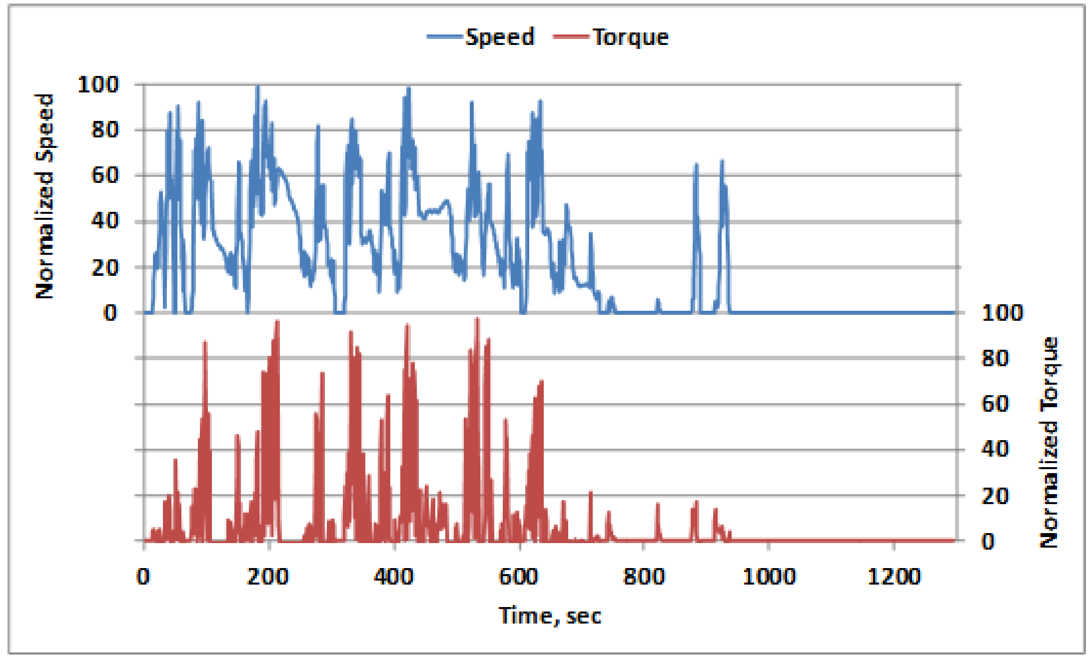

Translated Engine Test Profile

- 14.5% average load at speed
- 6% of max power
- 9% of max power moving
- 43% idle, 25% motoring

Real-World Vehicle Profile

- Class 8 Tractor, Drayage Truck, 6x4
- Volvo D13 430hp, 13-speed Manual
- 0.7 miles travelled (mostly first half)
- Average 7kph (14 kph moving)

V9892_CLUSTER 1 (SHADED AREA USED IN LLC)

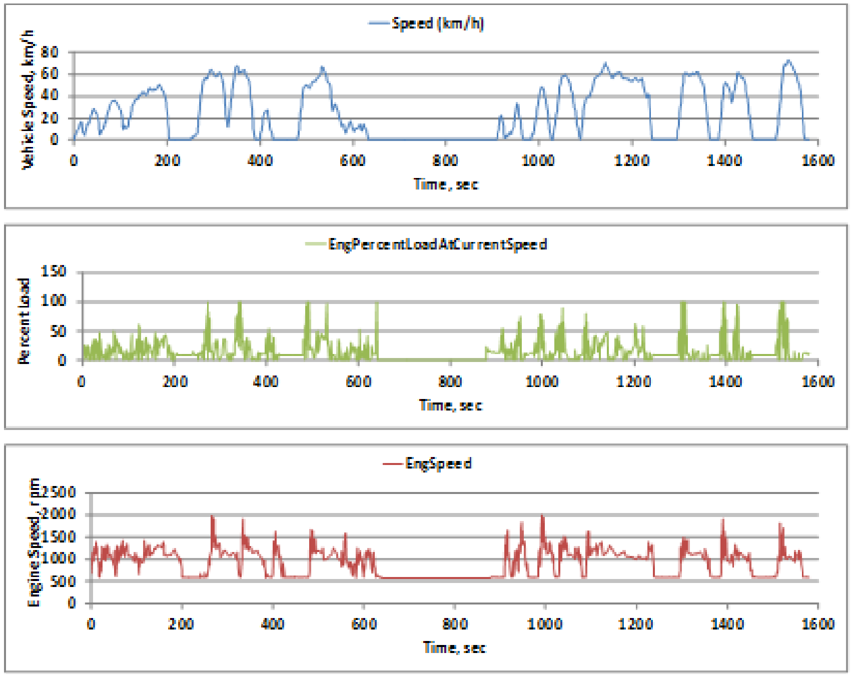

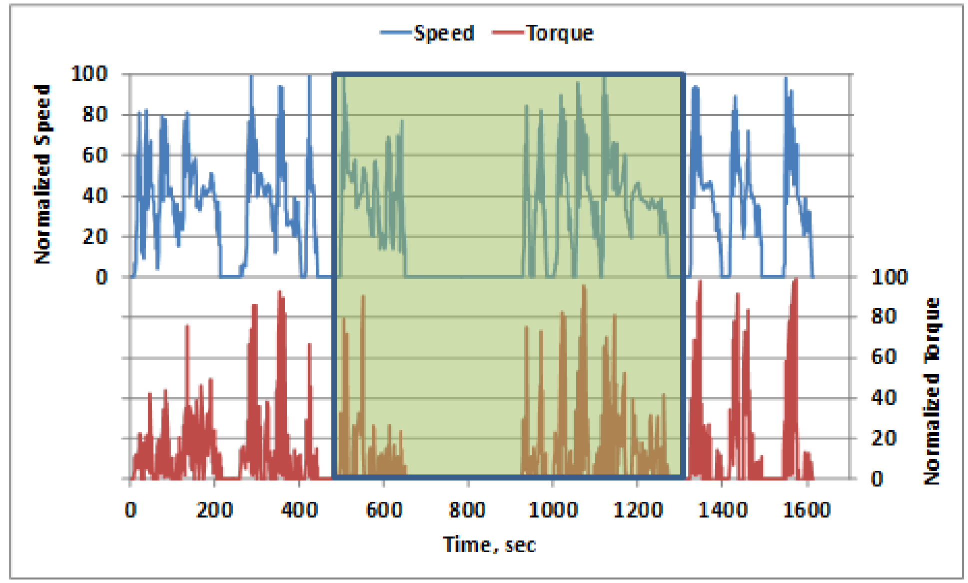

Real-World Vehicle Profile

- Class 8 Tractor, Food Delivery (Shamrock), 4x2
- Volvo D13 405hp, 12-speed AMT
- 6.3 miles travelled in 1600 secs
- Average 24kph (37kph moving)

Translated Engine Test Profile

- 14% average load at speed
- 9% of max power
- 13% of max power moving
- 34% idle, 18% motoring

V11646_CLUSTER 1

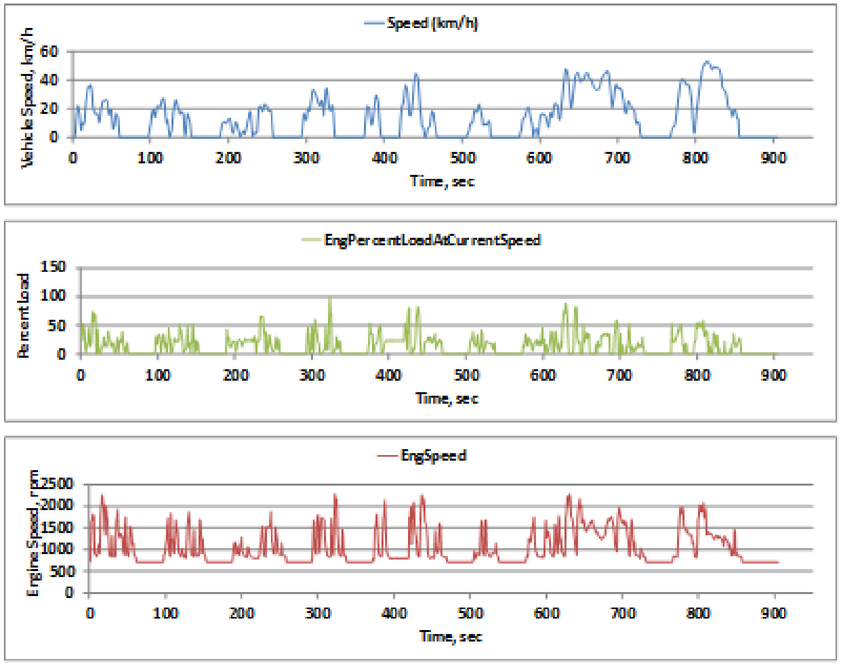

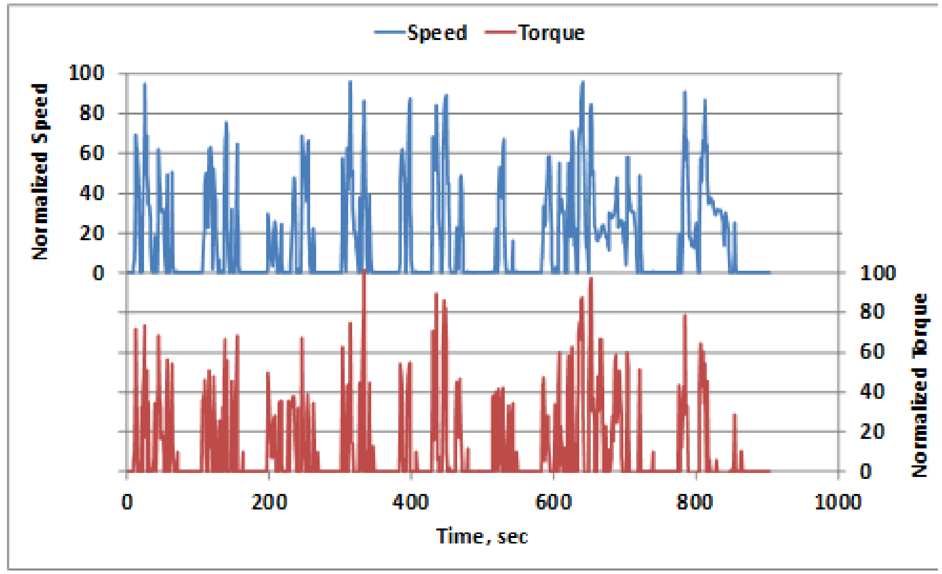

Real-World Vehicle Profile

- Class 6 Walk-In, Package Delivery (UPS), 4x2
- Cummins ISB 6.7L 200hp, 6-Speed Automatic
- 2 miles travelled in 900 secs
- Average 13 kph (21kph moving)

Translated Engine Test Profile

- 15% average load at speed
- 8% of max power
- 15% of max power moving
- 50% idle, 16% motoring

V11815_CLUSTER 1

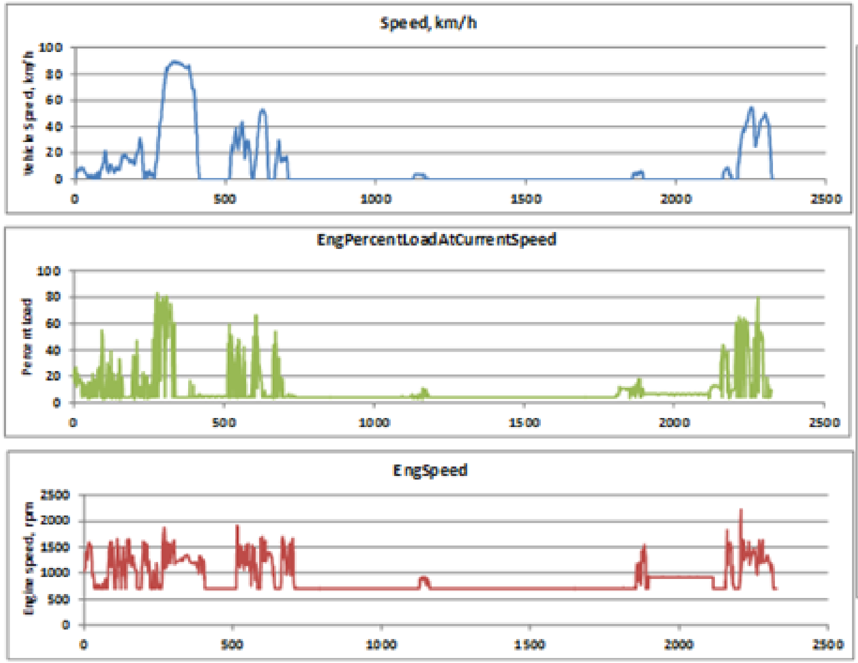

Real-World Vehicle Profile

- Class 8 Tractor, Transfer Truck (Southern CA), 6x4
- Cummins ISX 15, 13-speed MT
- 3.6 miles travelled in 1900 secs
- Average 11kph (26 kph moving)

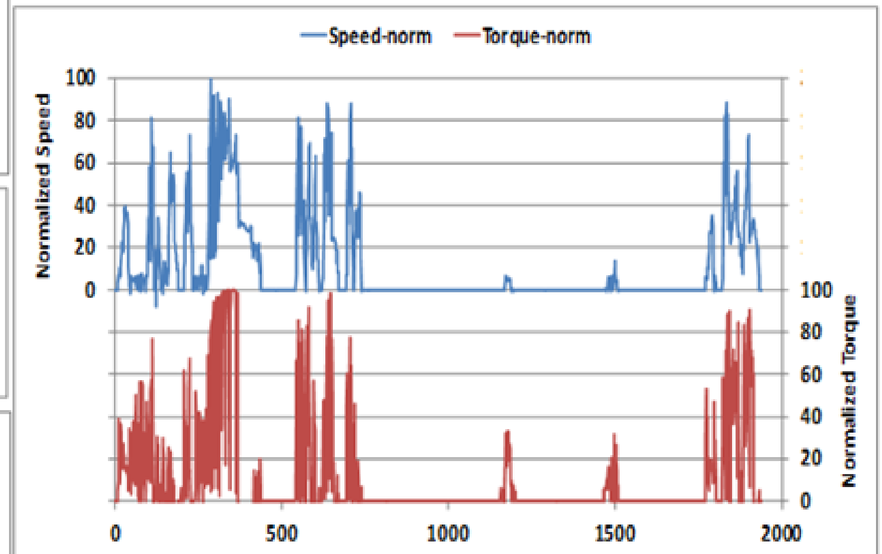

Translated Engine Test Profile

- 14% average load at speed
- 7% of max power
- 16% of max power moving
- 62% idle, 9% motoring

V073_CLUSTER 1 (SHADED PORTION USED IN LLC)

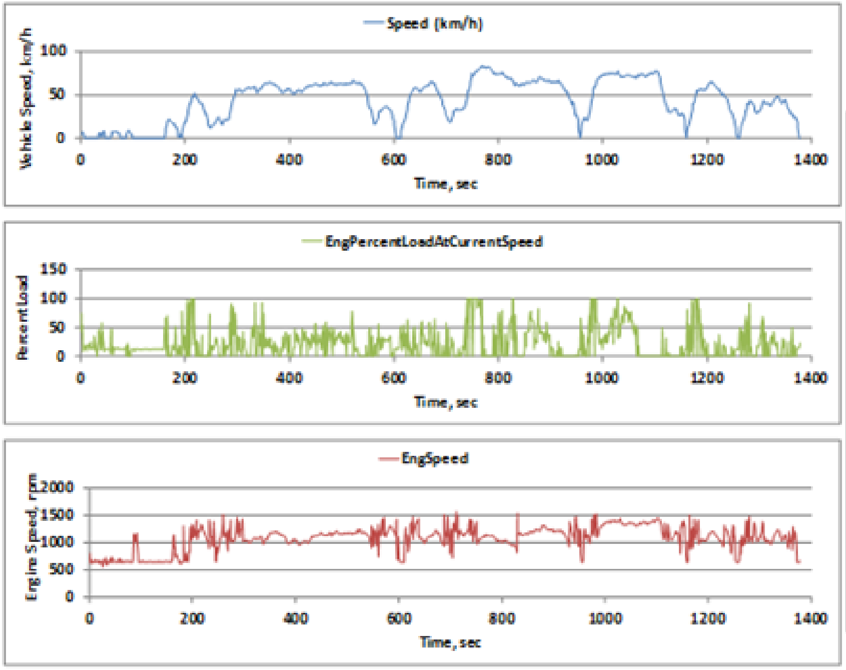

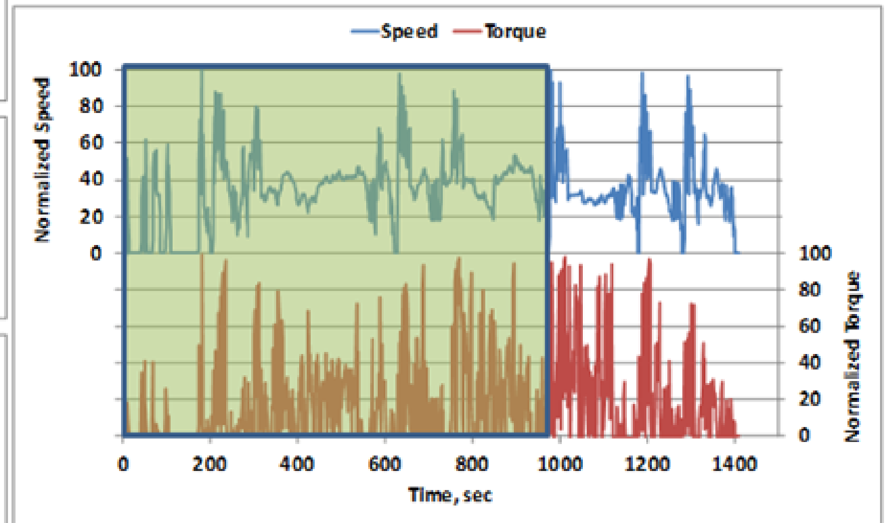

Real-World Vehicle Profile

- Class 8 Tractor, Drayage Truck (Southern CA), 6x4
- Mack MP8-415C, 10-speed AMT
- 10 miles travelled in 1400 secs
- Average 43kph (48 kph moving)

Translated Engine Test Profile

- 15% average load at speed
- 14% of max power
- 15% of max power moving
- 10% idle, 28% motoring

V11660_CLUSTER 5 (SHADED PORTIONI USED IN LLC)

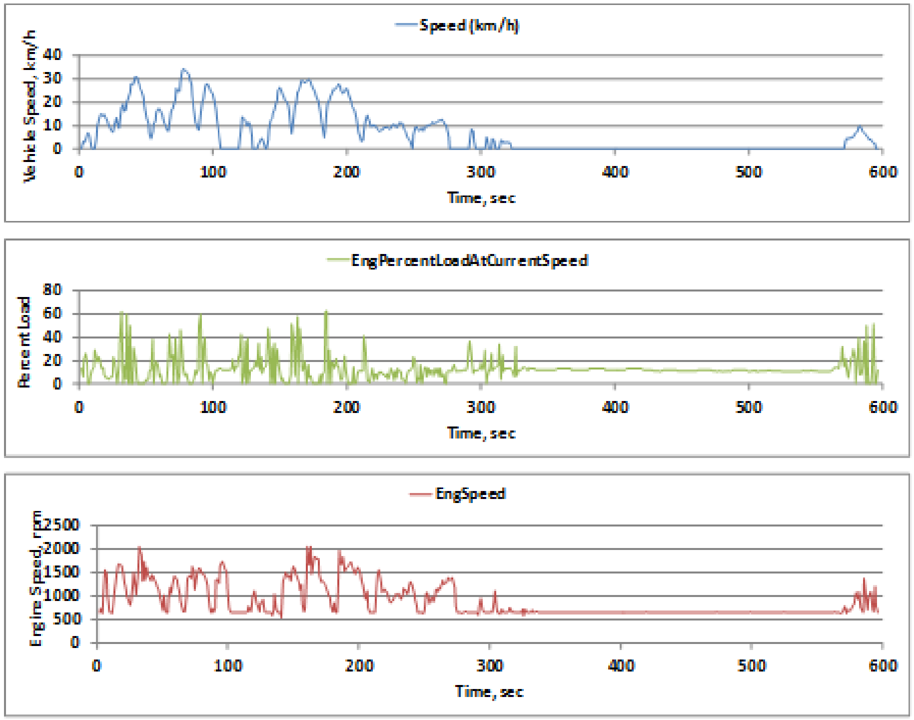

Real-World Vehicle Profile

- Class 8 Tractor, Drayage Truck, 6x4
- Volvo D13 430hp, 13-speed Manual
- 0.7 miles travelled in 600 secs
- Average 7 kph (14 kph moving)

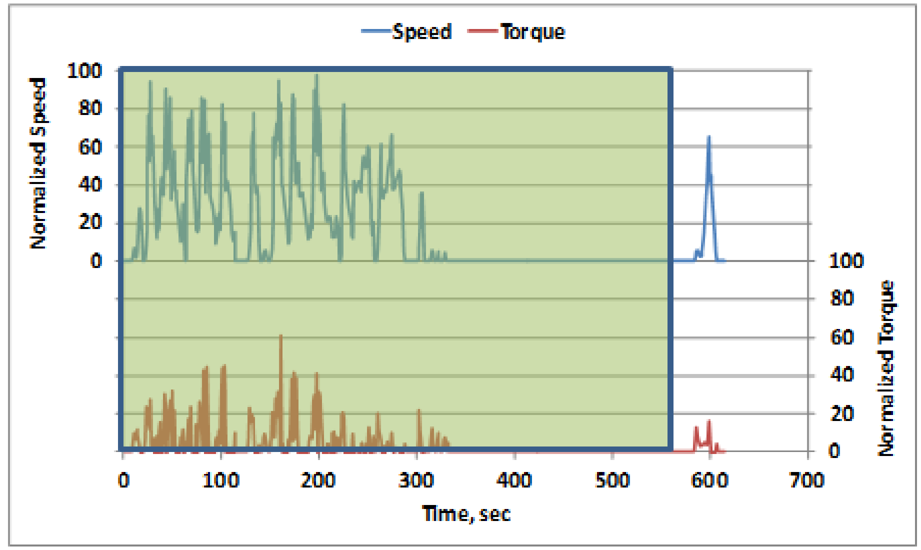

Translated Engine Test Profile

- 13% average load at speed
- 3% of max power
- 5% of max power moving
- 53% idle, 15% motoring

V11806_CLUSTER 5 (SHADED PORTION USED IN LLC)

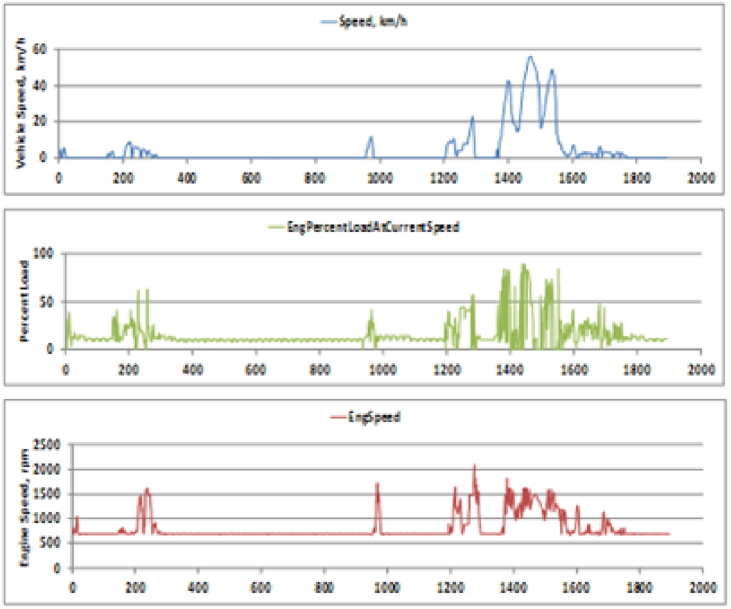

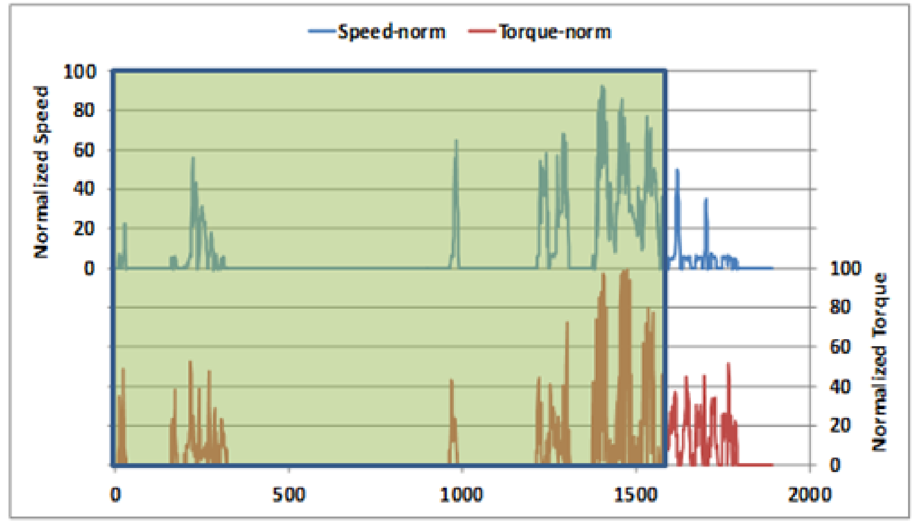

Real-World Vehicle Profile

- Class 8 Tractor, Transfer Truck (SCAQMD), 6x4
- Cummins ISX 12, 13-speed Manual
- 1.4 miles travelled in 1800 secs
- Average 4.5 kph (12 kph moving)

Translated Engine Test Profile

- 13% average load at speed
- 4% of max power
- 11% of max power moving
- 66% idle, 5% motoring

V11817_CLUSTER 5

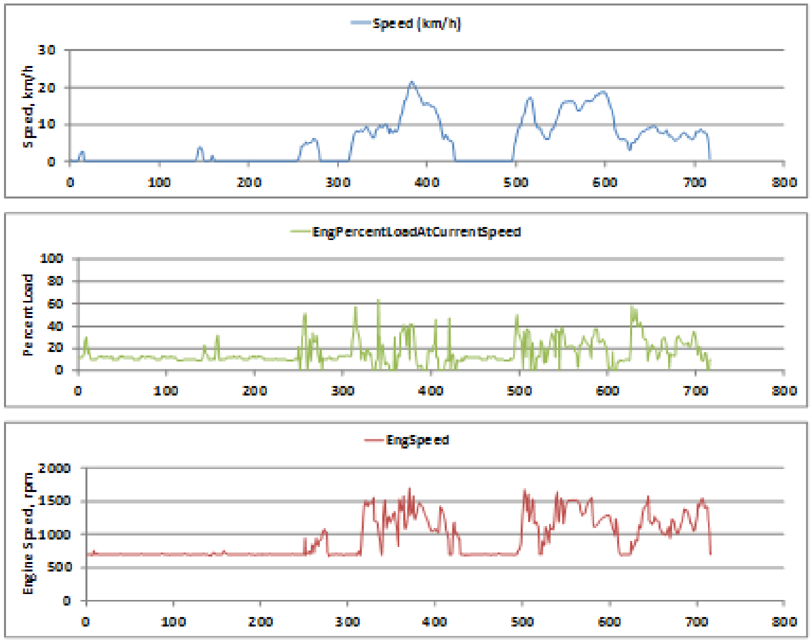

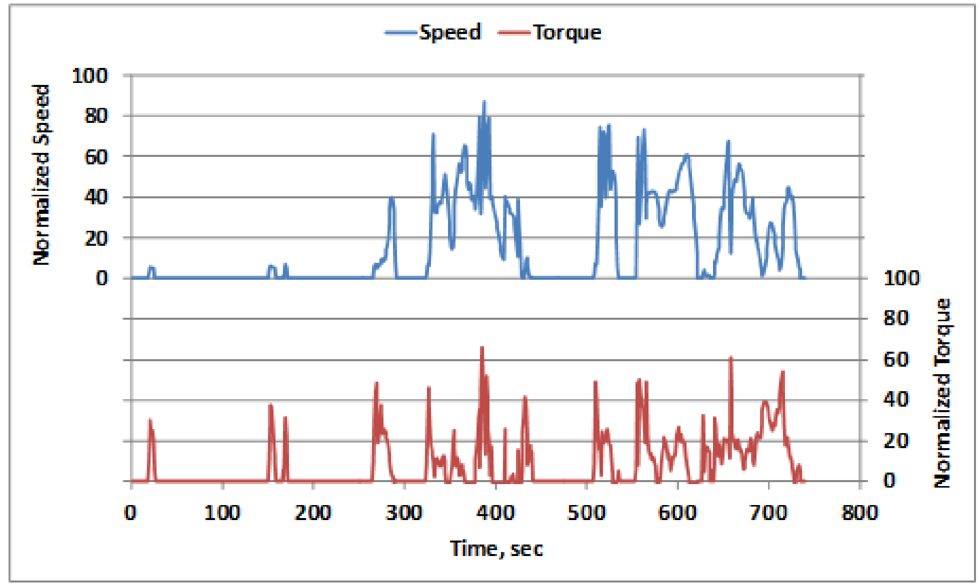

Real-World Vehicle Profile

- Class 8 Tractor, Transfer Truck (SCAQMD), 6x4
- Cummins ISM-385hp, 13-speed Manual
- 0.6 miles travelled in 740 secs
- Average 5kph, 9kph moving

Translated Engine Test Profile

- 13% average load at speed
- 4% of max power
- 8% of max power moving
- 32% idle, 18% motoring

APPENDIX B

ENGINE TEST DATA EXAMPLES FOR LOW-LOAD PROFILES

V9892_CLUSTER 0 – SUSTAINED LOW LOAD

FULL CYCLE DATA (4 REPEATS)

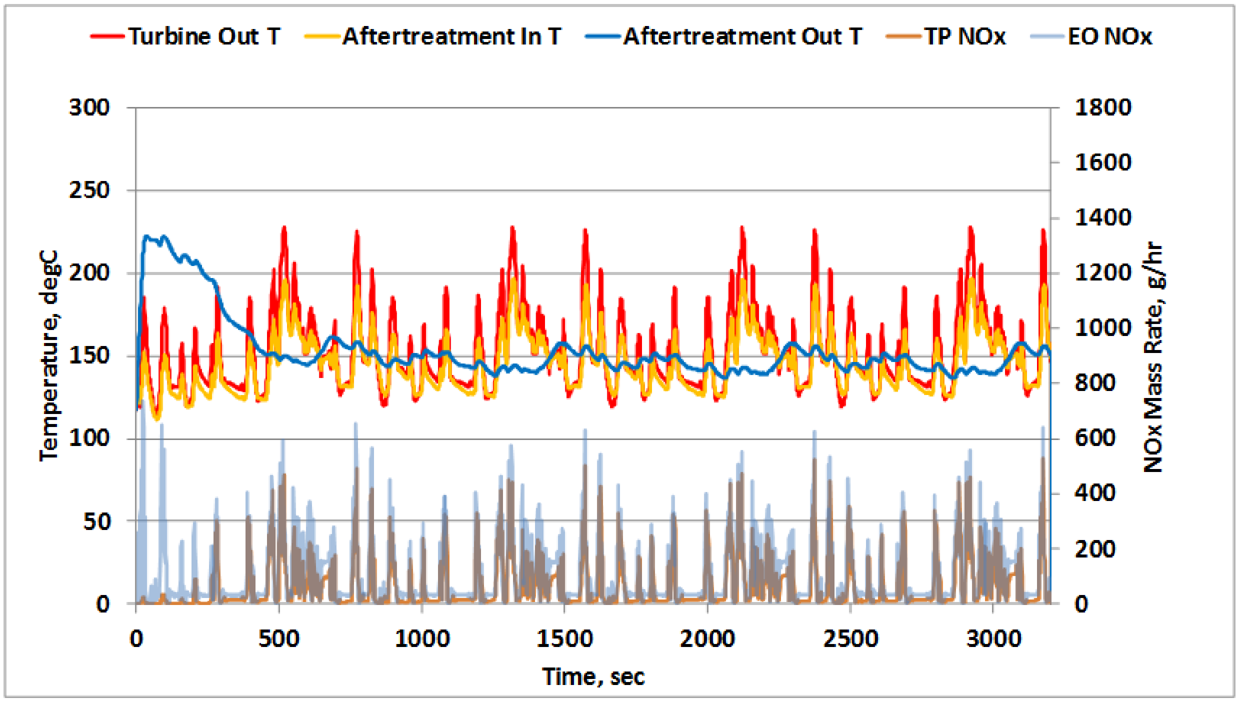

- 30% NOx conversion overall
- Note that field temperatures with MY 2012 engine indicated DPF-out temps ~ 120°C (145°C on this run with 2017 engine)

EQUILIBRIUM CYCLE DATA

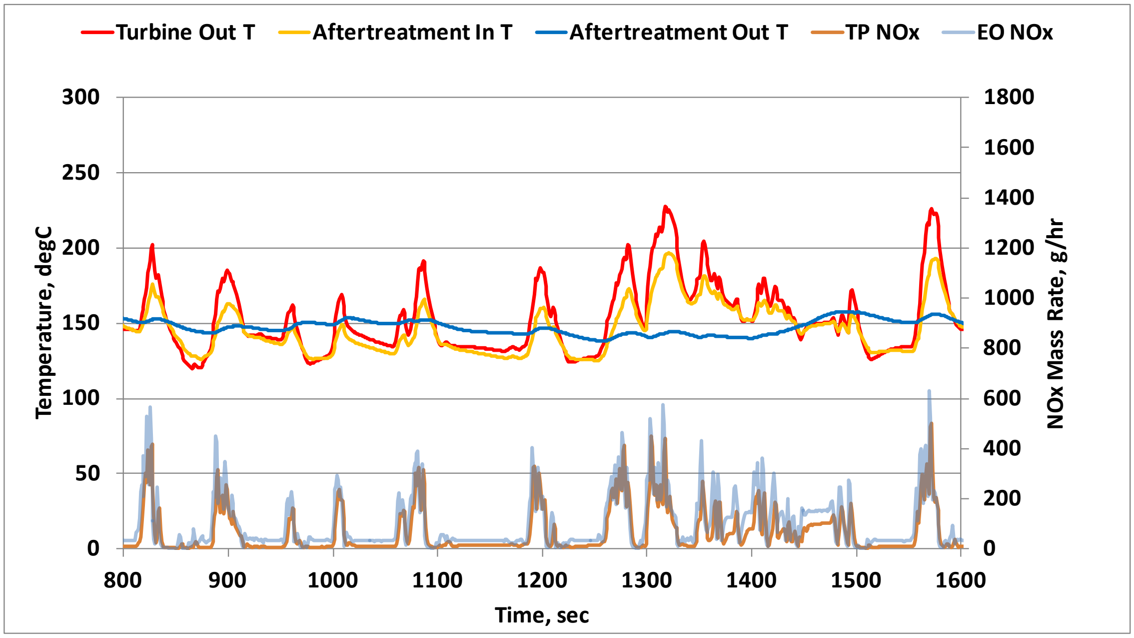

V075_CLUSTER 0
FIRST TWO CYCLES (TOTAL OF 3 REPEATS)

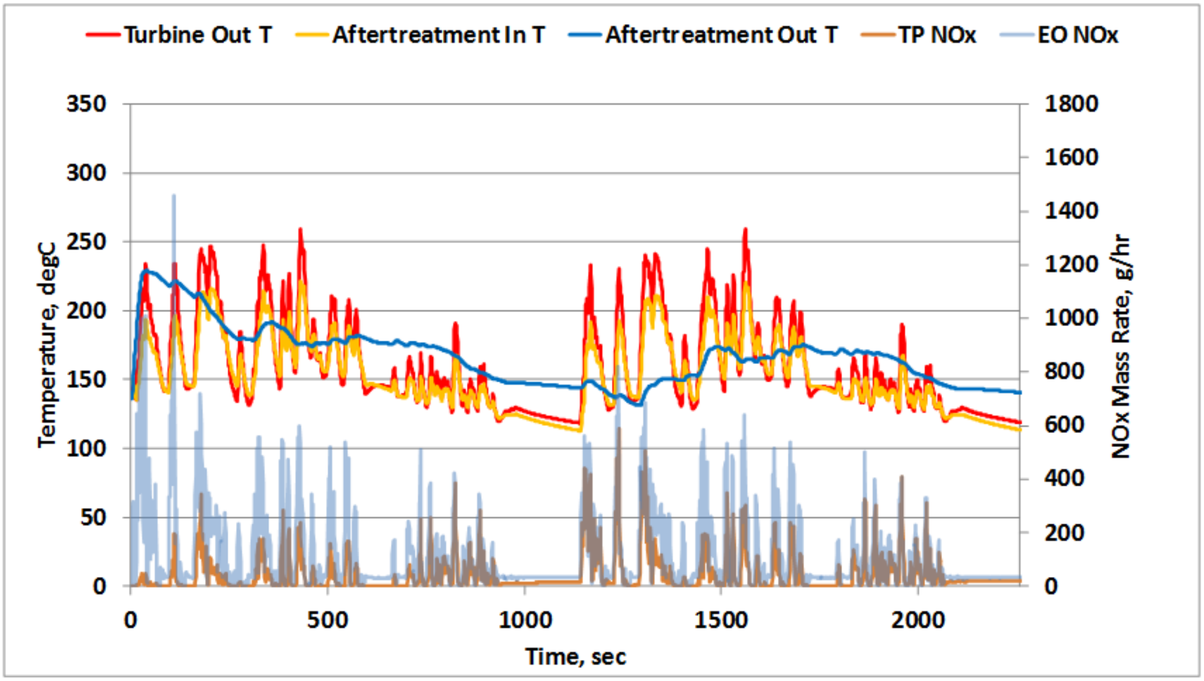

- Substantial cool off during the first 400 seconds from hotter condition
- First cycle was 72% conversion from FTP warm-up

EQUILIBRIUM CYCLE DATA

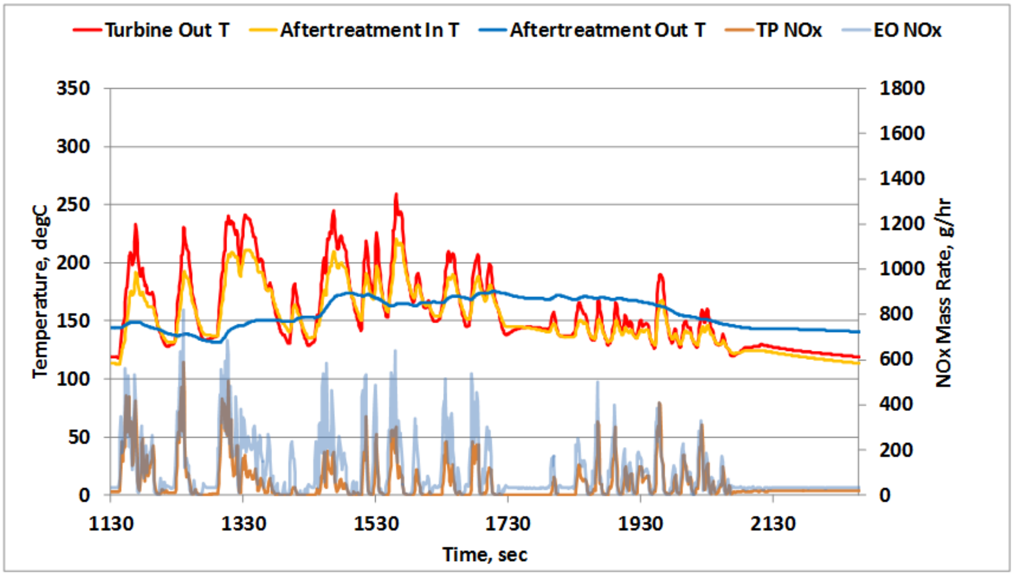

- First 600secs at 9% power, then later segment at 3%
- Only moderate heating at front
- 46% NO_X conversion

V11660_CLUSTER 0

FULL CYCLE DATA (3 REPEATS)

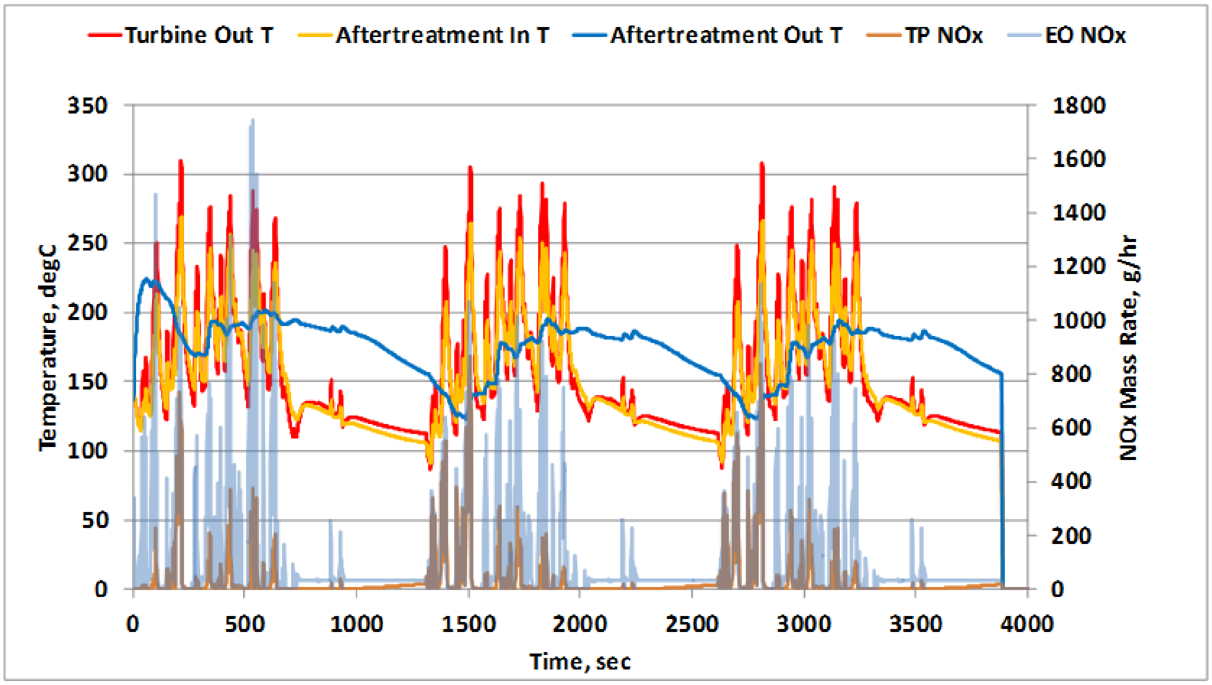

- Loaded portion is 11% max power
- Some cool down at end of that portion but idle at end is main cool portion
- Less effective unless placed after cool-down portion, does make effective cool-down prior to load in 20 minutes total

EQUILIBRIUM CYCLE DATA

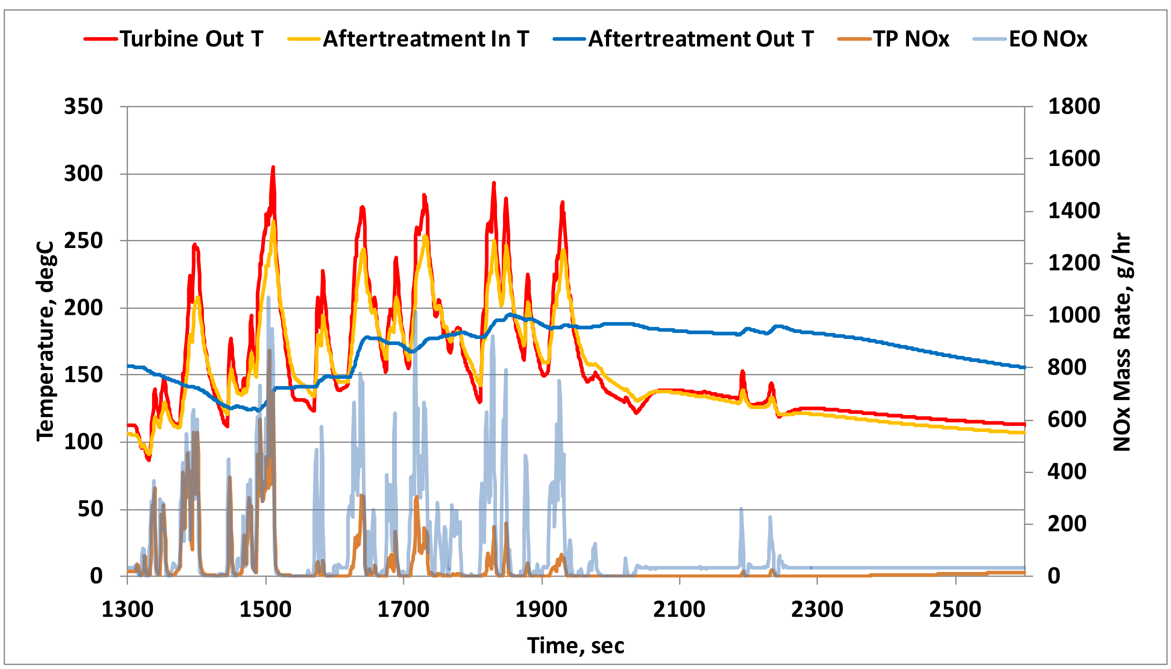

V9892_CLUSTER 1

FULL CYCLE DATA (2 REPEATS)

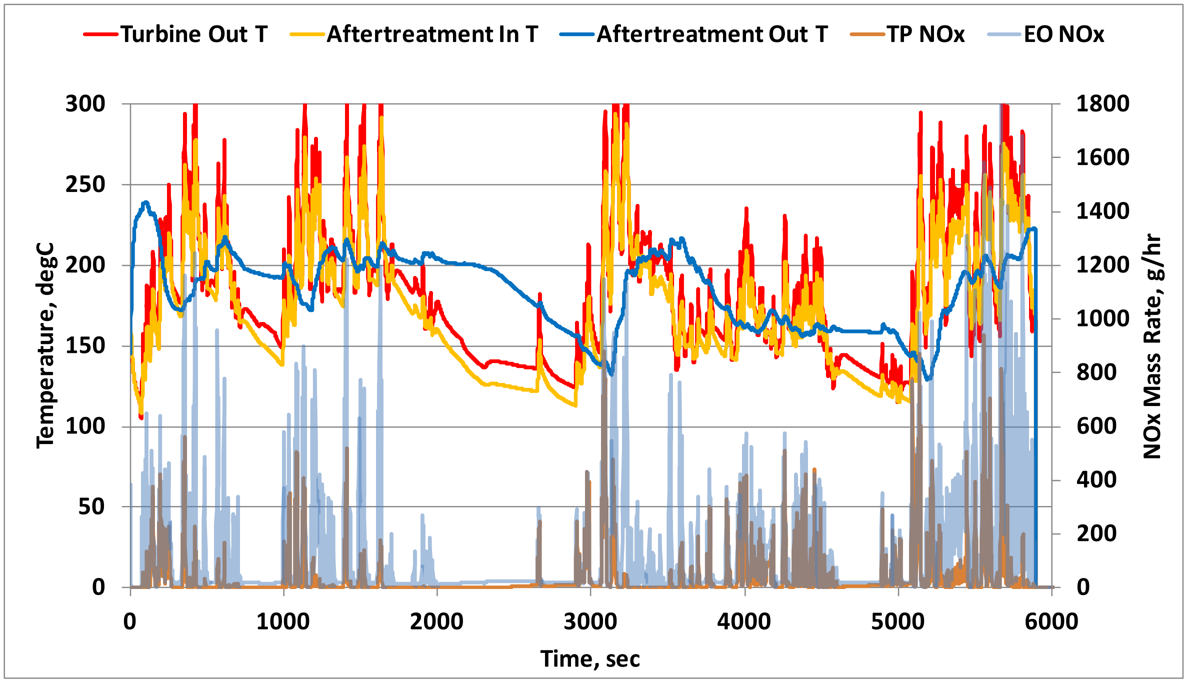

EQUILIBRIUM CYCLE DATA

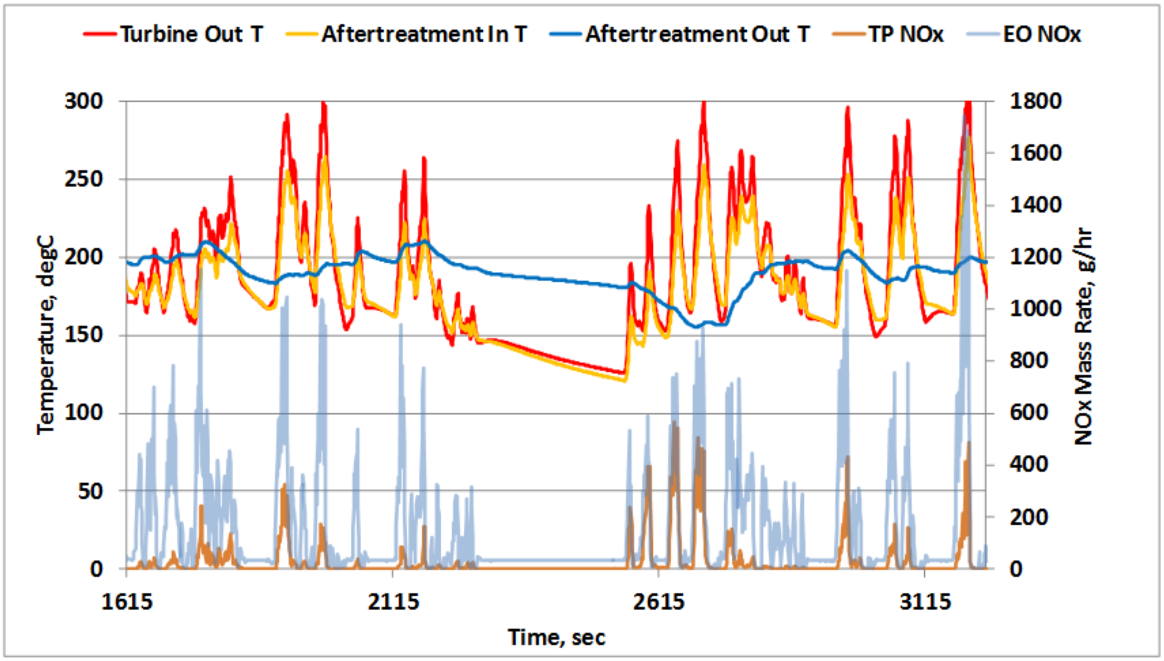

- Middle of range profiles, 9% average power with mix of operations
- 81% NO_X conversion due to significant breakthrough in middle
- Contains useful motoring/idle combination for cooling in middle

V11646_CLUSTER 1

FULL CYCLE DATA (4 REPEATS)

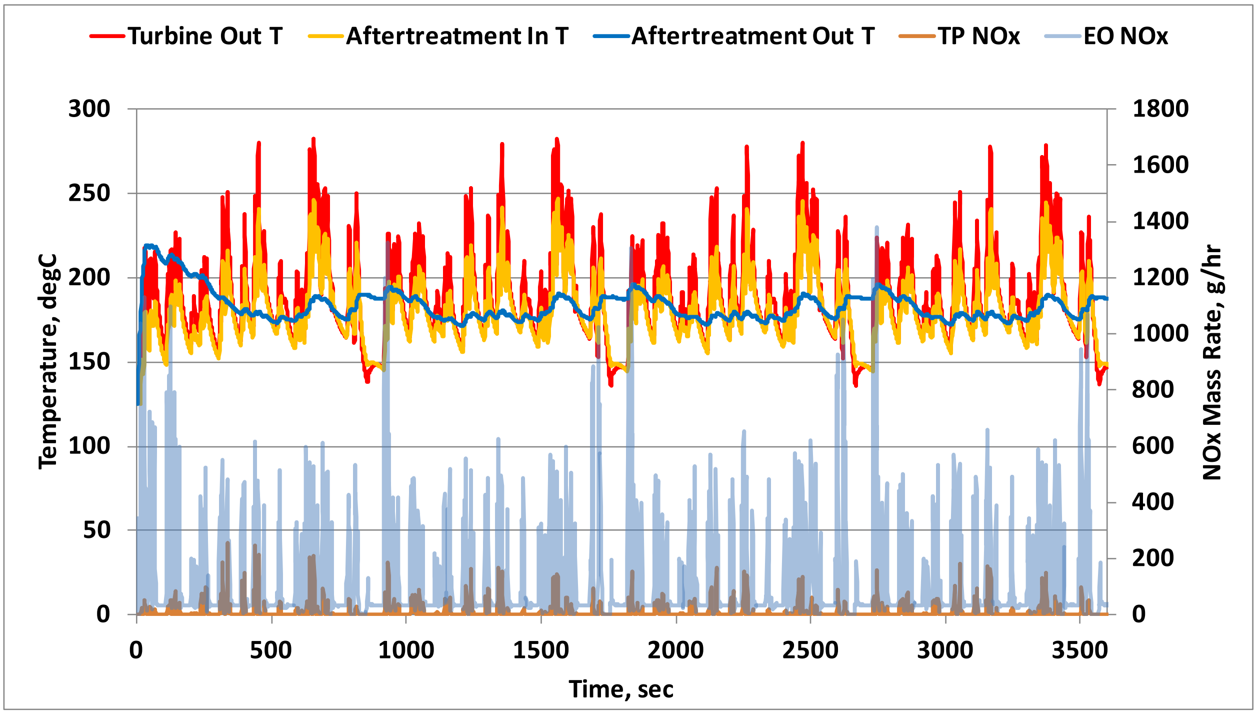

EQUILIBRIUM CYCLE DATA

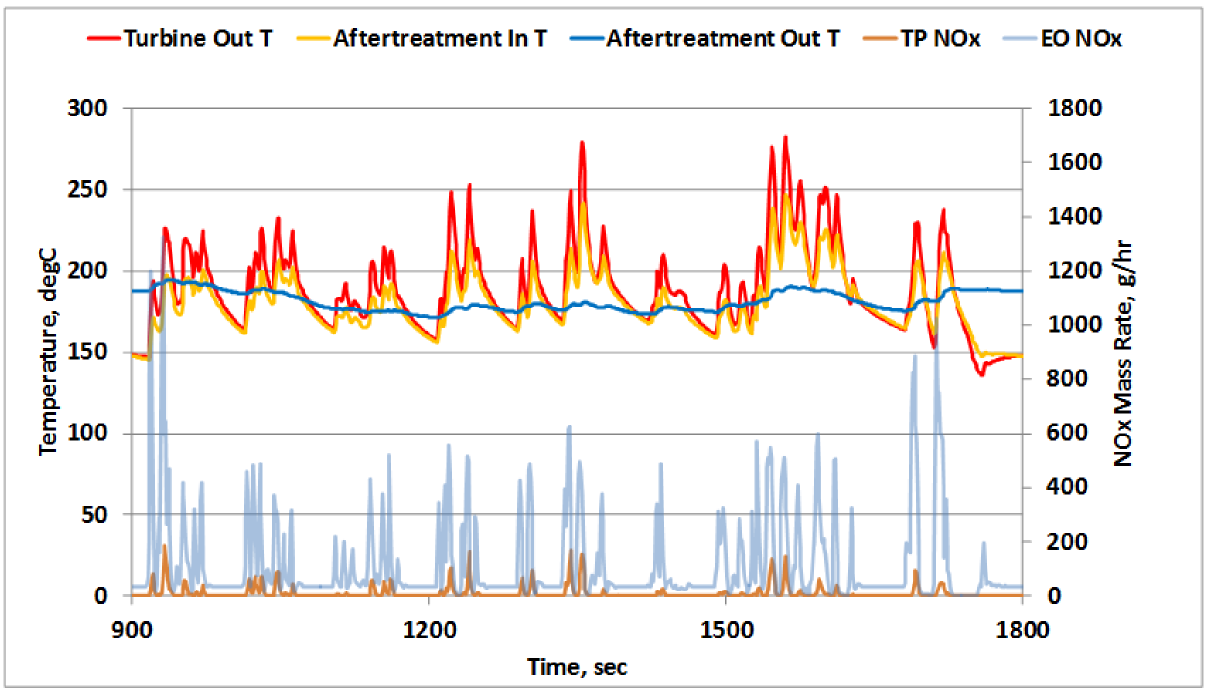

- Sustained low load but very intermittent between load and idle segments
- Little opportunity for significant cooling off, not much motoring
- 91% NO_X conversion, not a significant ATS challenge

V11815_CLUSTER 1

FULL CYCLE DATA (3 REPEATS)

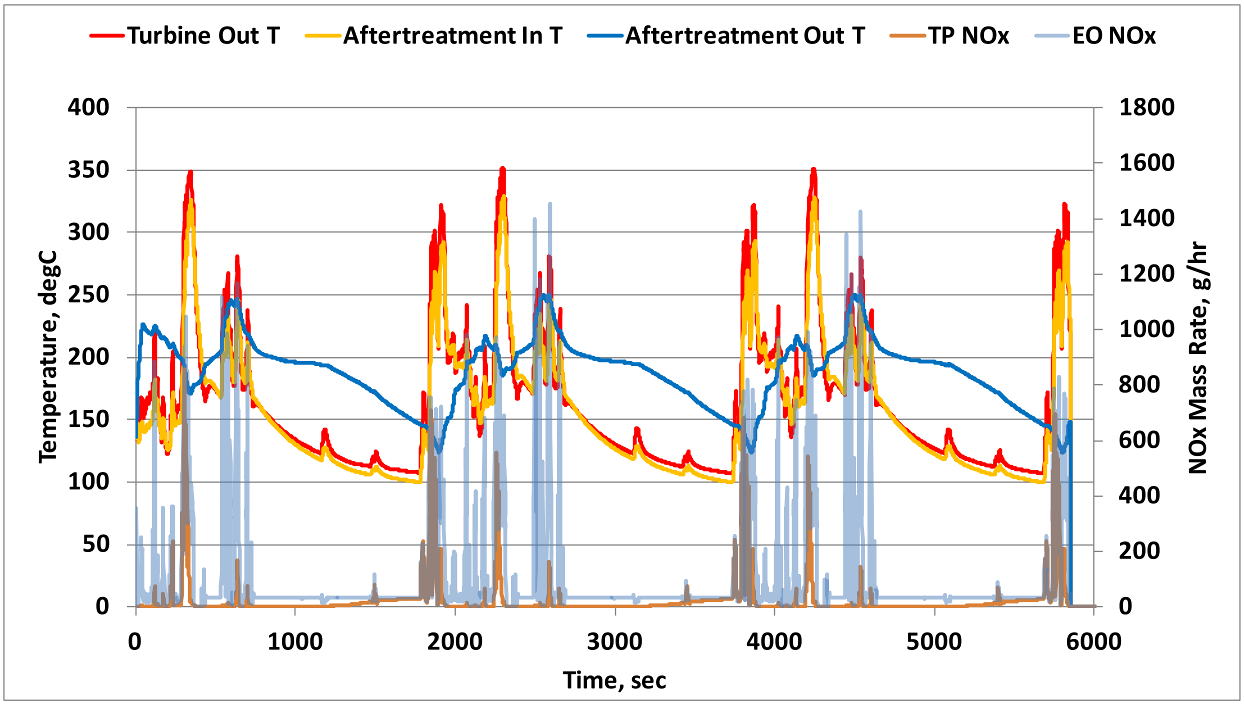

EQUILIBRIUM CYCLE DATA

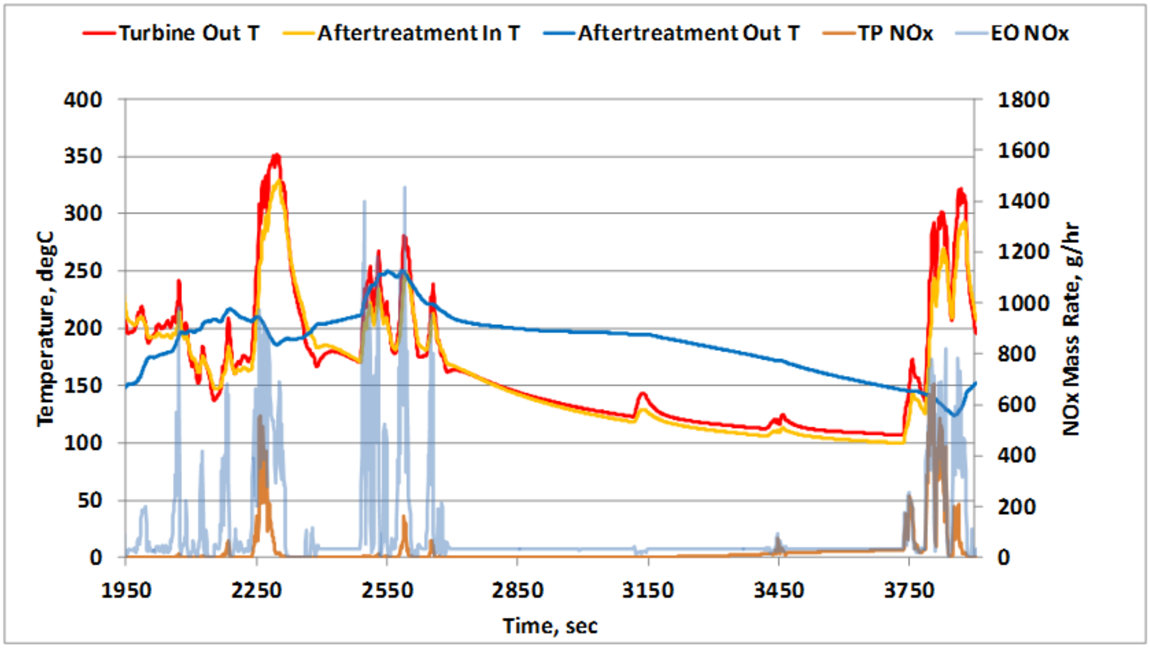

- High Load events bracketing long enough idle to lose performance
- Breakthrough after idle only…
- 76% NO_X conversion

V073_CLUSTER 1

FULL CYCLE DATA

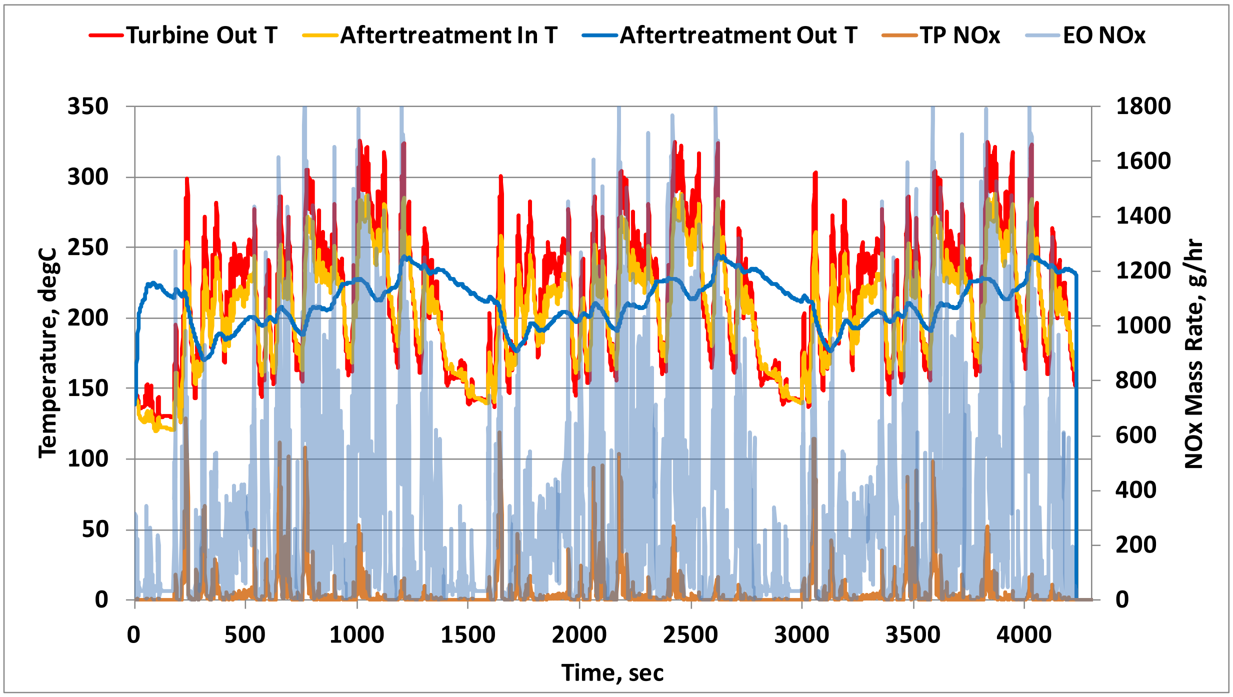

EQUILIBRIUM CYCLE DATA

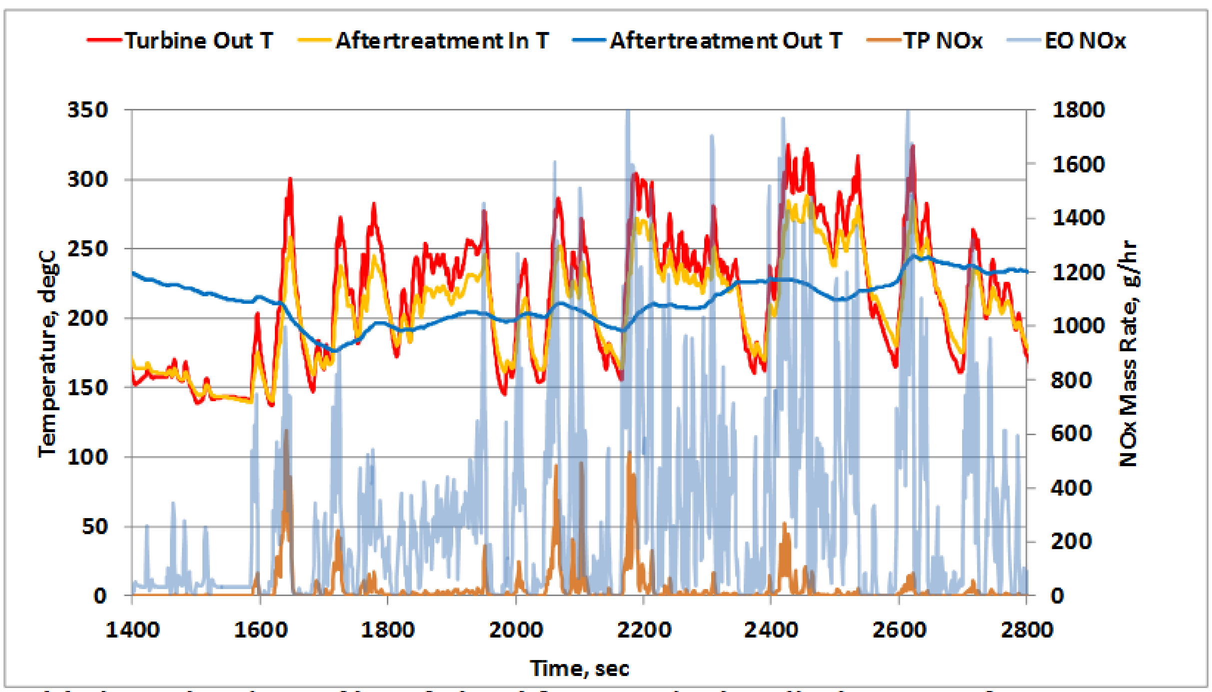

- Highest load profile of the 10, very little idle but significant motoring
- 91% NO_X conversion, but high EO NO_X so still 0.4 g/hp-hr TP NO_X
- Possibly more significant challenge after a low power segment

V11660_CLUSTER 5

FIRST TWO CYCLES (OF 4 REPEATS)

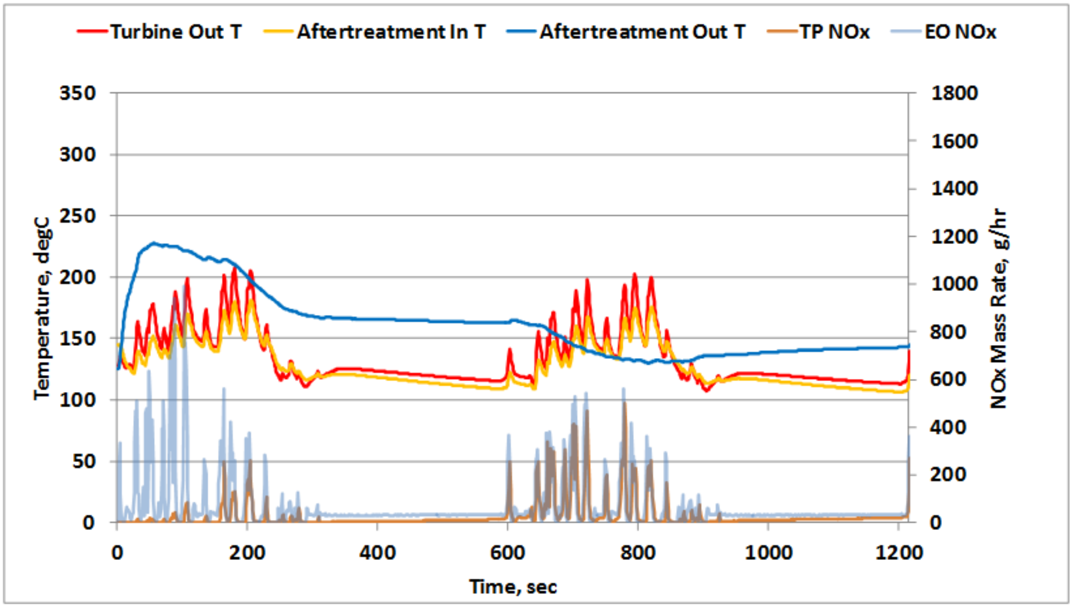

- Significant cooling after 200 seconds (even after initial residual heat)
- Motoring-to-idle segment at 250-300 secs, only 5 min idle
- Initial cycle repeat is 80% conversion (residual performance in first 200 secs)

EQUILIBRIUM CYCLE DATA

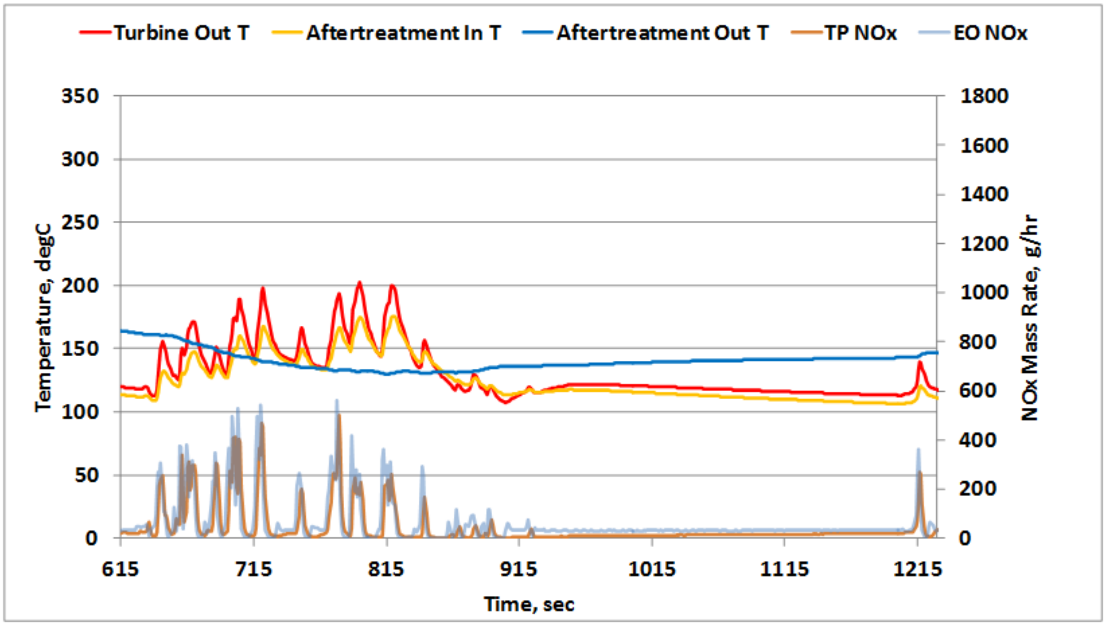

- Lowest Load profile of the 10 (3% max power), never gets much sustained load going
- 27% NO_X conversion, never really gets hot enough to get going
- Possibly useful as Sustained Low Load

V11806_CLUSTER 5

FULL CYCLE DATA (3 REPEATS)

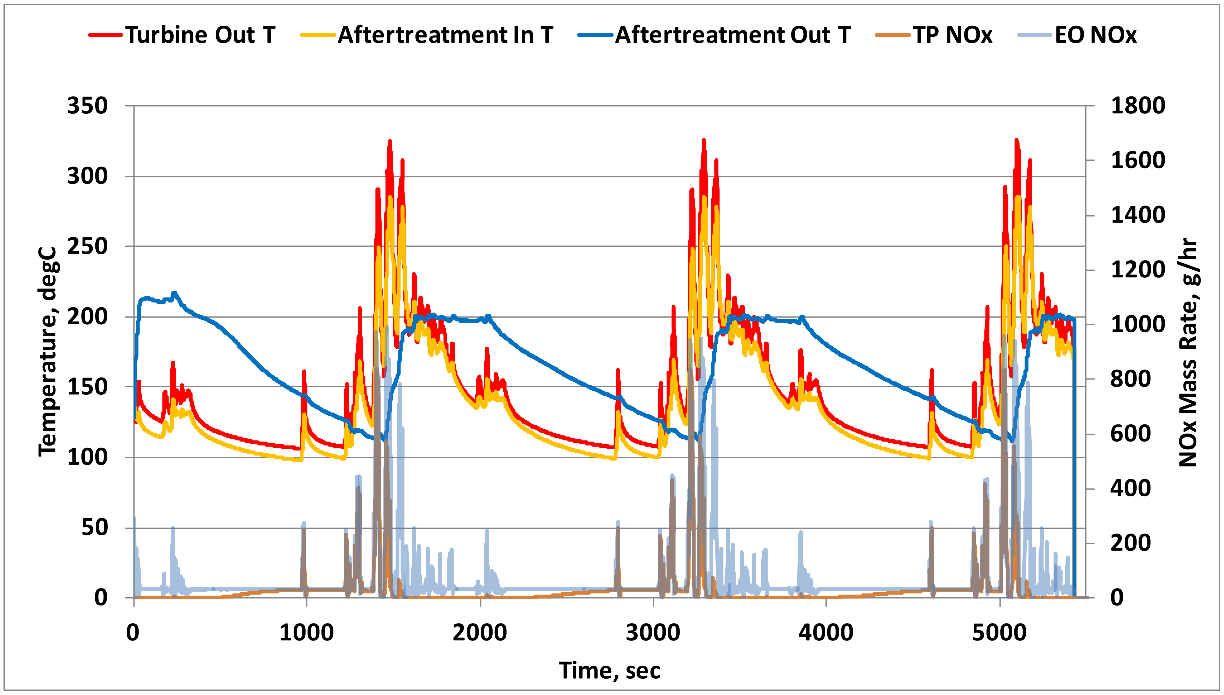

EQUILIBRIUM CYCLE DATA

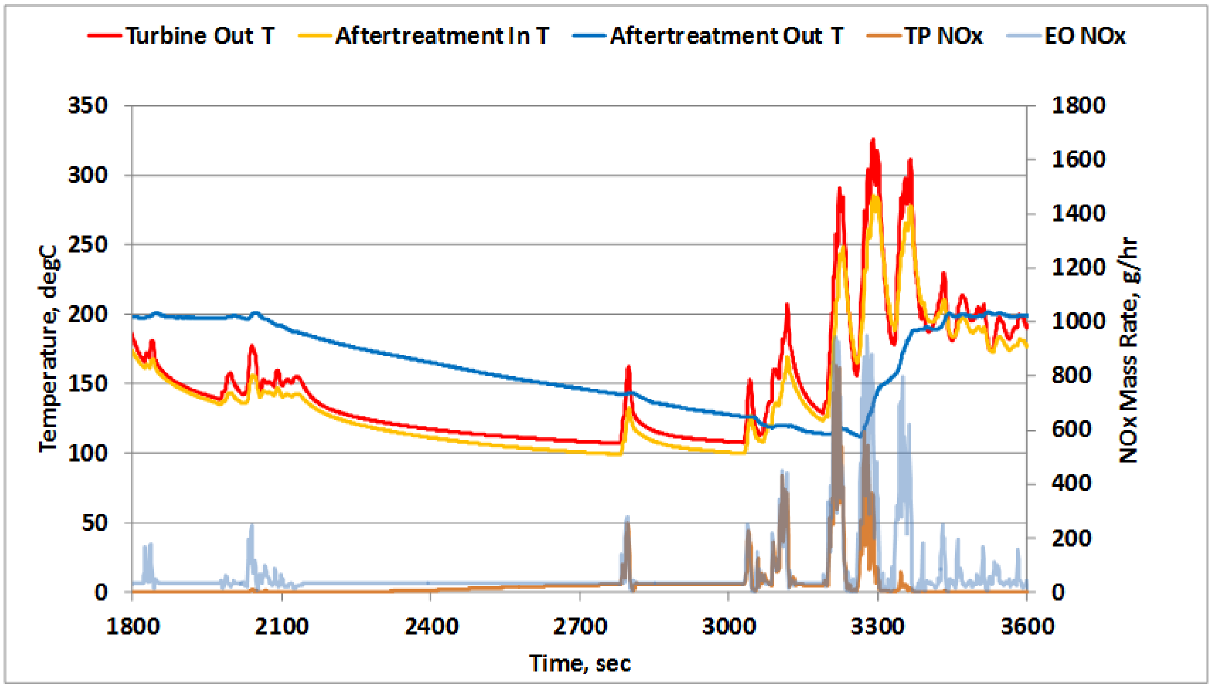

- Major low-to-high transition late in cycle, long idle lead in
- 55% NO_X conversion due to significant breakthrough in middle and loss of control at halfway point
- Good high load segment to use at the end of a cooldown (15% max power segment)

V11817_CLUSTER 5

FULL CYCLE DATA (4 REPEATS)

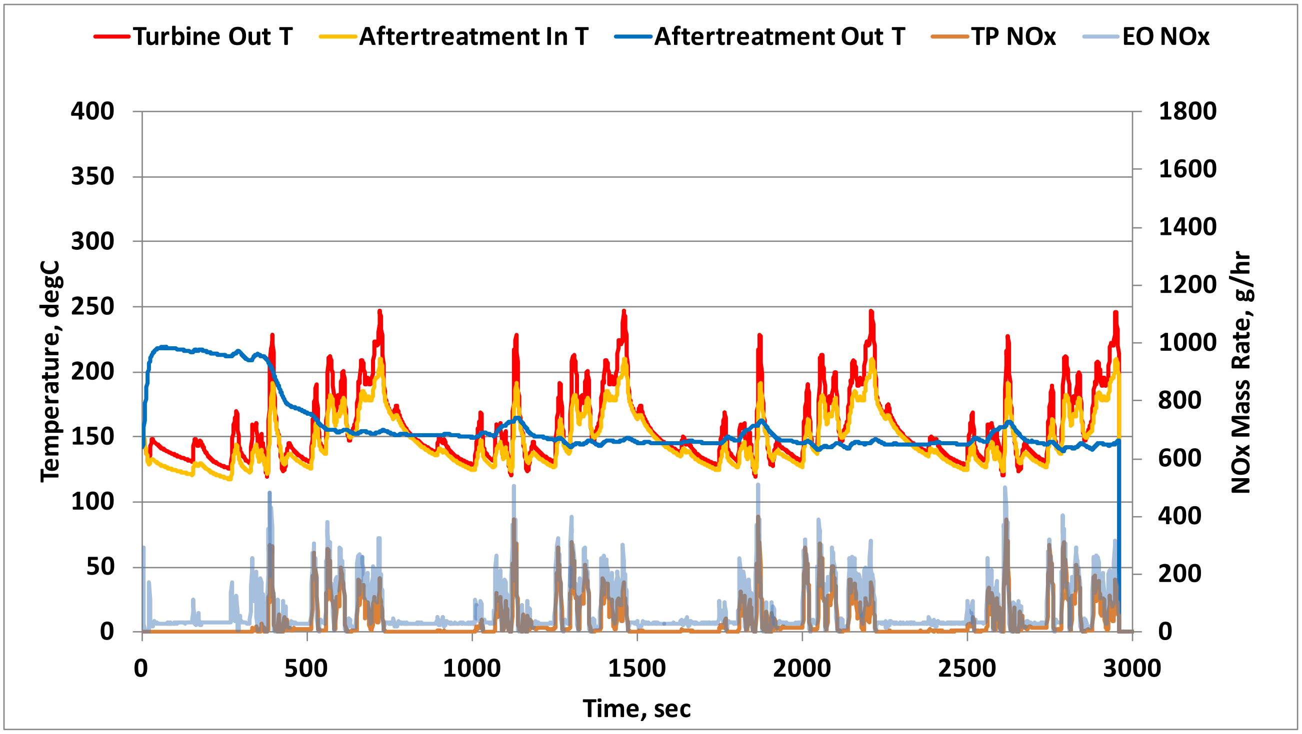

EQUILIBRIUM CYCLE DATA

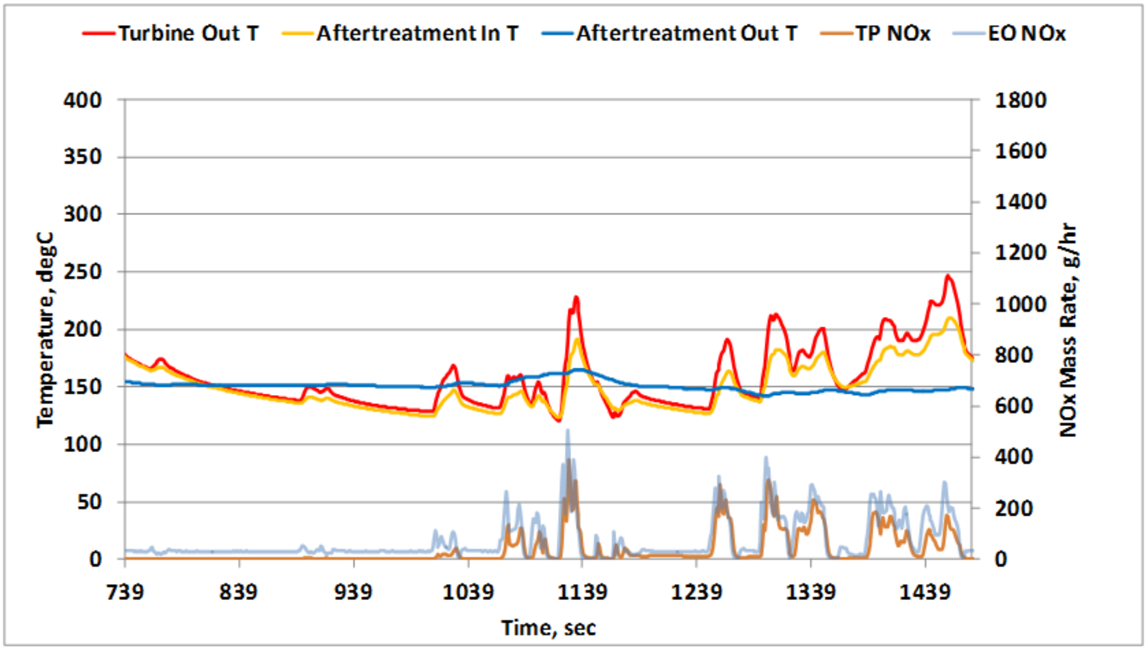

- Highest Cluster 5 load – marginal change in AT temps throughout profile
- 46% NO_X conversion, begin to see activity at end of profile